

Appendix K

Cap Placement Modeling

Introduction

Numerical model simulations of various cap placement factors played a critical part of the Palos Verdes Pilot Cap (PVPC) project. ERDC researchers primarily used two ERDC-developed models, the Short Term FATE of dredged material (STFATE) (Johnson and Fong 1995), and the Multiple Dump FATE of dredged material (MDFATE) (Moritz and Randall 1995), to develop predictions related to sediment dispersion and velocities in the water column, and cap material buildup and placement, respectively. A third model, the Dredging - Cornell Mixing Zone Expert System (D-CORMIX) (Doneker, Jirka, and Nash 1995) was used to estimate the bottom impact velocity of the cap material during direct pump-out through the hopper dredge draghead.

During the preliminary design phase (Palermo et al. 1999), MDFATE simulations were used to estimate the volumes of dredged material required to cover 300 m by 600 m cells with a given cap thickness. For the actual pilot study, MDFATE was used again to compute required volumes, both in the hopper and in the channel, to cover the target cells, LU and SU, with 15 cm of cap material. MDFATE also computed the area covered by both individual and multiple placements. The information on capping thickness and area coverage was needed to make decisions on the spacing and location of the various monitoring activities, e.g., the spacing and extent of the SPI stations and cores. Finally, MDFATE was used to assist in computing individual spacing and placement patterns within a given cell that would result in the desired cap buildup.

The STFATE model was used to predict the fate of the plume that remained in the water column, the impact velocity of the descending jet, and the bottom surge velocity. In addition, because of concern that the plume might adversely impact the inshore kelp beds, before the cap placement operations began, some STFATE simulations were conducted to predict the path and total suspended sediment (TSS) concentrations in the water column from a single placement of cap material. This TSS information was used to make a qualitative estimate of potential impact to the kelp beds. There was also concern over cap material placement impacts on the Whites Point Outfalls. However, the MDFATE simulations prediction of cap thickness showed essentially no accumulation at the outfall locations, so no STFATE simulations to predict water column plume tracks and concentrations in the direction of the outfalls were made.

As noted earlier, a major goal of the PVPC was to determine the ability of the FATE models to accurately predict the various aspects of the capping process. The bottom surge velocity is one of the most easily and accurately measured aspects of the aquatic portion of the cap placement process and is directly responsible for both potential resuspension of the EA sediments and the

ultimate extent of the cap. Therefore, prior to cap placement several STFATE simulations were also conducted to estimate the velocity of the bottom surge. This information was used to assist in locating the placement of the bottom-mounted current meters. After the cap placement operations, additional STFATE simulations were conducted to compare surge velocities measured with bottom-mounted instruments with STFATE predictions based on the actual conditions of the placements. In addition, during these additional simulations, the dimensions of the computed water column suspended sediment plume were compared with BBADCP data and computed TSS concentrations were compared with measurements obtained from water samples collected during the placement operations.

This Appendix describes the STFATE, MDFATE, and CORMIX models, and provides the input information for each. Modeling activities prior to placement, immediately prior to and during placement, and post placement are also included along with comparisons to measured data.

Model Descriptions

STFATE Description

The majority of the following information was excerpted from Moritz, Johnson, and Scheffner (2000).

Field evaluations by Bokuniewicz et al. (1978) and laboratory tests by Johnson et al. (1993) have shown that the placement of dredged material generally follows a three-step process: (a) convective descent during which the material falls under the influence of gravity, (b) dynamic collapse, occurring when the descending cloud or jet either impacts the bottom or arrives at a level of neutral buoyancy, in which case the descent is retarded and horizontal spreading dominates, and (c) passive transport-dispersion, commencing when the material transport and spreading are determined more by ambient currents and turbulence than by the dynamics of the disposal operation. Figure K-1 illustrates these phases.

Model development in this area was initiated in the early 1970's with the work of Koh and Chang (1973) and was continued with developments by Brandsma and Divoky (1976) and Johnson (1990). However, deficiencies remained in the model. Research in the Dredging Research Program (DRP), which resulted in the STFATE model, was directed at removing many of these deficiencies, e.g., inadequate representation of disposal from hopper dredges, the inability to represent the non-homogeneity of disposal material, the inability to model disposals at dispersive sites, the inadequate representation of the bottom collapse phase, and the inability to model disposal over bottom mounds. Basic concepts employed in STFATE are presented below. Details can be found in Johnson and Fong (1995).

Convective descent

In STFATE, multiple convecting sediment clouds that maintain a hemispherical shape during convective descent are assumed to be released. Figure K-2 illustrates the basic concept. By representing the disposal operation as a sequence of convecting clouds, both split-hull barge disposals as well as disposal from a hopper dredge can be modeled. For example, the material in each hopper might be contained in one cloud. This concept also allows for a more realistic representation of the disposal material when consolidation in the disposal vessel has occurred. Denser consolidated material might be represented by one cloud with the less dense, more fluid-like fraction overlying the consolidated material represented by a separate cloud. In addition, the use of multiple convecting clouds allows for a more realistic representation of disposal from a moving vessel where the disposal operation typically requires several seconds to perhaps 1-5 min for completion. As each small convecting cloud descends through the water column, material can be stripped from the cloud to settle with its particle settling velocity. Movement of the stripped material as small Gaussian clouds is discussed later.

Other than the concept of multiple convecting clouds and the stripping of material from those clouds, treatment of the convective descent phase for each of the convecting clouds is the same as initially developed by Koh and Chang (1973).

The equations governing the motion are those for the conservation of mass, momentum, buoyancy, solid particles, and vorticity. These equations are ordinary differential equations with time as the independent variable. Basic dependent variables are the cloud's radius, velocity, and density along with the concentration of each solid fraction.

Given a set of initial conditions, e.g., the total volume of disposal material, sediment concentrations, etc., along with ambient conditions such as the water column stratification and current, the governing system of equations are solved using numerical techniques. STFATE uses the forward Euler scheme. Given the idealized representation of the disposal operation and the uncertainty of initial conditions, the need for higher-order numerical schemes is questionable for most planning level applications of STFATE.

Dynamic collapse in water column

As the disposal cloud goes through the convective descent phase, its mass and momentum changes due to entrainment of surrounding water. The horizontal velocity of the cloud tends to approach that of the ambient fluid. Coincidentally, the disposed material concentration is greatly reduced and the cloud's vorticity becomes insignificant because of dissipation by ambient stratification and turbulence. If the cloud reaches the depth of neutral buoyancy, its momentum will tend to make it overshoot the neutrally buoyant point while the buoyancy force will tend to bring it back to the neutrally buoyant position. The combined action of these forces will make the cloud undergo a decaying vertical oscillation. As the vertical motion of the cloud is being suppressed, the cloud tends to collapse vertically and spread out horizontally, seeking hydrostatic equilibrium within the stratified ambient fluid. As the cloud collapses, its cross section

becomes elongated in the horizontal. The idealized shape that the cloud is assumed to take is that of an oblate spheroid.

With the exception of vorticity, the conservation equations used for convective descent still hold. Any differences are due to the additional dimension used to describe the cloud. Final results from the convective descent phase such as cloud size, position, and velocity become the initial conditions for the solution of these equations.

Dynamic collapse on bottom

As previously noted, the convective descent and water column collapse phases follow the development of Koh and Chang (1973). However, the manner in which collapse of the disposal cloud is treated when the bottom is encountered during convective descent is different.

Bottom collapse in STFATE is computed from a conservation of energy concept. When the cloud strikes the bottom, it possesses a certain amount of potential energy, which can be computed since the mass of the cloud and the location of its centroid are known. In addition, the kinetic energy of the impacting cloud can be computed since its velocity and mass are known. Thus, the total energy of the cloud at the moment of impact is known. This energy is then available to drive the resulting bottom collapse or surge.

A basic assumption is that the bottom collapsing cloud is one-half of an ellipsoid. If the bottom is flat, the cloud becomes one-half of an oblate spheroid. As illustrated by Johnson and Fong (1995), expressions for the time rate of change of the three cloud dimensions can be derived which are dependent on the cloud's kinetic energy. Actually, the surge of suspended dredged material that moves out from the impact point along the bottom takes the shape of a torus. For the depths, sediments and dredge operational conditions experienced during the pilot placement, the average speed of this torus over the first 50 to 75 m from the impact is on the order of 1 m/sec.

Given that the change in the total energy of the cloud, which is the sum of the kinetic and potential energies, is equal to work done by the cloud, the temporal variation of the kinetic energy can be determined. The potential energy of the cloud is easily computed and changes as the cloud density decreases due to entrainment of ambient fluid, the loss of sediment, and to the decrease of the height of the centroid of the cloud as the cloud spreads over the bottom. The kinetic energy of the cloud is then known since the change in kinetic energy can be computed once the work done by the collapsing cloud is quantified. Work must be done to overcome bottom friction, drag, the production of internal turbulence and the setting of the ambient fluid in motion. Given the kinetic energy of the cloud, the cloud shape can be determined from the expressions derived by Johnson and Fong (1995) relating the change in the cloud axis to the cloud's kinetic energy.

The STFATE model allows for the effect of bottom slope on the spreading of the cloud, but it is only a simplistic representation of the actual process. The basic approach employed in the model is to compare the bottom elevation at the centroid of the cloud's elliptical bottom with the bottom elevation at the centroids of the four quadrants of the ellipse. These four slopes are used to compute

changes in the rate of spreading, which are added to the cloud dimensions computed from the basic energy algorithm discussed above. The locations of the centroids of the four quadrants are then averaged to yield the new centroid of the overall cloud. When computing the spreading of the cloud due to its energy, the collapse is assumed to occur on a flat bottom. A more rigorous approach would be to model the surge movement with a fully three-dimensional model that contains all the basic physics (e.g., a non-hydrostatic pressure, required to accurately compute the transport of a sediment/water mixture as it descends through the water column, impacts the bottom, and is deflected laterally along a varying bottom bathymetry). Under the Dredging Operations and Environment Research Program such a model is under development (Johnson 2001).

Transport-diffusion phase

At most disposal sites, the convective descent and dynamic collapse phases only last on the order of a few minutes. When either the rate of spreading of the collapsing cloud becomes less than an estimated rate of spreading due to turbulent diffusion, or the energy of a bottom collapsing cloud becomes less than 0.01 percent of the initial energy, the collapse phase is terminated and the “longer” term transport-diffusion phase is initiated. In this phase, material in suspension is transported and diffused by the ambient current while undergoing settling. Any non-sediment constituents being modeled are also transported and diffused.

A basic assumption in the transport-diffusion phase is that material (or constituent) concentrations can be determined from a superposition of small clouds characterized by a normal or Gaussian distribution. These clouds are formed as material is stripped away during the descent of the convecting clouds as well as during the collapse phase. For collapse in the water column, small clouds are formed as material settles from the collapsing cloud. However, during bottom collapse, laboratory experiments by Johnson et al. (1993) and field data collected at Mobile, AL, by Kraus (1991), imply that fine-grained material is also lost to the water column at the top of the collapsing cloud.

At the end of each time-step, the input velocity field advects each cloud horizontally. In addition to the advection or transport of the cloud, the cloud grows both horizontally and vertically as a result of turbulent diffusion. If long-term output is desired at the end of a particular time-step, the concentration of each solid type is given at each grid point at a particular vertical location by summing the contribution from individual clouds. This approach for the transport-diffusion phase follows the work of Brandsma and Sauer (1983). The surface and all solid boundaries except the bottom are handled by assuming reflection from the boundaries.

In addition to the horizontal advection and diffusion of material, settling of the suspended solids also occurs. If a solid fraction is specified as being cohesive, the settling velocity is computed as a function of the suspended sediment concentration of that solid type. Therefore, at each net point the amount of solid material deposited on the bottom and a corresponding thickness are also determined. Since a normal distribution is assumed for material in the small clouds, deposited material is also assumed to take such a distribution on the bottom. A basic assumption in the model is that once material is deposited on the

bottom it remains there; i.e., neither erosion nor bed-load movement of material is allowed. However, deposition is prohibited if the computed bottom shear stress exceeds a specified critical shear stress for deposition for each solid fraction.

The discussion presented above for the transport-diffusion of solids also applies to the disposed fluid with its dissolved constituents. The constituents are assumed to be conservative with no further adsorption on or desorption from the solids in the water column or those deposited on the bottom. Computing the resultant time-history of constituent concentration provides information on the dilution that can be expected over a period of time at the disposal site and enables the computation of mixing zones in water column evaluations.

Other processes

Currents. STFATE assumes a current that is constant in time, called time invariant, over the length of the model simulation. The length of time the models simulate a single placement is generally 2 to 4 hr. STFATE has four options for modeling currents during an STFATE simulation. The first option is to select a single, depth-averaged current point value for a specified water depth used to maintain a constant, uniform flow rate or water flux through a grid cell. A depth-averaged current is the average of the current over the entire water column, both in speed and direction. The velocity is assumed to be uniform across the entire depth at each grid cell. For water bodies with relatively consistent currents over the entire water column, this is a reasonable assumption. It is also computationally easy and quick. To maintain a constant flux through all of the grid cells, the model increases the current as depths decrease from the specified depth and decreases the currents as the depths increase from the specified depth. For example, if the depth-averaged current is specified as 10 cm/sec at a bottom depth of 50 m, then everywhere on the grid where the depth is 50 m, the model will simulate a current of 10 cm/sec through the entire water column. If the depth decreases to 25 m, then the model will simulate a current of 20 cm/sec at those locations.

The second STFATE current option is the same as the first option except that the velocity is not assumed to be uniform throughout the depth of the water column within each cell; the velocity profile is assumed to be a log profile with depth. As in the first option, a depth-averaged velocity for a specified depth is given, and the program adjusts the average velocity as the depth varies to maintain a constant flow rate or water flux through all of the grid cells.

The third STFATE current option is a two point current profile, in which the user enters differing current velocities and orientations at two different depths. This option requires a flat bottom (no variable bathymetry).

The last STFATE current option allows the user to provide a depth averaged current field on the STFATE model grid (i.e., a depth averaged current for every grid point is supplied from an outside source). Current fields, which correspond to the STFATE model grid, can be obtained by horizontally interpolating current fields that are defined at other spatial locations onto the STFATE grid point locations. For example, the Surfacewater Modeling System (SMS) can interpolate a current field generated by the ADCIRC circulation model to the

STFATE grid.

Before the post-capping simulations (will be discussed later), modifications were made to STFATE so that vertical shear in the ambient current over a variable bathymetry site can be input. In addition, an algorithm was developed to spread point velocity data over the numerical grid in a more reasonable fashion.

Stripping of fine sediments. The fate of fine-grained dredged sediments stripped from the descending jet during conventional placement from a barge or hopper dredge can be an issue in some situations, e.g., concern over the impact of the water column plume on inshore kelp beds for this project, and especially during the placement of contaminated sediments (which was not a part of this project). Note that material is also released into the water column from the bottom surge. Typically, this is a much greater amount of material and is initially released near the bottom. As noted above, a major function of STFATE is tracking of the plume that remains following the bottom collapse phase. The following discussion provides a general description of stripping, which is a separate phenomenon from the main descent/bottom collapse phase.

As noted earlier, during open water placement of dredged sediments from a barge or hopper dredge; the vast majority of released dredged sediments descend rapidly to the bottom as a coherent, well-defined jet of material. However, some small fraction of fine-grained material can remain in upper and mid levels of the water column, and, depending on ambient currents, may be transported from the site. This fine-grained material may be released to the water column in different ways. As the descending cloud or jet moves downward, a circulation is set up such that ambient fluid is entrained into the backside of the cloud or jet. This entrained fluid decreases the overall density of the cloud and the turbulent mixing created in the cloud or jet separates some of the fine-grained material from the denser core of sediments. These fine-grained particles are then left behind at different levels in the water column as the cloud or jet continues its descent to the bottom. These fine-grained particles then settle at their particle-settling rate, but can become trapped in the water column if stratification exists (typically seen only in deep water). This is one form of what is commonly called stripping.

Truitt (1988) provides a good summary of approximately nine major field studies where measurements were made to estimate the volume of sediments that are stripped from the main jet and remain suspended in the water column a considerable length of time. For the five studies that dealt with mechanically dredged sediment placed in barges, three studies had suspended sediment masses of 1 percent, and two studies had suspended sediment masses of 2 to 4 percent. A study of dredged material disposal in Hong Kong, showed loss of sediments due to stripping during barge placement of fine sediments into disposal pits ranged from 1 to 3 percent (Land and Bray 2000).

Some portion of this 1 to 4 percent mass of suspended sediments stripped from the main jet of material likely deposits in the immediate vicinity of the placement and thus remains inside many disposal sites, although the size of this portion will vary considerably with site and sediment characteristics. In cases where the remaining portion of the stripped material is an issue of concern, it can either be tracked as it moves in the water column or the area of concern adjacent to the placement area can be monitored to determine if measurable amounts deposit there. Tracking fine material in the water column is a very expensive

undertaking, with considerable uncertainty involved in measuring small amounts of suspended sediment over a wide area. Similarly, monitoring an adjacent sensitive resource for minute amounts of fines and/or their associated contaminants is also very expensive, time consuming, and subject to some uncertainty. Therefore, such monitoring requirements are usually imposed in extraordinary situations, and only then to confirm numerical movement predictions through a limited number of monitoring events. To date, there has been no evidence that the amounts of “untracked” sediments stripped during the placement of contaminated have caused unacceptable environmental impacts. Thus for the vast majority of dredging projects, no attempt is made to collect quantitative data on the fate of the stripped fraction because it is not considered to be cost effective.

Due to concerns over the potential impacts on the nearshore kelp beds, a STFATE simulation was made specifically to examine this potential. However, the focus of this simulation was the main plume remaining in the water column, not just the stripped material. Several components of the placement monitoring activities also addressed tracking of the water column plume. This monitoring was conducted to primarily address potential impacts in the kelp bed. In the STFATE simulations of impacts on the kelp beds, the stripping option was invoked for all three sediment components, sand silt, and clay.

In MDFATE and STFATE, stripping is modeled as follows. As the clouds of dredged material move downward, material and fluid with dissolved contaminants may be stripped away. Stripped material is handled through the concept of Gaussian clouds described earlier. The model user can select whether or not to include stripping of the sand, silt or clay fractions. If the stripping option is selected, the amount of material stripped away and stored in the Gaussian clouds is computed as a coefficient times the downward velocity of the cloud times the cloud surface area. The value of the “stripping” coefficient is selected so that approximately 2 to 5 percent of the total volume of fine material is stripped away at placement sites with water depths of 60 m or less. Based upon field data collected by Bokuniewicz et al. (1978), along with the results of Truitt (1988) and Land and Bray (2000), this will result in the amount of stripped material being on the conservative side. The ambient current field then advects the stripped material in the Gaussian clouds, with the particles settling at their individual particle settling velocity.

Disposal at dispersive sites. In STFATE, a critical shear stress for deposition is specified for each sediment fraction. A computed bottom shear stress is then compared to the critical value to determine if suspended material can be initially deposited. If only currents affect the bottom shear stress and no waves are present, the shear stress computation is based upon the assumption of a log velocity profile. If waves are present at the disposal site, the approach derived by Madsen and Wikramanayake (1991) is used. With this approach, the ambient current angle, wave amplitude, wave period, and an initial value for the wave-current angle must be input.

STFATE Model use

Generally, STFATE is used to address environmental issues concerning individual disposal operations, e.g., the determination of mixing zones.

However, a streamlined version of STFATE comprises the short-term computations for individual disposals in MDFATE. In that version, many of the computations concerned with water column concentrations have been removed since they are not required to address mound formation and the long-term fate of those mounds.

Basic data required to operate STFATE are descriptions of the disposal material, disposal vessel, and the ambient environment at the disposal site. Therefore, information such as the bulk density of the material, the number of solid fractions and their concentrations, the barge length and width, and the ambient current and water column depth and stratification must be known. Basic outputs are the time history of water column concentrations in horizontal planes at particular depths and the initial deposition of material on the bottom.

Prior STFATE applications

Early STFATE applications focused primarily on model verification and involved comparisons of computed suspended sediment concentrations and computed extent of bottom deposition with actual field measurements. The first STFATE model verification efforts involved using field data collected under the USACE Dredged Material Research Program (DMRP) (Bokuniewicz et al. 1978). Data were collected at several sites, e.g., Lake Ontario and Duwamish Estuary for operations involving open water placement of fine-grained sediments. It is noted that Bowers and Goldenblatt (1978) conducted tank tests and related certain model coefficients such as the descent entrainment coefficient to the moisture content of the disposal material. These expressions are contained in STFATE.

Since the data collection efforts under the DMRP, other field data collection efforts have taken place. Data collected at Mobile, AL in 1989 (Kraus 1991) illustrated that the STFATE model could accurately reproduce the observed spread of the bottom surge, but that model modifications were required to accurately reproduce suspended sediment concentrations of fine grained material remaining in the water column. These modifications resulted in representing the disposal operation as a series of small disposal clouds rather than one large cloud. Thevenot and Johnson (1994) used the modified model to demonstrate that suspended sediment data collected during a disposal operation at Miami, FL, could be realistically reproduced.

Although STFATE computes the fate of material from a single disposal operation, individual results can be accumulated to represent the fate of multiple disposals. Nelson and Johnson (1992) showed that at the Port Gardner disposal site in Puget Sound the extent of the predicted disposal mound agrees quite well with bathymetric surveys of the actual mound resulting from the disposal of several hundred thousands of cubic yards of material. Since that study, many of the STFATE capabilities have been incorporated into a mound-building model called MDFATE (Moritz and Randall 1995).

Finally, under the Dredging Research Program (DRP), physical model tests were conducted to guide model developments such as the allowance for multiple disposal clouds noted above, improved bottom surge computations, and refined bottom surge distributions to more accurately represent suspended sediment

concentrations over the lower part of the water column. Those tests were conducted in a static tank in water depths ranging from 0.6 to 1.8 m. Several sediment types were tested in both moving and stationary disposals from a 1:50 scale split-hull barge and a vessel representative of a hopper dredge. Results presented by Johnson and Fong (1995) illustrate that the STFATE model accurately reproduced the deposition of material on the bottom as well as sediment concentrations in the water column.

In summary, although additional improvements to the STFATE model are desirable to more accurately represent processes such as the stripping of fine grained material during descent of disposal material through the water column and the impact of variable bathymetry on the bottom surge, both field data and physical model tests have demonstrated the model's ability to provide useful information on the short-term fate of dredged material disposed in open water.

STFATE Model limitations

STFATE was developed primarily as a planning level model, i.e., it has many assumptions that are appropriate for planning level studies. STFATE was developed when personal computers had limited amounts of memory, limited ability to use additional memory, and relatively slow processors. Thus, many of the more computationally intensive processes had to be considerably simplified. For the Pilot study, STFATE (and MDFATE) were not used for planning, but they were used to varying degrees for project-specific design. In this case, the model's limitations need to be recognized and factored into the predictions and interpretations. This section discusses the STFATE limitations and how they influenced the simulations for this project. For those cases where the same limitation pertains to both the STFATE and MDFATE models, it will be noted. MDFATE-specific limitations are discussed at the end of the section that follows describing the MDFATE model.

Perhaps the most notable limitation is the way STFATE and MDFATE represent currents. STFATE has a number of other limitations in how it models physical processes, which include: the rate of material leaving the barge, stripping, and no resuspension by surge currents. Other STFATE limitations include sensitivity to geotechnical parameters, idealized shapes of the clouds leaving the barge, how it treats dissolved contaminants, and model validation.

Currents. Depending on the situation, the STFATE limitations can potentially cause significant or minimal errors in predictions. STFATE was primarily used for two items, prediction of bottom impact velocities and the associated surge current, and the fate of the water column plume. For the bottom impact velocities, the time invariant current used in STFATE had very little impact. The short duration of the jet fall through the water column and the similarly short duration of the surge current were not significantly influenced by the time invariance of the current. They were perhaps somewhat influenced by the generally larger current predicted near the bottom when the full water column depth averaged current was used in the pre-placement simulations. Recall that vertical shear in the ambient velocity was allowed in the post-placement simulations.

STFATE's inability to have currents vary temporally reduces the model's

ability to simulate the fate of the water column plume; particularly as the length of time increases and the currents change (i.e., if a strong semi-diurnal tidal component exists that will vary over the 2- to 4-hr period the model is simulating). A constant, worst case current magnitude and direction was input for the pre-placement simulation of the plume's path and impact on the kelp beds. This likely resulted in over-prediction of the water column concentrations at the kelp beds, making this prediction even more conservative. The tidal change in current direction would likely have reduced the on-shore component.

Stripping limitations. Stripping of fine sediments from a descending plume is represented in STFATE during the convective descent phase as:

$$\Delta V = C_{\text{strip}} 2 \pi R^2 U C \Delta t$$

Where

ΔV = mass stripped

C_{strip} = stripping coefficient

R = plume radius

U = plume velocity relative to ambient current

C = concentration of solids in plume

Δt = computational time step

A major limitation of the stripping formulation in STFATE is that no real guidance can be given for the selection of the coefficient C_{strip} . As previously discussed, all that can be said is that a value of 0.003 results in 2-5 percent of the fines being stripped away from the descending plume in water depths of 30 to 60 m.

Again, this percentage of solids loss to the water column agrees with data published by Bokuniewicz et al. (1978), Truitt (1988), and Land and Bray (2000).

Other limitations. The determination and specification of model coefficients are another limitation in the STFATE and MDFATE models. STFATE has 14 default coefficients that define parameters such as drag and friction, which can be modified by the user. Details on model sensitivity to these coefficients are lacking, as are recommendations on how to adjust these coefficients for particular hydrodynamic environments. MDFATE has no provision to adjust any of the default coefficients.

STFATE and MDFATE assume dredged material is released at a pre-calculated rate over the duration of the specified placement. While this pre-calculated rate is likely reasonable, the actual release rate is not uniform over the entire dump duration. As the dump duration increases, and as the vessel velocity increases, the differences between actual and calculated release rates will induce additional uncertainties.

When STFATE and MDFATE simulate the exit of dredged material from a barge or hopper dredge, the models assume the dredged material is released as a

series of individual clouds of a given size and location. These clouds are assumed to be hemispherical in shape. Actually, the disposal for the dredged material at PVPC is continuous. However, an inspection of the vessel draft versus time plots revealed that the majority of the material generally was released in about the first minute. The impact of this on the post-placement modeling is discussed later.

STFATE and MDFATE are also sensitive to the geotechnical parameters of the sediments. During the pre-placement simulations, geotechnical data were limited. Initial STFATE simulations were based on samples collected during the late FY00 and early FY01 dredging of the Queen's Gate Channel. Geotechnical data from analyses of sediment samples collected out the hopper were used for STFATE hindcasting. However, these samples were collected from the surface of a thick (>3 m) layer and may not have been representative of the vast majority of the material in the hopper. Some additional thoughts on this fact are provide later in the appendix.

For this study a major limitation within STFATE and MDFATE, but particularly within STFATE, is the fact that resuspension of the native sediments (or previously placed sediment in the case of MDFATE) is not simulated by the model. STFATE and MDFATE simulations indicated that only the dredged material mound resulting from a single placement would result in a maximum thickness of several centimeters. SPI imagery has indicated that at the point of impact, a several centimeter thick layer of sediments was resuspended. Thus, any volume calculation from a single load, when compared with the SPI measurements, would likely show significant differences due to the inclusion of the resuspended sediments. This is much less of a problem for multiple placements. Each subsequent placement occurred over an area of the bottom that already had some thickness of dredged material from previous placements. Thus the vast majority of the material resuspended would be cap material, not native sediments.

STFATE allows the user to specify the concentration of a contaminant present in the dredged material. This concentration is determined by running a standard elutriate test. STFATE makes various assumptions related to contaminant concentrations: the contaminant concentration is uniform throughout the fluid fraction of the dredged material; the entire fluid fraction is released to the water column as a cloud during bottom collapse; the dissolved contaminant cloud diffuses vertically and horizontally as it is advected in the water column; and the dissolved contaminant is conservative and does not degrade, react, volatilize or adsorb to the solids originally in the water column. These are conservative assumptions for most contaminants, particularly non-polar organic contaminants. STFATE also assumes that there is not any further desorption or solubility of contaminants from the dredged material solids that have been dispersed in the water column. This latter assumption is not conservative, particularly for non-polar organic contaminants. Overall, the assumptions are conservative for all contaminants except non-polar organics, but are conservative for non-polar organics also, if the water column has its own source of clean suspended solids.

One final limitation of STFATE is that, beyond the field and laboratory work to develop and validate STFATE, additional field data for further validation of STFATE at other disposal sites have been limited.

MDFATE

MDFATE Background

Note that much of the following information was accepted from Moritz, Johnson, and Scheffner (2000).

MDFATE was developed under the Corps' Dredging Research Program (DRP) (Hales 1995). The MDFATE model was formerly known as Open Water Disposal Area Management Simulation (ODAMS) program (Moritz and Randall 1995). MDFATE is a site management tool that bridges the gap between the STFATE model (Johnson and Fong 1993), which simulates the placement of a single load of dredged material, and the Long Term FATE of dredged material (LTFATE) model (Scheffner et al. 1995) which predicts the long term stability (days to years) of dredged material mounds.

The STFATE model was described in the previous section. In MDFATE, the suspended solids and conservative tracer portions of STFATE are removed so the modified STFATE sub-model within MDFATE only models the convective descent, dynamic collapse, and passive diffusion processes. The LTFATE model combines hydrodynamics (waves, currents, and tides) and sediment transport algorithms to predict the stability of dredged material mounds composed of grain sizes ranging from small gravel/coarse sand down to silts and clays. MDFATE uses modified versions of STFATE and LTFATE to simulate multiple disposal events at one site to predict mound building and can be used to determine if navigation hazards are created, to examine site capacity and mound stability, to design capping operations, and to conduct long-term site planning. During the preliminary design effort (Palermo et al. 1999), a standalone version of the LTFATE model was used to model cap stability during storms.

Similar to LTFATE, local wave and tide information can be used in MDFATE along with actual disposal site boundaries and bathymetry. The disposal site bathymetry can be automatically generated as a flat plane at a constant depth or a flat plane with a constant slope. MDFATE can also import actual bathymetric data from an ASCII file.

Because of the modified LTFATE sub-model in MDFATE, the program can account for non-cohesive sediment transport and non-cohesive avalanching. In addition to being able to model the high-density jet from a conventional bottom dump, MDFATE also has a capping module that simulates the slow release of material from a barge/hopper so it may spread evenly on the bottom with a minimum amount of momentum imparted to the primary mound (i.e., particle settling).

MDFATE may be roughly categorized into three primary components: grid generation, model execution, and post-processing. The initial step in executing MDFATE and the foundation of the model is generation of the gridded version of site bathymetry. Subsequent to grid generation, MDFATE execution consists of running the STFATE and LTFATE sub-models, which provide information to update the grid with a revised bathymetry that reflects changes resulting from

placements and/or erosion. Post-processing consists of various plotting routines to present model results.

Grid generation

Disposal site grid generation is based on a user specified horizontal control (state plane or latitude-longitude) to create a horizontal grid. Presently, MDFATE can accommodate a grid with 40,000 nodes which will allow representation of a disposal site up to approximately 6,000 by 6,000 m when using a grid nodes spacing of 30 m. Grid corner points are specified by the user, and MDFATE creates the horizontal grid based on desired grid node intervals (typical grid node spacing range between 15 to 50 m).

Vertical control is based on a user-specified datum. MDFATE can automatically create a uniform flat or sloping bottom based on the datum of interest, or MDFATE can overlay actual bathymetric data in ASCII form and apply it to the horizontal grid by a multi-point polynomial interpolation. Similar to LTFATE, local wave and tide information can be used along with actual disposal site boundaries and bathymetry.

Model execution

Once grid generation is completed, MDFATE can simulate multiple disposal events (up to thousands) that can extend over a period of 1 year. The disposal operation is broken down into individual weeklong episodes during which long-term processes are simulated by the LTFATE sub-model. Within each week-long episode, the STFATE sub-model is executed for each load which simulates dredged material dumped into the water column to bottom accumulation. Cumulative results are generated for mound elevation, mound avalanching (the mound avalanches to a new, less steep side slope, when a critical angle is exceeded), and sediment transport by waves and currents.

The STFATE sub-model also generates a disposal mound footprint that identifies the extent of dredged material coverage for the disposal as well as mound volume and thickness. Water column currents can be accounted for as well as sloping or depression disposal areas. Differences in material composition can be considered, and layering of different materials in the hopper can be modeled. Based on material properties, currents and stripping of fines can be accounted for and an estimate of how the material accumulates on the sea floor is provided. More details on how stripping was modeled is provided later in the report.

Post-processing

For the weeklong simulations, the LTFATE sub model in MDFATE models the long-term processes affecting the created composite mound. The modeled processes include morphological changes resulting from cohesive and non-cohesive sediment erosion, non-cohesive sediment avalanching and cohesive sediment consolidation. For the sediment erosion processes, LTFATE sub-model requires hydrodynamic inputs. These data can often be most easily provided from tide and wave databases created during the DRP. The tide elevations and

currents database for the east, west, and Gulf Coasts were generated by an ADvanced two dimensional, finite element based hydrodynamic CIRCulation model (ADCIRC) (Hench et al. 1994). The tidal current time-series is generated from constituents contained in the ADCIRC database for the location of interest. Tidal currents can also be generated by other models, e.g., the CH3D Model (Chapman, Johnson, and Vemulakanda 1996). Wave statistics from the Wave Information Study (WIS) can be used (provided by the user for the site of interest) by the program HPDSIM to generate a wave time-series and ultimately wave induced currents for LTFATE. Other wave data can also be used. The net resulting tidal currents and wave orbital velocities are then used to drive the sediment transport portion of the model. The ADCIRC currents are also used by the STFATE sub-model within MDFATE to generate the water column currents that affect material settling for the short-term processes.

Additional details on the sediment transport algorithms used in the LTFATE sub-model in MDFATE can be found in *Cap Placement Modeling*, Appendix A of Palermo et al. (1999).

Output of results

STFATE sub-model estimates mound footprint coverage and thickness of bottom accumulation. MDFATE modifies the existing bathymetric grid according to the STFATE sub-model mound footprint and bottom thickness. Subsequent STFATE outputs are appended to the grid thus creating a composite mound.

Capping option

In addition to conventional bottom dumps where the vast majority of the material descends rapidly to the bottom, MDFATE can simulate capping using the spreading (particle settling) method, i.e., all the vertical kinetic energy of the material coming out of the dredge (or barge) is dissipated in the upper water column, allowing the sediments to experience passive transport, diffusion and settling of solids based on individual particle fall speed. The algorithms used for the spreading option are based on limited laboratory experiments conducted by Roberts et al. (1994). Two disposal methods can be simulated with the capping module. One method is the slow release of cap material through the slightly cracked (0.3-0.6 m) split hull of a split hull barge/hopper dredge. The second method simulates hydraulic pipeline discharge from a hopper dredge reversing its dredge pumps and pumping out through over the side pipes.

Platform

MDFATE is a FORTRAN program compiled to run on IBM-compatible personal computers (PCs).

MDFATE software application philosophy

To be effective as a planning tool, MDFATE was designed to run on PCs and not to require extensive amounts of input data. To accomplish this goal, two

dimensional (2D) depth averaged currents are used as opposed to 3D currents, which until very recently required a super computer and extensive data sets. MDFATE can also be used as a design tool. However, the user needs to be aware of the model limitations. At present, MDFATE is the only tool available to predict mound geometry from a series of disposals. As such, it has been used on a number of projects as described in the following section.

Prior MDFATE applications

MDFATE has been used to simulate placement of dredged material for a number of other projects, several of which involved contaminated sediments. MDFATE was used to model open ocean placement of clean maintenance sediments off North Carolina (Moritz and Randall 1995). In 1993, an early version of the capping option within MDFATE was used to design placement of a cap for a contaminated sediment mound consisting of material from New York Harbor and placed in the Mud Dump site off northern New Jersey (Randall, Clausner, and Johnson 1994). MDFATE was used to model placement of contaminated sediments removed from New York Harbor and placed in the Mud Dump site during the summer of 1997 (Clausner et al. 1998, Lillycrop and Clausner 1998). On the west coast, MDFATE was used to model placement of an *in situ* cap for the Palos Verdes Shelf (Clausner 1997).

MDFATE has also been used to model placement of dredged material in a borrow pit placement. Moreno and Risko (1995) used MDFATE to simulate placement of contaminated silt in a borrow pit in the mouth of the LA River. Clausner et al. (1999) used MDFATE to simulate placement of contaminated material and a cap in a borrow pit located in the harbor at Long Beach, CA. Also, Johnson et al. (1998) conducted an investigation of the ability of a historical disposal site located in natural depression in Chesapeake Bay to contain additional dredged material.

As the above discussions show, MDFATE has been used for a number of projects. For those projects where the model results were compared to actual projects, the agreement was reasonably good, and actual mound elevations were generally within 20 to 30 percent of those model predictions with overall mound geometries also showing good agreement. Considering that MDFATE uses only 2D depth averaged currents, and the amount of uncertainty in both placement locations (for some projects) and sediment characteristics, the agreement between actual and predicted mound geometries provided by MDFATE is good. In some cases, however, a fair amount of adjusting sediment properties is required to achieve good agreement.

MDFATE limitations

MDFATE has essentially all of the limitations of STFATE in regard to the water column hydrodynamics, sediment geotechnical relationships, and how the sediment is released from the hopper. With one exception, MDFATE's ability to simulate currents is more restricted. In addition, MDFATE has had limited verification and testing of how various geotechnical parameters influence results. These geotechnical-related limitations include: limited verification of avalanching angles, mound elevations, and apron limits, and consolidation

algorithms are crude and not fully tested. The following paragraphs discuss these limitations in greater detail.

Tidal current. MDFATE can simulate a depth-averaged current residual current in the identical manner it is simulated in STFATE. However, unlike STFATE, in MDFATE the residual current speed and direction can be changed once during the simulation. This is normally done to simulate a seasonal change in the residual current. MDFATE can also include a tidal current as noted in the model description section. When MDFATE simulates multiple placements, the program computes the number of placements per day, then computes the time in hours between placements. A different set of tidal constituents is used, based on the number of hours between the placements, which allows the tidal current magnitude and direction to vary between successive placements. A limitation in tide and current variation occurs when a series of individual placements are being simulated in separate simulations. In this case, the program always selects the same initial tidal current, so the tidal current will be the same for each simulation. Note that MDFATE is designed to simulate many individual placements, thus this limitation is a factor only in specialized situations like this.

Avalanching angle. The limited verification of avalanching angle did not likely have a major impact. Typically the avalanching angle only becomes an issue for mounds of significant height, say 1 m or more. Because the cap constructed at the PV shelf had a maximum elevation of perhaps 45 cm, the avalanching algorithms likely were not activated. For example, a change in elevation of 15 cm over a distance of 50 m (1/6 the width of the cell), equates to an angle of less than 0.2 deg. Typically, avalanching does not occur for angles less than 0.5 to 1 deg.

The limited verification of the consolidation algorithms in MDFATE did not likely have any influence on the accuracy of the PVPC monitoring. The Queens' Gate sediments in the hopper only had an average of about 5 to 10 percent clay, with the sediments on the bottom having even less. With over 80 percent sand, no consolidation was expected. Also, the clay was specified as non-cohesive, thus eliminating the consolidation routine from activating.

Essentially all of the MDFATE applications to date have been to simulate a mound of substantial elevation, say 1 m or more. As noted in the discussion of prior applications, simulated mound elevations within 20 to 30 percent of the actual after some fine-tuning of sediment properties. Much of this fine-tuning was required because solid/volume relationships of the dredged materials in the dredge and the as-placed void ratios were unknown. This was the first application of MDFATE where the desired mound thickness was less than 0.5 m. The initial mound target thickness was 0.15 m, and, for the single placements, a mound only a few centimeters thick was predicted. Considering the potential for the resuspended native sediments to be included in the single placements, the probability that MDFATE can accurately model these individual placements becomes less likely. We expected that MDFATE would be most successful for simulating mounds with 20 or more placements, where random variations in location, sediment properties, etc, would tend to average out because of the spreading from the multiple dumps.

Limitations in MDFATE's ability to model a near bottom current that potentially had a different magnitude and direction than the majority of the water

column likely limits the ability to model spread of the apron, the thinner outer section of the mound (typically 50 to 100 m from the point of impact). For conventional mounds, those with elevations in excess of 1 m, the apron is generally considered to be 15 cm or less. This thickness is based on the fact that mound thickness of 15 to 20 cm cannot be resolved with conventional fathometers. Also, the apron is generally composed of sediments that have been carried out significant distances from the placement point by the bottom surge. As described in the STFATE description section, MDFATE does not rigorously model the effect of bottom slope on bottom surge. This may cause some inaccuracy in the prediction of the apron.

D-CORMIX

Several mathematical models are available for estimating the growth and movement of discharge plumes caused by subaqueous emissions. The Cornell Mixing Zone Expert System (CORMIX) was specifically developed to provide a predictive tool for conventional or toxic pollutant discharges into waterways. The CORMIX modeling system was originally developed to address bottom discharges with low suspended solids concentrations or buoyant bottom discharges. Such discharges are typically associated with municipal wastewater, industrial waste outfalls, cooling water, freshwater releases in saline environments. Dredged disposal operations, on the other hand, typically involve surface or near-surface discharges, frequently with high suspended solids concentrations. Consequently, the original CORMIX package was not directly applicable to dredged material disposal operations (Chase 1994).

The Dredging Operations Mixing Zone (DROPMIX) program, now known as CDFATE, was developed to adequately address the need for modeling surface or near-surface dredge discharges (Havis 1994). The DROPMIX program takes data describing typical dredge discharge activities, and utilizes the CORMIX modeling system (with slightly-modified output routines) to predict water column concentrations and dispersion of the plume into the water column resulting from pipeline discharges and other discharges of a continuous nature into waterways. The DROPMIX routines transform the dredge discharge information (negatively or neutrally buoyant surface discharge) into an equivalent, mirror image, positively or neutrally buoyant, bottom discharge scenario with sedimentation. CORMIX analyzes the bottom discharge case to generate information on the mixing zone and turbidity/dissolved contaminant plume. This information includes the location and concentrations of effluent within the receiving waters.

The majority of effort required to transform a surface discharge case into an equivalent mirror image bottom discharge scenario is affiliated with the effluent and receiving water densities. For the CORMIX routines, receiving water density profiles are referenced to the receiving water bottom. However, for dredged material disposal, density differences are referenced to the water surface. Also, CORMIX references step density changes to the bottom. Once again a transformation must be made to reference any step changes to the surface.

In an effort to better model the dense fluid mud layer resulting from surface discharges of dredged material slurries from pipelines, Doneker, Jirka, and Nash (1995) developed CD-CORMIX, now known as D-CORMIX. D-CORMIX

models the transport of the fluid mud, entrainment of water into the fluid mud layer (growth and dilution), and sedimentation of particles from the fluid mud layer.

The D-CORMIX program was used in a limited manner during the pilot study, to estimate the impact velocity of the cap material jet with the bottom during direct pump-out through the dredge dragheads at various depths. This program predicts the time for the jet to descend through the water column and the size of the plume as a function of distance from the source. This is the only model for estimating the growth and movement of discharge plumes that provides sufficient output to compute the velocity of a jet as it impacts the bottom. Doneker, Jirka, and Nash (1995) discusses the D-CORMIX program, its capabilities, and outputs in greater detail. The impact velocities computed from the D-CORMIX simulations were used to determine if direct pump-out should be used during capping operation.

D-CORMIX limitations and assumptions

In order for CD-CORMIX to accurately simulate subaqueous discharges, the effluent must represent a continuous steady-state discharge. In addition, steady-state flow within the receiving water must exist. Of course, the condition of continuous flow is relative to the time over which mixing occurs.

With regard to the assumption of steady-state flow, flow through a pipeline or over a weir will not be “truly steady” due to minor variances in the flow rate. However, the time over which these variances occur is generally small compared to the time over which mixing occurs. Thus, the assumption of steady-state flow is assumed to hold. Not only is the flow presumed to be steady, but also the receiving water velocity is assumed to be uniform, that is, the velocity exhibits the same magnitude everywhere over its entire cross-section.

Changes in receiving water velocities associated with tidal effects may be ignored since these occur over much longer periods of time than mixing occurs (hours versus minutes). Alternatively, if long-term mixing results are desired, then it is possible to conduct a quasi-steady analysis. Typically in these cases the results from prior steady-state analyses are used as boundary or initial conditions for subsequent analyses.

Mixing within the receiving water is assumed to be due solely to hydrodynamic processes. In other words, dilution of the effluent concentrations is assumed to be the result of the interactions between effluent and receiving water velocities, densities, and geometries. The original CORMIX modules assume that the pollutant may be a conservative species or that it may undergo first-order physical, chemical, or biological reactions or decay processes. However, modifications to the program have incorporated in the DROP MIX whereby the mass of solids in suspension may decrease by a first-order process to model the effects of sedimentation (Havis 1994). Field studies suggest that results of CORMIX simulations accurately predict the mixing and the subsequent migration of contaminant plumes (Doneker and Jirka 1990).

Modeled Applications and Results

This section describes specific applications of the dredged material fate models, MDFATE, STFATE, and CORMIX, conducted as part of the pilot project, and the results of those applications. The vast majority of the MDFATE modeling simulations were made to predict the cap thickness and extent at cells LU, SU, and LD as a function of sediment characteristics (primarily grain size distribution), hopper dredge operating characteristics (speed, heading, duration of disposal), the volume and bulk density of material in the hopper, and ambient currents. A number of MDFATE scenarios were conducted at various times prior to, during, and following actual placement. Analysis of the model results included maximum mound thickness. During the prior to placement simulations, the primary items simulated were expected cap footprint and thickness from a single placement. This information was used to design the monitoring program. Later, MDFATE simulations of full cap placements were conducted to assist in determining the volume of cap material required.

The next suite of MDFATE simulations were conducted to estimate offset, the distance and direction between where the cap material is released and it comes to rest of the seafloor. The offset predictions were needed to insure cap material did not land directly on the bottom-mounted instruments. Immediately prior to and during the initial placements, MDFATE simulations were conducted to fine tune monitoring activities, confirm prior estimates of spacing between placements, and to confirm that the MDFATE predictions were reasonably close to the actual mound characteristics as determined by monitoring. This information provided confidence that the full cap placed would meet design expectations. The final sets of MDFATE simulations were conducted using actual data collected from monitoring to determine how well the MDFATE model could predict actual cap characteristics.

The final MDFATE predictions along with the final monitoring data on cap thickness and extent were used to make a prediction of the volume required to produce a given cap thickness for future capping operations.

STFATE applications prior to the actual placements included simulating water column concentrations of total suspended solids (TSS) of the plume moving towards the nearshore kelp beds, and predicting bottom impact velocities to assist in design of the bottom surge current monitoring effort. Following cap placements, STFATE simulations were conducted to compare the measured bottom surge current with measured currents, and to provide a qualitative comparison of far field plume TSS measurements.

As noted earlier, the CORMIX model was used to compare bottom impact velocities associated with direct pump out with the impact velocities from conventional surface release.

The remainder of this section describes the various scenarios modeled in detail. The following section presents the input data for each model and each scenario in detail. Results from the modeling simulations follow the section on input data, with recommendations for future modeling activities provided in the final section.

MDFATE

The majority of the MDFATE modeling simulations were made to predict the cap thickness and extent at cells LU, SU, and LD as a function of sediment characteristics (primarily grain size distribution), hopper dredge operating characteristics (speed, heading, duration of disposal), the volume and bulk density of material in the hopper, and ambient currents. A number of MDFATE scenarios were conducted at various times prior to, immediately prior to, during, and following actual placement.

Two types of placements were simulated: conventional and spreading. The vast majority of the simulations used conventional placement, where the hopper is opened fully to allow the dredged material to exit as rapidly as possible. A limited number of spreading placements, where the hull is cracked to allow turbulence to dissipate vertical kinetic energy (thus allowing the particles to settle at their individual settling velocity to minimize resuspension), were also simulated.

This section describes each MDFATE modeling scenario and its objective, the input data for each set of simulations, and the modeling results.

Pre-placement model scenarios

In the pre-placement model simulations, MDFATE was primarily used to model new bottom bathymetry resulting from the addition of the cap material. Because the relative change was so small in every case, the original bathymetry was subtracted from the new bathymetry to provide a bathymetry difference map. From the bathymetry difference map, the following items were often noted: the maximum mound elevation, the dimensions of the various cap thickness contours, and whether or not the contours were skewed in a given direction. While MDFATE can compute cap thickness of much less than 1 mm, the bathymetry change maps typically showed the 1 mm contour as the extent of the cap. However, for direct comparison with SPI measurements of cap thickness, the 1 cm contour was used because 1 cm was the thinnest cap that could be reliably measured using SPI. When the bathymetry difference maps are created, MDFATE also computes the change in volume, i.e., the volume of material contained in the cap. This volume was often compared to a theoretical maximum potential volume (often referred to as the potential volume), which is the volume that should be found on the seafloor if all the dredged material released from the dredge made it to the bottom within the simulated MDFATE grid. The ratio of the “actual volume” as calculated from the volume difference map to the theoretical maximum was sometimes calculated to indicate whether or not a significant percentage of the dredged material was carried beyond the boundaries of the grid by the currents.

MDFATE simulations were run for 5 different scenarios described below. Table K-1 summarizes the key input values varied for each set of simulations.

Scenario 1. This scenario consisted of MDFATE simulations for the initial sensitivity investigation conducted in March and April 2000. The purpose of these simulations was to observe the response of the maximum thickness, volume at seabed to the actual versus potential volume at seabed to the variable input

parameters, vessel speed, placement depth, and sediment characteristics. This information provided the data needed for planning level decisions on placement locations, scenarios, and monitoring program design.

Scenario 2. Scenario 2 consisted of MDFATE simulations conducted in May 2000 to determine the amount of offset for a range of currents to assist in adjusting the placement location for instrumented tripods that were deployed on the site bottom to measure the velocity and extent of the bottom surge. Offset is defined as the horizontal distance between where the dredge releases the material and where the material impacts the bottom. High currents were observed in USGS data (Noble 1994), which had the potential to occur during conventional dredged material placement. During the pilot study, the ARESS tripods (that measured currents, turbidity, and temperature) were deployed on the bottom some distance away from the expected deposit site prior to the load placement. It was critical for the pilot study to have an accurate estimation of where individual loads of dredged material would deposit. For the instrumentation to be effective, the load had to land in the desired location. The offset predictions were needed to ensure that cap material did not land directly on the bottom-mounted instruments. In addition, instrumentation could have been damaged if the descending jet from the dredged material landed directly on an instrument.

The primary input considerations of Scenario 2 simulations were the offset sensitivity due to different sediment characteristics, depths, vessel speeds, and current speeds and directions. The sensitivity of maximum mound thickness and volume at the seabed and actual versus potential volume at the seabed due to the variable input parameters was secondary considerations.

The initial round of Scenario 2 MDFATE simulations were run with low residual currents of 10 cm/sec, which are typical of the long-term average bottom currents. However, simulations in higher currents were thought to be needed to estimate the offset from currents that are more typical (i.e., greater) for the site. Depending on the amount of offset, it might have been necessary for the dredge to modify its release position so the material would land in the desired location relative to the pre-deployed instruments, or within the defined cell boundaries.

Scenario 3. This scenario consisted of MDFATE simulations with refined input parameters based on operational planning in June 2000. The primary goal of this scenario was to compute the volume of cap material required for various cap thicknesses and dimensions. Capping operation planning indicated that the dredge would make conventional placements while nearly stationary.

Scenario 4. Scenario 4 consisted of MDFATE simulations conducted immediately (1 to 3 days) prior to the initial actual placements, which occurred in early August 2000, to predict the expected mound geometry from the initial LU and SU placements. These simulations were based on the best input available at the time. Scenario 4 simulations provided the most up-to-date MDFATE prediction of the expected bottom footprint from a single load of Queen's Gate sediments (the finer than average classification) placed at cell LU (G3) on 2 August and SU (G1) placed on 8 August. These simulations assisted in deploying monitoring instruments and interpreting the data. In addition, the Scenario 4 simulations helped to demonstrate the ability of the model to accurately predict the mound configuration.

Scenario 5. This scenario consisted of capping sensitivity tested with eight MDFATE spreading mode simulations. The objective of this analysis was to determine the sensitivity of lateral plume movement to variable input parameters for comparison to the estimated fall velocity of sediment in order to estimate the lateral extent. Parameters varied included input grain size, current speed and direction, and placement location/depth. Borrow material sizes from A-II and A-III were used in these simulations.

MDFATE input data

When performing a series of MDFATE simulations, most of the input data remained constant between simulations. These constant data typically included bathymetry, model grid spacing, water density, and wave and current data. Also, the vessel characteristics did not change an appreciative amount. Input data that did vary generally included dredge velocities, currents, and sediment characteristics.

A range of scenarios was conducted prior to capping (pre-placement) to examine potential ranges of possible impacts because exact sediment properties, vessel loads, placement areas, vessel direction, heading, and speed, and current were unknown. As certain unknowns became more defined, the simulated scenarios became more focused. The remainder of this section describes the MDFATE simulation input.

Bathymetry/grid

CESPL provided ERDC with electronic bathymetric data from a 1999 multi-beam survey of the PV shelf. Data were provided in the California state plane system with horizontal distances in meters. The horizontal datum was NAD 83, and depths were meters below mean lower low water (mllw). MDFATE does not accept horizontal dimensions or depths in meters. Therefore the bathymetric data were converted to feet using TERRAMODEL software (Spectra Precision Software, Inc. 1997). After TERRAMODEL processing, the Palos Verdes Shelf bathymetry was imported into MDFATE with a grid spacing of 30 m (Figure K-3). One grid was used for all the calendar year 2000 simulations. The grid dimensions were 94 (north/south direction) x 104 (east/west direction).

MDFATE hindcast simulations conducted in FY2001 used the MDFATE model utilized in DAN-LA (Palermo et al. 2000; Pilot Cap Operation Plan). This model version allowed direct display of cap thickness in centimeters and facilitated comparison of MDFATE predictions of cap thickness with measured cap thickness from cores and SPI. Figure K-4 shows the baseline depth grid for the hindcast simulations. For the hindcast simulations the grid spacing was reduced to 15 m for more accurate comparisons with the SPI data. The reduced grid spacing resulted in a much greater number of grid points, which slowed computations. To overcome this limitation, for the hindcast simulations, smaller portions of the baseline grid were created centered around the cell of interest. Figure K-5 shows the MDFATE bathymetry input grid for simulations in cell LD.

Environmental conditions

Water density. A two-point water density profile was used for all MDFATE simulations. The water density at the surface was specified as 1.0245 g/cc and 1.025 g/cc at a depth of 715 m and was based on engineering judgment.

Waves. Water depths at the PVPC site range from 30 to 70 m. At these depths, average wave conditions are expected to have little effect on the material placed and were therefore neglected for the predictive and operational simulations. For the 2001 hindcast simulations, WIS wave data typical for the site were simulated.

Currents. Current values input into model simulations prior to the capping operation were based on summarized results of a PV shelf current study conducted as part of NOAA investigations of the PV site (Noble 1994). Current data were collected from May to September 1992. Representative current speed and direction values were derived from hour averaged time series of alongshelf and cross-shelf currents for Sites A and B at the surface, mid-depth, and near bottom. Site B currents were considered more representative of depths where sediment would be placed during the pilot project (Figure K-6). Tidal currents, winds, and waves do not play a large role in the residual (net current) currents at the PV shelf site. Subtidal currents with fluctuation periods of 10 to 15 days are the most dominant. The largest mean currents flow northwest and southeast along the depth contours. Mean hourly averaged currents, along the shelf at the mid-depth, and near bottom water column locations, were calculated over approximately 1 and 2 month periods, and range from 1 to 7.4 cm/sec. The maximum alongshelf mid-depth and near bottom current is approximately 40 cm/sec. During simulations, more likely maximum alongshelf shelf currents of 28 cm/sec to the northwest and 20 cm/sec to the southeast were used. The mean cross-shelf currents, at the mid-depth and near bottom water column locations, are slower and range from 0 to 6 cm/sec while the maximum cross-shelf mid-depth and near bottom current is approximately 20 cm/sec.

However, in most cases, simulations using the residual currents as determined from the Noble 1994 study showed that using a residual current resulted in unrealistically large predictions of mound offsets. These large predictions were due to the MDFATE program feature that always simulates the imposition of the residual currents for at least 1 week combined with the older, less sophisticated version of LTFATE sediment transport algorithms used in MDFATE. Apparently the critical velocity values for resuspension/deposition and the calculations that control resuspension/deposition and transport of the cap sediments predicted an excessive amount of transport during the 1-week-long simulations. Therefore, for some of the hindcast simulations, tidal currents, which change in magnitude and direction every 3 hr were used instead of residual currents. In some cases, no currents at all resulted in a simulation that best matched cap thickness and extent results determined by SPI monitoring.

Sediment characteristics

Three sets of sediment-related data were required to simulate placements with MDFATE. Those data were the grain size distribution (GSD) of the sediments, the volume fractions in the hopper for each type of sediment (gravel,

sand, silt, clay and clumps), and the void ratio of the sediments as deposited on the bottom. This section addresses how those data were determined for both the Queens Gate and Borrow Area A-III sediments.

Queen's Gate sediments

Grain size distribution – predictive and operational simulations. A range of sediment characteristics was used in MDFATE to simulate placement of Queen's Gate sediments during the predictive and operational phases of the pilot study. This sediment range was needed because there was sufficient variability in the Queen's Gate sediments such that a single sediment grain size distribution was not likely to adequately describe the expected potential range of cap geometries (footprint and thickness).

Sediment characteristics for the pilot study MDFATE simulations were developed following review of the grain size data distributed during a 20 January 2000 meeting at the Los Angeles District. A spreadsheet of grain size distributions, from samples collected by the contractor from the hopper bin during dredging of Queen's Gate channel between 29 November 1998 and January 2000, was the primary source of information. From these samples, SPL computed the following grain size distribution statistics: the finest, average, coarsest, and plus and minus one standard deviation from the average. The computed values were based on samples collected from the hopper, i.e., with an estimated loss of about 50 percent of the fines due to overflow when the mean hopper samples GSD was compared to the mean *in situ* GSD.

The initial MDFATE simulations used these data based on the assumption that the remaining material yet to be dredged was similar to that which had already been dredged. The statistical mean GSD as determined from the hopper samples was assumed to be the mean GSD for the sediments used in the pilot study MDFATE simulations. The mean -1 standard deviation was assumed to be typical of the sediments that are finer than the mean, and the mean +1 standard deviation was assumed to be typical of sediments that are coarser than the mean. The coarse and fine sediment values simulated were not the absolute extreme, but were thought to be typical of the coarser and finer sediments. These GSD values are plotted in Figure K-7. Table K2 shows the Queen's gate sediments characteristics for the MDFATE simulations that were developed from Figure K-7.

The GSD data from the dredge samples and the borings did not indicate specific percentages of silt and clay, only the percentage of material passing the number 200 sieve. The percentages of silt and clay were computed based on the assumption that the relative percentages of silt and clay as found in the overall project (reference boring report) would exist in the load placed as part of the pilot cap. The computed percentages were 80 percent silt and 20 percent clay, or a 4:1 ratio of silt to clay.

Grain size distribution – hindcast simulations. Data from the hopper samples collected during the pilot study were used for all the hindcast simulations and a few of the operational simulations. A description of the sampling methods is found in Chapter 3, Section 3.4.3, with additional details in SAIC 2002. For LU1, GSD results from the hopper sample for that placement were used, results are reported in Table K-3. For LU5, LU25, LU45, and LU71,

the average GSD for all 21 samples were used. See Appendix J, Table 3.11.5 for details. Similarly, the average GSD for all 7 SU hopper samples was used for the all the SU simulations. Table K-3 provides a summary of the values used.

Volume fraction calculation

Based on initial information from NATCO, the average hopper load for Queen's Gate (QG) sediments placed during the pilot study was expected to be 1,200 cu m at an average bin density of 1.4 g/cm³.

The density of water from the dredging site was assumed to 1.025 g/cu cm and the *in situ* particle density was assumed to be 2.70 g/cm³. Then the volume of voids (i.e., water) and solids in the hopper was computed by the following formula, where x is the volume fraction occupied by water and (1-x) is the volume fraction occupied by solid particles.

$$1.025x + 2.70(1-x) = 1.4$$

$$1.025x + 2.7 - 2.7x = 1.4$$

$$1.3 = 1.675x$$

$$x = 0.78 \text{ (volume occupied by water)}$$

$$1-x = 0.22 \text{ (volume occupied by sediment particles)}$$

Therefore the volume fraction, $V(f)$, of the sediments in the hopper was

$$V(f) = V(s)/V(t) = 0.22/1.0 = 0.22$$

where

$$V(s) = \text{Volume of the solids}$$

$$V(t) = \text{Total Volume}$$

NATCO staff also noted that the *in situ* density for Queen's Gate sediments, as determined from correlations with hopper volumes and surveyed volumes from the channel, was 1.936. If the *in situ* average particle density was assumed to be 2.70, then using the same logic as above, the volumes occupied by the solids and voids (i.e., water) were 0.456 for the water and 0.544 for the solid sediments. The average *in situ* void ratio of the Queens Gate sediment was then calculated as 0.84.

MDFATE uses the volume fraction to define the percentage, by volume, of each sediment component in the hopper. The volume fraction is calculated by multiplying the percentage of each sediment component, sand, silt, and clay, by the ratio of the volume of solids to the total volume, $V/V_T = 0.22$, calculated previously. Table K-4 provides the calculated volume fractions for each sediment component for the predictive simulations.

As-deposited void ratio

The as-deposited void ratio following placement was also needed when making MDFATE simulations. For the prior study (Palermo et al. 1999), an as-deposited void ratio of 1.39 was used. This value was based on limited tests conducted by Dr. Paul Schroeder (USAERDC/WES) for the consolidation tests as part of the Palermo et al. (1999) report. To provide some additional insight on the as-deposited void ratio for the pilot study, an estimate of the as-deposited void ratio for the Queen's Gate material removed by hopper dredge and deposited in the Western Anchorage during 1998 and 1999 was requested from SPL and the contractor. Unfortunately, the quality of these data were poor and could not be used for this calculation. Therefore, for this study, the as-deposited void ratio of 1.39 was input for the "average" sediments for the predictive and operational simulations. This value was adjusted to take into account the different percentages of sand and fines in the coarser and finer than average sediments also being simulated. The adjusted as-deposited void ratio for each sediment type was computed by multiplying the percent for each component, e.g., 80 percent sand for the coarse sediment times an assumed as-deposited void ratio for that sediment component (an as-deposited void ratio of 0.75 was assumed for sand). The as-deposited void ratio is a source of considerable uncertainty, particularly the assumed as-deposited void ratios for silt and clay.

Coarse sediment

$$e_t = 0.80 (.75) + 0.16(2.0) + 0.04(4.5) = 1.1$$

Average sediment

$$e_t = 0.63 (.75) + 0.30(2.0) + 0.07(4.5) = 1.39$$

Fine sediment

$$e_t = 0.56 (.75) + 0.35(2.0) + 0.09(4.5) = 1.53$$

Once actual data from post placement cores became available, the as deposited void ratio for sediments placed in cell LU was computed to be 1.04, based on core data that gave an average bulk density in the cap material as 1.79 g/cm³ with particle specific gravities of 2.72. As described in Chapter 3, and in considerable detail in the SAIC (2001) monitoring report, the geotechnical data from the SU cores was unreliable due to coring artifacts. A range of as deposited void ratios were used for the MDFATE hindcast simulations, based on as deposited sediment bulk densities ranging from 1.60 to 1.79, that resulted in as deposited void ratios of 1.04 (LU and SU) to 1.10 (LU) to 1.27 (SU). Table K-3 summarizes void ratio and related sediment data for the individual sediment components for the hindcast simulations, details are in the following paragraphs.

Sediment properties required to compute as-deposited void ratios for MDFATE hindcast simulations in LU, SU, and LD were based on the GSD from the hopper samples and core data. It was decided to use the post LU45 cores as a basis for all the LU as deposited sediment properties because these cores had the greatest amounts of cap. Reviewing the core bulk density and water content results, the range of bulk densities was from 1.61 to 1.99 g/cm³ (Appendix J (SAIC 2002), Section 3.11.4 and Appendix J, Appendix C (SAIC 2002)). In general, the lower bulk densities were for depths of 15 to 18 cm, were some

mixing with the native EA sediments was likely. It was decided to model the as deposited void ratio as the average bulk density of 1.78 g/cm^3 . This value was also checked based on an average water content of 36.27 percent and an average particle SG of 2.68. Based on these values, an as-deposited void ratio of 1.04 was computed and used for the MDFATE simulations. To achieve the composite void ratio of 1.04, the as deposited void ratios for the individual sediment fractions (sand, silt, clay) were adjusted as shown in Table K-3.

Similar to LU, it was decided to use cores from the post SU21 coring effort as a basis for the SU as deposited sediment properties. Problems with coring artifacts have been documented in Chapter 3 and Appendix J (SAIC 2001). The bulk density of cores SUC46 and SUC47 were judged most likely to have cap material. The bulk density value at 2 cm was 1.95 and 1.73, respectively, with values lower in the cores ranging from 1.43 to 1.5 at 6 and 8 cm, respectively. A bulk density value of 1.70 g/cm^3 was selected based on engineering judgment. This value is about 5 percent less than the value used for the LU simulations and was thought to reflect additional entrained water as a result of the greater depth. Based on this value an as-deposited void ratio of 1.27 was computed. The as-deposited void ratios of the individual sediment fractions were adjusted to achieve a composite void ratio of 1.27 as shown in Table K-3.

Borrow area sediment: A-II & A-III

Grain size distribution. As noted earlier, SPL conducted a geotechnical investigation of two potential borrow sources offshore and adjacent to the Queen's Gate Channel. These two borrow sites were designated A-II and A-III. Vibracorer samples from Borrow areas A-II and A-III provided the percentages of sediment components used in the MDFATE simulations. Sediments from borrow areas A-II and A-III were classified as a poorly graded, fine to medium-grained sands with less than 5 percent fines. Table K-5 provides the percent sediment components for the A-II and A-III Borrow areas.

The data reported in Table K-5 for the average top 1 m for A-III and the average top 0.75 m for A-II. This was the assumed thickness to be removed during hopper dredging of the area, to acquire capping material. The D_{50} of A-III was 0.33 mm, and the D_{50} from A-II was 0.40 mm. When using the spreading mode, MDFATE allows only a single grain size to be simulated during a single run. Based on the sediment data from A-II and A-III, the initial predictive spreading simulations were made with 0.33 and 0.40 mm sediments.

Data from hopper samples collected during the pilot study were used to determine the GSD for the hindcast simulations. The data from the seven hopper samples collected from loads taken to cell LD were considerably finer than the 0.33 mm D_{50} from samples of the A-III borrow area. We are unsure whether the material from the hopper samples is finer than that found during the pre-dredge coring inadequate correlation of the core log data with the specific locations used for dredging, or because the finer sediments settled out last and thus the surface layer of the material in the hopper is finer than the vast majority of the material in the hopper. Using the average of the hopper sample data from the LD loads, the D_{50} is about 0.22 mm. The initial set of MDFATE simulations in cell LD used a D_{50} of 0.25 mm, slightly coarser than the D_{50} from the hopper samples. The simulation of all nine placements in cell LD used the D_{50} of 0.22 mm.

Volume fraction calculation. Predictive spreading simulations with A-II and A-III material were conducted assuming the hopper load to be half solids and half water. The volume fraction is then 0.5 for A-II and A-III sediments, corresponding to a bin density of 1.86 g/cm³. Table K-3 lists the volume fractions used for the spreading simulations during the hindcast simulations.

As-deposited void ratio. The as-deposited void ratio for the predictive simulations with A-II and A-III material was assumed to be 0.70, which is about the same value used for Queen's Gate sand components.

After hindcast GSD data became available showing the finer grain size, the as deposited void ratio was increased to 0.75. A later review of the supplemental core data completed after the MDFATE simulations had been completed showed a likely bulk density of about 1.85 g/cm³, which equates to an as deposited void ratio of 1.0. Barring other factors, this increase in void ratio would result in an increased thickness of four percent. A new set of simulations using the increased void ratio should be considered for future design work.

Hopper dredge characteristics/volumes/loads

Queen's Gate sediments. NATCO's *Sugar Island* hopper dredge was used to place the cap during the pilot study. The *Sugar Island* has a total hopper capacity of 2,735 cu m; the dredge length is 85 m, and the beam is 16 m. From information supplied by NATCO, the loaded and empty drafts were initially assumed to be 5.5 m and 3.0 m, respectively.

The volume or load of material expected was the subject of some confusion initially. ERDC personnel interpreted initial information supplied by NATOC on expected loads for the *Sugar Island* to be 1,200 cu m at an average bin density of 1.4 g/cm³. Most of the initial simulations made between January to late May 2000 used this volume, bin density and the associated volume fractions.

Following a meeting in Los Angeles in late May 2000 and subsequent phone conversations with NATCO, it was learned that our initial impression of how NATOC defined a hopper load was in error. When NATCO reported the "load" for the Queens Gate dredging, it reports cubic meters. However, this value is not the number of cubic meters in the hopper bin. The full hopper volume of 2,735 cu m includes a volume of settled sediments and the more-fluid slurry above it. Because the contractor is being paid on material removed from the channel, it makes sense to report the load of dredged material removed as the equivalent number of cubic yards that have been removed from the channel. This makes it easier for the Corps to determine progress and make estimated payments. Thus, while the hopper is typically filled with a mixture of the solid sediment particles and water, this is the equivalent of a much smaller volume of material in the channel at the *in situ* density, which is much higher than the density of the combined sediments, and water in the hopper. A later section on cap volume computation describes in detail how bin volumes, loads, and *in situ* channel volumes are related and computed.

Based on this new information, all subsequent MDFATE predictive simulations made from June up through the initial operational simulations were made with the following values of hopper volumes and volume fractions.

The expected average Queens Gate hopper load was 925 cu m, at an average bin density of 1.4 g/cm³, and was based on loads from Queens Gate in April and May 2000. Because the average bin density did not change, the volume fraction in the hopper remained the same as described above (0.22). Thus the volume fractions for each component as noted in Table K-4 remained the same. However, the total volume placed did change, and the volume placed was the full hopper volume or 2,735 cu m.

The new data for April and May 2000 from NATCO indicated that the *in situ* density of the material in the channel was 1.84. It was decided to average the two values of *in situ* channel density, 1.936 and 1.84. The resulting value was rounded up to 1.90. Using this information, the average *in situ* void ratio of the Queens Gate sediments was recalculated as 0.92.

Borrow Area A-III sediments. The *Sugar Island* hopper dredge was also used to place the A-III material and all MDFATE simulations of A-III material used the *Sugar Island* hopper characteristics. For the simulations, the loaded and empty drafts were initially assumed to be 5.5 and 3.0 m, respectively. The volume for each hopper load was assumed to be 1,988 cu m with a bin density of 1.86 g/cm³.

Results of MDFATE Simulations

Like the description of model input, the results section is split along the three modeling phases, predictive, operational, and hindcast. As might be expected, a greater emphasis is placed on the hindcast simulations where actual data from the placements were available.

Prior to the discussions of the results a short description of terms placement, load, and volume is in order. In common USACE terminology, a load is the full mass (or weight) of dredged material inside the hopper bin when the dredge has finished loading. In addition to the weight of dredged material (as determined by the change in dredge displacement), the load of dredged material also occupies a certain volume inside the hopper dredge. Because the weight of the dredged material, or load, is more easily determined than the volume, the dredging contractor routinely calculates the load in tons. However, the dredging contractor is paid based on the volume of dredged material removed from the channel. Thus the dredging contractor often determines the relationship between the volume and weight of the channel material, i.e., the bulk density of the channel sediments. By knowing the bulk density of the material in the channel, the bulk density of the material in the hopper, and the relationship between the two, the contractor often converts the hopper load in tons to an equivalent in channel volume.

When the contract is finished loading the dredge, he takes the load to the placement site where the load is placed. The terms placement and load are interchangeable, for this report the term placement is used.

Predictive simulations

This section describes the conventional placement simulations conducted using MDFATE prior to the placement operation for cells LU and SU. The

primary goal of this portion of the study was to establish the sensitivity of the resulting mound thickness, lateral extent, volume on seabed, actual versus potential volume, and offset distance to variations in vessel speed, current speed and direction, and sediment characteristics. A large number of simulations were conducted due to the range of values simulated. The reader will note when looking at the tables in this section that not all of the results from every simulation were computed. In many cases, only a limited number of values were computed to identify trends or make decisions on what to variables to examine in subsequent simulations.

Scenario 1. The results, summarized in Table K-6, show the variation in mound characteristics due to different vessel speeds, placement depth (i.e., the difference between placing material in 42 m at LU and 62 m in SU), and grain size. A fairly wide range of characteristics was modeled to determine their influence on cap geometry. All placements were modeled with a dredge heading of 315 deg, which is northwest and roughly parallel to the depth contours. The results in Table K-6 show that increasing vessel speed has a modest impact on the maximum thickness, volume at the seabed, and actual volume versus potential volume, particularly for SU. The largest value of the maximum mound thickness in LU was 3.3 cm at a vessel speed of 0.5 knots for simulation G3A02 while the maximum thickness was 2.2 cm at a vessel speed of 2.0 knots for simulation G3A04. The variation in volume at the seabed is only 2 to 3 cy between the different vessel speeds for placements at the same location.

There are differences in the maximum thickness, volume at the seabed, and actual volume versus potential volume between the shallow and deep placement locations. The maximum thickness corresponding to the shallow placement location with a depth of 42 m was about 3 cm while the maximum thickness corresponding to the deep placement location with a depth of 62 m is about 1.5 cm. The volume at the seabed corresponding to the shallow location was about 703 cu m while that of the deep location is about 632 cu m. The ratio of actual volume/potential volume for the shallow location was 0.81 while that of the deep location was 0.73. These simulations show that there is a 10 percent decrease in volume at the seabed when placing material at the deeper depth compared to the shallow depth location.

A second set of simulations for Scenario 1 were aimed at determining the general behavior of the mound at the shallow and deep cells while varying the sediment type (coarse and fine) and vessel speed (0.5 and 2.0 knots). As expected, the maximum thickness, volume on the seabed, and actual versus potential volume at the seabed were smaller for the fine sediment compared to the coarse sediment (Table K-6). For example, the actual/potential volume ratio for the fine sediment was 0.11 smaller than the value for the coarse sediment at a depth of 42 m (0.88 vs. 0.77) and 0.16 smaller at a depth of 62 m (0.82 vs. 0.66).

Scenario 2. These simulations examined the offset distance sensitivity due to different sediment characteristics, depths, vessel speeds, and current speed and directions. Representative predominant along-shelf currents were varied between NW 28 cm/sec and SE 20 cm/sec. These shore parallel currents are typical maximum currents and therefore provided a worst-case estimate of offsets. A secondary consideration was the sensitivity of maximum mound thickness, volume at seabed and actual/potential volume ratio due to the variable input parameters. The variable input parameters and results are summarized in

Table K-7. For all the Scenario 2 simulations, the dredge was assumed to have a heading of 315 deg.

The first eight simulations used the coarse sediment as defined in the MDFATE Input section. In the simulation for the 42 m depth, G3C2Z, the dredge velocity was 0.5 knots to the NW, which is about the same direction as the 28 cm/sec residual current. For this case, the offset distance was 120 m. Important contributions to the offset distance are the distance traveled by the dredge and therefore the speed of the dredge and for low dredge speeds, the direction of the dredge with respect to the residual current. During the 180-sec duration of the placement, the dredge moved 47 m. The maximum mound thickness was 2.4 cm in this case. Simulation G3C2Y was identical to G3C2Z except the residual current was 20 cm/sec to the SE, which is opposite of the dredge heading. In this case, the offset was 16 m while the dredge moved 47 m in the opposite direction. Simulation G3C4Z was identical to G3C2Z except the dredge had a speed of 2 knots rather 0.5 knots. Interestingly, the 78-m offset from this simulation was less than that from G3C2Z even though the dredge speed was increased by a factor of 4. In this case, the dredge traveled a distance of 182 m during the disposal time and the maximum mound thickness was 1.6 cm. Simulation G1C2Z was identical to G3C2Z except that the placement was in 62 m water depth. The resulting offset for simulation G1C2Z was 147 m, which was 20 m more than the offset for the corresponding placement at the 42 m depth (G3C2Z). The maximum mound thickness was less than 1 cm and was less than the 2.4 cm thickness for G3C2Z.

The coarse sediment simulations also showed a decrease in volume at the seabed and actual/potential volume ratio when comparing the 42 m and 62 m depth placements. The volume at the seabed for the 42 m depth placements range from 663 to 676 cu m, while that of the 62 m depth placements range from 632 to 648 cu m. The actual/potential volume ratio at the seabed showed a similar trend with an average value of 0.87 for the 42 m depth placements and 0.84 for the 62 m placements.

The next 8 simulations shown in Table K-7 are with the fine sediment as defined in the MDFATE Input section. As expected the fine sediment, with its smaller settling velocity allowing greater displacement, had less volume at the seabed, less mound thickness, greater dispersion of mound, and larger offset distances than the coarse sediment simulations. Average volume at the seabed for the 42 m and 62 m depth simulations was 619 cu m and 418 cu m, respectively. The actual/potential volume ratio at the seabed for the 42 m and 62 m depth simulations was 0.67 and 0.46, respectively. For simulation G1F4Z, 62 m depth simulation, the offset distance was 300 m and the maximum mound thickness was less than 1 cm.

These simulations were very conservative due to limitations in the MDFATE model. The residual current applied to the mound acts for a minimum of 7 days. A more appropriate simulation time would be several hours. Offset distances were not computed in every case, just in a sufficient number of cases to allow decisions to be made. The size of the offset distances with a moving dredge indicated that having the dredged stationary was the most desirable option.

Scenario 3. Scenario 3 MDFATE simulations included a nearly stationary dredge as indicated by capping operational planning and the predicted

results from the Scenario 2 simulations. Offset distance and volume at the seabed sensitivity tests were performed with a vessel speed of 0.1 knots and a heading of 315°. Also, the simulated volume of the hopper was changed from 1,660 cu m to 2,735 cu m during these simulations because the error in the interpretation of dredged volume reported by the contractor as described earlier.

The first four simulations shown in Table K-8 are the results for the fine sediment and the maximum expected current, 28 cm/sec to the NW and 20 cm/sec to the SE. The volumes at the seabed were similar to the Scenario 2 fine sediment simulations with a dredge speed of 0.5 knots. The offset distances for the simulations at the 42 m depth, G3F0X and G3F0W, were greater than similar simulations with coarse sediment in Scenario 2. The offset distance for G3F0X was 174 m and 120 m for G3C2Z. The offset distance for G3F0W was 49 m and 16 m for G3C2Y. The offset distances for corresponding coarse and fine simulations at the 62 m depth were similar. The offset distance for G1C2Z is 147 m and 145 m for G1F0X.

The remaining six simulations in Table K-8 included the increased hopper volume and a residual current of 15 cm/sec directed toward the northwest, which is the predominant current direction. These simulations show a trend of increasing volume at the seabed as the sediment type moves from coarse, to average, and to fine at the 42 m depth. This seemed counter intuitive, we have no ready explanation for this. While at the 62 m depth, at least for the fine sediment type, there was a decrease in volume at the seabed compared to the coarse and average sediment type seabed volumes. The actual/potential volume ratios show a decreasing trend as the sediment type moves from coarse to fine for both the 42 m and 62 m depths. The decrease was more dramatic for the 62 m depth.

These results provided more evidence that the offset predictions from MDFATE, due the requirement to simulate the full currents acting on the mound for an entire week, greatly over-predicted the offset over what would actually occur in the field. The actual offset of the impact point due to the current falling through the water column is extremely small due to the short duration for the jet to reach the bottom, just a few seconds as shown in the STFATE calculation. However, the relatively high intensity current acting on the mound for a solid week was apparently sufficient for the erosion and transport algorithms in MDFATE to shift the center of the mound up to hundreds of meters. It was believed this would not actually occur and thus the decision was made to model with little or current currents for the most of the rest of the simulations.

Scenario 4. Scenario 4 simulations were conducted immediately (1 to 3 days) prior to the initial placements at LU and SU to provide a model prediction of the expected mound geometry for these placements. These simulations were based on the best input available at the time and provided the most up to date MDFATE prediction of the expected bottom footprint from a single load of Queen's Gate sediment (using the finer than average classification). A range of current directions were simulated to indicate the likely offset distance which would correspond to the portion of the tidal cycle present at the time of placement. These simulations were intended to assist in deploying instruments, interpreting monitoring data, and to demonstrate the ability of the model to accurately predict the mound configuration.

The results of these simulations are shown in Table K-9 and have similar trends to the previous simulations. As expected, higher currents, in this case 10 cm/sec, produce less volume at the seabed and larger offset distances. There is also a general decrease in volume at the seabed and greater offset distances for placements made at the deeper location in Cell SU. The volume at the seabed for LU and SU placements is about 1,376 and 1,300 cu m, respectively. The average dimensions of the resulting circular shaped mounds for the placements in Cell LU are about 600 m in diameter, based on the 0.1 cm contour and between 3 and 4 cm maximum thickness. The mounds for the SU placements are similar in horizontal dimensions and shape but tend to be more elongated in the direction of the current and slightly bigger. The maximum thickness of the SU mounds, between 1 and 2 cm, are less than that of the LU mounds.

Scenario 5. Scenario 5 consisted of ten sensitivity MDFATE spreading mode simulations for the planned placements using the spreading mode in cell LD (Table K-10). (Two of the simulations are with no current velocity.) The objective of this analysis was to determine the sensitivity of the cap configuration and offset distance to variable input parameters and to compare to the estimated fall velocity of sediment to estimate the cap lateral extent. Input grain size, current speed and direction, and placement location/depth were varied. The sediment used in these simulations was based on the A-II and A-III borrow material. Two sediment types were simulated, $D_{50} = 0.4$ and 0.33 mm (MDFATE can only model a single grain size in the spreading mode). The load for each simulation was 1,990 cu m and the vessel speed was 1.5 knots with a north/south heading. The placement area was 490 m in the north/south direction and 60 m in the East/West direction. This simulation was conducted with 3 vessel tracks, each of 488 m length and separated by 30 m increments. The simulation time for capping was 30 min. This simulation length was based on using an Island Class hopper dredge and similar sediments (D_{50} of 0.4 mm) for capping at the New York Mud Dump site (Lillycrop and Clausner 1998).

Based on the work of Noble described previously, worst case residual currents were varied between 28 cm/sec at 290 deg and 20 cm/sec at 115 deg. Since the direction for the current in the tidal.dat file could not be controlled easily, the tidal current was neglected and the total representative current was specified as the residual current.

As a first order approximation, the Shore Protection Manual (1984) Equation 4-8 for fall velocity of spherical particles was used compute to determine the time the A-III sediment would be in the water column and available for the ambient current to act on it. The particle diameter was 0.4 mm and the kinematic viscosity was 1×10^{-6} . From the calculations, the fall velocity was 0.053 m/sec.

As a very conservative estimate, it was assumed that during spreading, the sediments would have a maximum initial vertical momentum as they exited the dredge, falling a distance equal to the draft of the dredge. The assumption was that the particle would fall a distance of 12.2 m (the 6.1 m draft of the dredge plus another 6.1 m) before beginning to settle at the particle settling speed of 0.053 m/sec. Thus the conservative time for an individual particle to reach the bottom at the LU was:

$$42.5 \text{ m} - 12.2 \text{ m} = 30.3 \text{ m} / 0.054 \text{ m/sec} = 560 \text{ sec (9 min)}$$

Assuming a maximum current of 0.28 m/sec, the particles could travel 2,000 m, or well beyond the cell. For a placement in cell SU, using the same logic, the time for an individual particle to reach the bottom after falling:

$$50.3 \text{ m}/0.054 \text{ m/sec} = 931 \text{ sec (16 min)}$$

Assuming a maximum current of 0.28 m/sec, the particles could travel over 3,000 m.

For shallower depths and more typical currents of 15 cm/sec or less, the material would settle out within the domain of the MDFATE model grid.

Simulations PVSP34 and PVSP38 computed the cap footprint size and location with no current. A current directed at 290 deg (to the west) shifted the footprint to the west about the width of the footprint (150 to 200 m) and slightly north. The current directed at 115 deg (southeast) shifted the footprint to the east and slightly south. The modeled shifts in location due to currents were much less than the conservative estimates based on pure particle settling described in the prior paragraphs. As expected, the 0.33 mm material had a bigger footprint than the 0.4 mm material. At the shallower depth near cell F4 there was less north/south shifting of the footprint. All resulting volumes on the seabed are within a few cubic meters of each other and were 0.97 of the maximum potential volume.

The potential for A-III borrow material to move some distance from the placed location caused considerable concern with for the monitoring effort. Also, the 30-min placement time would have required the dredge to make three passes over the cell. Attempting to track the plume resulting from multiple passes would have been logistically impossible with the available vessels and equipment. Thus, a decision was made to increase the rate of release of dredged material such that all the material exited in a single pass over cell LD. The target was to have all material exit in 10 min and at 1.5 knots, so that the dredge would travel a distance of 300 m, or half the length of the cell. The faster rate of release would also increase the vertical momentum, reducing the potential for ambient currents to move the cap material beyond the cell and out of monitoring range.

Operational model simulations

From a few days prior to the actual placements until a few days following the actual placements, a series of MDFATE predictions and hindcasts were conducted for initial placements in Cells LU and SU and cap building placements in LU. The cap building simulations included the first 5 and 25 placements in LU. Inputs for these simulations were based on the best available data. Hopper characteristics such as grain size distributions from hopper samples, hopper volume (water and solids), loaded and unloaded displacement, placement location, and dredge speed and heading were of primary importance for these simulations. For those simulations conducted a few days after the placements, comparisons of the resulting mounds were made with available SPI data. The purpose of these simulations was to fine tune monitoring activities, confirm prior estimates of spacing between placements, confirm that the MDFATE predictions were reasonably close to the actual mound characteristics as determined by monitoring, and provide confidence that the full cap placed would meet design expectations. Most of the discussions provided below are

based on those simulations conducted a few days after the placement when actual data were available.

Initial LU placement. Once grain size distributions and preliminary SPI results from the initial LU placement were available, a set of MDFATE simulations was conducted. Results from the MDFATE simulations were compared with SPI measurement of cap thickness and rough estimates based on the SPI data of apparent volume and horizontal extent. Initial attempts to simulate this event resulted in much smaller mound volumes than indicated by the SPI measurements. In order to increase the simulated mound volume, tests were conducted using various percentages of clumping (there was visual evidence of this in hopper and cores/SPI –clumping is when the clay fraction was assumed to be clumps at a relatively low bulk density, not individual particles), increasing as placed void ratio, and simulating the solid material in the hopper only as opposed to the entire hopper volume (water and solids). These tests were unsuccessful. In hindsight, the apparent cap volume and thickness indicated by the SPI measurements likely included at least a 2 cm of native sediments that had been resuspended during cap placement, particularly near the point of impact from each load. This would have increased the estimated cap thickness and volume measurements based on the SPI measurements.

During the simulations that attempted to match the footprint thickness and horizontal extent of the LU single placement SPI data, the sediment grain size data from the hopper load samples were used (Table K-11). These data include the volume fractions and grain size from the LU HOP 1 sediment geotechnical analysis.

The density of the sediments in the hopper was calculated using the following equation:

$$[\text{Loaded displacement} - \text{light displacement (short tons)}] * 0.9702 [\text{metric tons/short ton}] / \text{volume of sediments in the hopper [cy]} * 0.7646 [\text{cubic meter/cy}] = \text{bulk density}$$

$$[(7200 - 3452) * 0.9702] / [(2774) * 0.7646] = 1.603 \text{ g/cm}^3$$

The volume fractions of the material in the hopper were then calculated as shown previously. The resulting volume fractions were 0.54 for sediments and 0.46 for water. Based on the sand (0.78), silt (0.19), and clay fractions (0.03) from the samples, the volume fraction constituents used in the MDFATE simulations were sand (0.42), silt (0.10), and clay (0.016). Using the logic described earlier, the composite as placed void ratio assuming the as deposited void ratios for sand (0.90), silt (2.5), and clay (4.5) was 1.3.

Decreasing the composite void ratio to 1.3 and modeling the total hopper volume at the channel *in situ* density (1.9 g/cm^3) provided the best comparison to the SPI data. Figure K-8 shows the simulated mound in the LU cell and the comparison to the mound from the inferred SPI data, respectively. The maximum thickness of the simulated mound was 6.3 cm, which was similar to the maximum SPI thickness of approximately 6 cm. The model 2 cm contour was reasonably close to that of the SPI but the model mound has a more circular shape. Note that the SPI thickness likely includes at least 2 cm of resuspended EA sediments in the center of the mound. Additional discussions on the influence of the resuspended EA sediment contribution to the SPI measured cap

thickness are discussed in considerable detail in the MDFATE hindcast results section.

Initial SU placement. One day prior to the initial SU placement (called SU1) on 8 August 2000, several MDFATE predictions were made based on the LU1 hopper load and current measurements that indicated a depth averaged current of 17 cm/sec. These simulations resulted in mound with offset distances of about 60 m, which was much greater than indicated for the LD placements. Similar to LU1, several simulations were conducted a few days after placement that included with the best available data from the placement (load, heading, etc.), initial GSD, to allow comparison to the preliminary SPI data. To match the SPI measured cap thickness, which once again had a maximum thickness of about 6 cm, several simulations were made with clumping and with increased void ratios. The increased void ratio gave the best result when compared to SPI data. Once again it should be noted that the SPI thickness likely includes at least 2 cm of resuspended EA sediments in the center of the mound.

Attempting to match the footprint thickness and horizontal extent of the SU single placement SPI data, the sediment input data from the hopper load were used (Table K-11). This included the volume fractions and grain size from the SU HOP 1 sediment geotechnical analysis.

Bin density for the SU1 placement was calculated to be:

$$[(7250 - 3250) * 0.9702] / [(3325) * 0.7646] = 1.526 \text{ g/cm}^3$$

The volume fractions of the material in the hopper were then calculated as shown previously. The resulting volume fractions were 0.277 for sediments and 0.723 for water. Based on fraction of sand (0.90), silt (0.09), and clay (0.01) from the samples, the volume fraction constituents used in the MDFATE simulations were sand (0.25), silt (0.025), and clay (0.003). Using the logic described earlier, the composite as placed void ratio assuming the as deposited void ratios for sand (1.5), silt (2.5), and clay (4.5) was 1.62.

Figure K-9 shows the simulated mound in cell SU and the comparison to the mound from the inferred SPI data. The maximum thickness of the simulated mound is 3.4 cm, which was similar to the initial estimated maximum SPI thickness of approximately 3.5 cm. The model 2 cm contour was much different than that of the SPI. The model 2 cm contour was located downslope of the placement location while the SPI inferred 2 cm contour was both upslope and downslope of the placement location. Also the model 2 cm contour extended about half the area of the SPI inferred 2 cm contour.

LU 5 placement. MDFATE hindcast simulations were conducted and compared to SPI data collected after the first five placements at Cell LU (called LU 5). The best comparison for this case was simulated with the sediment characteristics from LU HOP1 with an as deposited void ratio of 1.1. These placements were modeled with solid material only at the *in situ* density, not the total hopper volume, which includes a significant volume of low-density slurry above the settled sediments. Therefore the hopper volumes are about half of the actual hopper volumes. Each of the five hopper loads set at 990 cu m, the average of the four LU placements on 13 August and the one LU placement on 2 August.

Sediment characteristics, volume fractions and as placed void ratio for simulation G3L5D, the best simulation for the 5 LU placements are described in Table K-11. Like the LU1 operational simulation in which the was 1.6 g/cm^3 , assuming the hopper contained settled solids only at *in situ* density of 1.94 g/cm^3 provided the best match with the SPI measured mound thickness. The volume fractions and void ratio were the same as for the single LU placement on 2 August.

Figure K-10 shows the simulated mound and the comparison to the mound from the inferred SPI data. The maximum thickness of the simulated mound was 12 cm compared to the SPI thickness of greater than 7 cm. The model 3 cm contour was similar in lateral extent to that of the SPI except in the upslope direction, where the preliminary SPI results showed more of the mound extending in upslope. Also the SPI 3 cm contour extends about the width (300m) of Cell LU while the model 3 cm contour was about 200 m in diameter.

LU25 placements. MDFATE hindcast simulations were also conducted and compared to SPI data collected after the first twenty-five placements at Cell LU. The best comparison for this case was simulated, similar to the LU5, with the sediment characteristics from LU HOP1 with an as deposited void ratio of 1.1. These placements were modeled with solid material only at the *in situ* density, 1.9 g/cm^3 . Therefore the hopper volumes are about half of the actual hopper volumes. Each of the five hopper loads set at 990 cu m. Placement locations defined at the nearest model grid points to the plan developed during the capping operation.

Figure K-11 shows the simulated mound and the comparison to the mound from the inferred SPI data. The 5 cm model contour extends over most of Cell LU and the 10 cm contour extends over about the middle third of Cell LU. The maximum thickness of the modeled mound is 22 cm. The SPI data ranges between 5 and 10 cm near the edges and up to 12 or 15 cm near the center of the cell. There is a limitation to the SPI thickness data in that the device did not penetrate the sediment to a depth that will allowed it to measure the entire cap thickness.

Hindcast results

Once all the monitoring data had been collected, processed, analyzed, and reported, hindcasting using the best available data was initiated in March 2001 and continued into September 2001. While the monitoring program was well thought out and executed, a number of monitoring techniques did not work as well as expected. The failure of the coring effort to produce accurate estimates cap thickness proved to have the greatest impact on our ability to compare modeled cap thickness with actual cap thickness in areas where the cap thickness exceeded the depth of penetration of the SPI. The lack of reliable core data also limited our ability to accurately determine the as deposited void ratio (calculated from bulk density and water contents) in cells SU and LD.

Selected hindcast MDFATE model simulation results are presented herein. Data for placements related to dredging, (location, speed, duration, etc.) were developed from ADISS data. Table K-12 summarizes the results from the hindcast simulations including the cell, number of placements, scenarios simulated, dimensions of the 1 cm contour, maxim cap thickness, volume on the

seabed, and percent retained (the actual volume predicted by the model to reside on the seafloor divided by the maximum potential volume had all the sediment settled inside the model grid). When the 1 cm cap thickness contour dimensions are listed, the first dimension is the length and the second dimension is the width. The length is the shore parallel length, i.e., the direction parallel to the long, 600 m cell axis. The width dimension of the contour will be the shore normal direction parallel to the 300 m long cell axis. These definitions of contour lengths and widths are used in the following discussions.

The MDFATE simulations of conventional placement in cells LU and SU are presented in this order: the initial single placements in LU and SU; followed by the cap building multiple placements in LU (5, 25, 45, and 71); and the multiple placements in SU (5 and 21). The MDFATE simulation of the spreading placements in cell LD are discussed next, with the single placement discussed first followed by the multiple placements.

LU 1 placement. As noted in the operational simulation section, initial attempts to simulate this event with MDFATE resulted in much smaller mound volumes and thickness (maximum about 2.9 cm) than indicated by the SPI measurements (greater than 5 cm). To increase the simulated mound volume, simulations were conducted using various percentages of clumping (clumping was observed in the hopper and cores/SPI), increasing as-placed void ratios, and simulating the solid material in the hopper only. These test simulations were unsuccessful in matching the SPI measurements. In hindsight, the apparent cap volume and thickness indicated by the SPI measurements included at least two or more centimeters of native sediments that had been resuspended during cap placement, particularly near the point of impact from each load. Figure K-12 (SAIC 2001; Figure 3.7-11) shows the estimated depth of disturbance of the EA layer. A visual estimate of the average depth of disturbance results in a value between 1.5 and 2.0 cm, with a depth of disturbance in excess of 2.4 to 3.0 cm at the two central stations. Assuming the EA sediments are mixed evenly from an areal perspective, then the individual SPI cap thickness, particularly at the central portion of the cap would need to have about 2 cm subtracted to yield the actual cap thickness due solely to the Queens' Gate sediments. Because MDFATE does not include resuspension it is almost impossible to have the MDFATE simulations match the SPI measurements using realistic inputs.

Hindcast simulations to match the footprint thickness and horizontal extent of the LU1 placement SPI data used grain size data from hopper samples collected during this placement. As noted earlier, the overall hopper load density was calculated to be 1.6 g/cm³. Figure K-13 shows the hindcast simulated mound and the comparison to the mound from the inferred SPI data. The maximum thickness of the simulated mound is 2.9 cm, which is less than the maximum SPI thickness of 5 to 5.5 cm.

Figure K-13 is similar to several other figures where MDFATE simulations of predicted cap thickness and extents are compared to SPI predictions. In these figures, the MDFATE cap thickness contours, in centimeters, will typically be shown as thick solid or dashed lines. The contours are labeled, often with the labels at an angle, and always with a decimal point (e.g., 1.0, 2.0, 5.0, etc.). In Figure K-13, the 1.0, 2.0, and 2.5 cm MDFATE cap thickness contours are shown. The 1.0 cm MDFATE thickness contour is generally assumed to be the effective outer edge of the cap. MDFATE does predict cap thickness out to a

millimeter or less, however, the 1 cm contour is the practical limit for most SPI applications, therefore the 1 cm contour is used for the MDFATE limit. The SPI predicted cap thickness can be shown two ways, one is with a color ramp, where a range of cap thickness are shown a single shade of color with thicker portions of the cap shown in progressively darker colors. The boundaries between the colors, narrow black lines, are single contour lines. For example, in Figure K-13, the outer most color, light tan, represents an average SPI cap thickness measurement of from 1.5 to 2.5 cm. The darkest color represents a cap thickness of 5 to 5.5 cm. In the color ramp scheme, the outer contour is the 1.5 cm cap thickness; the next contour is 2.5 cm, etc.

Because the color contours are drawn by algorithms in ArcView, in some cases the contours are thought to be somewhat misleading due to the relatively small number of data points. Thus, in many of the MDFATE cap thickness compared to the SPI cap thickness figures the actual location of the individual SPI stations are shown, also color-coded according to thickness, with zero thickness as white, with light yellow through orange and to red for the thick caps. For these cases, the measurement of cap thickness from SPI, in centimeters, is often labeled with a single number, an integer with no decimal point to distinguish it from the MDFATE thickness contour labels. In most cases the SPI thickness label is black in color, however when the label falls on a dark background, the label may be white or light gray.

On most of these MDFATE and SPI comparison figures, depth contours are also shown, often as dashed lines with the water depth (in meters) displayed.

In Figure K-13, the best MDFATE simulation was realized with no currents (residual or tidal), stripping of all the sediments, and modeling the full hopper volume of dredged material, 2,120 cu m, at an overall bulk density for the entire hopper load of 1.63 g/cm. The overall as placed bulk density of 1.81 g/cm³ from cores converted to as placed void ratio of 1.10. Data from the LU1 hopper samples were used to compute required sediment characteristics. Other pertinent sediment data for the hindcast simulations are summarized in Table K-12.

The overall shape of the MDFATE contours agrees quite well with the SPI predictions. The overall location of the MDFATE contours is shifted slightly to the southeast compared to the SPI contours. The MDFATE 1 cm contour has a maximum length of 250 m and width of 205 m. The SPI 1 cm contour has a maximum length of 245 m and maximum width of between 160 and 210 m. Major differences occur at the center of the cell, where the MDFATE predicted thickness are much less, for example the 2.5 cm contour is only 85 m long by 77 m wide while the SPI 2.5 contour is about 215 m long by 165 m long. The ship shaped polygon (in green) shows the location of the dredge at the start of the placement with the green triangle indicating the center of the hopper. The red triangle indicates the position of the center of the hopper at the end of the placement.

For this simulation the MDFATE predicted cap volume was 1,390 cu m, out of a maximum possible of 1,560 cu m, or 89 percent of the material was retained in the site. The cap volume computed from SPI measurements was 1333 cu m, or extremely close to the MDFATE volume. However, inspection of Figure K-12, shows that the EA layer was disturbed to an average depth of about 1.5 cm over an area approximately 210 m long by 140 m wide. The volume of the EA

layer resuspended and likely mixed with the cap and included in the SPI estimate of cap volume is 540 cu m. This results in a net volume of cap material from SPI of about 790 cu m, considerably smaller than the MDFATE estimate of 1,560 cu m.

A number of other simulations were made in an attempt to better match the LU1 placement. These simulations included a tidal current, which displaced the location of the mound to the southeast about 80 m. Several simulations using the average sediment characteristics for the entire set of LU placements and with and without stripping, with and without tides, etc, were also conducted. Also simulated was the hopper load at a higher volume fraction where the volume equivalent to the in channel volume at density of 1.90 g/cm^3 , a volume equal to 1,022 cu m, was done. This simulation was also good, however, the mound was more compact, symmetrical (the 1 cm contour was 158 m long and 147 m wide), and more displaced to the south. It also had a higher maximum thickness, 4 cm (Table K-12).

SU1 placement. MDFATE hindcast simulations to compare to the SU1 placement SPI data used grain size data from hopper samples collected during the actual placement. Figure K-14 shows the simulated mound thickness and the comparison to the SPI mound thickness. This MDFATE simulation was based on the entire hopper load and had a higher overall void ratio (1.62), than the other MDFATE simulations of LU placements. The logic for this was that the bulk density of the native EA sediments in cell SU have a surface layer average bulk density of 1.49 g/cm^3 , which corresponds to a void ratio of 2.39, and that a considerable amount of relatively lower bulk density EA sediments were mixed in with the placed cap material. These preliminary MDFATE simulations indicated as placed volume of 1,760 cu m, while the SPI volume was 2,460 cu m. However, if the volumes of sediments associated with the EA sediments resuspended into the cap are included, the agreement is reasonable. If the EA sediment volume entrained in the mound is assumed to be a cylinder 1.5 cm thick and 300 m in diameter (see discussion below), this represents a volume of 1,060 cu m, adding this volume to the MDFATE volume gives a total of 2,820 cu m. This is reasonable agreement (2,460 versus 2,820 cu m) considering the uncertainty in the various bulk densities, void ratios, and SPI method computation of volume based on a limited number of data points.

The MDFATE cap thickness contours are shown as dashed lines, the SPI cap thickness contours are shown as solid lines. The maximum thickness of the MDFATE simulated mound is 2.4 cm, and is compared to the maximum SPI thickness of approximately 6 cm. The 1 cm MDFATE contour has dimensions of 285 m long by 245 m wide, while the STFATE contours are 325 m long by 300 m wide. The model 2-cm contour (dashed line) is much smaller than that of the SPI, it is 100 m long by 73 m wide while the 2 cm SPI contour is 240 m long by 215 m wide. Also the model 1-cm contour covers about the same area of the SPI inferred 2-cm contour but is shifted more downslope.

Figure K-15 shows the thickness of the EA layer disturbed by the SU1 placement. Most of the thicknesses are in the 1 to 3 cm range. When the EA layer depth of disturbance thicknesses are subtracted from the SPI cap thickness as shown in Figure K-14, the agreement between the SPI and MDFATE simulated thicknesses is much better.

Multiple placements in cells LU and SU

As noted earlier, beyond the initial placements in cells LU and SU, total hopper volume and load were not available, thus the volumes simulated were the contractors equivalent in-channel volumes at a density of 1.9 g/cm^3 . The LU multiple placement simulations used the average sediment characteristics from all the LU hopper samples. Tables K-4 and K-12 summarize the data from the various simulations. Additional details on the GSD can be found in Appendix J, Table 3.11-5. Similarly, the SU simulations used the average sediment characteristics from the SU hopper samples, with Tables K-4 and K-12 providing a summary and Appendix J, Table 3.11-5 providing additional details.

Based on the results of the predictive, operational and initial hindcast simulations, which showed significant offsets when simulating residual currents, none of the simulations of multiple placements used a residual current. In general, the simulations were done with tidal currents as computed from ADCIRC constituents and without tidal currents. In most simulations, stripping of all the sediments fractions into the water column was specified, however in some cases no stripping of the sediment was specified.

One final general observation, like the single placements, all the SPI measurements of cap thickness where the camera penetration exceeded cap thickness include the estimated thickness of EA disturbance. Estimates of the thickness of EA layer disturbance in areas where cap thickness was greater than SPI penetration were based on earlier SPI monitoring data, e.g., during the monitoring episodes following 1 and 5 placements.

LU 5 placements. As noted earlier, after the initial LU placement, four additional placements were made at approximately the same location as the initial LU placement. Two different LU simulations best bracket the SPI measured mound dimensions. The details on these simulations are summarized in Tables K-4 and K-12.

Figure K-16 shows the MDFATE simulation with no currents (residual or tidal) and with stripping of all sediment fractions. The MDFATE contours are fairly circular, with the center of the MDFATE cap displaced down-slope about 20 m. The MDFATE 1-cm contour agrees reasonably well with the SPI data, particularly for the NW, S, and SE portions of cell LU. Note that there were no SPI stations outside of the LU cell boundaries for this round of monitoring. North of the placement point, this MDFATE simulation under predicts the cap thickness, though the cap thickness includes a considerable volume of EA sediments. For example, at the station directly onshore of the center near the northeast cell border, the SPI cap thickness is listed as 5 cm. At this location the depth of disturbance averages 3.3 cm (Figure K-17). Similarly, the 3 cm SPI thickness directly south of the cell center and just inside the southwest cell boundary, the average depth of disturbance is 1.3 cm. At the center of the cell, the MDFATE simulation over predicts the cap thickness compared to the SPI measurements. Maximum MDFATE cap thickness is 18 cm, which is located within the small 15 cm contour (55 m long by 40 m wide) near the center of LU. This peak is the result of integrating the cap thickness from each placement with no resuspension of the previously placed loads. The SPI predictions of the cap thickness in the center are in general 7 to 8 cm, however, in almost every case the

cap thickness exceeded camera penetration. SPI stations with pink dots are locations where cap thickness exceeded SPI penetration depth. Overall, the 5 and 10 cm contours seem to match reasonably well with the SPI measurements.

The as placed volume from the MDFATE predictions was 4,570 cu m remaining inside the grid, which is 84 percent of the maximum possible. The SPI estimated volume was 4,745 cu m, however the reliability of the volume is quite questionable. First, an estimated 2,000 cu m of EA sediments are included based on the area covered and an average of 2 cm of EA sediments. Second, because the cap thickness exceeded the penetration depth in the center, the volume estimate does not include the cap thickness greater than penetration in the estimate.

In an attempt to better match the SPI predictions, a second MDFATE simulation was made that included tidal currents. Figure K-18 shows the results from this simulation. Two features are immediately obvious. First, the contours are much less circular; they are stretched in the major tidal axis direction increasing the length of the 1.0 cm contours from 340 m (no tidal currents) to 425 m while reducing the width. These contours do not match the SPI measurements nearly as well, which show a much more circular mound. Second, the maximum cap thickness is reduced, from 18 to 13 cm, which appears to match the SPI predictions better. The volumes retained are nearly identical to the no tidal currents simulation.

Overall, the MDFATE simulation with no tidal currents simulation seems to provide a slightly better match to the SPI measurements, only the cap thickness is over predicted over a small, approximately 50 to 75 m diameter circle in the center of the cell. Some LU5 simulations without any stripping of sediments were performed. These simulations showed a large increase in the predicted central cap thickness, with similar results on the rest of the mound as to the non-stripping simulations. Also, without any currents or stripping, almost all the material reached the seabed (97 percent). As shown in Table K-12, the maximum thickness increased to 25 cm with tides and 28 cm without tides. Neither of these simulations was thought to provide an accurate representation of the actual cap.

LU 25 placements. The MDFATE simulations of 25 placements in LU, without tidal currents and with tidal currents, provided essentially identical results on cap extent and thickness and similar comparisons with SPI measurements, as did the 5 placements in cell LU. Figure K-19 shows the LU25 MDFATE simulation with no tidal currents and stripping of sediments. Maximum mound thickness was 28 cm with the 1-cm contour of cap thickness being 865 m long and 640 m wide. The mound is fairly symmetrical about a longitudinal centerline. The MDFATE simulated cap is slightly displaced down slope, the 1 cm contour is a maximum of 180 m farther offshore than the seaward LU cell boundary, while the maximum landward extent of the 1 cm contour is 150 m. The 5 cm MDFATE contour covers most of cell LU, with the 10 cm contour covering an area 475 m long by 210 m wide. The central mound peak of 28 cm is surrounded by a fairly small 20 (130 m long by 85 cm wide) and 25 cm (50 m in diam) contour.

Comparing the MDFATE thickness with SPI measurements shows a similar trend to the LU5 simulations. With the exception of four SPI stations, all the

stations have cap thicknesses greater than SPI penetration. Central SPI stations tend to be slightly thicker than the outer stations, with thicknesses of 13 to 14 cm, while the majority shows cap thicknesses of 9 to 12 cm. Overall the MDFATE and SPI predictions agree reasonably well with the MDFATE slightly under predicting cap thickness on the outer portion of the cell and over predicting in the center portion of the cell. Note that no SPI measurements were taken outside the cell on this monitoring effort. Like the LU5 placements without tidal currents but including stripping, 85 percent of the placed material is retained within the confines of the LU grid.

Like LU5, a second MDFATE simulation that included tidal currents was made, the results are shown in Figure K-20. Also, like LU5, this simulation resulted in a reduced maximum cap thickness; the mound peak in the center was 17 cm as opposed to 28 cm with no tidal currents. Also, the cap thickness contours were stretched in the tidal current directions, NW and SE and reduced in the shore perpendicular direction. While the peak was reduced for the simulation with tidal currents, an overall better match with the SPI measurements was with the MDFATE simulation with no tidal currents (similar to the case with the LU5 simulation).

LU 45 placements. MDFATE hindcast simulations were also conducted of the first 45 placements in LU with the results compared to SPI and core data. As noted earlier, in the initial planning, the placements in LU were to end after 45 placements because this was predicted to result in a 15 cm cap over the entire cell. Consequently, a full suite of monitoring data was collected following these placements. Therefore, the MDFATE prediction for the 45 placements provided the best opportunity to compare the predicted cap geometry with the actual mound geometry.

Figure K-21 shows the MDFATE-predicted cap when no tidal currents and no residual currents are simulated, compared to the SPI measured cap thickness. Figure K-21 shows the MDFATE simulated mound has a maximum thickness of 30 cm with a pronounced peak in the center of the cell, with the 10 cm contour covering almost the entire cell. The overall shape of the MDFATE-predicted mound is reasonably symmetrical with only a slight displacement down slope of the 1 and 5 cm contours.

The 1 cm contour has a maximum length of about 1,060 m and a width of 720 m. The entire mound footprint is shifted slightly downslope by a distance of about 30 m. The 1 cm contour is a maximum of 225 m seaward of the SE cell boundary, 190 m landward of the NE cell boundary, and about 250 m beyond the NW and SW cell boundaries.

It was assumed that a peak with this amount of excessive thickness (compared to the remainder of the central thicknesses) would not actually occur because the bottom surge currents from adjacent placements would tend to preferentially resuspended the material forming the peak and thus reduce its thickness. As noted earlier, MDFATE does not model resuspension of existing bottom sediments during the placement process. MDFATE can only simulate sediment transport of placed sediment due to ambient currents and waves during the “longer term” simulations where LTFATE algorithms simulate sediment transport.

Because of the peak, cap thickness predicted by this MDFATE simulation with no tidal currents is considerably thicker than SPI thickness at the center of the cell. When SAIC correlated the core thicknesses with SPI thicknesses for locations where the cap thickness exceeded penetration, they concluded that in most cases, the cap thickness exceeded the SPI thickness by about 6 cm. Using this logic, the thickness of the cap over much of the center of the cell is about 15 to 18 cm thick. Note that the SPI measurements includes the EA sediments that were resuspended and mixed into the sediment, and thus likely add at least 2 to 3 cm to the overall cap thickness. If this is true, then the cap thickness due solely to the cap material added is on the order of 13 to 16 cm thick, which is reasonably matched by this MDFATE simulation with the exception of the peak.

Outside the cell, the MDFATE-predicted thicknesses match the SPI measurements reasonably well (within a few centimeters), particularly if the SPI cap thickness is reduced by 2-3 cm. Figure K-22 shows the depth of disturbance in the SPI stations outside the LU cell boundaries. The distance outside the cell boundaries where the EA layer was disturbed indicated that the bottom surge disturbed sediments a greater distance in the down-slope direction compared to the along-slope and upslope directions.

Another simulation was conducted that included a tidal current as determined by ADCIRC tidal constituents. Figure K-23 shows the resulting MDFATE simulation with the SPI information superimposed. The tidal current significantly reduces the maximum thickness and spreads the mound in the direction of the tidal current major axis approximately 300 to 120 deg. A definite peak still exists in the center of the cell, however, the maximum predicted thickness is reduced from the no current simulation thickness of 30 to 19 cm. The small contour in the center of Figure K-23 is the 18-cm contour. The 15-cm contour also fairly small, only 240 m in diameter in the depth contour parallel direction. The 5-cm contour covers the entire cell, with the 1-cm contour having a length of well over 1,100 m. Once again, the cap is reasonably symmetrical with a slightly greater spread down slope. Overall, the simulation with tidal currents predicts a cap that is about 2 to 3 cm thinner within cell LU than the simulation without tides.

LU 71 placements. As noted in Chapters 1 and 3, a decision was made to attempt to create a cap that reached a thickness of 45 cm over a small portion of the center of cell LU. A hindcast of the full 71 loads placed in cell LU was made using essentially all of the input parameters developed for the 45 simulation hindcasts. Also, like the simulations for 45 placements, two simulations were made, one with tidal currents and one without any currents. Results were similar to the LU45 simulations.

At the time this report was written, it was virtually impossible to make a meaningful comparison of the MDFATE simulation of 71 placements in LU to the actual cap thickness dimensions because following the post 71 placements, because the cores collected had inconclusive results of cap thickness. The SPI data collected following 71 placements were meant only to define the how far from the cell boundaries the cap material extended.

Figure K-24 shows the LU71 MDFATE simulation with no tidal currents. A pronounced peak developed, with a maximum cap thickness of 42 cm, the 10-cm

contour effectively covers the entire cell, and the 1-cm contour is less than 1,100 m long (very similar to the 45 simulation). As expected, beyond the cell boundaries, there is little added cap thickness. As before, in hindsight, a peak with this excessive thickness was not expected to have occurred.

Figure K-25 shows the L71 MDFATE simulation with tidal currents. Again, a pronounced peak developed, but the tidal currents reduce the maximum cap thickness from 42 to 30 cm. The 1-cm contour extends beyond the size of the modeling grid, the estimated extent is about 1,500 m. The 10 cm contour is just over the cell length. The maximum mound thickness is 31 cm, and the maximum lengths of the 30- and 25-cm contours were about 100 and 215 m, respectively.

Maximum cap extent in cell LU. While the maximum cap thickness and cap thickness over the cell and immediately adjacent to the cell are primary concerns in cap design and simulation, the maximum extent of the cap is also of interest. Monitoring to define maximum cap extent was done following the 71 placements in cell LU. The monitoring consisted of SPI stations spaced 25 m apart over two transects of 7 and 8 stations starting 125 m northeast (on-shore direction) of cell LU and 100 m SE of cell LU (up current direction) (Appendix J Section 3.7.4.6) (Figure K-26). The prediction of the maximum cap extent in the up current direction as defined by the MDFATE 1.0-cm from the no tidal currents simulation agrees quite well with the SPI measurements, a distance of 220 m (SPI) versus 240 m (MDFATE). The MDFATE simulation with tidal currents greatly over predicted this extent, by over 200 m.

The maximum cap extent in the shoreward direction beyond the cell boundary is 120 m as measured by observable cap (1.0 cm) in the SPI image. The MDFATE simulations over predicted the cap extent, predicting 215 m in the no tidal currents simulation (over prediction of 95 m) and 185 m in the tidal currents simulation (an over prediction of 65 m).

SU multiple placements

SU 5 placements. Similar to the LU5 simulations, MDFATE simulations of SU5 were done with and without tidal currents, with and without stripping, and using LU average sediment characteristics and SU average sediment characteristics. Results varied somewhat from those in cell LU. Once again, only having SPI stations within the cell boundaries reduces the accuracy of the comparisons because thinner portions of the cap, say 3 cm or less, did spread outside the cell.

The MDFATE simulations showed that the spread of material was greater at SU than in LU, the various simulations of SU5 showed 1 cm contours ranging from 450 to 525 m in length and 295 to 400 m in width (Table K-12). In contrast, the LU 5 simulations showed the 1 cm contour length to range from 340 to 450 m (Table K-12). The SPI predicted contours for SU5 showed the 1 cm contour to be a minimum of 400 m long and perhaps as much as 600 m long. The extent of the SU5 mound as determined by SPI was difficult to compute because there was still significant thickness at the outer stations as shown in Figure K-27, which is also what was seen for the LU5 placements in Figure K-18. However, there does appear to be slightly greater spread for the cap at SU.

Note that the five LU placements totaled of 4,950 cu m, while the five SU placements totaled 5,470 cu m, or 10 percent more than LU.

As noted in 3.6.2.2, the SPI and core data indicated a cap of 5 cm and greater over an area of 250 m in the center of the cell with maximum cap thickness of 8 to 10 cm at a minimum. The MDFATE simulations with the SU sediment characteristics and stripping with tidal currents (Figure K-27) predicted a maximum cap thickness of 8 cm, with the 5 cm contour having a length of 170 m and width of 100 m. If the depth of the EA layer disturbance (Figure K-28), which average about 2.5 cm in the center of the cell, are subtracted from the total SPI cap thickness, then the agreement between the MDFATE simulation and SPI measured thicknesses is reasonably good, typically within a centimeter or two. The greatest difference between the two is in the inshore portion of cell SU, where the MDFATE mound's lack of a circular shape and downslope displacement causes greater discrepancies between the SPI and MDFATE predictions.

The overall shape of the MDFATE cap simulation shows that the combinations of slope and depth resulted in a mound that is stretched or displaced in the downslope direction. For example, the 1 cm contour extends 225 m downslope from the approximate center of the mound and only 177 m upslope, a difference of 50 m. Also, the center of the mound from the MDFATE simulation is about 30 m downslope from the center of the cell. In contrast the SPI mound appears to be more circular, though the slope effects can be seen in that the three center, outer SPI stations upslope have thicknesses of 3, 3, and 5 cm, compared to the three center, outer SPI stations downslope which have thickness of 4, 5, and 6 cm.

The MDFATE simulations with LU sediment characteristics (made before the SU core data had been fully analyzed) had thinner mounds than those with SU sediment characteristics as shown in Table K-12, while the MDFATE simulation using SU sediments, no tides, and no stripping produced a relatively thicker mound with a maximum thickness of 13 cm. While this simulation had better agreement in the very center of the mound, the remainder of the cap thicknesses were under predicted.

SU 21 placements. The full 21 placements in cell SU were simulated with MDFATE. Because of uncertainty in the post 21 core data, the initial simulations used the sediment characteristics from the LU45 and LU71 simulations, with a composite as deposited void ratio of 1.04. A full range of SU21 simulations, with and without tides and with and without stripping, was conducted (Table K-12). Later, when the supplement core data were examined, a second set of simulations using sediment data that appeared to be more typical of cell SU, with a lower bulk density and correspondingly higher as-deposited void ratio, 1.27, were done. The results between the two sets of simulations were consistent with results from the LU simulations, with the non-tidal simulations producing thicker mounds with higher peaks and fairly circular shapes, while the simulations with tidal currents produced thinner mounds with less pronounced peaks, with thickness contours stretched in the direction of the major tidal axis. Simulations with no stripping produced mounds of excessive thickness, e.g., a maximum mound thickness of 26 cm with no tides and no stripping. As would be expected, due to the increased void ratio, the simulations with the SU sediments were resulted in mound that were slightly thicker than those with the LU sediments,

generally by about 1 to 2 cm at the center of the mound. Compared to the SPI measurements, the non-tidal simulations with SU sediments provide the best match, though the tidal simulations with SU sediments are nearly as good.

Figure K-29 shows the results of the SU21 simulation with the SU sediment characteristics, no tidal currents, and stripping. The solid contours are the MDFATE prediction with the contour thickness in centimeters placed next to the contour and labeled with a decimal point, e.g., 1.0, 2.0, etc., while the SPI measured cap thicknesses in centimeters labels are placed next to the colored dots, are whole numbers (e.g., 1, 2, 12, etc.), and are oriented vertically. Figure K-30 shows the depth of disturbance of the EA layer, in most cases the EA depth of disturbance was 2.5 cm or more. The maximum cap thickness predicted by MDFATE was 17 cm, as with the LU placements, it is believed this is more than would actually occur. The majority of the center of the cell is covered by about 12 to 14 cm of cap. As noted in other simulations, if resuspension were included, the maximum thickness in the center of the cell would be less. The cap is relatively symmetrical with the 1 cm contour having dimensions of 780 m long by 740 m wide.

SPI measurements show cap thickness greater than penetration thicknesses of 11 to 15 cm in the central portion of the mound with 5 to 8 cm covering a large portion of the mound. One to 3 cm of cap extend beyond the cell boundaries with thicknesses of 3 to 8 cm of cap just outside the cell boundary in the onshore and offshore directions. These greater thicknesses in the upslope direction are likely due to material from placements in LU moving down slope. Correcting for the EA depth of disturbance the agreement between SPI and the MDFATE simulation is generally within 1 to 3 cm.

Figure K-31 shows the MDFATE simulation with tidal currents, stripping, and SU sediments. Like the previous simulations, this reduced the peak and overall mound thicknesses, in this case the maximum thickness is 11 cm, a slightly better match to the SPI data. As with other simulations with tides, the contours are stretched in the NW to SE direction. The 1.0 cm contour has a diameter in the depth contour parallel direction of 855 m, while the shore normal diameter is about 530 m. The cap thicknesses predicted at the cell borders and outside the cell, particularly in the shore normal directions, are much less than SPI measurements. The MDFATE-predicted mound is also skewed downslope by about 100 m. The 1 cm contour is 200 m seaward of the seaward boundary of cell SU, while in the upslope-direction; the 1 cm contour is only 60 m inshore of the inshore boundary.

The SU21 simulations using the LU sediment characteristics resulted in similar patterns with slightly thinner mounds as would be expected with the reduced void ratios (Table K-12). It is likely that some intermediate combination of SU and LU sediments could provide a slightly better agreement with the SPI measurements. However, until good quality core data are available, the MDFATE simulations provide a reasonable estimate of actual cap dimensions.

Maximum cap extent. A set of SPI stations to those in conducted in cell LU to compute the far field extent of the cap placed in cell SU were performed. Appendix J, Figures 4.7-17 and 4.7-18 (SAIC 2001) show the cell locations and results. Our interpretation differs slightly from SAIC's. In the alongshore direction, up current direction (SE), the maximum cap extent is about 100 m

from the SU cell boundary. However, the closest placement to these SPI stations was some distance inside the cell boundary. The actual distance of maximum cap extent from the nearest placement was approximately 250 m, slightly greater than that seen in LU and consistent with the observation that footprints from individual placements in cell SU are larger due to the greater depth. The SU21 MDFATE simulation with no currents and SU sediment characteristics matches the SPI measurement of maximum cap extent almost exactly almost exactly (Figure K-29).

In the offshore, down slope direction (SW), the maximum extent of the cap was about 240 m from the SW cell SU boundary, but only 225 m from the closest placement point which was slightly outside the cell boundary. Note that the SU21 far field survey and SU 21 post placement survey had slightly different results on the interpretation of far field cap extent (Appendix J, Figures 4.14 and 4.17). In this interpretation, we chose to go with the SU21 post placement results. The SU21 MDFATE simulation with no currents and SU sediment characteristics (Figure K-29) also agreed almost exactly with the SPI measurements.

LD placements

As described earlier, placements in LD were done in “spreading” mode to minimize the potential for resuspension. MDFATE has a set of spreading algorithms that were used for these simulations. However, to confirm that the spreading mode option provided answers that better matched the SPI measured cap dimensions the initial LD placement was also modeled using the conventional placement mode.

Spreading simulation of initial LD load. Figure K-32 shows the results of the single LD spreading simulation compared to the SPI measurements. As noted earlier, MDFATE can only simulate spreading based on east to west or north to south placement (east to west was modeled in all cases). Illustrated in Figure K-32, the MDFATE simulated cap has a maximum thickness of 1.0 cm, the 0.9 cm contour (dashed line) is 440 m long and 40 m wide, while the 0.5 cm contour is 590 m long and 135 m wide. This simulated cap is considerably thinner than the SPI-estimated cap which is 800 m long with rounded ends (dog bone shaped) and also shown in Figure K-32. SPI cap thicknesses in the lighter brown area between in Figure K-31 are between 1.0 and 1.5 cm thick and the darker brown areas at the ends are between 1.5 and 2.5 cm thick. The width of the lighter brown center section is 140 to 260 m with the larger end sections, where the majority of material was placed, having widths of 260 to 300 m.

The dog bone shape is due to lateral spreading after the descending jet impacts the bottom and reflects the uneven rate of placement documented in the SAIC (2001) monitoring report. The ADISS data collected documented that higher rates of placement occurred after the hopper was initially opened in the SE section of cell LD, was less in the center, and increased again in the NW portion of the cell. Note that MDFATE cannot take into account the uneven rates of release.

However, it is unlikely that the SPI estimated thickness is all sand from borrow site A-III. The borrow sand in the LD SPI images was quite clear, it is

assumed that the estimate of cap thickness is just based on the thickness of the “golden sand” visible in the SPI images. However, Figure K-33 shows that there was between 0.8 and 2.0 cm of EA sediment disturbance over the impacted area. If the estimated EA disturbed layer thickness is subtracted from the total thickness, then the cap thickness due to the A-III sediments only is in the 0.5 to 1.0 cm range, quite good agreement with the thicknesses predicted by MDFATE.

Further verification of this explanation can be found by examining volumes. It is assumed that the EA sediment volume is included in the cap thickness measurement. To address this question, SAIC estimated the cap volume from the SPI thicknesses as 2,230 cu m. This is much larger than the volume placed 967 cu m and the MDFATE predicted volume on the seafloor of 835 cu m. While some bulking is possible following placement, this volume appears too large. It is suspected that over half the SPI cap volume is actually resuspended native material.

To investigate this fact, Figure K-33 was reviewed. The size of the EA layer disturbed was visually estimated as a rectangle 200 m wide by 775 m long and an average of 0.8 cm thick. The volume represented by the EA layer disturbed during LD1 placement is 960 cu m. If the total SPI thickness volume is divided by the 200 m wide by 775 m long footprint, then the average cap thickness is 1.4 cm, or 0.6 cm thicker than the EA layer. This 0.6 cm thickness of A-III cap material represents 930 cu m. This value compares well to the 967 cu m volume estimated by the NATCO load and the MDFATE predicted volume of 835 cu m.

If the above reasoning is correct, then the MDFATE spreading simulation estimate of cap thickness is reasonably close to the actual in an average sense.

Conventional simulation of initial LD load. For comparison, the initial LD placement was also simulated using conventional placement. The result is shown in Figure K-34. For this simulation, 75 percent of the load was simulated as being placed over the SE most 245 m of the cell, point at which ADISS measurements showed 75 percent of the load had exited the dredge. This was done in hopes of most accurately modeling the eastern portion of the cap. As can be seen in Figure K-34, a very narrow and peaked cap was predicted. The 1 cm contour only has a width of 95 m, compared to over 200 m as measured by SPI. Also, the maximum cap thickness as predicted by MDFATE was over 5 cm, much thicker than the SPI peak of just of 2-2.5 cm, which includes the resuspended EA layer.

Based on these results, it was decided to model the remainder of the LD placements using the spreading mode.

Spreading simulation of LD9. The MDFATE simulation and SPI results of the full nine placements in cell LD are shown in Figure K-35. The brown color ramp shows the SPI estimates of cap thickness, with the darker colors indicating greater cap thickness as predicted by SPI data. SPI thickness contours are in centimeters and are labeled as integers. The bright green colored lines are the MDFATE cap thickness contours, also in centimeters. The MDFATE contours are larger and have a decimal (e.g., 5.0). Depth contours are negative values in meters. The dog bone shape noted in the single placement continues for the full nine placements reflecting the difficulties in achieving a uniform release rate. The action of the surge current to disperse material cap beyond the cell boundaries is also evident. Possibly, a greater factor in the spread of material is

the fact that in the spreading mode, some of the material does not reach the bottom rapidly and remains in a cloud that settles more slowly allowing greater spreading.

Considering the limitations of the spreading mode capabilities in MDFATE, the predicted values agree quite well with the SPI predictions. Once again, it should be noted that the SPI cap thicknesses along the longitudinal axis of the cell under predict the cap thickness because the SPI camera could not penetrate the full cap thickness. Also, the SPI over predicts the cap thickness by including about 2 cm of EA sediment in the cap due to resuspension.

The maximum thickness predicted by MDFATE is 12 cm, while the maximum SPI prediction is greater than 11 cm. Note that the supplemental box cores taken in cell LD estimated cap thickness (visually – assumed to be mostly A-III sediments) as 11.5 and 12 cm. This location was near the >11 cm SPI estimate in the western portion of LD. The biggest difference between MDFATE and SPI are on the thinner portions of the cap outside the cell boundaries. The MDFATE prediction for the 1.0 cm contour is 620 m long and 315 m wide. In contrast, the SPI measurements show the 1.0 contour to extend greater than 1000 m long with a width of 500 to 620 m. As the cap gets thicker, the MDFATE and SPI measurements become closer. For example, the MDFATE 9-cm contour is 340 m long and 90 m wide while the SPI 9 cm contour is 460 m long and 130 m wide. The MDFATE 11-cm contour is 215 m long and 40 m wide.

The MDFATE and SPI contours are quite symmetrical. This is no surprise for the MDFATE thickness contours because no currents were imposed. The SPI contours are also quite symmetrical, showing little if any impact of slope.

The cap volumes in cell LD were also estimated and compared. The MDFATE simulation resulted in an estimated cap volume of 8,400 cu m, 99 percent of the maximum potential volume that would be on the bottom based on the placed volume of 10,300 cu m from the NATCO/ADISS records. Looking at the dog bone shaped footprint from SPI measurements, the overall average maximum length is about 800 m and the average width is about 500 m. In reviewing Figure K-36, the EA disturbance thickness estimate appears to average about 1.2 cm in thickness, over an area estimated to be 800 m long by 400 m wide, resulting in a volume from the EA layer of 3,800 cu m. The cap volume from the SPI data was 10,920 cu m within the cell boundary and 17,000 cu m total. If the 3,800 cu m of EA sediment volume is added to the MDFATE volume, the total becomes 13,200 cu m, 3,800 cu m less than the SPI volume. Part of the difference could be in the estimate of the EA thickness volume. Most likely, however, are the computer-generated contours of cap thickness from the SPI point measurements, when the number of points are limited, the accuracy of the contours, particularly at the edges of the area, is suspect.

These LD simulations used an as deposited void ratio of 0.75. Later investigations provided the estimates of bulk density from supplemental cores. These cores indicated a bulk density of 1.85 that translates to a void ratio of 1.0. A simulation with this as placed void ratio would increase potential volume and likely increase the MDFATE predicted thickness. Visual estimates from the supplemental box cores showed a cap thickness of 11.5 cm, this likely does

not included the mixed cap/EA layer. Some additional simulations at the higher as deposited void ratio could be worthwhile.

MDFATE model observations from the hindcast simulations. The SU simulations showed the sensitivity of MDFATE to the volume of the vessel. Applied Science Associates modified the version of MDFATE in DAN-LA to allow input files with multiple placements to be run in batch with all the pertinent variables associated with each placement included in the file. However, even though batch file provides the load, which was calculated equivalent volume removed from the channel at the *in situ* density (and approximately equal to the settled solids volume), the program still needs a vessel a vessel volume from another location in the input file. When this volume was out of the range of reasonable values (i.e., too large) the thickness of the cap became too thin, probably due to excessive spreading due to reduced volumetric concentrations. This aspect needs to be examined before additional modeling is done if possible.

MDFATE is also very sensitive to the depth at which the currents are measured is specified in the program. Deeper depths specified for a given current equate to greater bottom currents at a given depth when MDFATE computes a depth averaged current, which results in more dispersion and thinner mounds when tidal currents are specified. The assumptions made when the ADCIRC tidal constituents were computed should be examined before the next round of MDFATE simulations.

Cap volume estimates

In addition to the MDFATE simulations to predict detailed operational parameters, a good estimate of the in-channel and in-hopper volumes required to construct a pilot cap of a given thickness and area was needed to allow SPL and EPA personnel to make decisions on the volume of material to place during the Pilot study. This volume estimate was needed to compute a cost for the dredging and placement portion of the Pilot study. The volume to be dredged was then used to determine the best overall combination of cap volume placed and the amount of monitoring to achieve the project objectives. Many of the procedures used for these prior-to-placement volume estimates were developed during the prior *in situ* capping study and are described in Palermo et al. 1999. However, the techniques used to calculate cap volume estimates for the pilot study are more detailed, based on actual values, and are therefore thought to provide a better estimate of in-channel or in-hopper volumes required for a cap of a specific dimension. These procedures can also be used to make future estimates of required cap volumes. While MDFATE simulations are a part of this procedure, it involves a number of steps beyond those needed for the other MDFATE simulations.

The volume estimates are, in fact, a rough sediment mass balance for the dredging, transportation, and placement process for this project. Because the volume during each phase changes due to differing densities of material, the best method to track the amount of material is by mass. The appropriate mass to volume conversion can then be made as needed. A number of assumptions are required for the mass/volume estimate. In some cases, solid information on which to base the assumptions was not readily available. A major part of this effort was to compute the volumes required for a range of capping scenarios (cap

thickness and extent). For brevity, only the option selected for implementation during the pilot cap project (i.e., the modest cap option) is presented. The remainder of this section lists the steps required to compute the volume.

Steps required to compute the PV shelf cap volume

The following steps were followed to compute the in-hopper and in-channel volumes required to produce caps of a specified size. The section following these steps describes how each of these calculations was conducted and the source of the information.

- a. The *in situ* density of the sediment in the channel prior to dredging was determined to estimate the mass of material retained in the dredge during each load and the volume of sediment removed from the channel to create this load.
- b. The mass of the sediments retained by the dredge for each load was computed by estimating the volume and density of the material in the hopper.
- c. NATCO provided an estimate of the sediment volume lost during dredging followed by a subsequent calculation by ERDC.
- d. NATCO estimated any sediment losses that occurred during transportation to the PV shelf.
- e. Material losses during placement were estimated from the MDFATE model simulations.
- f. Required as-placed mound volumes for the selected capping scenarios, a 15 cm cap over all of LU and SU, and ten loads in LD, were determined from simple mound geometry.

Addendum A to this appendix provides details of information sources and calculation methods to the steps described above.

Cap Volume Results

The actual in-hopper and in-channel volumes required to achieve the desired cap volumes were computed using the data from the MDFATE simulations and the other computations described above. With this information, the number of hopper loads was computed to estimate costs and the in-channel volumes were computed so that SPL could determine if sufficient volume was available for dredging.

Table K-13 provides a summary of cap volume calculations described in detail in Appendix A. The following information was used by SPL and EPA to make a decision on the project, i.e., the likely number loads to place at 925 cu m per load for the Queen's Gate sediments. The modest cap scenario was 600 m long by 300 m wide by 15 cm thick, as modified based on 16 June 2000 MDFATE simulations. The cap volume estimate for the shallow cell LU was 43,000 cu m to be placed from 46 hopper loads, and the cap volume estimate for the deep cell SU was 67,000 cu m to be placed from 73 hopper loads. Additionally, 10 spreading loads from borrow area A-III were included.

Potentially, the total estimated volume of material was 110,300 cu m from 129 hopper loads.

STFATE Applications

The objective of STFATE simulations prior to placement was to examine bottom impact velocities, horizontal surge velocities, and plume impacts on kelp beds from individual loads. After placement, STFATE simulations were conducted for single load events and results were compared to measured horizontal surge velocities, BBADCP data illustrating plume dimensions, and TSS concentrations. This section describes the data input into the STFATE model and the simulation results.

Model input

Input for simulations made after placement utilized field data collected during the capping operation. The general input for the STFATE model simulations is described below.

Bathymetry

The STFATE simulations used the same multi-beam bathymetric survey data collected by CESPL as that used in the MDFATE simulations. The overall grid produced for most of the STFATE simulations were 44 (north/south) by 64 (east/west) with a uniform grid cell size of 30 m. A 54 by 47 grid with 60m cells was used for the pre-placement A-III borrow material simulation (Figure K-37).

Environmental Conditions

Water density. A four-point water density profile was used for all STFATE simulations. The water density was specified as 1.02158 g/cc at a depth of 6, 15, 23, and 40 m based on engineering judgment.

Current. Current values used in model simulations prior to the capping operation were based on summarized results of a PV shelf current study conducted as part of NOAA investigations of the PV site (Noble 1994). This study is described in greater detail in the previous section. For each STFATE simulation a representative depth averaged current was selected for use during the entire simulation. As will be discussed later, vertical shear in the ambient currents was modeled in the post-capping simulations.

Sediment characteristics used during STFATE simulations

The sediment used for STFATE simulations prior to actual placements was the fine sediment and the A-III borrow area sediment with 0.4 mm diameter described in the MDFATE Input section. Sediment characteristics are defined in STFATE by the following parameters: specific gravity, volume fraction of each type, fall velocity, as deposited void ratio, critical shear stress, cohesive, mixing,

stripping. See Table K-14 for values used in the pre-placement simulations. Table K-15 shows similar values used in the post-placement simulations.

Hopper dredge characteristics/volumes

The same hopper dredge characteristics as used in the MDFATE simulations were used for pre-placement STFATE simulations. Hopper load volumes used for STFATE simulations prior to the capping operation were 1650 cu m and 2,120 cu m. Volumes used in the STFATE post-capping hindcast simulations are presented later.

Placement scenarios/locations

Pre-placement STFATE simulations were performed with single loads of Queen's Gate material in order to look at the bottom impact velocities, horizontal velocity on the ambient sediment and impact of plume concentration on kelp beds. Also a simulation was performed with A-III borrow material placed in the LU cell using conventional placement. Post-placement simulation scenarios and locations were similar, except for the LD1 spreading operation.

STFATE results from pre-capping simulations

As noted earlier, resource agencies expressed concerns about the potential impact of cap material placed on the Palos Verdes shelf on the kelp beds. Concerns centered on increased turbidity levels associated with the placement activities. To address this concern, EPA requested CHL conduct an STFATE simulation to determine potential impacts associated with cap placement.

For this simulation of a nominal worst-case scenario, a constant current of 20 m/sec through the entire water column flowing at an angle of 60 deg (true north) was simulated. A current flowing at this angle is moving directly towards. Thus, the dredged material plume from a cap placement will have the greatest impact on the kelp beds under this scenario. The current amplitude and direction were derived from hour averaged time series plots of along-shelf and on-shelf currents measured during the USGS study of the PV conducted in the early 1990s (Noble 1994). The predominant current component is along-shelf in the northwest and southeast directions, but there is an on/off shelf component that averages about 10 cm/sec and reaches 20 cm/sec at times. Because this simulation was intended to be conservative, a constant on-shelf current of 20 cm/sec was used.

The results from this nominal worst-case STFATE simulation of a single load dredge material placement are shown in Figures K-38 thru K-46. The contours of the peak concentration in the plume anywhere in the water column for the first 2 hr of the simulation are shown at 15 min increments starting 19 min after the placement. The placement of a single load of dredged material removed from the Queen's Gate deepening is located at about the middle of cell LU and is indicated by the first black diamond symbol in the first snap shot, Figure K-38. Based on information provided by the Los Angeles District and EPA, the most seaward extent of the kelp beds are assumed to the 30 m contour. The green line with dots represents the 30-m contour on the figures.

The snap shots show that by the 3rd time increment or 49 min (Figure K-40) after the placement the plume has reached the 30 m contour with maximum peak concentrations of 70 to 100 mg/l. The diameter of the plume at this time increment is about 185 m measured from the 1 mg/l contour. Had this scenario been simulated with a 10 cm/sec current the plume is expected to reach the 30 m contour in about twice the time or approximately 2 hr.

While this simulation is unrealistic in the sense that the current is not likely to be constant over a distance from the placement cells to the shore it is reasonable to expect a constant current over the distance from the placement cells to the 30 m contour. The 30 m contour is within about 300 m of cell LU and the time for the plume to reach the 30 m contour is 1 to 2 hr given the range of onshelf currents. An increase in the plume travel time and distance to the 30 m contour is expected when an alongshore component is combined with the onshelf component and realistic time and spatially varying currents are simulated. For time and spatially varying currents the plume is expected to travel in a curved path rather than a straight line.

Figure K-46 shows the footprint of the placement. The maximum thickness is about 1.5 cm. Note that no sediments settling outside the placement area are shown, and those sediments that are not deposited initially remain in the water column for the entire 2-hr simulation.

The STFATE model can present TSS concentrations at four different depths and for the full range of sediment constituents, i.e., sand, silt and clay. Thus the results could be presented based on sediment constituents, time, or depth. The output from this simulation was shown as the maximum suspended sediment concentration anywhere in the water column, i.e., the worst case.

Also, for this simulation, the conditions which would produce a maximum concentration in the water column were used. This includes the high stripping option and assumes the silt and clay components are non cohesive, i.e., they will not floc to form larger particles which would tend to settle faster.

STFATE Results from Post-Capping Simulations

In 2001, STFATE was used to hindcast the monitored placements in cells LU and SU. An inspection of Acoustic Doppler Current Profiler (ADCP) data indicated that significant vertical shear in the ambient current existed during some of the disposals. Therefore, CHL staff decided that STFATE should be modified to allow for vertical shear in ambient currents over a variable bathymetry. These simulations are referred to as post-placement simulations. They involved simulations for the LU1-LU5 and SU1 placements, as well as, one new simulation involving the initial spreading placement operation in cell LD1.

Ambient current modifications in STFATE

Previously when applying STFATE over a variable bathymetry two options were available. One was to import a vertically averaged flow field and the other was to specify the velocity at one point along with the water depth at that location. A flow field was then created on the numerical grid by multiplying the specified velocity by a ratio of the specified depth and the water depth at a particular grid point. In some situations this can lead to unreasonable flow fields. For example, in an estuarine situation, if the specified velocity is located in a channel, velocities in the shallow areas will be much larger when in reality they should be smaller due to frictional effects.

Code modifications in STFATE now allow for a single specified velocity to be spread over the numerical grid based on frictional considerations if the disposal is in either a riverine or estuarine area. If the disposal takes place in a coastal environment (such as the Palos Verdes Shelf), Green's Law which relates tidal amplitudes to water depths is employed. In the first case, at depths shallower than the water depth where the data were collected, the velocity decreases. In the second case, since the tidal amplitude increases as one moves toward the shore, the algorithm implemented results in the velocity increasing at shallower depths.

In both cases, STFATE now allows the user to specify vertical shear in the ambient velocity over variable bathymetry. Three depths and the two velocity components at each depth are now specified, with linear interpolation of the velocity components at depths between the specified values.

Validation of STFATE Using LU1 Disposal Data

Data collected on 2 August 2000 for the LU1 disposal operation have been employed to validate STFATE with the latest information on ambient currents and the placement operation. These data consist of surge speeds from a bottom mounted current meter, near-bottom suspended sediment concentrations from bottle samples collected at several locations away from the disposal operation, and acoustic backscatter data along transects that crossed the suspended sediment plume. The acoustic backscatter data do not provide suspended sediment concentrations, but do yield information on the location and extent of the suspended sediment plume resulting from the disposal operation.

STFATE Input Data

Numerical Grid: When applying STFATE, a Cartesian numerical grid must be constructed, with bathymetry then assigned to each grid point. The grid used in all the simulations contains 64 x 44 computational cells, with the dimensions of each cell being 100 x 100 ft. The bathymetry placed on the grid is shown in Figure K-37. It can be seen that water depths at the LU site range from about 26 to 280 m. The location of the disposal operation occurred at a depth of about 40 m in the upper right part of the numerical grid (see Figure K-37). This is the same grid as employed in the earlier Palos Verdes' applications of STFATE.

Ambient Environment: Based on an inspection of data from the bottom mounted current meters, the ADCP data, and an analysis of drogue data (see Figure K-47) from SAIC (2002), the velocity magnitudes and directions of Table K-16 were specified at depths of 15, 30 and 40 m (49.2, 98.4, and 131.2 ft).

Depth (m)	Magnitude (cm/sec)	Direction (deg from north)
15	21	310
30	18	300
40	15	280

In addition to the ambient current, the water density must be prescribed. A surface value of 1.0255 gm/cc was specified with a linear stratification of 1.67×10^{-5} gm/cc/ft of water depth specified to reflect an increasing water temperature with depth.

Disposal Operation: The disposal vessel is a 280-ft-long and 5-ft-wide split hull barge. Figure K-48 illustrates that the vessel drifted slightly to the north during the disposal operation, which started at 19:21:03 (GMT) (see Table 3.2.2 in SAIC (2002)). However, Figure K-49 implies that the placement operation actually started closer to 19:20:30. About 180 sec were required to completely empty 2774 cu yd of material, with an average bulk density of 1.6 gm/cc. However, from an inspection of Figure K-49, it can be seen that only about 80 percent of the material was released over the first minute or so. Since STFATE doesn't allow for the impact of a continuous disposal operation on the movement of the bottom surge, the disposal operation was modeled in STFATE as a single instantaneous cloud of 2219 cu yd (80 percent of 2774). In the earlier application, the entire load was modeled. It is believed that the speed of the bottom surge that is first detected by a bottom mounted current meter is controlled by the initial rapid release of the disposal material.

Disposal Material: The disposal material was primarily fine sand and silt, with a small amount of clay. The fine sand had a d_{50} of 0.09 mm and made up 78 percent of the total solids in the barge. The silt fraction had a d_{50} of 0.05 mm and made up 19 percent of the solids. The remaining 3 percent of the solids were clay with a d_{50} of 0.005 mm. Settling velocities specified for the sand and silt fractions were 0.02 fps and 0.006 fps, respectively. Since the clay fraction was assumed to be cohesive, a settling velocity for the clay was computed within STFATE. A description of the settling algorithm employed in STFATE can be

found in Johnson and Fong (1995). In addition to the settling velocities, another important parameter that must be prescribed for each solids type is the critical shear stress for deposition. This parameter determines how/when small clouds of suspended sediment are created and whether or not material will be deposited. The values for the critical shear stress for deposition for the fine sand, silt, and clay fractions specified were 0.015 lb_f/cu ft, 0.009 lb_f/cu ft, and 0.002 lb_f/cu ft, respectively.

Model Coefficients: The coefficients in STFATE that have the greatest impact on model results are the entrainment (ALPHA0) and drag (CD) coefficients during the convective descent phase, the fraction of kinetic energy (S1) at impact lost due to the bottom impact, the drag coefficient (CDRAG), the friction coefficient (FRICTN) between the bottom surge and the sea bottom, and the horizontal turbulent dissipation parameter (ALAMDA) and vertical diffusion coefficient (AKY0). The following values were selected in the current application of STFATE at Palos Verdes.

$$\text{ALPHA0} = 0.68$$

$$\text{CD} = 0.20$$

$$\text{S1} = 0.50$$

$$\text{CDRAG} = 0.30$$

$$\text{FRICTN} = 0.003$$

$$\text{ALAMDA} = 0.002$$

$$\text{AKY0} = 0.005$$

The value of 0.68 for ALPHA0 was increased from 0.50 in the earlier applications, but still agrees fairly well with Bokuniewicz et al. (1978) and Proni (1994). Assuming the descending cloud is in a turbulent state, Lindeburg (1992) gives a value of 0.2 for CD. Bokuniewicz et al. (1992) discusses the loss of kinetic energy of the cloud in the form of elastic waves in the bottom sediments at bottom impact. Energy calculations by Bokuniewicz et al. (1992) substantiates the assumption that half of the cloud kinetic energy is lost at bottom impact. From Lindeburg (1992), since the expanding bottom surge takes the shape of a torus, an appropriate value for CDRAG in fully turbulent flow is about 0.3. The shear stress acting between the cloud bottom and the sea floor is assumed to be quadratic. A friction coefficient of 0.003 is typical for estuaries such as Chesapeake Bay. As discussed by Brandsma and Divoky (1976), values of ALAMDA should range from 0.0001 to 0.005. Values of vertical turbulent diffusivity coefficients are much less than horizontal values. Three-dimensional hydrodynamic model studies in estuaries such as Chesapeake Bay show that although there are times when the vertical diffusivity coefficient can attain values of 50-100 cm²/sec, e.g., during strong wind events, most of the time minimum values of 0.2 to 0.4 cm²/sec yield good salinity modeling results. Thus, a value of 0.005 cu ft/sec for AKY0 appears appropriate. Variations of the above values were tested in STFATE before settling on the final values that gave the best comparison with the field data collected during the LU1 disposal operation.

Model Output

Output from STFATE can be grouped as convective descent computations, bottom collapse computations, and water column suspended sediment computations. A brief summary of model results from the current simulation of the LU1 disposal operation is presented before discussing the comparison of model results with field data.

The descent of the single disposal cloud through the water column takes 7.4 sec before the leading edge impacts the bottom. From an initial radius of 30.6 ft the disposal cloud grows to a final radius at bottom impact of 80.2 ft as a result of entrainment of ambient water. The difference between the bulk density of the disposal cloud at impact and the ambient water is 0.0569 gm/cc. The insertion velocity of the disposal cloud was 9.6 fps, and increased as a result of gravity to a maximum velocity of 12.6 fps during the descent. However, as a result of the dilution of the cloud and resistive forces acting on the cloud, its velocity at bottom impact decreased to 7.3 fps.

As a result of the kinetic energy of the disposal cloud, the cloud begins to collapse vertically and spread horizontally over the sea floor. The change in potential energy of the collapsing cloud is converted to kinetic energy, which continues the horizontal spreading. As the cloud spreads on the sea floor, kinetic energy is dissipated through resistive forces acting on the collapsing cloud. The bottom spreading continues until either the rate of spreading becomes less than a rate estimated due to horizontal diffusion or the cloud energy becomes less than 0.01 percent of the energy at impact. Basic output from STFATE during the bottom collapse phase consists of the cloud thickness, its horizontal dimensions, and its bulk density. For the LU1 disposal, the bottom spreading ends at 740 sec after the initiation of the disposal operation. The cloud thickness at the end of bottom collapse is 3.1 ft and the horizontal dimensions are 982 by 977 ft. Although it is not significant, the impact of the bottom slope can be seen since the horizontal dimensions are not the same.

STFATE also generates a table during the collapse phase that shows the average speed of the front of the bottom surge or collapsing cloud for various distances from the disposal point. These speeds are a combination of (1) the change in the horizontal dimensions of the cloud as a function of time, (2) the movement of the cloud centroid as a result of the bottom slope, and (3) the movement of the cloud centroid due to the ambient current. The major component of the initial surge speed is due to the kinetic energy possessed by the cloud at the moment of bottom impact. However, the longer-term movement is due to the surge's potential energy being converted to kinetic energy.

As previously discussed, during both convective descent and bottom collapse, suspended solids can be separated from the main cloud. The material separated from the main cloud is inserted into small clouds that are assumed to have a Gaussian distribution. The user specifies those solid fractions that can be stripped during convective descent. For the current LU1 simulation, only the silt and clay fractions were allowed to be stripped during the descent of the cloud through the water column. In the pre-placement applications, the fine sand was also allowed to be stripped.

After the cloud impacts the bottom and the collapse phase is initiated, solids continue to be separated from the collapsing cloud for those fractions that could be stripped during descent. If either a shear stress computed from the rate of spreading of the collapsing cloud or one computed from the ambient current is larger than the critical shear stress for deposition for a particular solids fraction, material is separated from the collapsing cloud and inserted in small Gaussian clouds located at the top of the collapsing cloud. For solids that are not stripped, when neither shear stress is greater than the critical stress for deposition, material is inserted in Gaussian clouds with a very small thickness and placed at the sea bottom. This results in immediate deposition of material from these clouds. Each small Gaussian cloud settles at the specified particle-settling rate for its particular sediment type, and are transported and diffused by the ambient current.

Since the critical shear stress for the clay fraction is smaller than the shear stress computed from the ambient current, none of the material from clay clouds ever settles. However, 88 percent of the fine sand and 1.5 percent of the silt settles to the bottom within 780 sec, with the remainder of the sand settling to the bottom in the next 240 sec. At the end of 30 min after the beginning of the disposal operation, about 24 percent of the silt is on the sea bottom.

During the settling, transport, and diffusion of the small Gaussian clouds, the user can request concentration output on the horizontal numerical grid at various depths in the water column. Concentrations are computed by superimposing the small-suspended Gaussian clouds.

Comparison of Model Results to Available Field Data

The field data available for comparison with model results were data from current meters located about 100 m and 165 m downslope from the disposal point. These locations are given in SAIC (2002). The average speed of the bottom surge computed by STFATE and the speed based on field data showing the time required to travel to each meter are shown in Figure K-50. The average surge speed from the moment it struck the bottom until the front moved past the first meter (100 m away) was 91 cm/sec; whereas, the average speed during its travel to the second meter (165 m away) was 68 cm/sec. The average speeds computed by the model were 81 and 65 cm/sec, respectively. The model bottom surge speed computations show good agreement with the field data. However, it should be noted that the times of arrival of the surge in the field at the bottom meters were determined from Figure 3.3.6 presented in SAIC (2002), where the time axis covers in excess of 1 hr. Thus, there could be small errors in the timing estimates from these plots, resulting in some uncertainty in the field average surge speeds displayed in Figure K-50.

In addition to the current meter data, plots of backscatter intensity along the transects shown in Figure K-51 were available at various times after the disposal operation had begun. These plots are presented in Figures K-52 thru K-57. As discussed by Tubman in SAIC (2002) these plots do not yield information on suspended sediment concentration in the water column. However, they can be used to qualitatively assess the extent and width of the suspended plume. The higher intensity levels shown on the plots are a strong indicator that material from the disposal operation was detected by the towed BBADCP. In areas where

the background variability is large, there is greater uncertainty in the interpretation of results from the instrument, resulting in the smaller intensities displayed in the backscatter plots.

From an inspection of Figure K-52 (Transect 1), it can be seen that, at sometime during the first 180 sec after the beginning of the LU1 disposal operation, material from the disposal was detected over the upper 25-30 m of the water column at a distance of about 75-100 m downstream from the disposal point (ambient current is directed toward the northwest). The width of the plume at that time and location was about 50 m. From a depth of about 5 m to 20 m, the centroid of the plume is located about 50-75 m to the right (looking in the northwest direction) of that portion of the plume located at a location of about 20 – 30 m below the surface. This correlates with the paths of two drogues released at the disposal site at depths of 15 m and 30 m (see Figure K-47) and the velocities specified in STFATE (Table K-16).

Figure K-53 shows results along Transect 2 at 2 min after the end of the disposal at a location about 200 m away from the disposal point. Once again the plume can be viewed as being composed of two parts, with the upper water plume continuing to move along the path of the drogue released at 15 m and that portion of the plume located between 20 – 30 m following the path of the drogue released at 30 m. Little horizontal diffusion appears to have taken place between Figures K-52 and K-53. Some material appears to be located near the bottom along Transect 2. It is difficult to say whether this material is reflective of the bottom surge or material suspended in the water column that is being transported and diffused by the currents. The total width of the material occupying the lower 5-10 m of the water column appears to be in excess of 300 m.

Results at 9 min after the disposal ended along Transect 3, which is located about 200 m away from the disposal point, are shown in Figure K-54. These results show that material is suspended throughout the water column. The width of the plume at a depth of 20 – 30 m is about 250 m. Near the bottom it appears that the width of either the bottom surge or the material in suspension is about 400 m.

Sixteen minutes after the termination of the disposal, at a distance of 300 m from the disposal point (Transect 4), the backscatter results indicate the upper water column plume now has spread over a distance of about 200 m, and that portion of the plume located at a depth of 20–30 m has diffused to a well-defined width of about 300 m (see Figure K-55). Material near the bottom has now spread about 350 m. It is important to realize that although all of these transects cut through some portion of the plume, they do not show where the leading edge of the plume was located when the transect was run.

Figure K-56 displays results 22 min after disposal ended at a location 400 m from the point of disposal (Transect 5) shown in Figure K-48. These results show a well-defined upper and middle water column plume with the width of the upper portion being about 200 m and the middle water column plume being about 400 m wide. The lower water column plume is less well defined.

At 30 min after the disposal was completed, Figure K-57 (Transect 6) shows that the plume hasn't spread horizontally substantially from the widths illustrated in Figure K-56 (note that the scales are different). Again, recall the note above about not knowing where the transect lies in the body of the plume.

These results seem to imply that since the disposal material is composed of fairly fine-grained material a suspended sediment plume will persist for a long time. In fact it is difficult to envision that the clay fraction will ever completely settle to the ocean floor. Obviously, over time the plume will become more and more diffuse, and the material from the plume will eventually become part of the background.

The suspended sediment plume computed by STFATE at depths of 50 (15.2 m), 90 (27.4 m), and 39 m (39 m) at the end of bottom collapse and at times of 1,500 and 1,800 sec after the disposal began are presented in Figures K-58 thru K-66. Note that an "X" identifies the disposal point, and that the suspended sediment plume for each case is shown as a "zoomed in" plot. The distance between the grid points displayed is 100 ft (30.5 m). It can be seen from Figures K-58 thru K-60 that at the end of bottom collapse the maximum concentrations at 15 m are 50-100 mg/l and 250-500 mg/l at 27 m. The high values at 27 m are due to the clay and silt fractions being sheared from the top of the collapsing cloud. At the end of collapse, concentrations near the bottom at 39 m are relatively small, i.e., 25-50 mg/l. The plume width varies from about 185 m (182.9 m) at 15 m to about 400 m (396.3 m) at 39 m. At 1,500 sec after the disposal occurred (see Figures K-61 thru K-63), the maximum concentrations at 50 and 27 m have decreased to 25-50 and 100-250 mg/l, respectively, whereas, those at 39 m have increased to 250-500 mg/l. The reason for this increase is due to settling of material in the water column. Plume widths have increased to about 215 m (213.4 m) at 15 m below the water surface and to about 1185 m (487.8 m) near the bottom at 39 m. After 1,800 sec, Figures K-64 thru K-66 show that the maximum concentrations at 15 m are 10-25 mg/l, whereas, those at 27 m and 39 m are still in the same ranges as at 1,500 sec. Plume widths have increased slightly over those after 1,500 sec.

Note that the centroid of the plume at all depths has moved to the northwest, with the distance being less in the lower water column. This is a result of the vertical velocity profile shown in Table K-16. Also note that since water depths to the northeast of the disposal point are less than 39 m no water column plume exists there.

Total suspended solids concentrations were collected in the field very near the bottom. After about 3 min, values as high as 1,600 mg/l were collected at a depth of 40.5m (132.8 m). This can't be compared with computed results since no suspended concentrations are computed until the end of bottom collapse, i.e., about 745 sec after the disposal began. In addition, there is no way to tell if all of this concentration is due to disposal material rather than material that has perhaps been eroded from existing bottom sediments. At the end of 5 min (600 sec), one sample showed a concentration of 1,600 mg/l at 19.4 m (63.6 ft), indicating that material is indeed separated from the top of the collapsing cloud. After 35 min, the field data indicated concentrations close to 100 mg/l at 40.8 m (133.8 ft), whereas, after 30 min, STFATE computes values in the range of 250-500 mg/l at 39 m.

Both the computed plume and the observed plume data show that the width of the plume increases with depth. Although the computed plume widths do not agree exactly with the widths determined from the backscatter data, they are generally fairly close. For example, the backscatter data imply that 30 min or so after the disposal the upper water column plume ranges from about 200 m wide

in the upper water column to about 400 m wide in the lower water column. Corresponding widths of the computed plume are about 200 m and 450-500 m, respectively. Much uncertainty exists in the observed widths. The location of the transect in the body of the plume is unknown, and the determination of the horizontal extent of the plume from Figures K-52 thru K-57 is very subjective. The entire plume, at a particular depth, can be seen in the computed results.

Computed concentrations at lower depths do not show a consistent decrease in suspended sediment concentrations over the time period shown. This is because suspended material settles throughout the water column. For example, as material settles from the 27 m level material from above settles into the 27 m level. In addition, it could be that some material suspended below this level diffuses upward. However, after a sufficiently long period of time, concentrations throughout the water column will decrease due to settling and horizontal diffusion.

STAFATE Validation Conclusions

Available field data consisted of current meter data at two locations away from the point of disposal, backscatter plots from a BBADCP that qualitatively show the horizontal extent of the suspended sediment plume at various distances away from the disposal point at various times, and suspended sediment concentrations near the bottom. The BBADCP plots do not provide information on water column concentrations nor on the locations of the leading edge or centroid of the plume. In future studies, data taken continuously over time along a single transect located some distance from the disposal is desirable. This would provide more definitive information on the speed and size of the suspended sediment plume.

The computed average bottom surge speeds agree well with the current meter data located down slope from the disposal. Given the simplistic nature of how STFATE computes the bottom collapse phase, i.e., as a collapsing ellipsoid, it is difficult to determine an up slope speed. One could compute a speed with no bottom slope to determine the contribution of the slope component to the total speed and then subtract that component twice from the speeds reported here to obtain an estimate.

Comparison of the computed and observed water column plume is very qualitative. However, the results do generally support the conclusion that the computed suspended sediment plume compares well with the estimated size of the observed plume. It is difficult to directly compare computed suspended sediment concentrations with those from water samples collected in the field. However, the limited comparison after about 30 min appears reasonable.

It can be concluded that results from the current application of STFATE compare quite well with the observed data. This application contains a more realistic representation of the ambient currents, and, for the purpose of computing bottom surge speed as accurately as possible, the disposal operation is more accurately modeled than in the earlier application. However, to accurately compute the spatial distribution of the bottom surge resulting from the disposal of dredged material in open water, a more rigorous three-dimensional computational model is required. Such a model is being developed under the DOER Program.

Application of STFATE to Other LU Disposals

LU2 Disposal

The LU2 disposal operation began at 7:32:02 (GMT) on 13 August 2000 at the same location as the LU1 disposal (see Figure K-48). At the time of this disposal operation, the ambient current contained significant vertical shear. The magnitude of the ambient velocity and its direction at 15, 30 and 40 m are shown in Table K-17:

Depth (m)	Magnitude (cm/sec)	Direction (deg from north)
15	10	60
30	8	200
40	8	240

This profile was determined from the bottom mounted current meters and ADCP data presented in SAIC (2002). No drogue data existed for the LU2 disposal.

The material disposed was slightly different from the LU1 material. The fine sand fraction constituted 90 percent of the solids, with the silt constituting 9 percent and the clay fraction only 1 percent. The grain sizes were the same as for LU1. Thus, settling velocities and critical shear stresses were the same as specified for the LU1 simulation. The disposal vessel, depths prescribed on the numerical grid, and the ambient stratification were also the same as for the LU1 simulation.

An inspection of Figure K-67 showing the vessel draft versus time reveals that less material was immediately released than in the LU1 disposal. In addition, Figure 3 shows a much greater northerly drift of the vessel during the disposal operation. Based on Figure K-67, it was assumed that only 60 percent of the full load was immediately released.

Since the bulk density of the material is slightly higher than for the LU1 material (1.7 versus 1.6 gm/cc), the injection velocity is slightly higher, i.e., 10.2 ft/sec versus 9.6 ft/sec. The downward velocity increased to 13.0 ft/sec and then decreased to 6.9 ft/sec by the time the bottom was impacted after 7.7 sec. With a total volume of disposal material of 1584 cu yd (60 percent of 2640 cu yd), the initial radius of the disposal cloud was 27.3 ft and grew to 78.2 ft at the moment of bottom impact.

Computations for the collapse of the cloud continued for 838 sec, with the final bottom cloud being 3.1 ft thick and having horizontal dimensions of 943 x 984 ft. A comparison of the computed and measured surge speeds is given in Figure K-68. It can be seen that the agreement is not as good as for the LU1 simulation, although, the rate of decrease of the average surge speed with

distance compares well. Other than uncertainty in how much of the total load initially contributes to the bottom surge speed and the fact that there was much more movement of the disposal vessel away from the targeted release point, the reason for the greater discrepancy is unknown.

After 900 sec, 88 percent of the fine sand and about 0.1 percent of the silt have deposited on the sea floor. There is no deposition of clay particles during the complete simulation. After 1,140 sec, all of the fine sand and about 0.2 percent of the silt have deposited. There is virtually no additional deposition of silt for the remainder of the simulation. The reason for little deposition of silt is because the suspended material near the bottom is transported into deeper water to the southwest of the disposal point by the ambient current (see Table K-17).

No plume tracking took place for either the LU2 or the LU3 disposal operations. The computed suspended sediment plume at depths of 15, 27, and 39 m at the end of bottom collapse and 1,800 sec after the disposal operation began are presented in Figures K-69 thru K-74. At the end of collapse at 842 sec, maximum concentrations were 25-50 mg/l and 100-250 mg/l at depths of 50 and 27 m, respectively. At 39 m the maximum concentrations were only 25-50 mg/l. After 1,800 sec, the maximum concentrations were 10-25, 50-100, and 100-250 mg/l at depths of 15, 27, and 39 m, respectively. Note that these concentrations are slightly lower than those in the LU1 disposal. However, recall that less material is disposed in the model results in the LU2 disposal. Plume widths show the same pattern of increasing with water depth.

Figures K-69 thru K-74 show that the centroid of the upper water column plume moves toward the northeast, whereas, the lower column plume moves more toward the south or southwest. An inspection of Table K-17 reveals that this is the proper behavior given the vertical velocity profile input to STFATE.

LU3 Disposal

The location of the LU3 disposal was the same as for the LU1 and LU2 disposals and occurred at 10:58:14 (GMT) on 13 August 2000. The disposal material had a bulk density of 1.71 gm/cc and the solids were composed of 83 percent fine sand, 16 percent silt, and 1 percent clay. An inspection of the vessel draft versus time in Figure K-75 resulted in the assumption that about 60 percent of the disposal load was released very quickly, with another quick release about 1 min later. The remaining load was released at a slower rate. Based on data from the bottom mounted current meters and ADCP data presented in SAIC (2002), the vertical distribution of the ambient current near the disposal point shown in Table K-18 was employed.

Table K-18 Vertical Profile of the Ambient Current During the LU3 Disposal		
Depth (m)	Magnitude (cm/sec)	Direction (deg from north)
15	6	150

30	4	80
40	4	800

All operational parameters and model coefficients were the same as for the other LU disposals. Impact of the descending cloud with the sea bottom occurs at 7.7 sec after the release of the disposal cloud. Due to entrainment of the ambient water, the radius of the cloud grows from 27.5 ft (reflecting a disposal volume of 60 percent of 2,676 cu yd) to 78.4 ft at the moment of impact. The injection velocity was 10.3 ft/sec and increased to a maximum of 13.1 ft/sec before decreasing to 6.9 ft/sec at bottom encounter.

Collapse of the disposal cloud on the bottom ended at 786 sec after the initial release of material. The final dimensions of the bottom cloud were 3.0 ft thick and 947 x 991 ft. After 840 sec, 87 percent of the fine sand and 7 percent of the silt are on the seafloor. After 960 sec, all of the fine sand and 22 percent of the silt have settled to the bottom. About 70 percent of the silt settles to the seafloor within 1,800 sec after the disposal operation was initiated. Note that the transport of suspended material in the lower water column is toward the northeast into shallower water.

Results presented in Figure K-76 show that the computed and measured surge speeds compared well at 80, 160, and 240 m from the disposal point. The computed speed is slightly higher at 80 m and slightly lower than the field data at the other locations. Thus, the computed rate of decrease of the surge speed with distance is slightly greater than that reflected by the field data.

Figures K-77 thru K-82 show plan form plots of the suspended sediment plume at 15, 27, and 39 m immediately after the bottom collapse phase was terminated and again near the end of the simulation at 1,800 sec after the disposal occurred. Maximum concentrations and plume widths at depths of 50 and 27 m are similar to those for the other LU disposals. The impact of the ambient current input to STFATE can be seen, i.e., the plume at 15 m moves to the southeast, whereas, the plume at 27 m moves in an easterly direction.

LU4 Disposal

The location of the LU4 disposal was taken to be identical to the other LU disposals. Thus, the same disposal depth of 128.1 ft applied. This disposal occurred on 13 August 2000 at 16:59:09 (GMT), with plume tracking conducted along the transects shown in Figure K-83.

The path of the vessel during the disposal operation is shown in Figure K-48. It can be seen that instead of a slow northerly drift as occurred in the LU1 disposal, the disposal occurred while the vessel turned. Figure K-84 shows that about 70 percent of the disposal material exited the vessel fairly quickly. Again, as in the other simulations, it is assumed that the bottom surge initially detected by the current meters is due to this initial rapid release of disposal material.

Based on results from the bottom current meters, ADCP data and the paths of two drogues released at 15 and 30 m (see Figure K-85), the following velocity

distribution of Table K-19 was specified in STFATE, with velocities at other grid points being computed as previously discussed.

Table K-19 Vertical Profile of the Ambient Current During the LU4 Disposal		
Depth (m)	Magnitude (cm/sec)	Direction (deg from north)
15	14	300
30	14	300
40	14	30

It can be seen that for the LU4 disposal, no vertical shear in the ambient current was specified even though some shear is implied by the drogue data. The reason for not specifying any vertical shear is because no vertical shear was detected by the ADCP, and an inspection of the backscatter plots did not imply that any was present.

The solids in the disposal material consisted of 90 percent fine sand, 8 percent silt, and 2 percent clay. The bulk density was 1.71 gm/cc and, based on Figure K-84, the volume of disposal material was 1873 cu yd (70 percent of 2676 cu yd). This yielded a disposal cloud with an initial radius of 28.9 ft. At the moment of bottom encounter at 7.2 sec after the disposal, the radius was 79.1 ft. The injection velocity was 10.3 ft/sec. The maximum velocity the descending cloud attained was 13.3 ft/sec but decreased to 7.4 ft/sec at bottom impact.

The collapse of the cloud on the sea floor continued for 735 sec. The final dimensions of the cloud were 2.8 ft thick with horizontal dimensions of 1,037 x 1,007 ft. Figure K-86 shows a comparison of the computed surge speeds with measured results from the bottom mounted current meters at distances of 70, 135, and 240 m down slope of the disposal point. Excellent agreement is seen at the 70 m location, with the computed average surge speed being too high at the other locations. The computed rate of decrease is too low from 70 to 135 m, but compares well with the field data from 135 to 240 m.

After 780 sec, 85 percent of the fine sand and 6 percent of the silt have deposited on the bottom. After 900 sec all of the fine sand and 20 percent of the silt have settled to the bottom. With the ambient current being 14 cm/sec throughout the water column, none of the clay fraction ever deposited. After 1,800 sec, about 66 percent of the silt is on the bottom.

Computed suspended sediment concentrations at depths of 15, 27, and 39 m below the water surface are presented in Figures K-87 thru K-95 at 900, 1,200, and 1,560 sec after the disposal occurred. Since the ambient current is uniform throughout the water column and directed toward the northwest, it can be seen from the plots that the computed plume moves toward the northwest at all depths. After 900 sec, maximum concentrations are 25-50, 100-250, and 25-50 mg/l at depths of 15, 27, and 39 m, respectively. The water column plume varies in width from about 150 m (152.4 m) to 400 m (396.3 m).

After 1,560 sec, concentrations at 15 m have decreased, with the maximum concentrations at 90 and 39 m being 100-250 mg/l. Plume widths of about 185 m (182.9 m) and 1150 m (457.3) at depths of 50 and 39 m are computed. The upper right corner of the plume at 39 m is not plotted. As noted previously, this is because the water depths at those locations are less than 39 m.

Water samples collected very near the bottom yielded concentrations as high as 3400 mg/l after 1 min, with those concentrations decreasing to about 15 mg/l after about 30 min. The same comments made in the LU1 discussion about comparing model results with the water sample data apply here also.

Figures K96 thru K-98 present backscatter plots along transects that are about 100 m upstream of the disposal point (see Figure K-83). These show disposal material in the upper part of the water column even though the ambient current is directed in the opposite direction. If the disposal operation had been stationary, it is unlikely suspended material in the upper water column would be detected at these transects. However, with material being released while the disposal vessel moves (see Figure K-48), the resulting suspended sediment plume is more complex and interpretation of the backscatter results is more difficult. Since the disposal operation is modeled in STFATE as an instantaneous stationary operation, model results do not show an upper water column suspended sediment plume upstream of the disposal point. Figures K-96 thru K-98 also show disposal material near the sea bottom. This is likely material in the bottom surge that remains in suspension.

Figures K-99 thru K-101 show backscatter results along Transects 6, 7, and 8, respectively, (Figure K-83) from 17 to 31 min after the disposal ended. These results show a suspended sediment plume with a width of perhaps 300-400 m in the upper and mid-water column; whereas, the model computes a corresponding plume width of about 200 m. However, recall that about 20 percent of the disposal material was released while the disposal vessel was making a wide turn. Thus, one would expect a larger upper water column plume to be generated than the one computed by STFATE. Note that Figures K-99 thru K-101 show a plume that is fairly uniform throughout the water column, indicating little vertical shear in the ambient current.

LU5 Disposal

The LU5 disposal began at 20:19:00 (GMT) on 13 August 2000. Based on drogue data (see Figure K-102), bottom mounted current meters, and ADCP data, the vertical distribution of the ambient current at the disposal site is shown in Table K-20:

Table K-20 Vertical Profile of the Ambient Current During the LU5 Disposal		
Depth (m)	Magnitude (cm/sec)	Direction (deg from north)
15	15	60
30	12	275
40	5	275

As can be seen, there is a great difference in the direction of the water movement from the upper water column to the lower. Thus, one would expect the upper water column suspended sediment plume and the lower water column plume to move in different directions.

Based on the vessel draft versus time plot in Figure K-103, the volume of the LU5 disposal was taken to be 2141 cu yd (80 percent of 2676 cu yd), resulting in an initial disposal cloud with a radius of 30.22 ft. The solids were composed of 87 percent fine sand, 9 percent silt, and 4 percent clay fractions. The bulk density was the same as that of the LU3 and LU4 material; namely, 1.71 gm/cc. All other parameters such as bathymetry, ambient density, etc were the same for all LU disposals.

The injection velocity of the descending cloud was 10.3 ft/sec and increased to a maximum speed of 13.6 ft/sec before decreasing to 7.8 ft/sec at bottom impact. The final radius of the descending cloud was 80.1 ft.

The bottom collapse phase ended at 831 sec after the initiation of the disposal operation. The final bottom surge dimensions were computed to be 3.1 ft thick and 995 x 1,048 ft in the horizontal. As can be seen from Figure K-104, only one current meter was in operation for the LU5 disposal. The computed bottom surge speed agrees well with the measured data at that one location (140 m).

After 840 sec, 85 percent of the fine sand and 0.7 percent of the silt are computed to be on the bottom. After 1,080 sec, the amount of deposited material increases to 100 percent of the fine sand and 18 percent of the silt. After 1,800 sec, 42 percent of the silt is on the bottom.

Figures K-105 thru K-113 show the suspended sediment plume computed by STFATE at depths of 15, 27, and 39 m below the water surface at 1,080, 1,500, and 1,860 sec after the disposal began. As expected, the plume at 15 m moves toward the northeast, whereas, the plume at 90 and 39 m moves basically toward the northwest. After 1,080 sec, maximum concentrations of 25-50, 100-250, and 100-250 mg/l are computed at 15, 27, and 39 m, respectively. Plume widths are generally about 150 m (152.4 m) in the upper water column and about 1150 m (457.3 m) over the lower water column.

Figure K-111 shows an interesting behavior after 1,860 sec. It appears that the plume has broken into two separate plumes. However, note that the concentrations are very low (1-10 mg/l). It is likely that nonzero concentrations exist between the two plumes but are below 1 mg/l so that they are not plotted. Maximum concentrations after 1,860 sec are 10-25 mg/l in the upper water column and 100-250 mg/l over the lower water column. The plume width over the lower water column is about 1,800 ft (548.8 m).

Water samples yielded a maximum concentration very near the bottom of 2700 mg/l after 1 min and concentrations less than 50 mg/l after 32 min. Again, it is difficult to compare the computed plume suspended sediment concentrations with the field data.

Figure K-114 shows the locations of the transects along which the BBADCP was towed. It can be seen that two transects were basically run across the point of disposal. Figure K-115 shows results along Transect 1. A plume of fairly constant width through the water column of only about 50 m is centered slightly down slope (to the south/southeast) of the disposal point at 8 min after the termination of the disposal. This does not correlate with the vertical shear in the ambient current since the ambient current is directed toward the northeast over the upper 15 m of the water column (see Table K-20). Figure K-116 shows results along approximately the same transect as in Figure K-115, but the plume has moved up slope (to the north/northeast) as the ambient current indicates it should. The width of the near bottom plume appears to be about 500-600 m after 18 min, which agrees well with the computed width. Figure K-117 shows results after 22 min along Transect 3 which is located about 100 m from the disposal point. These results imply a suspended sediment plume that extends over the complete water depth with no vertical shear and a relatively constant width of 400 – 500 m. The computed results show a water column plume with material in the upper water column moving to the northeast while material in the lower water column moves to the west/northwest.

The constant width plume over the water column shown in the Figure K-117 doesn't agree with the general shape of a plume increasing in size with water depth that the field data showed for the LU1 disposal operation. However, as for the LU4 disposal, the disposal vessel was in a turn during the disposal, resulting in perhaps a larger suspended sediment plume over the upper and mid-water column than the one generated during the LU1 disposal. At 49 min after the disposal ended, results from Transect 6 (Figure K-118) show a near bottom plume about 600 m long. Since the width and length of the plume are about the same, this indicates that the plume is basically circular.

Conclusions on LU Disposals

The major differences between the simulation of each of the LU disposals was the ambient current specified in STFATE and the amount of the total load that was considered to be released instantaneously. All other ambient conditions, operational parameters, and material characterization were quite similar.

A comparison of computed average surge speeds with data from bottom mounted current meters show relatively good agreement considering the simplistic nature of how STFATE computes bottom surges. The reason for the good agreement is probably because the speed of the bottom surge is more a function of the energy it possesses at bottom impact than the bottom slope near the disposal point. As previously discussed, the kinetic energy at bottom impact appears to control the initial speed of the surge, with the surge's potential energy controlling the surge speed away from the disposal point.

Data from the BBADCP can only be viewed in a qualitative sense. Data from the LU1 disposal seemed to be the most consistent when viewed along with the tracks of drogues released at depths of 15 and 30 m in the water column and

data from an ADCP. The general shape and size of the computed water column plume and that interpreted from the BBADCP results agreed. The plume tends to increase in size with depth, and the rate of diffusion of the plume tends to increase with depth. Generally, after 30 min or so the suspended sediment plumes from both STFATE and the LU field data have a width of 150-200 m in the upper water column and 400-600 m near the bottom.

No BBADCP data were taken for the LU2 and LU3 disposals. Due to some of the disposal material being released while the vessel was turning (see Figure K-48), BBADCP data for both the LU4 and LU5 disposals were more difficult to interpret.

Application of STFATE to the SU1 disposal

On 8 August 2000 at 18:34:29 (GMT), a disposal was initiated at the SU site shown in Figure K-37. The same numerical grid as employed in the LU disposal simulations was employed in STFATE. However, the disposal point is now located in the lower left hand part of the grid. The depth at the disposal point was 199 ft. Based on data from the bottom mounted current meters, ADCP data, and drogues released at 10 and 30 m, (see Figure K-119) the velocity profile of Table K-21 was specified in STFATE.

Table K-21 Vertical Profile of the Ambient Current During the SU1 Disposal		
Depth (m)	Magnitude (cm/sec)	Direction (deg from north)
15	16	125
40	6	65
60	5	160

Model coefficients and the ambient water stratification were the same as in the LU simulations previously discussed.

The bulk density of the disposal material was 1.486 gm/cc, with the solids being composed of 90 percent fine sand, 9 percent silt, and 1 percent clay. The gradation of the solids was the same as the LU disposal material. Thus, settling velocities and critical shear stresses were the same as in the LU simulations. The total volume of material disposed was 3325 cu yd. However, an inspection of Figure K-120 resulted in assuming that 80 percent was released immediately from the disposal vessel. This resulted in a disposal cloud with an initial radius of 32.5 ft.

With the deeper water depth at the SU site, the time of descent until bottom encounter was 17.4 sec. With the increased descent time, the entrainment of ambient water increased, resulting in a disposal cloud with a radius of 119.4 ft at bottom impact. Due to the smaller bulk density of the disposal material compared to the LU material, the injection velocity was 9.8 ft/sec. The maximum velocity attained by the descending disposal cloud was 12.0 ft/sec, with the velocity at bottom impact being reduced to 4.8 ft/sec.

As can be seen from Figure K-121, the STFATE average surge speeds are a little higher than the observed average surge speed at 115 and 170 m from the disposal point, but the rate of decrease of surge speed with distance compared well. Comparing the behavior of the surge at the SU site with that at the LU site, it can be seen that the speed is not reduced as much from the first current meter to the second one at the SU site. This is likely due to the increased bottom slope at the SU site over that at the LU site.

The bottom collapse phase continued for 1,262 sec. At the end of the collapse phase, the final cloud was 4.0 ft thick with horizontal dimensions of 1,779 x 1,583 ft. Although STFATE doesn't accurately compute the impact of bottom slope on a spreading bottom surge, the impact of the large slope at the SU site can be seen since one horizontal dimension is almost 200 ft larger than the other. The impact of the deeper depth can also be seen in the increased size of the bottom surge. This agrees with data collected by Bokuniewicz et al (1978).

At 1,320 sec after the disposal occurred, 89 percent of the fine sand is computed to be on the bottom, with 0.6 percent of the silt having been deposited. After 1,620 sec, essentially all of the fine sand and 2 percent of the silt are computed to be on the sea floor. Even after 2,400 sec only about 6 percent of the silt has deposited. Comparing these percentages with those from the LU simulations, it can be seen that at the deeper site more of the material remains in suspension for a longer period of time. Also note that the ambient current is directed to the southeast near the bottom, resulting in the transport of suspended material into deeper water.

Figures K-122 thru K-133 show the computed suspended sediment plume at depths of 50, 100, 150, and 127 m at the end of the bottom collapse and at times of 2,040 and 2,460 sec after the disposal occurred. At the end of bottom collapse, maximum water column concentrations range from 10-25 mg/l in the upper water column to 50-100 mg/l in the lower water column. Near the end of the simulation, at 2,460 sec after the disposal occurred, maximum concentrations are less than 10 mg/l over the upper water column and less than 50 mg/l over the lower water column. The width of the plume at the end of collapse ranges from about 515 m (167.7 m) in the upper water column to about 1215 m (518.3 m) in the lower. After 2,460 sec, the plume widths are about 215 m (213.4 m) and 2,100 ft (640.2 m), respectively. Note that due to the ambient current profile in Table K-21, the plume in the upper part of the water column is directed to the southeast, whereas, that in the middle of the water column is directed to the northeast and that in the lower part of the water column is directed toward the south.

Water samples for determining suspended sediment concentrations were collected during the SU1 disposal operation. After 3 min, at a depth of 60-61 m, the concentration was 27 mg/l. After 22 min at the same depth it was 10 mg/l. This correlates fairly well with computed concentrations of less than 50 mg/l at 127 m (57.9 m) after 34 min. However, after 52 min at a depth of 58.6 m a concentration of 1100 mg/l was measured from a water sample. Such a high concentration almost 1 hr after the disposal appears questionable.

Figure K-134 shows transects along which the BBADCP was towed at different times. Figure K-135 displays backscatter data along Transect 3, at 19 min after the end of the disposal operation, from about 35 m below the water

surface to the bottom. After 19 min, there is a basic core of suspended sediment of about 150 m wide over the disposal point.

After 31 min, results in Figure K-136 for Transect 4 show a plume between 35 and 50 m below the surface that is located at the disposal point and has a width of about 250 m. Its centroid is about 50 m away from the disposal point toward the south (down slope).

Figure K-137 for Transect 5 shows that part of the suspended sediment plume at depths greater than 35 m still resides over the disposal point 39 min after the disposal ended. The width is about 200 m at a depth of 35 m, whereas, at a depth of 50 m the width is 400 m or more, with the centroid directed up slope (to the northeast). Figures K-127 and K-128 show a computed plume at the disposal point at the same time with a width of about 120 m at a depth of 100 ft (30.5 m) and 400 m at a depth of 115 m (45.7 m). The computed plume in Figures K-127 and K-128 clearly imply that the BBADCP data were taken on the backside of the plume and that at a depth of 115 m the plume is moving to the northeast. Therefore, one can conclude that the BBADCP data and the computed results agree quite well.

After 60 min, Figure K-138 for Transect 7 shows that the length of the plume at mid-depth is about 250 m. After 70 min (see Figure K-139 at Transect 8), the BBADCP data indicates the suspended sediment plume is barely detectable.

Disposal at the SU site occurred in deeper water than those at the LU site and on greater bottom slope. As a result of the increased bottom slope, there is not as much of a drop off in surge speed from the first bottom mounted current meter to the second. This is reflected in both the field data and in the STFATE surge speeds.

Generally, the computed results agreed well with the BBADCP data. Being able to view the entire computed plume at a particular depth, with the disposal point marked, enables one to better understand BBADCP data taken over transects that cut through a suspended sediment plume at various times.

Application of STFATE to the LD1 disposal

The first disposal event in the LD cell shown on Figure K-37 began at 19:15:23 (GMT) on 15 August 2000. This disposal was different from those in LU and SU since the purpose was to release the material slowly as a spreading operation. Figure K-140, as well as Figure K-141, shows that the material was released along the center of the LD cell over about 10 min. A total of 1265 cu yd were released. This operation was modeled in STFATE as a series of six disposal clouds released over 10 min, with each cloud containing 211 cu yd of material. The numerical grid that was available from the earlier applications of STFATE did not completely cover the LD cell. However, since the bathymetry in the LD cell is very similar to that in the LU cell (SAIC 2002), it appeared reasonable to model the disposal operation as if it occurred in the LU cell.

Based on data from the bottom mounted current meters, the ADCP, and drogues (Figure K-142), the velocity profile of Table K-22 was specified at the disposal point.

Table K-22 Vertical Profile of the Ambient Current During the LD1 Disposal		
Depth (m)	Magnitude (cm/sec)	Direction (deg from north)
15	20	300
30	15	285
40	9	285

The disposal material in LD was coarser than that in the LU and SU disposals (SAIC 2002). Thus, the material was assumed to be composed of 95 percent sand, 4.5 percent silt, and 0.5 percent clay. With the sand being coarser, the settling velocity of the sand was taken to be 0.025 ft/sec instead of the 0.02 ft/sec used in all other simulations. Values for the silt and clay were the same as for the LU and SU simulations.

With a total volume of 211 cu yd for each of the 6 clouds, the initial radius was 13.9 ft. The injection velocity was computed to be 10.4 ft/sec, with a value of about 2.5 ft/sec at bottom impact for each cloud. The final radius of each descending cloud was about 77 ft. The impact velocity and final radius were slightly different for each cloud since the water depths where the clouds were released were slightly different. Collapse of each cloud continued for about 635 sec, with the final dimensions being about 5.8 ft x 585 ft x 527 m. After 1,200 sec, 78 percent of the sand has deposited along with about 15 percent of the silt. After 2,280 sec, 99 percent of the sand and 49 percent of the silt have deposited.

Figure K-143 shows a comparison of the average surge speeds from STFATE and those computed from timings provided by the bottom mounted current meters at distances of 60, 140, and 240 m from the center of the disposal cell. It can be seen that due to the smaller disposal clouds, the surge velocities are not as large as those generated by the LU and SU disposals.

Figures K-144 thru K-152 show the computed suspended sediment plume at times of 1,500, 2,040, and 2,240 sec at depths of 15, 27, and 39 m. After 1,500 sec, maximum concentrations are less than 10 mg/l at 15 m, less than 50 mg/l at 27 m, and mostly 250-500 mg/l at 39 m. By 2,240 sec after the disposal started, maximum concentrations at 27 m are 10-25 mg/l and 100-250 mg/l near the bottom at 39 m. After 2,240 sec, the width of the upper water column plume is about 1,000 ft (304.8 m) and 1150 m (457.3 m) in the lower water column. Due to disposal of the material being along a northwestern path (see Figure K-141), along with the fact that the ambient current is in that direction (see Table K-22), the plume is elongated in the northwestern direction.

Figure K-153 shows transects along which BBADCP data were taken. These data are presented in Figures K-154 thru K-158. Figure K-154 for Transect 2 shows the sediment plume along Line 2 at about 400 m from where the disposal started at 6 min after the disposal was completed. It can be seen that the upper water column plume is slightly sheared in the down slope (to the southwest) direction with a width of about 175 m. The lower water column plume appears to be symmetric around the disposal line with a width of about 300 m.

Figure K-155 shows results along Transect 3, at 15 min after the disposal stopped, at about 500 m from where the disposal started. The width of the upper water column plume is now about 200 m, with the width of the lower plume being about 325 m. Corresponding plume widths computed by STFATE are comparable (see Figures K-144 thru K-146). Figure K-156 shows results along Transect 4 back near the same location as Transect 2 (see Figure K-154), but at 24 min after the completion of the disposal operation. Most of the lower water column plume no longer exists. However, an upper water column plume is still visible with a width of about 225 m at 20 m below the surface. At this time (see Figures K-147 thru K-149), STFATE still computes a lower water column plume with maximum concentrations of 100-250 mg/l.

Figures K-157 thru K-158 show results along Transects 5 and 6, respectively. At 34 min after the disposal operation terminated, an upper water column plume remains, but after 47 min no plume anywhere in the water column is visible back at 400 m from where the disposal started.

Suspended sediment concentrations determined from water samples were quite low, e.g., less than 20 mg/l, except for one sample at 11 min after the disposal terminated (21 min from the beginning of the disposal). This sample gave a concentration of 350 mg/l at a depth of 43.8 m (143.7 ft). From Figure K-146, it can be seen that STFATE computes maximum concentrations of 250-500 mg/l at 1,500 sec (25 min) from the beginning of the disposal operation at a depth of 39 m.

The LD disposal operation was different from all the others. The disposal was conducted to spread material along the entire length of the LD cell. STFATE modeled the disposal as a series of six instantaneous clouds released at different locations over the length of the cell. The STFATE average surge speeds compared well with those computed from timings obtained from the bottom current meters at locations of 60 and 140 m from the center of the cell. Since the bottom collapse phase in STFATE terminated before the surge reached the meter at 240 m, no comparison could be made there.

Based on data from the BBADCP transects, the size of the computed suspended sediment plume appears about right. Comparing the computed suspended sediment concentrations with data from collected water samples is difficult. However, one value collected near the bottom at 21 min after the beginning of the disposal operation compared well with the computed value near the bottom at 25 min after initiation of the spreading operation.

STFATE Summary

The numerical model called STFATE has been applied to simulate seven dredged material disposal operations that took place on the Palos Verdes Shelf during August 2000. Six of these simulations had previously been made. However, when those simulations were made some of the field data were not available, e.g., ADCP data. In addition, in the earlier simulations STFATE did not allow for specifying vertical shear in the ambient current. Therefore, before making new simulations, modifications were made to STFATE to allow for vertical shear in the ambient flow field. In addition, a new algorithm was implemented to yield more realistic ambient velocities over the entire numerical grid when data are available at only one point.

Six of the disposal operations were made at a point, with the bottom doors opened quickly while the disposal vessel attempted to remain stationary. However, in all cases some drift of the vessel occurred, making accurate estimates of how far the disposal point was from bottom mounted current meters more difficult. The seventh disposal operation was one in which the dredged material was slowly released as the vessel moved along a disposal line. In other words, the aim was to spread the material over the bottom for capping purposes. The point disposals were simulated in STFATE as instantaneous releases of a single disposal cloud, whereas, the spreading disposal was simulated by releasing multiple disposal clouds along the disposal line.

Output from STFATE consisted primarily of average bottom surge speeds and water column concentrations at various times and depths in the water column. These were then compared with available field data, both in a validation effort for the LU1 disposal, as well as, for the other six disposal operations.

STFATE Conclusions

Various coefficients in STFATE were selected through numerous simulations of the LU1 disposal. With reasonable values of the coefficients, model results compared favorably with field data for both the bottom surge speed and the water column suspended sediment plume. Even in some simulations where the computed average surge speeds differed from the field data by 20 percent or so, the variation of the surge speed with distance from the disposal point compared well with the field data.

Given the uncertainty in trying to determine the exact dimensions of a suspended sediment plume from a limited number of BBADCP transects, the size of the computed water column plume tended to agree well with the plume picked up by the BBADCP. Generally it was difficult to compare computed suspended sediment concentrations with values from water samples collected in the field. Most of the samples were collected very near the bottom. Concentrations from samples collected before the surge had dissipated its energy could not be compared with STFATE results since suspended sediment concentrations are only available from STFATE after the bottom collapse phase terminates.

A major conclusion that can be drawn from these simulations is that allowing for vertical shear in the ambient current is extremely important for accurately transporting suspended material throughout the water column. In addition, spreading velocity data collected at one point over the entire numerical grid should be done in a reasonable manner. However, the algorithm implemented does not yield a mass conservative flow field. One would have to apply a numerical hydrodynamic model to achieve a mass conservative flow field.

Another important conclusion is that attention should be directed to how the disposal operation occurred. For example, if the interest is in computing bottom surge speeds, one needs to determine how much of the disposal material leaves the vessel rapidly, and then set the volume of the instantaneous disposal cloud accordingly rather than assume all of the material leaves instantaneously.

[JIM, I suggest keeping this CORMIX discussion in this appendix, since it is part of the modeling analysis. tlp]

References

- Bokuniewicz, H. J., Gilbert, J., Gordon, R. B., Higgins, J. L., Kaminsky, P., Pilbeam, C. C., Reed, M., and Tuttle, C. (1978). "Field study of the mechanics of the placement of dredged material at open-water disposal sites, Volume 1: Main text and Appendices A-I," Technical Report D-78-7, U.S. Army Engineer Waterways Experiment Station, Vicksburg, MS.
- Bokuniewicz et al. (1992). Page 49
- Bowers, G. W., and Goldenblatt, M. K. (1978). "Calibration of a predictive model for instantaneously discharged dredged material," EPA-600/3-78-089, U.S. Environmental Protection Agency, Corvallis, OR. In text it is spelled Bowers, page 7
- Brandsma, M. G., and Divoky, D. J. (1976). "Development of models for prediction of short-term fate of dredged material discharged in the estuarine environment," Contract Report D-76-5, U.S. Army Engineer Waterways Experiment Station, Vicksburg, MS, prepared by Tetra Tech, Inc., Pasadena, CA.
- Brandsma and Sauer (1983). Page 4
- Bray, R. N., Bates, A. D., and Land, J.M. (1997). *Dredging, A Handbook for Engineers*. Second Edition, New York, John Wiley & Sons. Not in text
- Chapman, R. S., Johnson, B. H., and Vemulakonda, S. R. (1996). "User's guide for the Sigma stretched version of CH3D-WES," Technical Report HL-96-21, Hydraulics Laboratory, U.S. Army Engineer Waterways Experiment Station, Vicksburg, MS.
- Chase, D. (1994). "Dropmix user's manual," draft report prepared for the Environmental Laboratory, U.S. Army Waterways Experiment Station, Vicksburg, MS.
- Clausner, J. E., Gailani, J. Z., Lillycrop, L. S., Rollings, M. P., Torrey, V. H., and Allison, M. C. (In Preparation). "Summer 1997 Capped Category II mound in the mud dump site - Draft Report," Report for the U.S. Army Engineer District, New York, U.S. Army Engineer Waterways Experiment Station, Vicksburg, MS.
- Clausner, J. E. (1997). Page 13
- Clausner et al. (1998). Page 13
- Clausner et al. (1999). Page 13
- Clausner, J. E., et al. (Date). "Title of report," NEIE Report for Los Angeles District.
- Doneker, R. L., and Jirka, G. H. (1990). "Expert system for hydrodynamic mixing zone analysis of conventional and toxic submerged single port discharges (CORMIX1)," U.S. Environmental Protection Agency, Environmental Research Laboratory, Athens, GA.
- Doneker, R. L., Jirka, G. H., and Nash, J. D. (1995). "CD-CORMIX for continuous dredge disposal mixing zone analysis, Version 1.0," Final Draft

Contract Report, EPA Contract No. 68-C3-0374, U.S. Environmental Protection Agency, Office of Science and Technology, Newport, OR.

- Gailani, J. Z. (1998). "LTFATE cohesive sediment transport model," DOER Technical Note N1, <http://www.wes.army.mil/el/dots/doer/technote.html>. Not in text
- Hales, L. (1995). "Accomplishments of the Corps of Engineers Dredging Research Program," *Journal of Coastal Research* 11(1), p 66-88.
- Havis, R. N. (1994). "Mixing zone simulation model for dredge overflow and discharge into inland and coastal waters," U.S. Army Engineer Waterways Experiment Station, Vicksburg, MS.
- Hench, J. L., Luettich, R. A., Jr., Westerink, J. J., and Scheffner, N. W. (1994). "ADCIRC: An advanced three-dimensional circulation model for shelves, coasts, and estuaries - Report 6 - development of a tidal constituent database for the eastern north Pacific," Dredging Research Program Technical Report DRP-92-6, U.S. Army Engineer Waterways Experiment Station, Vicksburg, MS.
- Jepsen, R., Roberts, J., and Lick, W. (1997). "Long Beach Harbor sedimentation study," Department of Mechanical and Environmental Engineering, University of California, Santa Barbara, Draft Contract Report prepared for the U.S. Army Engineer District, Los Angeles, Los Angeles, CA. not in text
- Johnson, B. H. (1990). "User's guide for models of dredged material disposal in open water," Technical Report D-90-5, U.S. Army Engineer Waterways Experiment Station, Vicksburg, MS.
- Johnson, B. H. (2001). "need the name of the article," IEB article.
- Johnson, B. H., and Fong, M. T. (1995). "Development and verification of numerical models for predicting the initial fate of dredged material disposed in open water, Report 2: Theoretical developments and verification results," Dredging Research Program Technical Report DRP-93-1, U.S. Army Engineers Waterways Experiment Station, Vicksburg, MS.
- Johnson, B. H., McComas, D. N., McVan, D. C., and Trawle, M. J. (1993). "Development and verification of numerical models for predicting the Initial fate of dredged material disposed in open water, Report 1: Physical model tests of dredged material disposal from a split-hull barge and a multiple bin vessel," Technical Report DRP-93-1, U.S. Army Engineer Waterways Experiment Station, Vicksburg, MS.
- Johnson, B. H., O, H. R., Teeter, A. M., Cerco, C. F., and Wang, H. V. (1998). "Modeling the fate and water quality impact of dredged material placed at Site 104," Technical Report, Coastal and Hydraulics Laboratory, U.S. Army Engineer Waterways Experiment Station, Vicksburg, MS.
- Koh, R. C. Y., and Chang, Y. C. (1973). "Mathematical model for barged ocean disposal of wastes," Technical Series EPA 660/2-73-029, U.S. Environmental Protection Agency, Washington, DC.
- Kraus, N. C. (1991). "Mobile Alabama, field data collection project, 18 August - 2 September 1989, Report 1: Dredged material plume survey data report,"

- Technical Report DRP-91-3, U.S. Army Engineer Waterways Experiment Station, Vicksburg, MS.
- Land and Bray (2000). page 6
- Lillycrop and Clausner. (1998). Page 13
- Lindeburg, M. R. (1992). *Civil Engineering Reference Manual*. Sixth Edition, Professional Publications, Inc., Belmont, CA.
- Madsen and Wikramanayake (1991). Page 7
- Moreno, J. D., and Risko, A. J. (1995). "Borrow pit capping," Draft Report, Navigation Section, U.S Army Engineer District, Los Angeles, Los Angeles, CA.
- Moritz, H. R., Johnson, B. H., and Scheffner, N. W. (2000). "Numerical models for predicting the fate of dredged material placed in open water," in *Handbook of Coastal Engineering*, pp. 16-1 - 16-27.
- Moritz, H. R., and Randall, R. E. (1995). "Simulating dredged-material placement at open-water disposal sites," *Journal of Waterway, Port, Coastal, and Ocean Engineering* 121(1), January/February 1995, ASCE.
- Nelson, E. E., and Johnson, B. H. (1992). "Analysis of dredged material deposition patterns," *Proceedings Ports '92*, Seattle, WA.
- Noble, M. (1994). "Circulation on the Palos Verdes Shelf 1992 Summer Deployment," United States Geological Survey. [need to finish this reference]
- Pace, S. D., Dorson, D. L., and McDowell, S. E. (1998a). "A surveillance system for dredged material disposal," *Proceedings of Ports '98*, American Society of Civil Engineers, Reston, VA. Not in text
- Pace, S. D., Dorson, D. L., and McDowell, S. E. (1998b). "An automated surveillance system for dredged material transport and disposal operations," *Proceedings XVth World Dredging Congress 1998*, CEDA, Amsterdam, The Netherlands, p. 293-307. not in text
- Palermo et al. (1999). Page 1-52
- Palermo et al. (2000). Page 19
- Proni.....Dredging 94. page 49
- Randall, R. E., Clausner, J. E., and Johnson, B. H. (1994). "Modeling cap placement at New York mud dump site," *Proceedings of Dredging '94*, ASCE, New York, NY, p. 1,295-1,304.
- Roberts et al. (1994). Page 12
- Rollings, M. (1997). "Recommended sampling plan for geotechnical evaluation of sediment properties for North Energy Island borrow pit project, Long Beach Harbor," Letter Report for the Los Angeles, District, U.S. Army Engineer Waterways Experiment Station, Vicksburg, MS. Not in text
- SAIC. (2002).

- Sea Surveyor, Inc. (1994). "Queens Gate dredging - geotechnical and chemical investigation," report prepared under contract HD-5420 for the Port of Long Beach, CA. Not in Text
- Scheffner, N. W., Thevenot, M. M., Tallent, J. R., and Mason, J. M. (1995). "LTFATE: A model to investigate the long-term fate and stability of dredged material disposal sites, user's guide," Dredging Research Program Instruction Report DRP-95-1, U.S. Army Engineer Waterways Experiment Station, Vicksburg, MS. Not in text
- Shore protection manual.* (1984). 4th ed., 2 Vol, U.S. Army Engineer Waterways Experiment Station, U.S. Government Printing Office, Washington, DC.
- Spectra Precision Software, Inc. (1997). "TERRAMODEL, Version 9.31," 13 June 1997, Atlanta, GA.
- Tavolaro, J. F. (1984). "A sediment budget study of clamshell dredging and ocean disposal activities in the New York Bight," 6(3), *Environmental Geology and Water Science*, 133-140. not in text
- Thevenot, M. M., and Johnson, B. H. 1994. "Verification of numerical modeling of the fate of disposed dredged material," *Proceedings of Dredging '94*, Orlando, FL.
- Truitt, C. L. (1988). "Dredged material behavior during open-water disposal," *Journal of Coastal Research* 4(3), 389-397.
- Wiley, M. B. (1994). "DAMOS Capping Model verification," Science Applications International Report No. SAIC-91/7603&C95, Contribution #89, U.S. Army Engineer Division, Waltham, MA. Not in text
- Wiley, M. B. (1995). "Deep Water Capping," Science Applications International Report No. SAIC-91/7609&C96, Contribution #98, U.S. Army Engineer Division, Waltham, MA. Not in text

Table K-1 MDFATE Input for Predictive Modeling Scenarios					
Input Categories	Scenarios*				
	1. Sensitivity Tests	2. Offsets	3. Stationary Vessel	4. First LU and SU Placements	5. Spreading Mode
Time frame	March to April 2000	May 2000	May to June 2000	July and August 2000	April 2000
Sediment type	Average, Coarse, Fine	Coarse, Fine	Average, Coarse, Fine	Fine	D ₅₀ = 0.33 and 0.4
Vessel speed (knots)	0.0, 0.5, 1.0, 2.0	0.5, 2.0	Stationary (0.1 knots)	Stationary (0.1 knots)	1.5
Vessel heading	300 deg NW	315 deg NW	Stationary	300 deg NW	North/South
Placement depth (m) and cell	42 (LU) 62 (SU)	42 (LU) 62 (SU)	42 (LU) 62 (SU)	42 (LU) 62 (SU)	42 (LD)
Placement duration (min)	3	3	3	3	30
Residual current	5 cm/sec at 315 deg NW	Between 28 cm/sec NW and 20 cm/sec SE	Between 28 cm/sec NW and 20 cm/sec SE, and 15 cm/sec NW	10 and 15 cm/sec NW 5 cm/sec NE 5 cm/sec SE 5 cm/sec NW	28 cm/sec at 290 deg 20 cm/sec at 115 deg
Single load volume (cu m)	1,659	1,659	1,659 and 2,873	2,873	1,988 (each load)
* Simulations for Scenarios 1 through 4 were conducted using Queen's Gate sediment data. Borrow Area A-III data were used to make Scenario 5 simulations.					

Table K-2 Queen's Gate Sediment Characteristics for MDFATE Predictive Simulations of Pilot Study Placements						
Sediment Type	Percent Sand	Sand Grain Size (mm)	Percent Silt	Silt Grain Size (mm)	Percent Clay	Clay Grain Size (mm)
Coarse	80	0.17	16	0.03	4	0.003
Average	63	0.12	30	0.03	7	0.003
Fine	56	0.09	35	0.03	9	0.003

Table K-3 Summary of Sediment Characteristics in MDFATE Hindcast Simulations				
Scenario/ Sediment Types	Specific Gravity (g/cu m)	Volume Fraction (percent of sample)	Particle Size D₅₀ (mm)	As-Deposited Void Ratio
Scenario LU 1 – Based on Full Hopper Volume				
Sand	2.7	0.27 (79)	0.09	0.75
Silt	2.7	0.065(19)	0.05	2
Clay	2.7	0.0103 (3)	0.003	4.5
		Total 0.34		Composite 1.10
Scenario LU5, LU 25, LU45, LU71, SU 5 and SU 21 with Average LU sediments (based on bulk density of 1.79 g/cu m				
Sand	2.72	0.4078 (79)	0.09	0.75
Silt	2.72	0.0878 (17)	0.05	1.75
Clay	2.72	0.0206 (4)	0.003	4
		Total 0.52		Composite 1.04
Scenario SU1, SU 5, SU 21 – SU sediments with Bulk Density of 1.50				
Sand	2.72	0.40 (77)	0.09	0.85
Silt	2.72	0.06 (11)	0.05	2.70
Clay	2.72	0.01 (2)	0.003	4.00
Clumps	1.40	0.05 (10)	5.00	2.00
		Total 0.52		Composite 1.27
Scenario LD1 Initial				
Sand	2.68	0.50 (100)	0.25	0.75
Scenario LD1 Later, LD Full Placements				
Sand	2.68	0.47 (100)	0.22	0.75

Table K-4 Volume Fractions Used for MDFATE Predictive Simulations Using Queens Gate Sediments			
Sediment Type	Sand	Silt	Clay
Coarse	0.1760	0.0352	0.0088
Average	0.1386	0.0660	0.0154
Fine	0.1232	0.0770	0.0198

Table K-5 Percent Sediment Components Used in MDFATE Predictive Simulations Using Borrow Area Sediments		
Sediment Component	Borrow Areas	
	A-II	A-III
Coarse gravel	0	1
Fine gravel	2	2
Coarse sand	6	2
Medium sand	39	31
Fine sand	50	62
Fines	2	1

Table K-6 Summary of Scenario 1 MDFATE Simulations – Conventional Placement							
File Name*	Water Depth (m)	Dredge Velocity (knots)	Sediment Characteristics	Maximum Cap Thickness (cm)	Volume at Seabed (cu m)	Actual Volume/Potential Volume	Offset Distance (m)
G3A01	42	0	Average	2.9	705	0.81	
G3A02	42	0.5		3.3	705	0.81	
G3A03	42	1.0		2.9	703	0.81	
G3A04	42	2.0		2.2	703	0.81	
G1A01	62	0		1.5	633	0.73	
G1A02	62	0.5		1.6	632	0.73	
G1A03	62	1.0		1.4	632	0.73	
G1A04	62	2.0		1.2	631	0.72	
G3C02	42	0.5	Coarse	4.2	673	0.88	42
G3C04	42	2.0		2.9	671	0.88	
G1C02	62	0.5		2.0	630	0.82	
G1C04	62	2.0		1.6	627	0.82	
G3F02	42	0.5	Fine	2.6	711	0.77	
G3F04	42	2.0		1.8	710	0.77	
G3F02	62	0.5		1.2	606	0.66	
G1F04	62	2.0		0.9	604	0.66	

* G3 = Cell LU, G1 = Cell SU

**Table K-7
Summary of Scenario 2 MDFATE Simulations – Conventional Placement**

File Name*	Water Depth (m)	Dredge Velocity Range (knots)	Sediment Characteristics	Maximum Cap Thickness (cm)	Volume at Seabed (cu m)	Actual Volume/ Potential Volume	Offset Distance (m)	
G3C2Z	42	0.5	Coarse	2.4	668	0.87	120	
G3C2Y		0.5		> 3	676	0.88	16	
G3C4Z		2.0		1.6	663	0.86	78	
G3C4Y		2.0			673	0.88		
G1C2Z	62	0.5		> 1	633	0.83	147	
G1C2Y		0.5			648	0.85		
G1C4Z		2.0			632	0.82		
G1C4Y		2.0			645	0.84		
G3F2Z	42	0.5	Fine		596	0.65		
G3F2Y		0.5			648	0.70		
G3F4Z		2.0			589	0.64		
G3F4Y		2.0			644	0.70		
G1F2Z	62	0.5				366	0.40	
G1F2Y		0.5				481	0.52	
G1F4Z		2.0		> 1	364	0.40	300	
G1F4Y		2.0			457	0.50		

*G3 = Cell LU, G1 = Cell SU

**Table K-8
Summary of Scenario 3 MDFATE Simulations with Conventional Placement and a Stationary Dredge**

File Name	Water Depth (m)	Dredge Velocity (knots)	Sediment Characteristics	Residual Current (cm/sec)	Volume at Seabed (cu m)	Actual Volume/ Potential Volume	Offset Distance (m)
G3F0X	42	0.1	Fine	28 NW	590		174
G3F0W				20 SE	649		49
G1F0X	62			28 NW	371		145
G1F0W				20 SE	476		86
G3C0V	42		Coarse	15 NW	1130	0.89	
G1C0V	62				1096	0.87	
G3F0V	42		Fine		1237	0.81	
G1F0V	63				1009	0.66	
G3A0V	42		Average		1194	0.83	300
G1A0V	62				1109	0.77	

Table K-9 Summary of Scenario 4 MDFATE Simulations Conducted 3 to 4 Days Prior to Placement – Conventional Placement with Dredge Stationary							
File Name	Water Depth (m)	Current Velocity (cm/sec)	Sediment Characteristics	Maximum Cap Thickness (cm)	Volume at Seabed (cu m)	Actual Volume/Potential Volume	Offset Distance (m)
Prediction for 2 August 2000 Placement at Cell LU							
G3FN1	42		Fine		1,318	0.87	36
G3FN2	"		"		1,405	0.92	23
G3FNE	"		"		1,388	0.91	3
G3FSE	"		"		1,404	0.92	15
G3FSW	"		"		1,389	0.91	23
Prediction for 8 August 2000 Placement at Cell SU							
G1FN1	62		Fine		1,184		
G1FN2	"		"		1,324		40
G1FNE	"		"		1,300		13
G1FSE	"		"		1,293		35
G1FSW	"		"		1,258		44

Table K-10 Matrix of MDFATE Simulations – Spreading					
File Name	Target Location	Current Speed (cm/sec)	Current Direction (deg)	D50 (mm)	Volume at Seabed (cu m)
PVSP24	West corner G2	28	290	0.4	1,635
PVSP25		20	115	0.4	1,633
PVSP26		28	290	0.33	1,633
PVSP27		20	115	0.33	1,635
PVSP34		0	0	0.4	1,634
PVSP28	Center F4	28	290	0.4	1,637
PVSP29		20	115	0.4	1,638
PVSP30		28	290	0.33	1,635
PVSP31		20	115	0.33	1,634
PVSP38		0	0	0.4	1,638

Table K-11 Sediment Characteristics for MDFATE Simulations Immediately Prior to and During Placement of LU1 and SU1						
Sediment Type	Percent Sand	Sand Grain Size (mm)	Percent Silt	Silt Grain Size (mm)	Percent Clay	Clay Grain Size (mm)
LU HOP 1	78	0.09	19	0.03	3	0.003
SU HOP 1	90	0.11	9	0.03	1	0.003
LU HOP 1*	78	0.09	19	0.03	3	0.003
* For MDFATE Simulations of 5 and 25 Placements in LU						

Table K-12 Hindcast Simulations Summary					
Cell # Placements, Sediment Characteristics	Scenario Simulated	1 cm contour Dimensions L x W (m)	Maximum Simulated Cap Thickness (cm)	Maximum SPI Cap Thickness (cm)	Percent of Volume retained
LU 1, LU1 Sed	Full hopper volume	250 x 205	2.9	5	89
LU1, LU Avg Sed	In Channel volumes	170 x 115	4.0	5	90
LU 5, LU Sed	No Tides, Stripping	380 x 330	18	Min 8-10	84
LU 5, LU Sed	Tides, Stripping	450 x 240	13	Min 8-10	84
LU 5, LU Sed	No Tides, No Stripping	340 x 275	32	Min 8-10	97
LU 5, LU Sed	Tides, No Stripping	425 x 265	25	Min 8-10	97
LU 25, LU Sed	No Tides, Stripping	865 x 640	28	>15 cores	85
LU 25, LU Sed	Tides, Stripping	1,200 x 560	17	>15 cores	80
LU 45, LU Sed	Tides, Stripping	1,520 x 655	19	>15 cores	71
LU 45, LU Sed	No Tides, Stripping	1,065 x 700	30	>15 cores	86
LU 71, LU Sed	Tides, Stripping	>1,500 x 750	31	22-24 est. cores	76%
LU 71, LU Sed	No Tides, Stripping	1,075 x 760	42	22-24 est. cores	84
SU 1, SU Sed	No Tides, Stripping	285 x 245	2.4	6	69
SU 5, LU Sed	No Tides, Stripping	525 x 400	7	Min 8-10	85
SU 5, LU Sed	Tides, Stripping	450 x 295	6	Min 8-10	72
SU 5, SU Sed	No Tides, Stripping	515 x 395	8	Min 8-10	77
SU 5, SU Sed	No Tides, No Stripping	490 x 350	13	Min 8-10	87
SU 21, LU Sed	Tides, Stripping	910 x 535	10	> 15	62
SU 21, LU Sed	No Tides, Stripping	770 x 725	16	>15	85
SU 21, SU Sed	No Tides, No Stripping	715 x 563	26	>15	87
SU 21, SU Sed	Tides, Stripping	885 x 530	11	>15	56
SU 21, SU Sed	No Tides, Stripping	780 x 740	17	>15	79

**Table K-13
PV Pilot Cap In Channel Volumes, Hopper Volumes, and As Placed Volume Calculations**

	PV Shelf Capped Area Dimensions Thickness (cm)	Length (m)	Width (m)	Total Volume Vertical Sides (cubic m)	Percent Volume Retained in Cell w/ vertical sides (%)	Percent Retained During Placement As Simulated by MDFATE (%)	Inverse of Percent of DM lost During Transport (%)	Overall Multiplier PV Shelf volume to hopper volume	Hopper Volume Required at As Placed void r (cu m)
Shallow Cell LU	15	600	300	27,000	44	87	0	2.61	70
Deep Cell SU	15	600	300	27,000	33	74	0	4.10	110
Totals									
Spreading Total Loads									

STFATE Model Applications and Results – Tables

Table K-14 Sediment Properties Used for Predictive Simulations											
Type	Volume Fraction (Percent)		Fall Velocity (ft/sec)		Void Ratio		Critical Shear Stress (psi)		Cohesive	Mixing	Stripping
	Fine	A-III	Fine	A-III	Fine	A-III	Fine	A-III			
Fine Sand	12.32	9.5	0.02	0.025	0.75	0.7	0.015	0.015	No	No	Yes
Silt	7.70	4.5	0.006	0.006	2.00	2.00	0.09	0.09	No	No	Yes
Clay	1.98	0.5	0.000025	0.000025	4.50	4.50	0.002	0.002	Yes	No	Yes
$SG_{sand} = SG_{silt} = SG_{clay} = 2.70$											

Table K-15 Sediment Properties Used During Post Placement Simulations UPDATE!!											
Type	Volume Fraction (Percent)		Fall Velocity (ft/sec)		Void Ratio		Critical Shear Stress (psi)		Cohesive	Mixing	Stripping
	Fine	A-III	Fine	A-III	Fine	A-III	Fine	A-III			
Fine Sand	12.32	50.0	0.020	.025	0.75	0.70	0.015	0.015	No	No	Yes
Silt	7.70	0	0.006	0.006	2.00	2.00	0.09	0.09	No	No	Yes
Clay	1.98	0	0.000025	0.000025	4.50	4.50	0.002	0.002	Yes	No	Yes
$SG_{sand} = SG_{silt} = SG_{clay} = 2.70$											

Table K-16 Vertical Profile of the Ambient Current for the LU1 Placement		
Depth (m)	Magnitude (cm/sec)	Direction (degree from north)
15	21	310
30	18	300
40	15	280

Table K-17 Vertical Profile of the Ambient Current During the LU2 Disposal		
Depth (m)	Magnitude (cm/sec)	Direction (degree from north)
15	10	60
30	8	200
40	8	240

Table K-18 Vertical Profile of the Ambient Current During the LU3 Disposal		
Depth (m)	Magnitude (cm/sec)	Direction (degree from north)
15	6	150
30	4	80
40	4	800

Table K-19 Vertical Profile of the Ambient Current During the LU4 Disposal		
Depth (m)	Magnitude (cm/sec)	Direction (degree from north)
15	14	300
30	14	300
40	14	30

Table K-20 Vertical Profile of the Ambient Current During the LU5 Disposal		
Depth (m)	Magnitude (cm/sec)	Direction (degree from north)
15	15	60
30	12	275
40	5	275

Table K-21 Vertical Profile of the Ambient Current During the SU1 Disposal		
Depth (m)	Magnitude (cm/sec)	Direction (degree from north)
15	16	125
40	6	65
60	5	160

Table K-22 Vertical Profile of the Ambient Current During the LD1 Disposal		
Depth (m)	Magnitude (cm/sec)	Direction (degree from north)
15	20	300
30	15	285
40	9	285

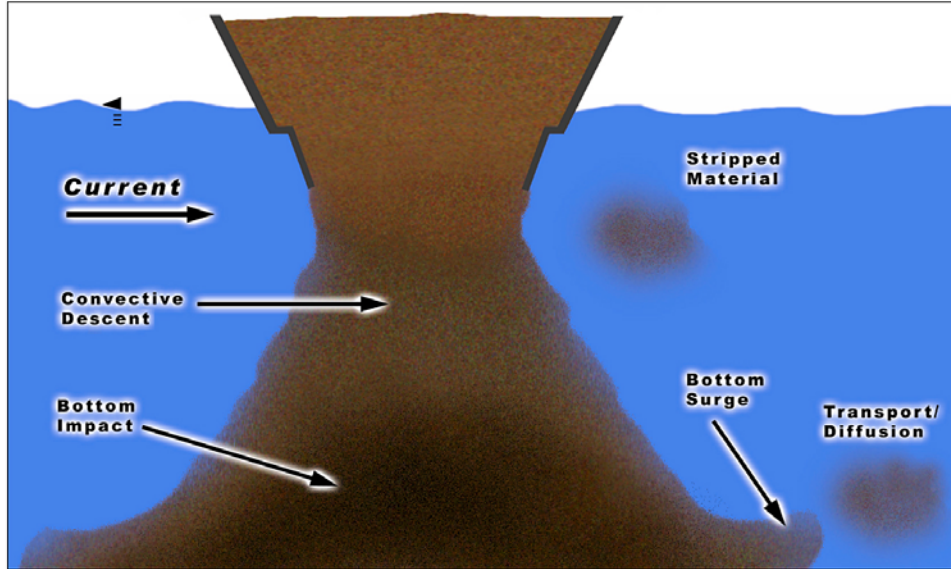


Figure K-1. Processes modeled in STFATE

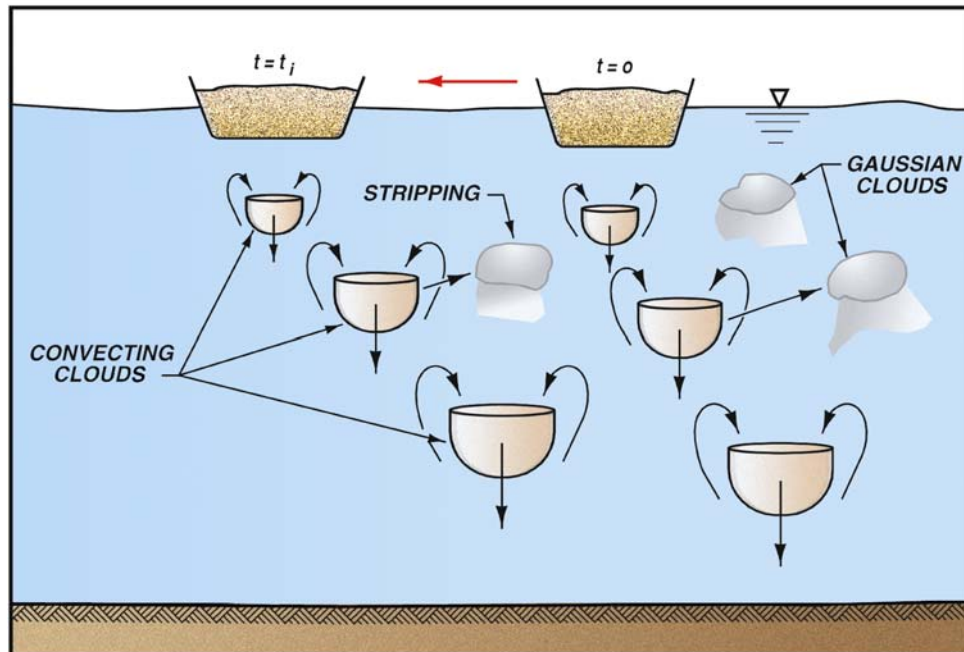


Figure K-2. Multiple convecting clouds as simulated by STFATE

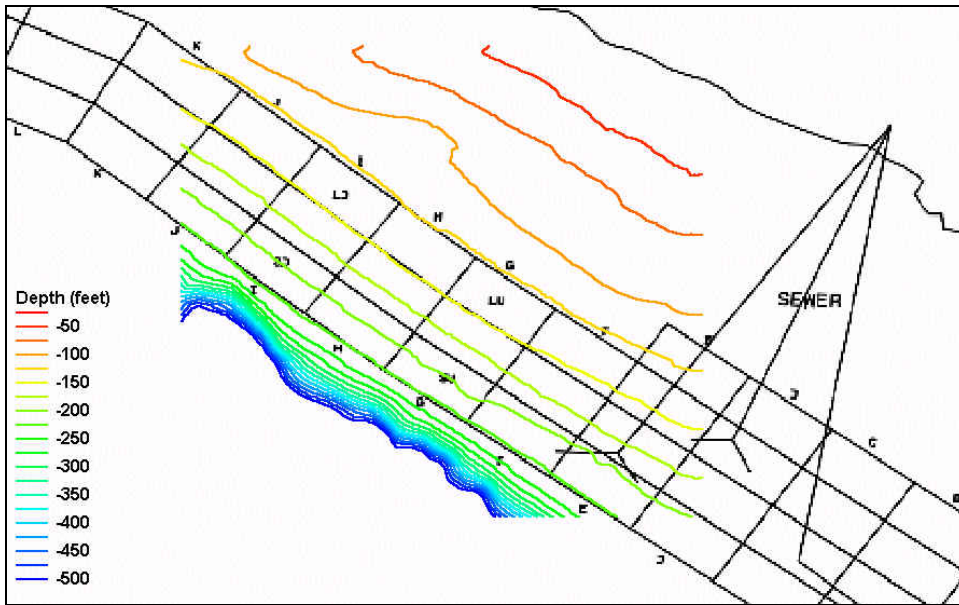


Figure K-3. MDFATE bathymetry grid used in the predictive and operational simulations

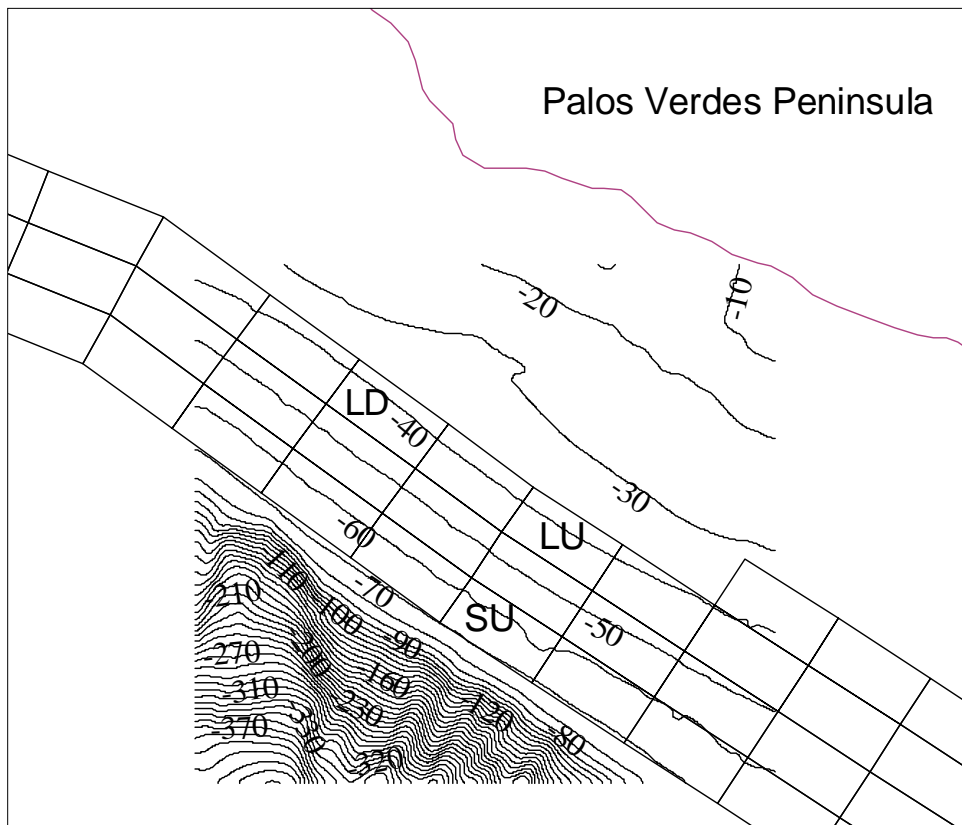


Figure K-4. Baseline bathymetry grid (depths in meters) from which MDFATE grids used for hindcast simulations were extracted

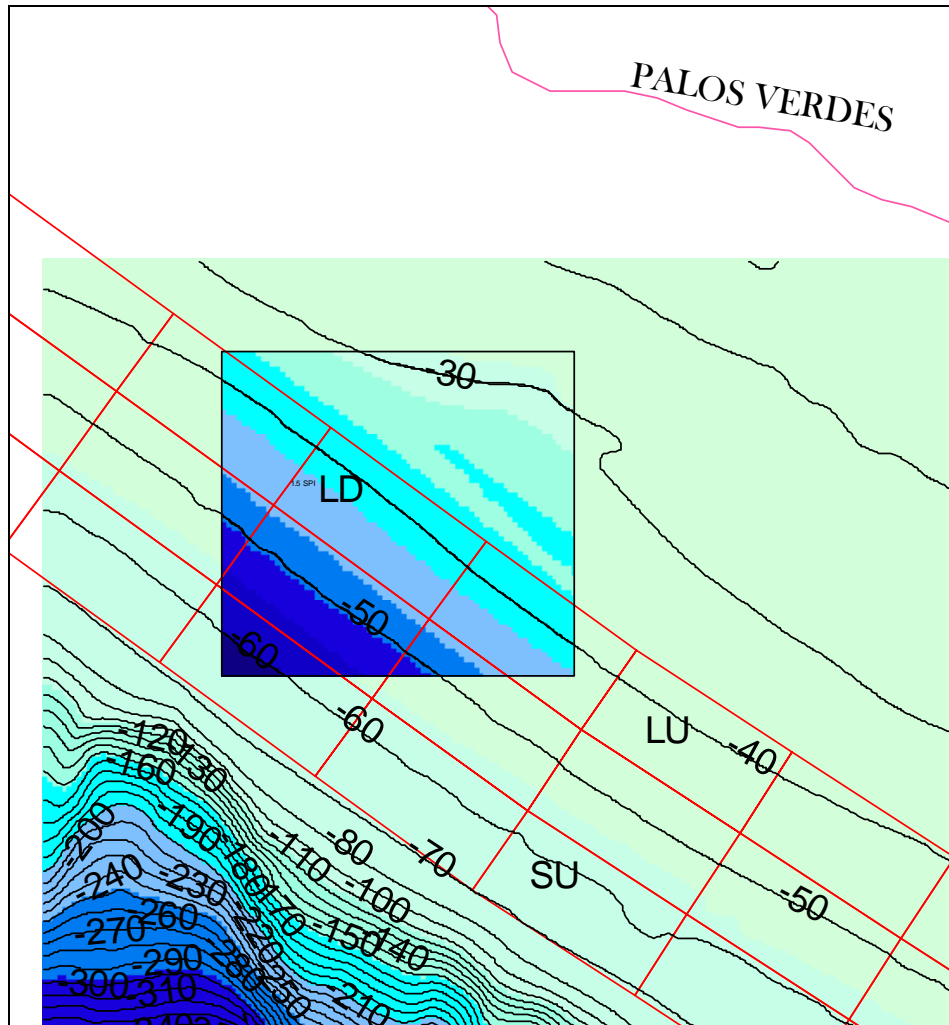


Figure K-5. MDFATE hindcast grid bathymetry (depths in meters) used for simulations in cell LD

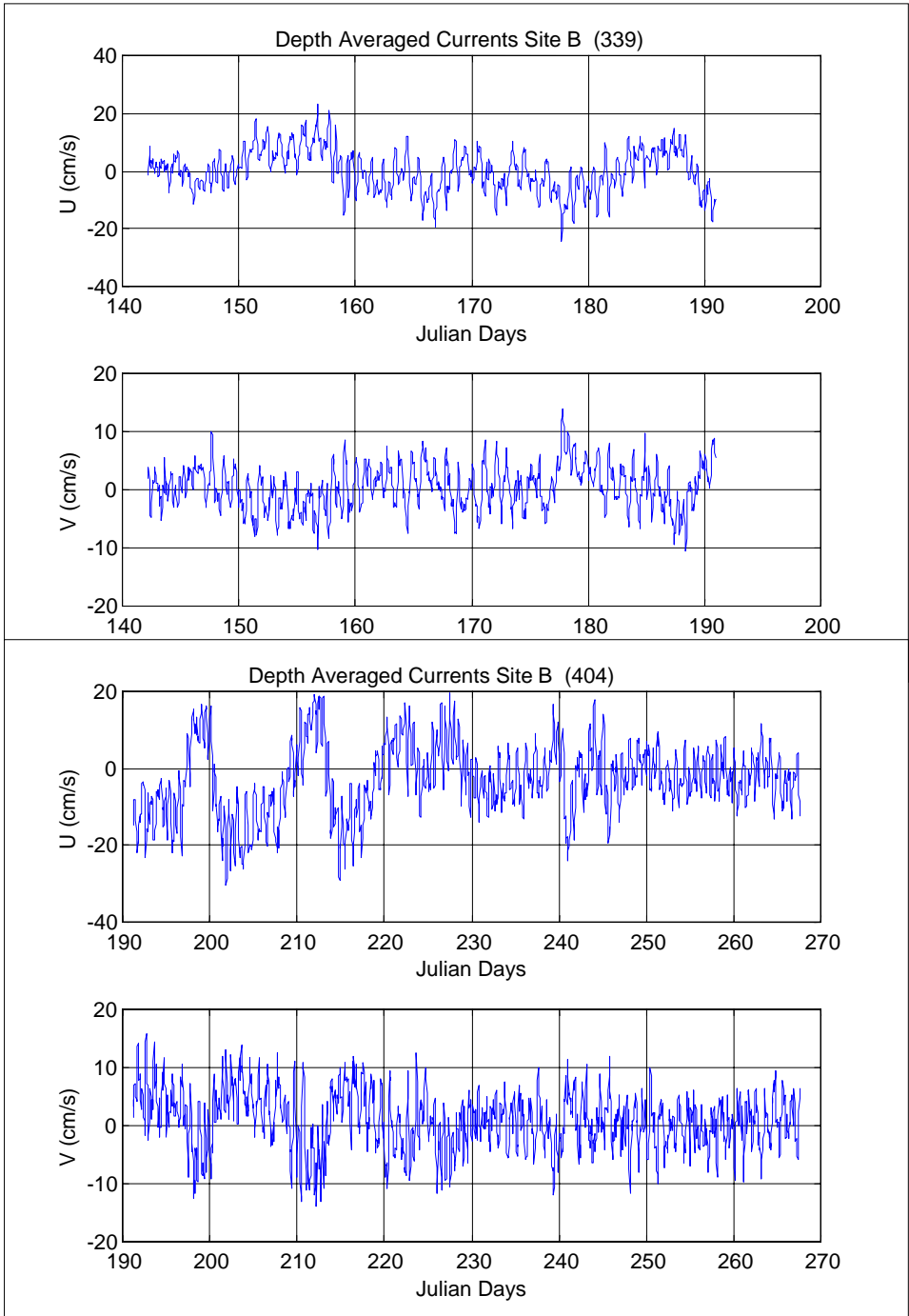


Figure K-6. Averaging of Site B surface, mid-depth, and near-bottom currents

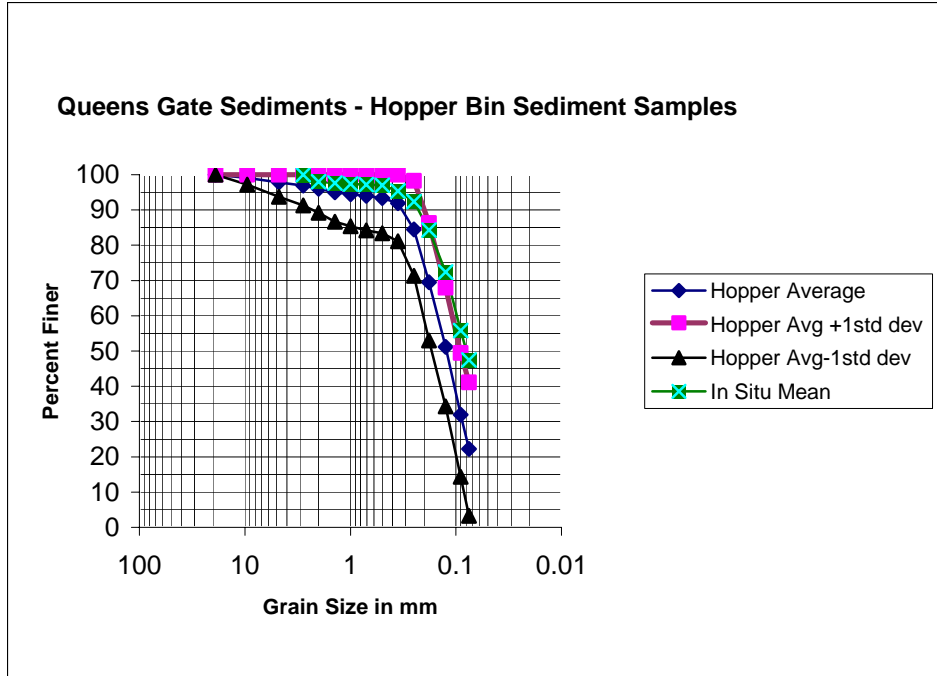


Figure K-7. Queen's Gate dredged sediment grain size distributions

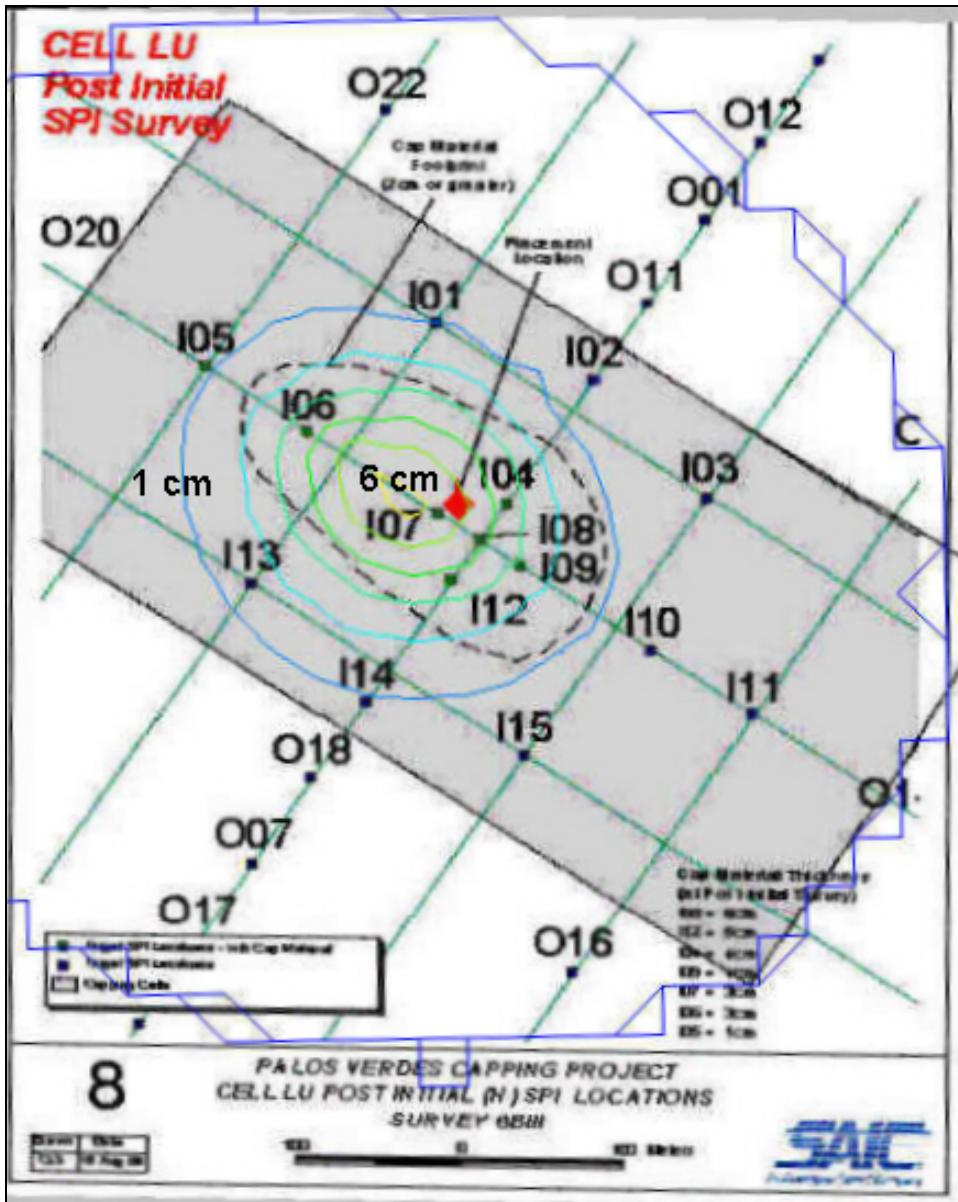


Figure K-8. Operational MDFATE simulation of LU1 placement compared to SPI data. Colored contours are MDFATE thickness predictions; the dashed line is the 2-cm contour as predicted by preliminary evaluation of the SPI results

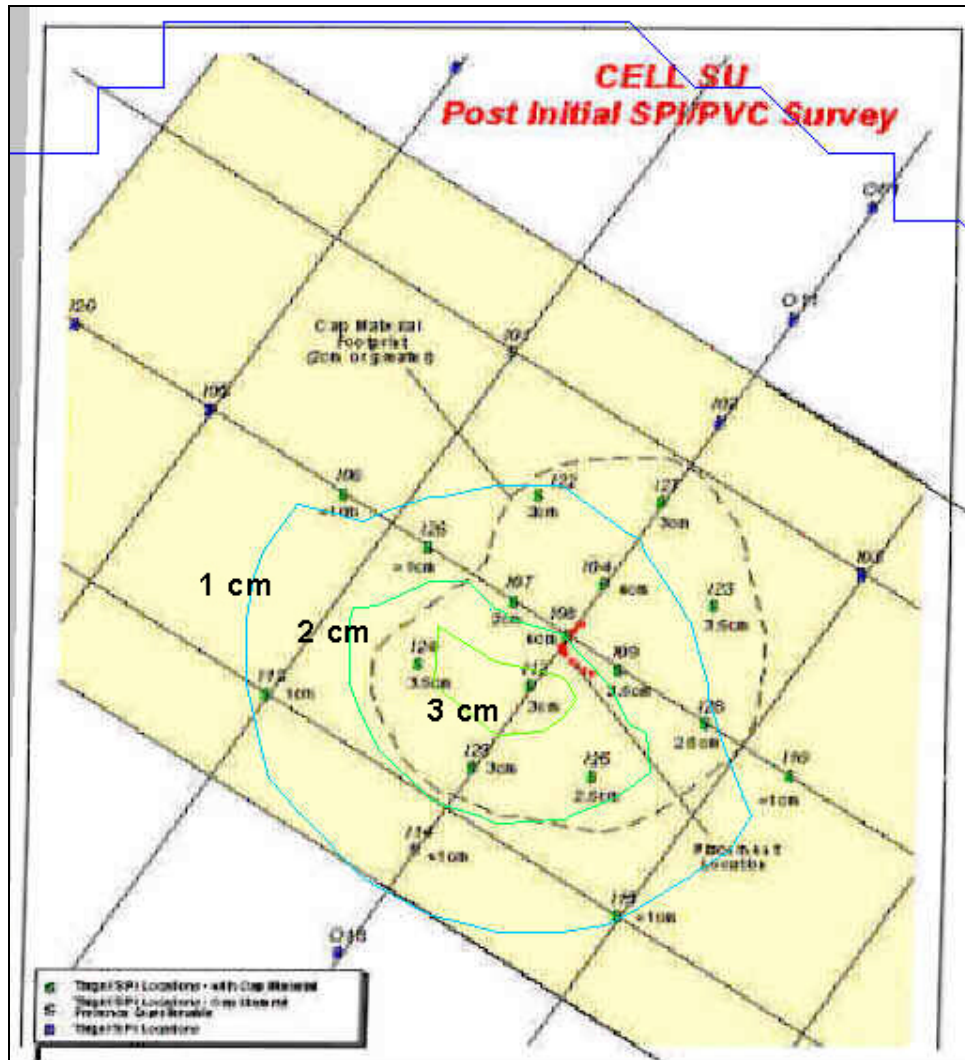


Figure K-9. Operational MDFATE simulation of SU1 placement compared to SPI data. Colored contours are MDFATE thickness predictions; the black dashed line is the 2-cm contour as predicted by preliminary evaluation of the SPI results

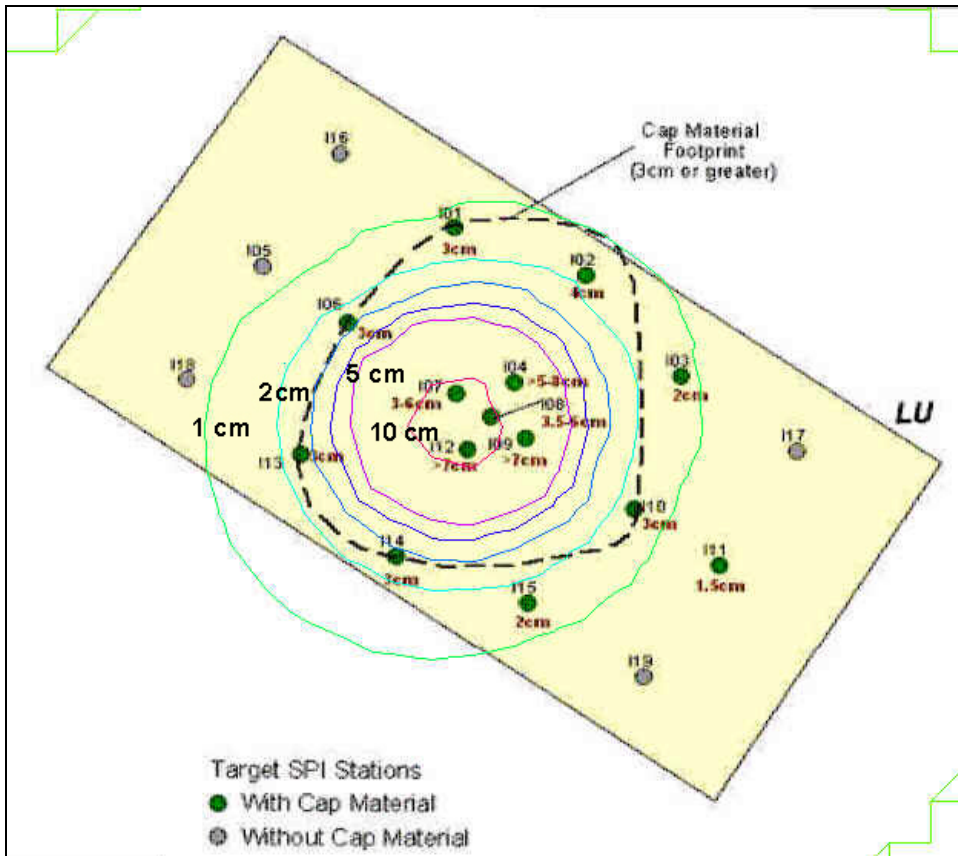


Figure K-10. Operational MDFATE simulation of LU5 placement compared to SPI data. Colored contours are MDFATE thickness predictions; the black dashed line is the 3-cm contour as predicted by preliminary evaluation of the SPI results

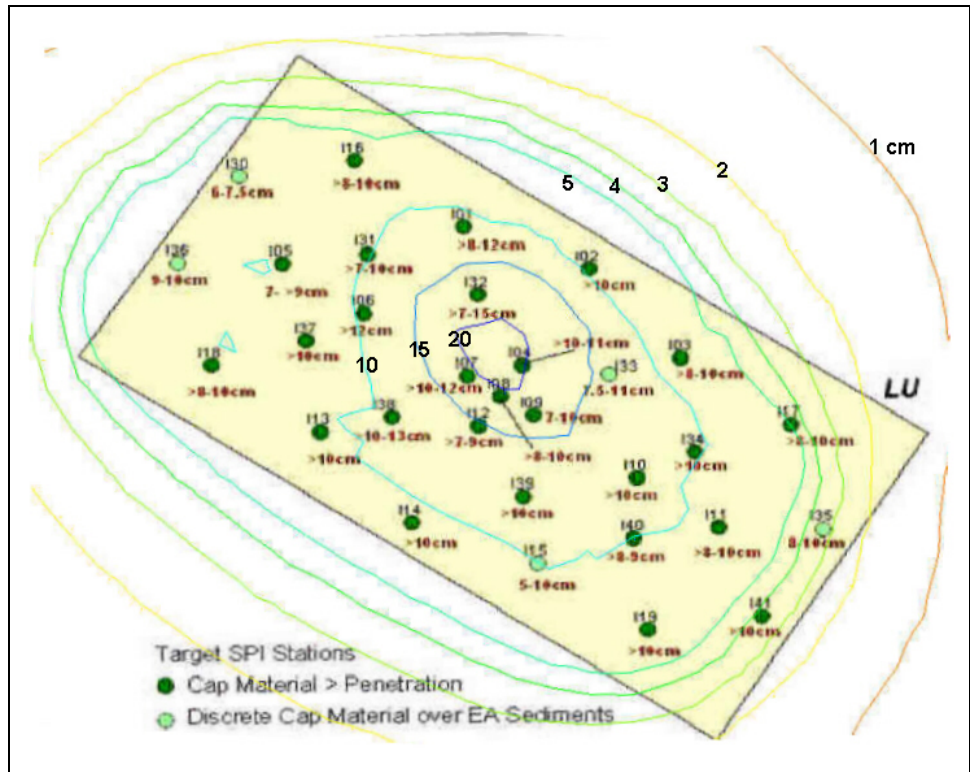


Figure K-11. Operational MDFATE simulation of LU25 placement compared to SPI data. Colored contours are MDFATE thickness predictions; SPI measured thicknesses are listed next to the SPI stations

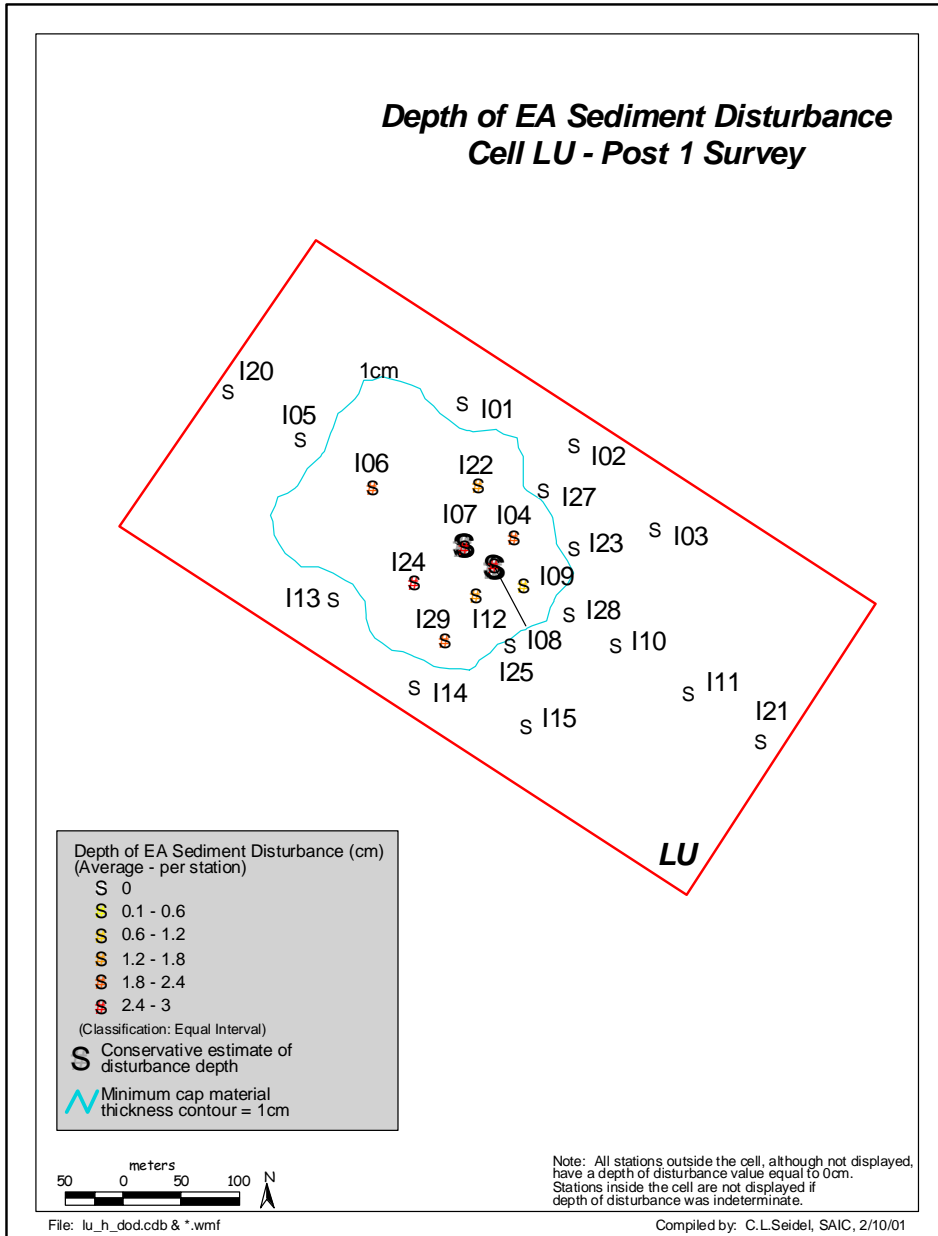


Figure K-12. EA layer depth of disturbance from LU1 placement as estimated from SPI data (SAIC 2002; Figure 3-7.11)

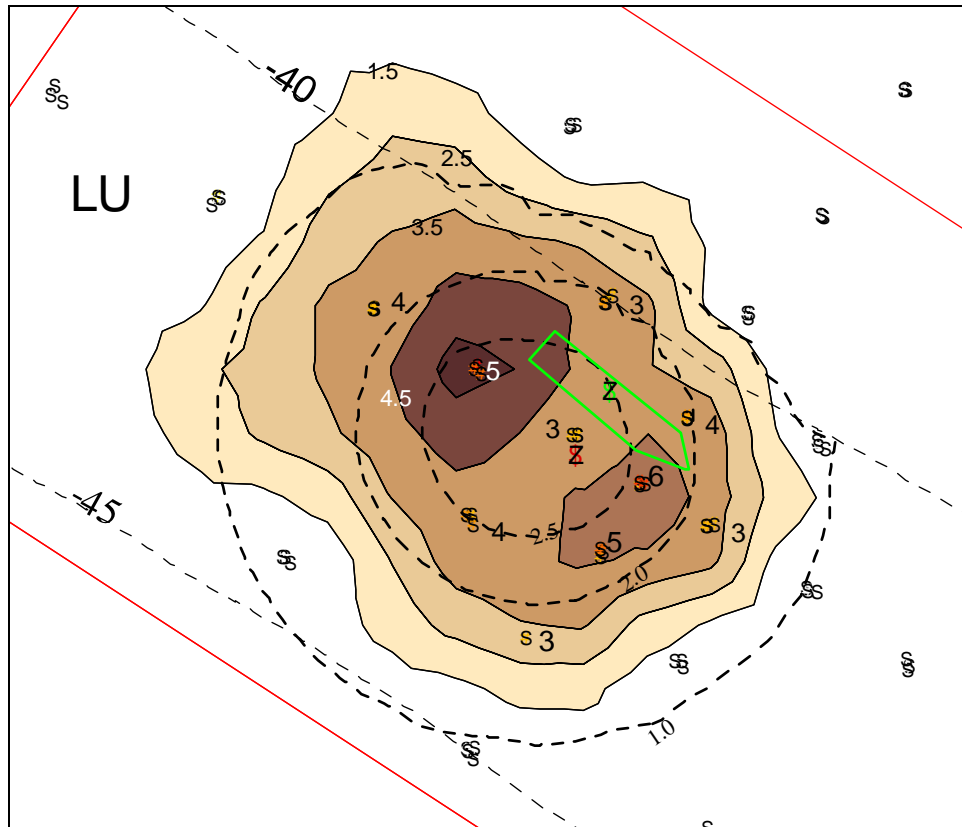


Figure K-13. MDFATE and SPC inferred cap thickness (cm) of initial LU placement. MDFATE cap thickness contours (labeled 1.0 and 2.0 at a 30 deg angle) (dashed lines) are in cm, SPC cap thickness contours are solid lines, with horizontal labels – 1.5, 2.5 cm, etc. Brown shading also indicates SPC thickness, dots are SPC stations, labels next to the dots are the SPC thickness at that point. Green line shows vessel position at start of placement, green triangle is center of hopper, red triangle is center of hopper at end of placement

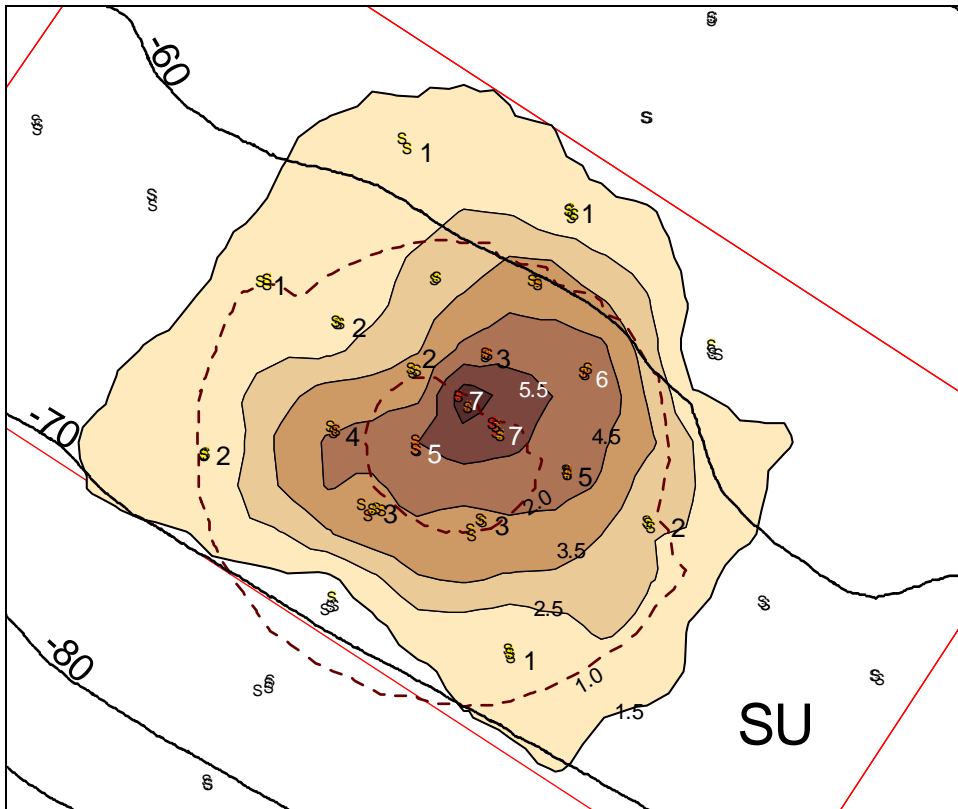


Figure K-14. MDFATE and SPC inferred cap thickness (cm) of initial SU placement. MDFATE cap thickness contours (labeled 1.0 and 2.0 at a 30 deg angle) (dashed lines) are in cm, SPC cap thickness contour (solid lines, horizontal labels – 1.5, 2.5 cm, etc.) with brown shading also indicating thickness, dots are SPC stations, labels next to the dots are the SPC thickness at that point

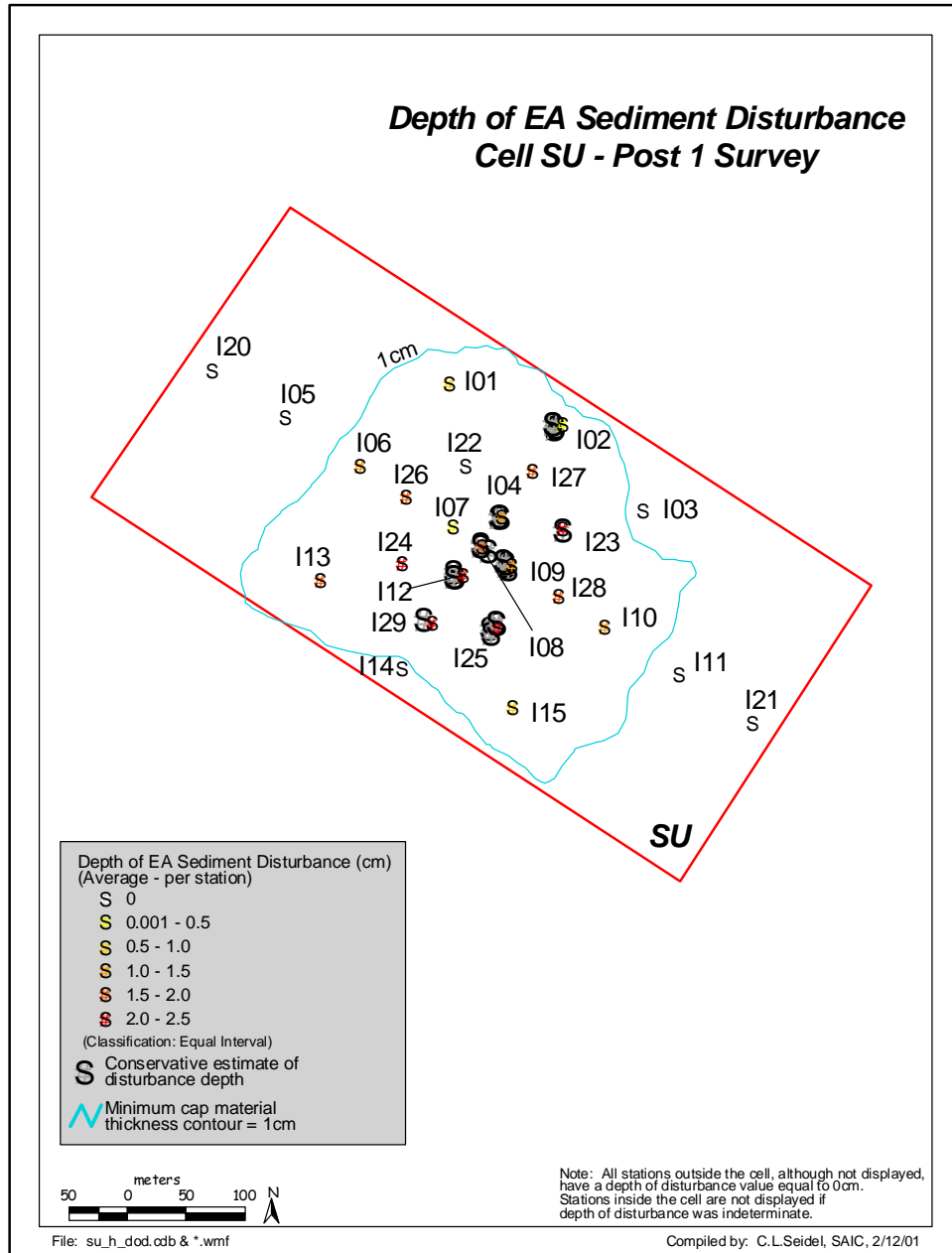


Figure K-15. EA layer depth of disturbance from SU1 placement as estimated from SPI data (SAIC 2002, Figure 4.7-8)

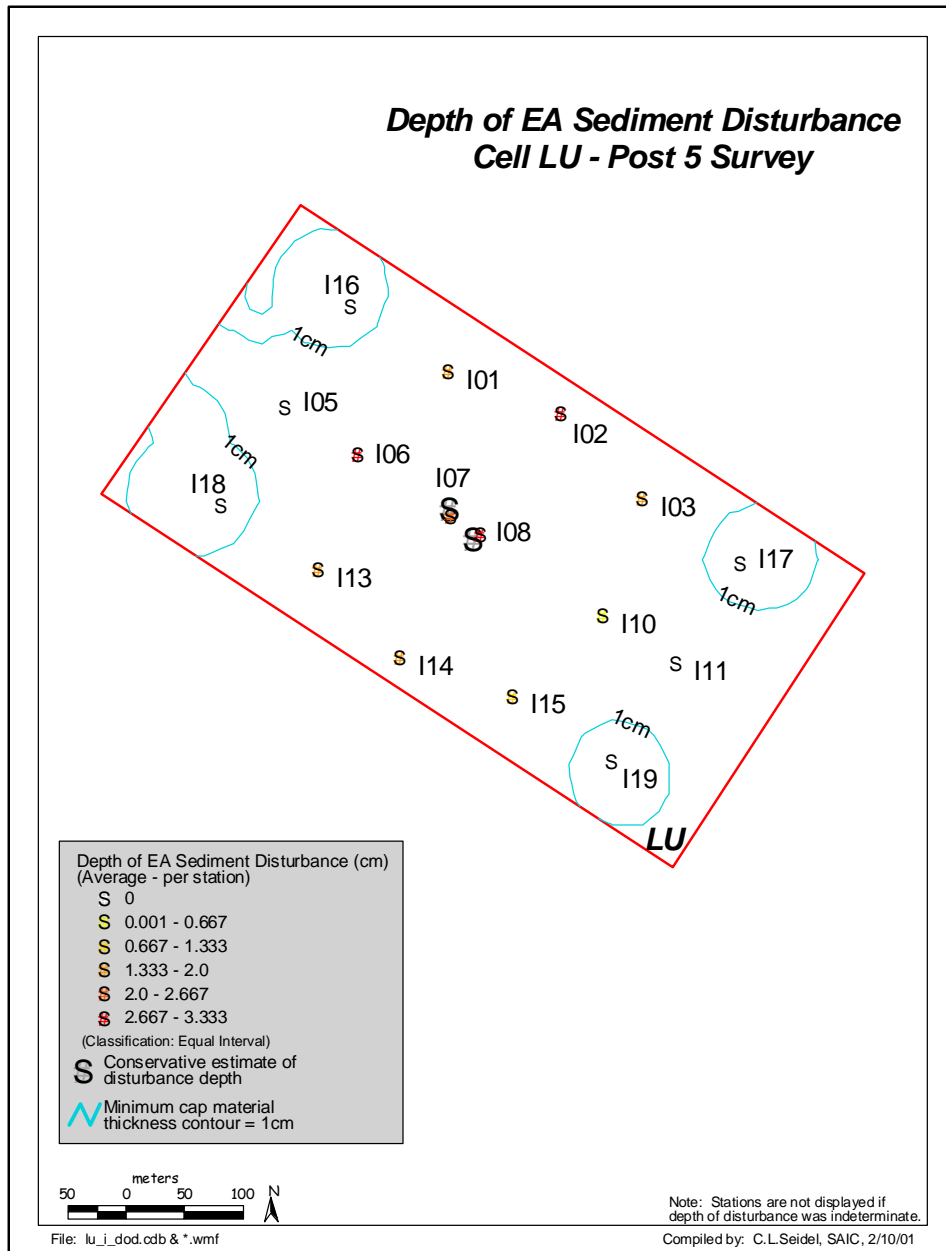


Figure K-17. EA layer depth of disturbance from LU5 placements as estimated from SPI data (SAIC 2002, Figure 3.7-16)

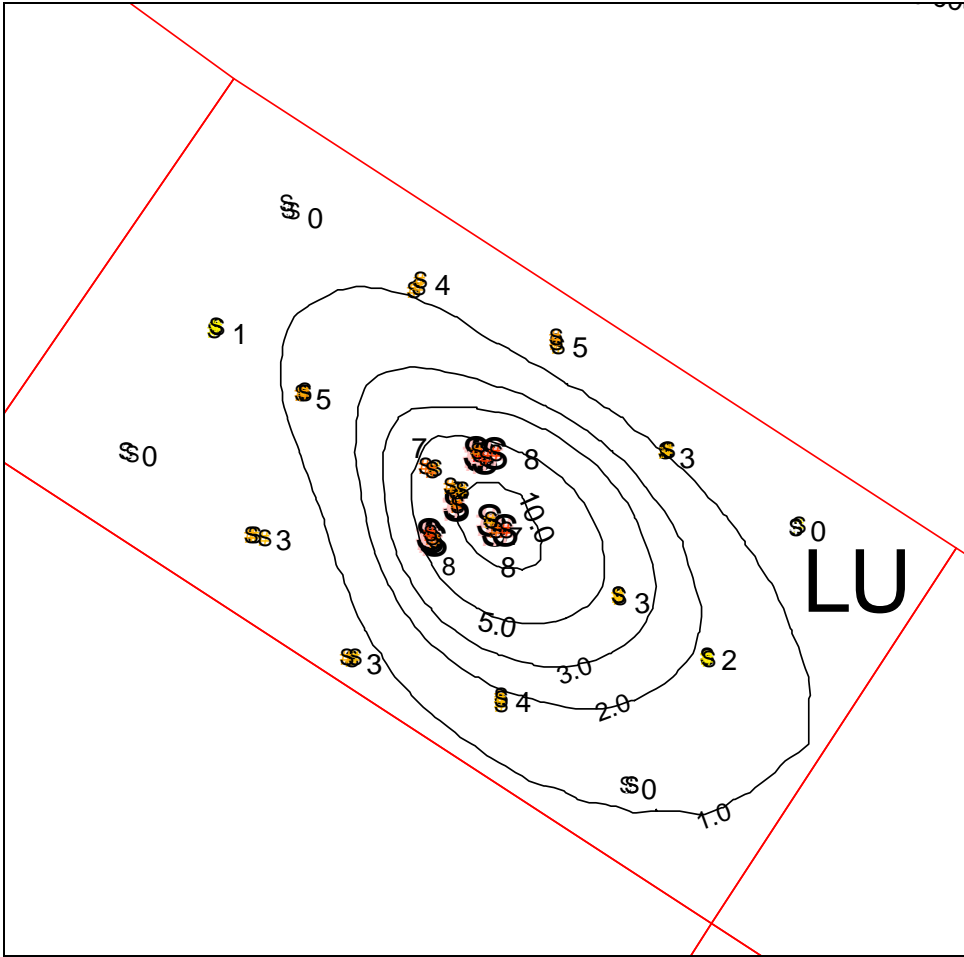


Figure K-18. MDFATE simulation of LU5, with tidal currents, and stripping of sediments. Depth contours (x.0) are MDFATE cap thickness in cm, colored dots indicate SPI stations, SPI thicknesses are in cm (whole numbers), pink dots are locations where cap thickness exceeded SPI penetration depth

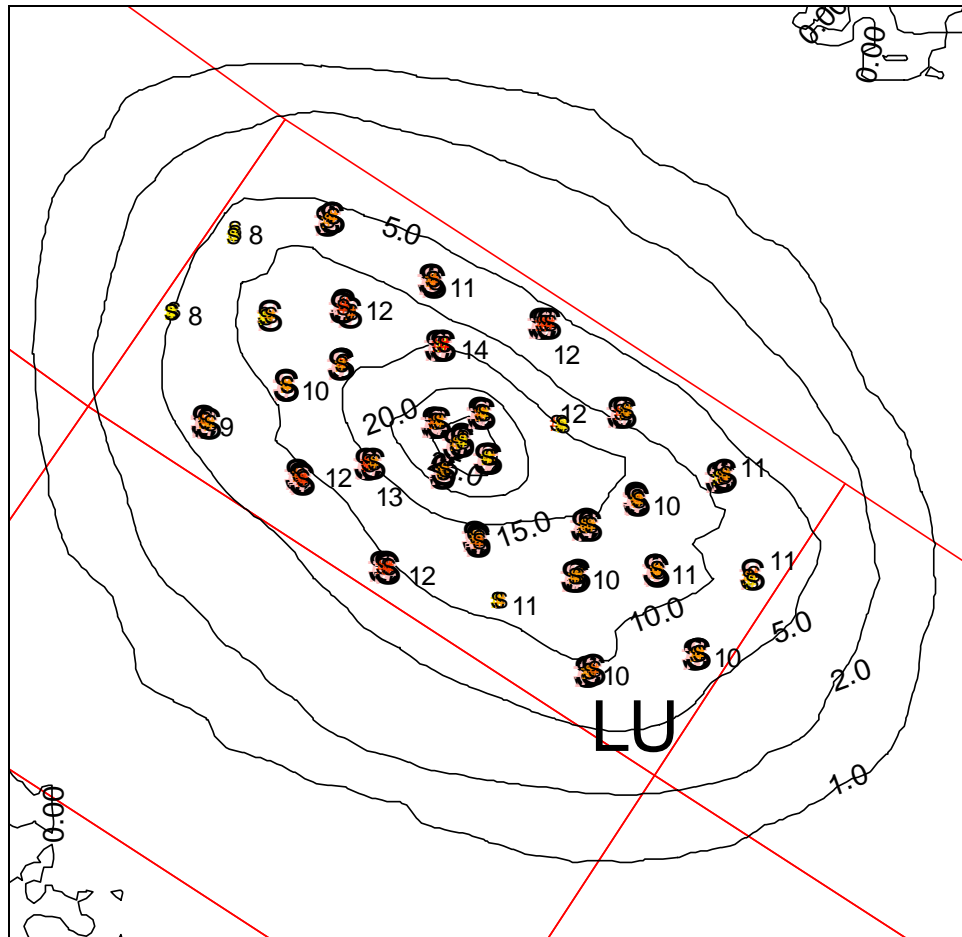


Figure K-19. MDFATE simulation of LU25, without tidal currents, and including stripping of sediments. Depth contours (x.0) are MDFATE cap thickness in cm, colored dots indicate SPI stations, SPI thicknesses are in cm (whole numbers), pink dots are locations where cap thickness exceeded SPI penetration depth

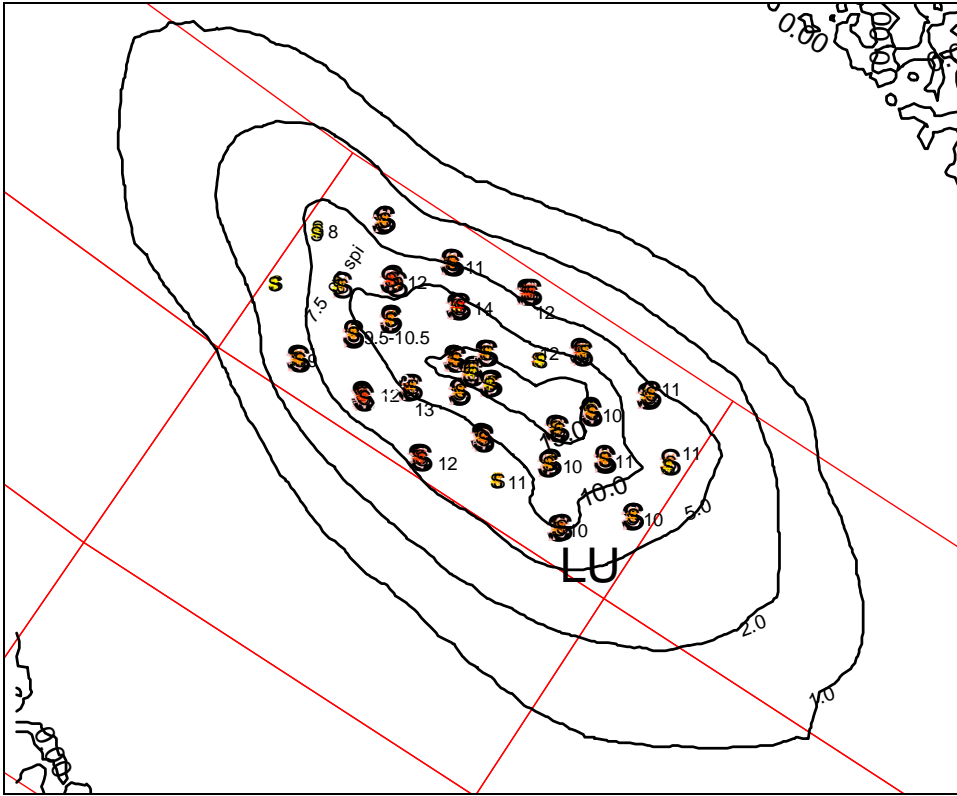


Figure K-20. MDFATE simulation of LU25, with tidal currents, and including stripping of sediments. Depth contours (x.0) are MDFATE cap thickness in cm, colored dots indicate SPI stations, SPI thicknesses are in cm (whole numbers), pink dots are locations where cap thickness exceeded SPI penetration depth

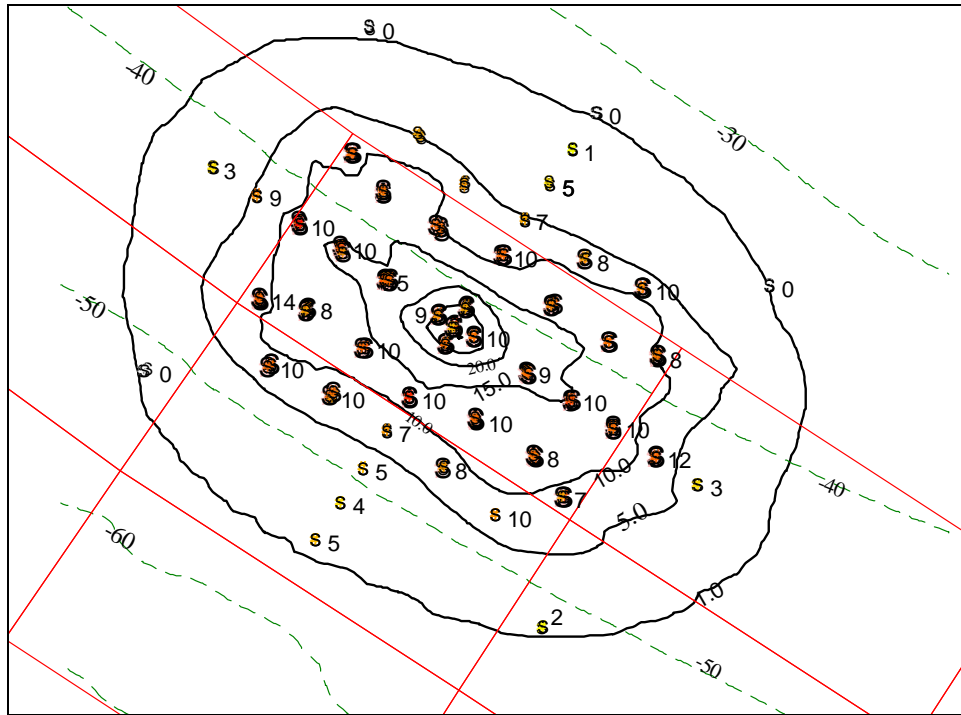


Figure K-21. MDFATE simulation of LU45, without tidal currents, and including stripping of sediments. Depth contours (x.0) are MDFATE cap thickness in cm, colored dots indicate SPI stations, SPI thicknesses are in cm (whole numbers), pink dots behind colored dots are locations where cap thickness exceeded SPI penetration depth

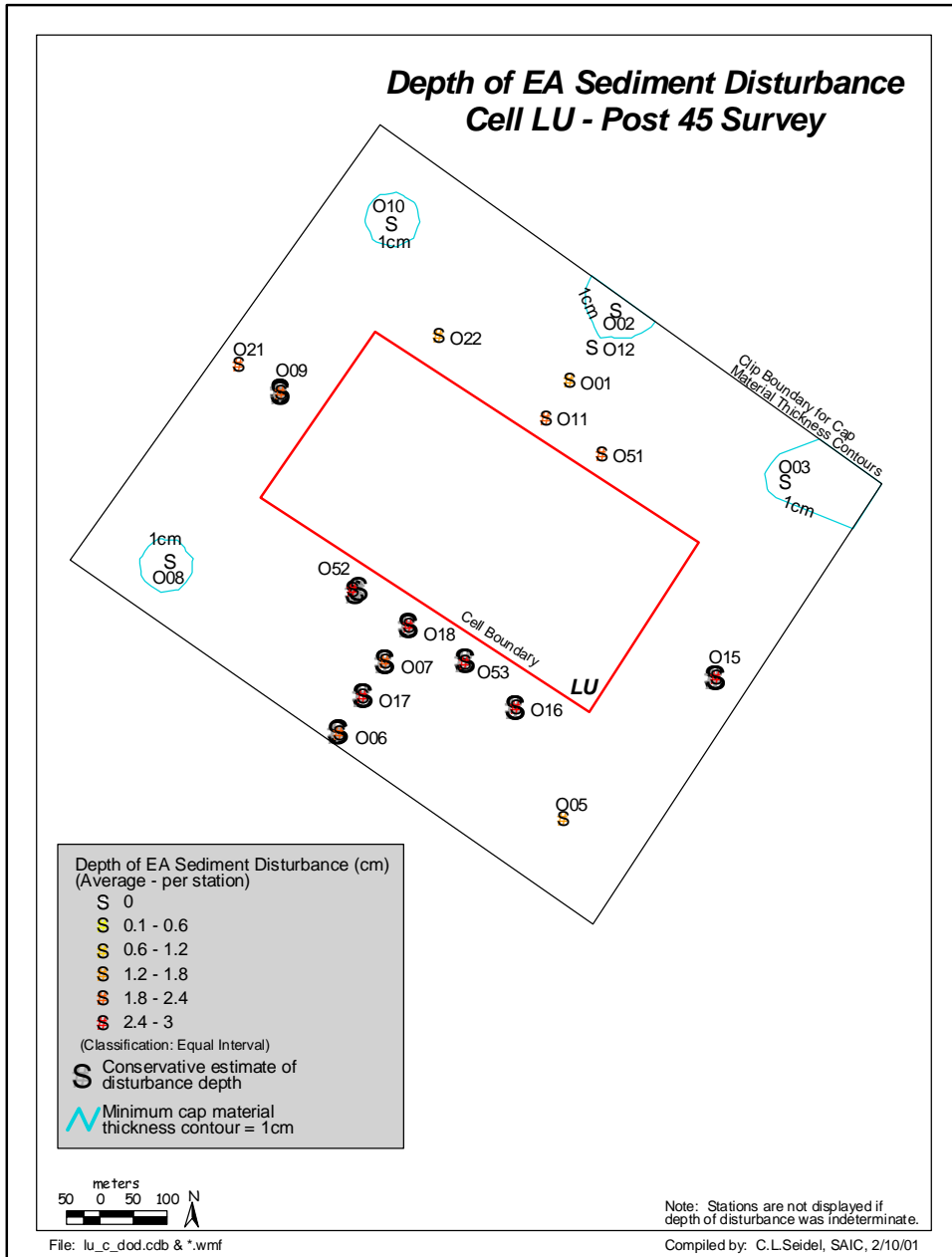


Figure K-22. EA layer depth of disturbance from LU45 placements as estimated from SPI data (SAIC 2002, Figure 3.7-24)

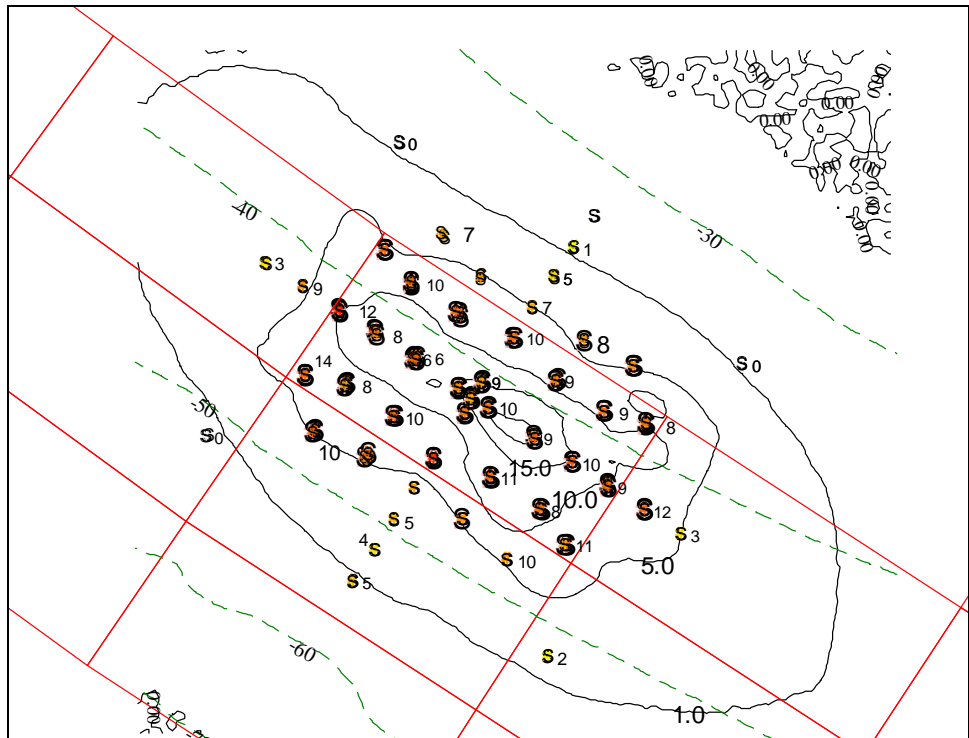


Figure K-23. MDFATE simulation of LU45, with tidal currents, and including stripping of sediments. Depth contours (x.0) are MDFATE cap thickness in cm, colored dots indicate SPI stations, SPI thicknesses are in cm (whole numbers), pink dots behind colored dots are locations where cap thickness exceeded SPI penetration depth

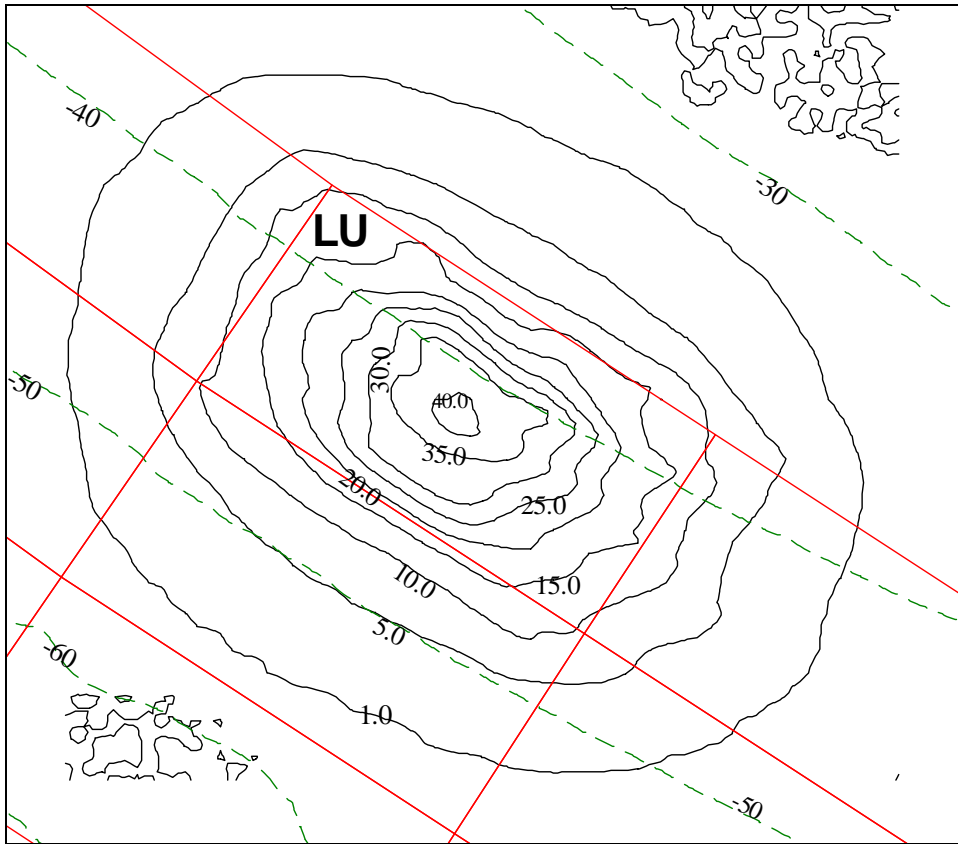


Figure K-24. MDFATE simulation of LU71, without tidal currents, and including stripping of sediments. Solid contours are MDFATE cap thicknesses in cm, dashed contours are water depths in meters

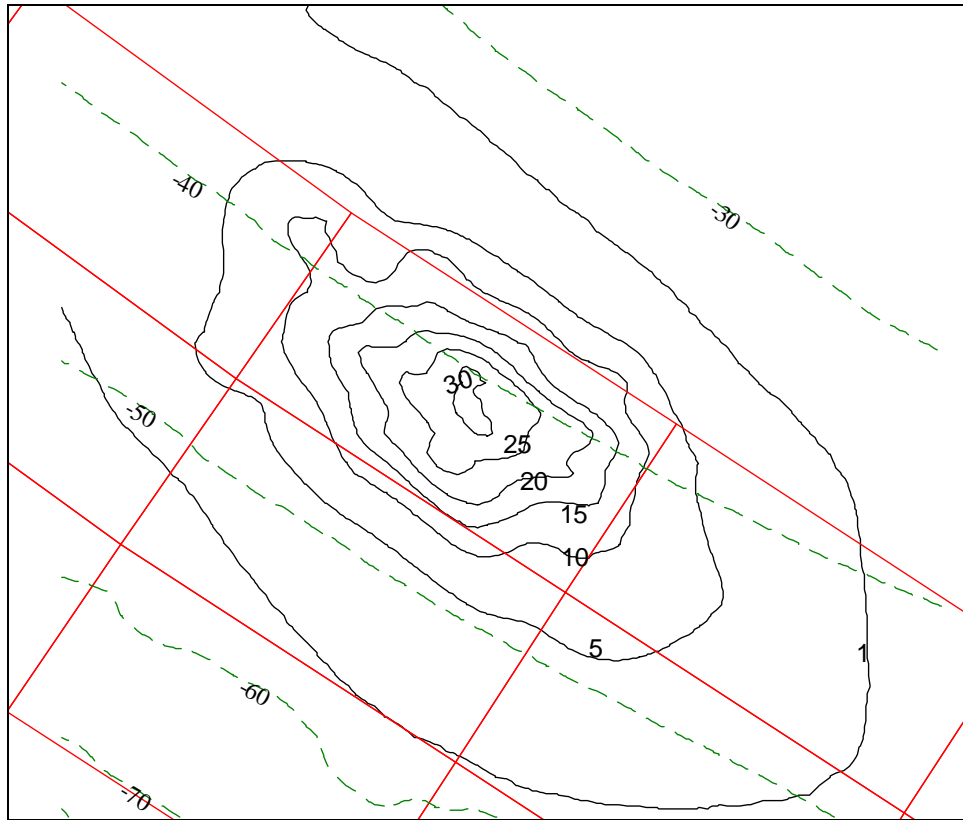


Figure K-25. MDFATE simulation of LU71, with tidal currents, and including stripping of sediments. Solid contours are MDFATE cap thicknesses in cm. Dashed contours are water depth in meters

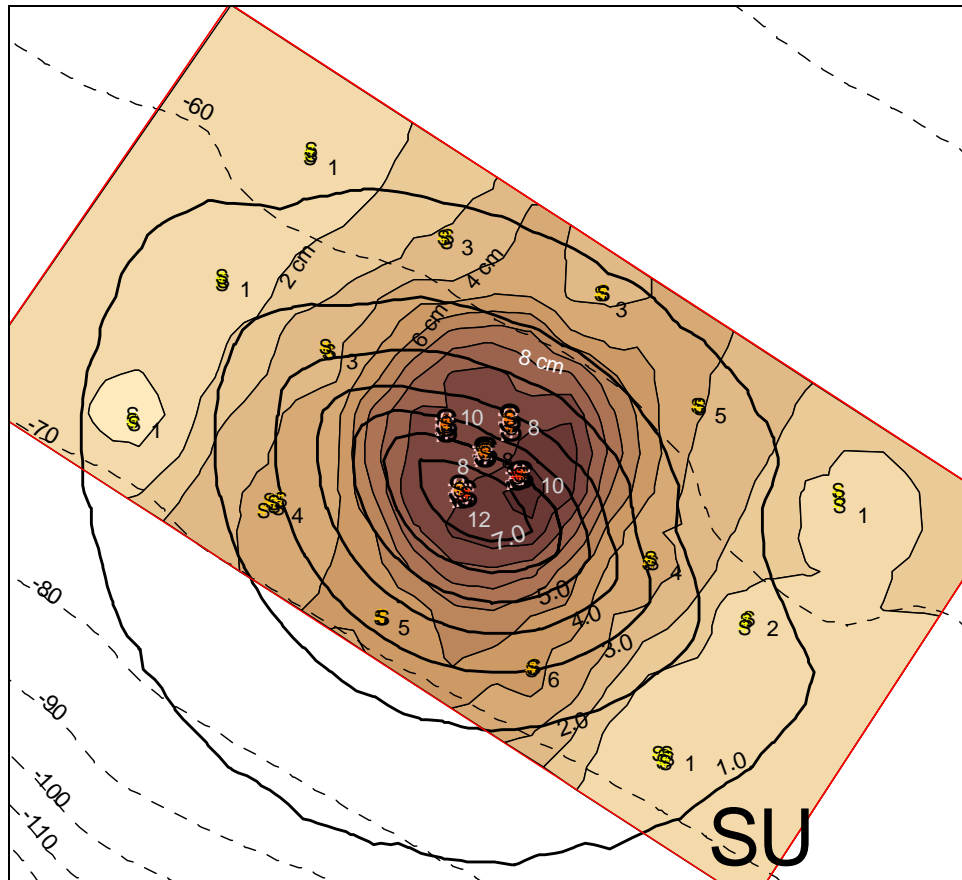


Figure K-27. MDFATE simulation of SU5, with tidal currents, and including stripping of sediments. Depth contours (x.0) are MDFATE cap thickness in cm, colored dots indicate SPI stations, SPI station thicknesses are in cm (whole numbers), pink dots behind colored dots are locations where cap thickness exceeded SPI penetration depth, SPI contours and color ramp based on average thickness are labeled as 2 cm, 4 cm, etc.

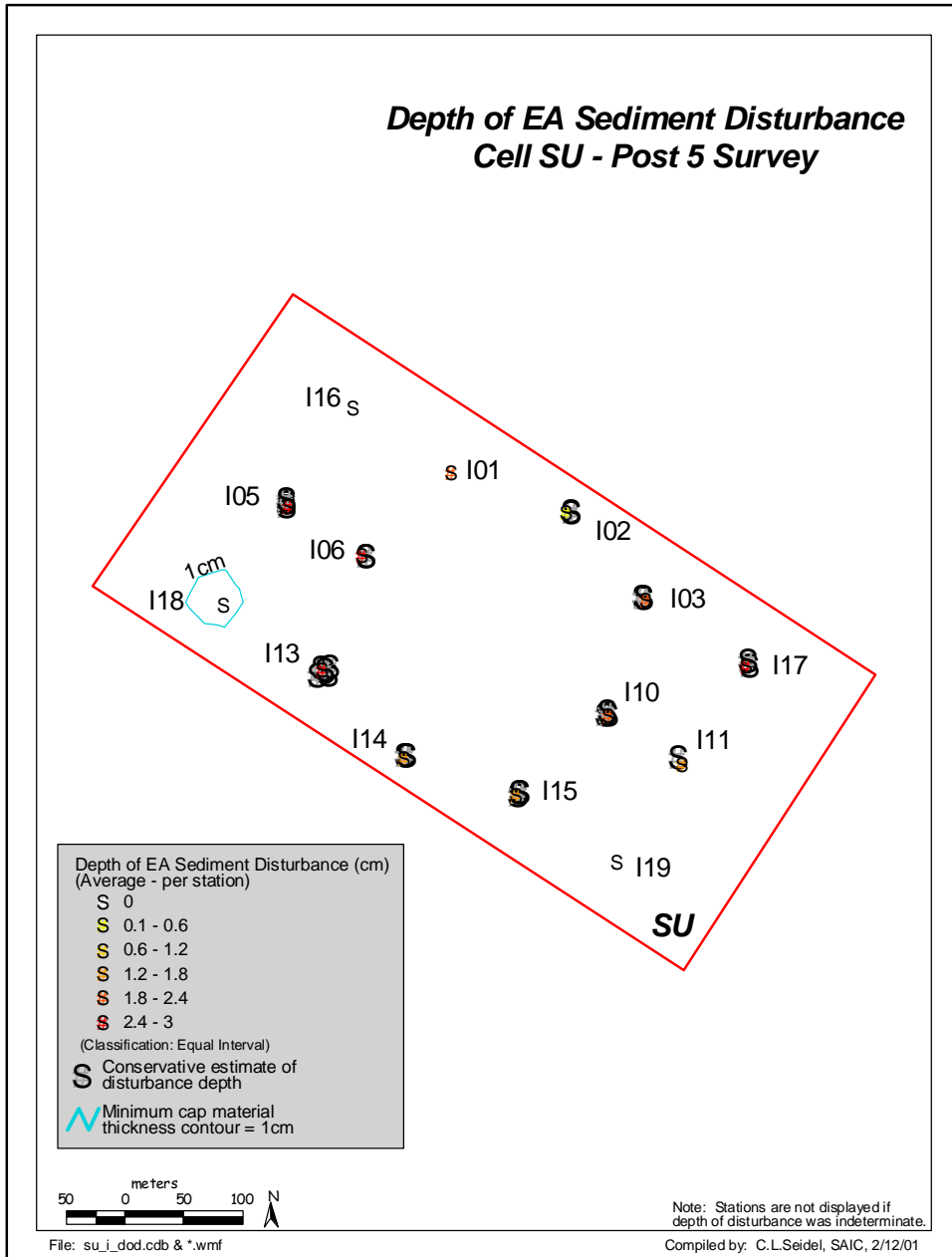


Figure K-28. EA layer depth of disturbance from SU5 placements as estimated from SPI data (SAIC 2002, Figure 4.7-12)

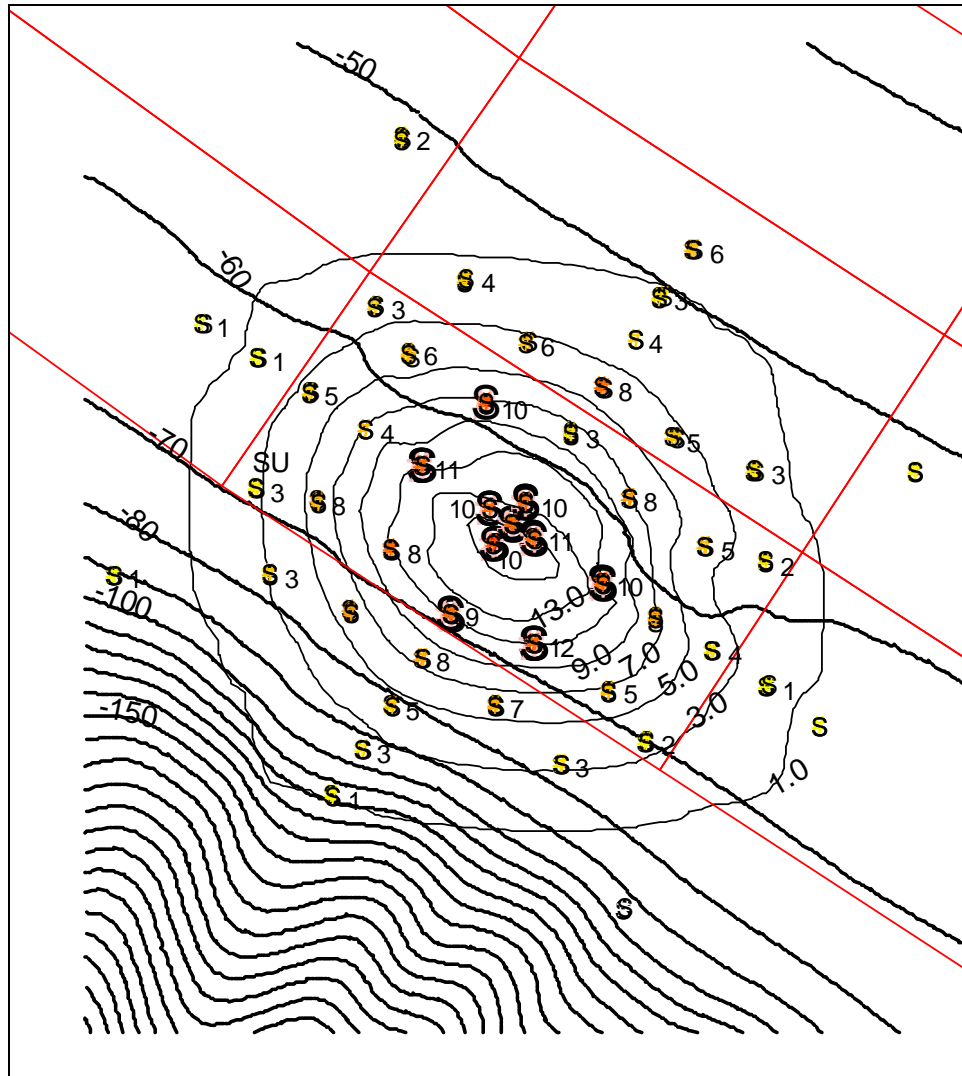


Figure K-29. MDFATE simulation of SU21 with no tidal currents, no stripping compared to SPI cap thickness measurements. Solid contours are MDFATE cap thickness measurements in cm (labeled as x.x), dots represent SPI stations, adjacent labels are cap thickness in cm. The dark solid lines are depth contours in meters

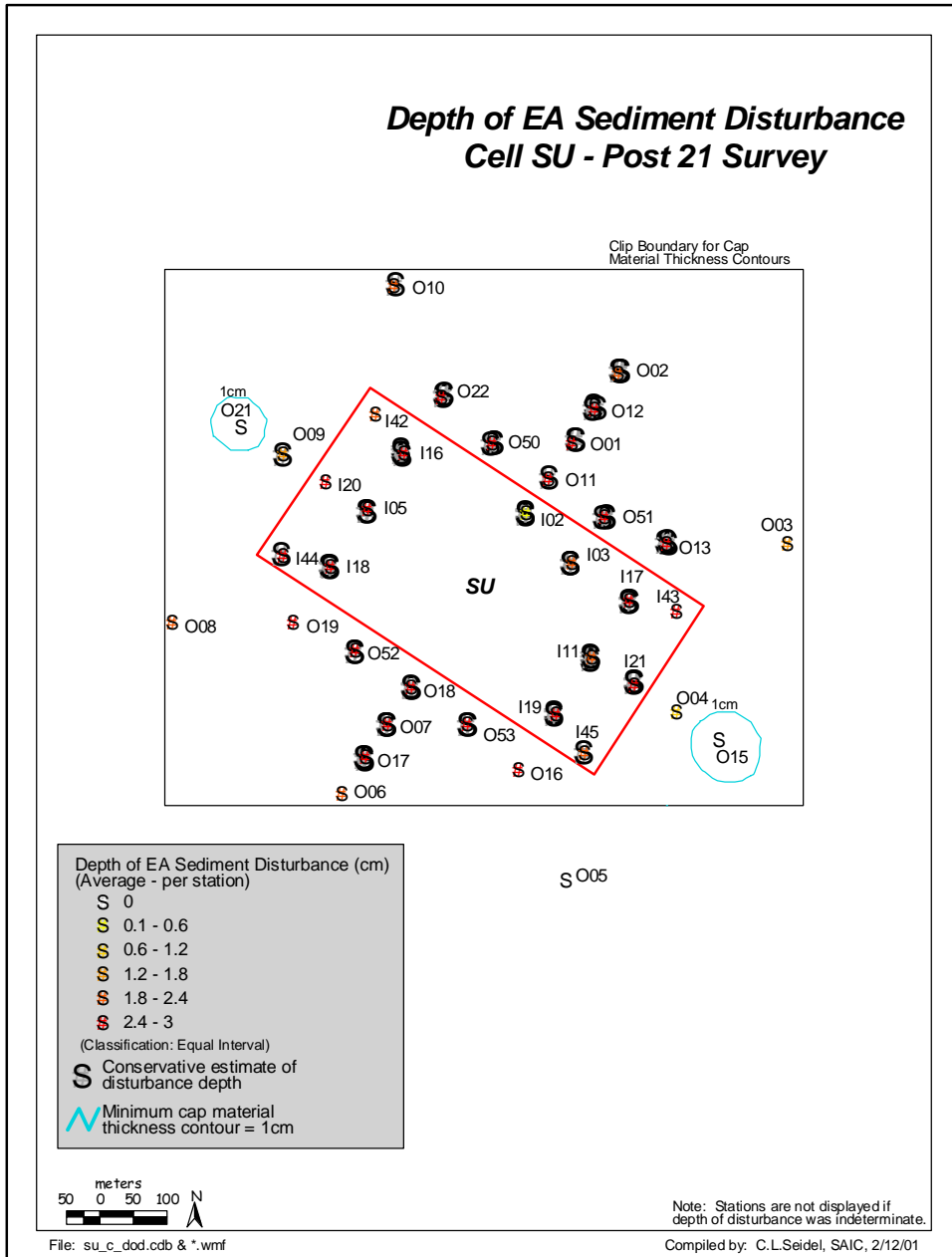


Figure K-30. EA layer depth of disturbance from SU21 placements as estimated from SPI data (SAIC 2002, Figure 4.7-16)

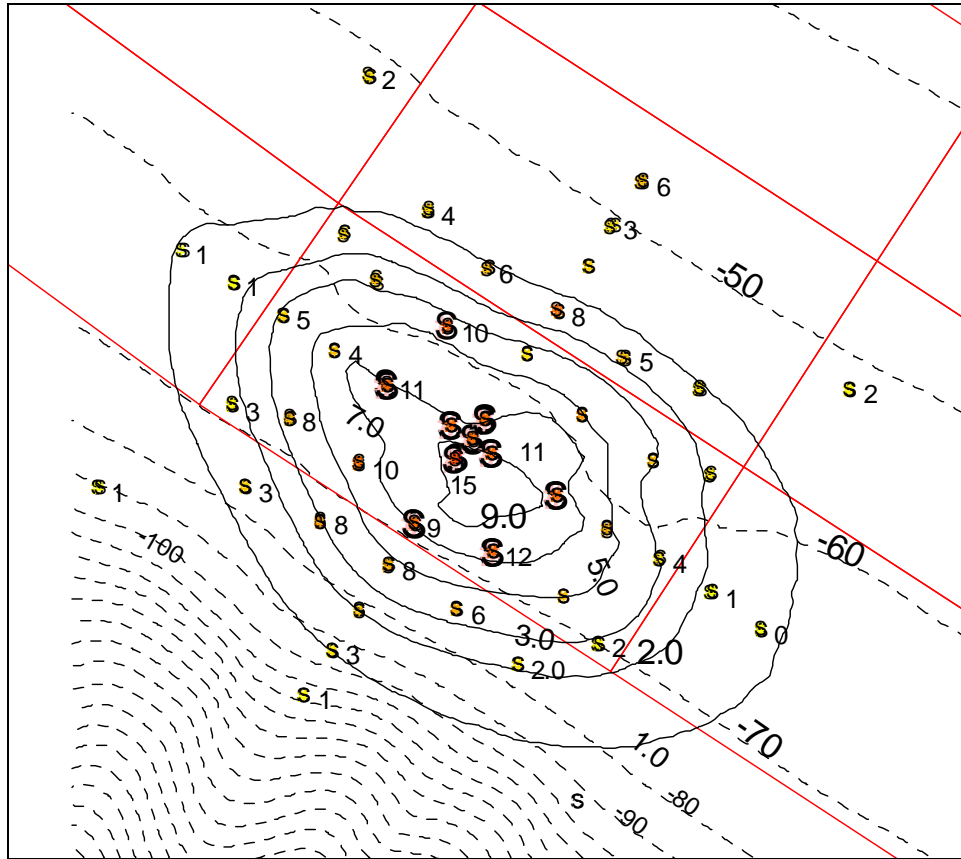


Figure K-31. MDFATE simulation of SU21 with SU sediment characteristics, includes tidal currents and stripping compared to SPC cap thickness measurements. Solid contours are MDFATE cap thickness measurements in cm (labeled as x.x), dots represent SPI stations, adjacent labels are cap SPC thickness in cm (integers)

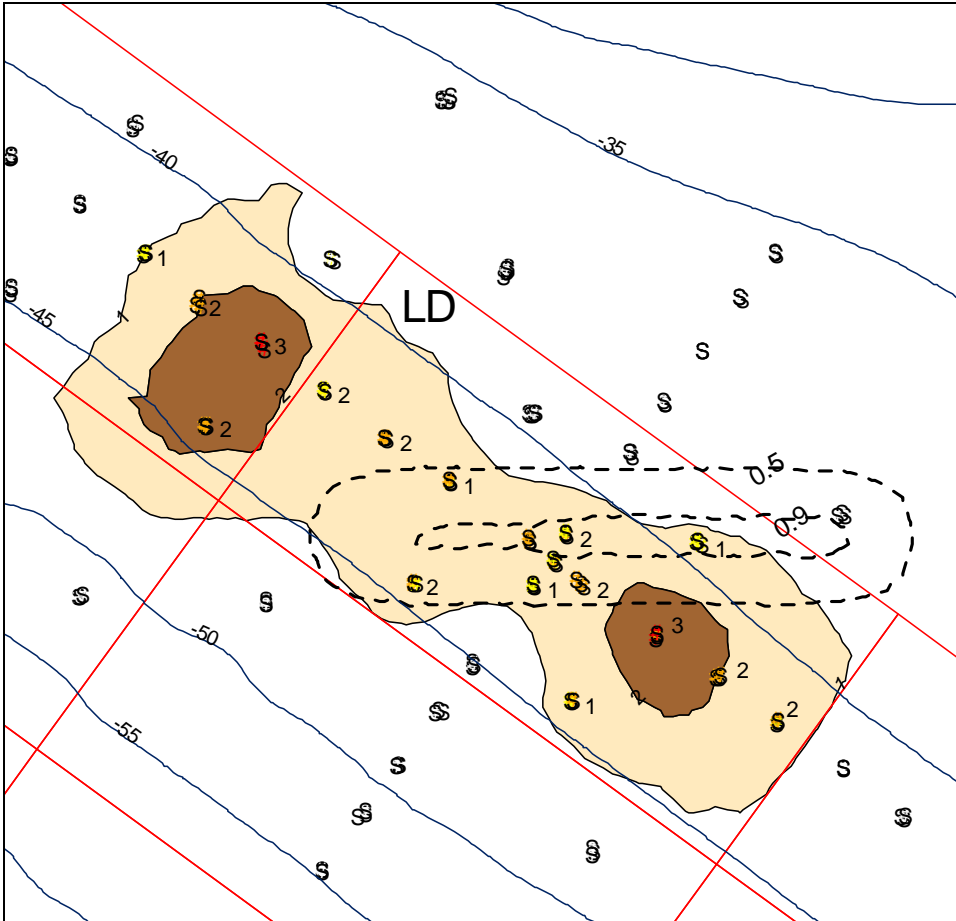


Figure K-32. MDFATE hindcast simulation in spreading mode of LD1 placement and SPI inferred cap thickness (cm). Bold dashed lines are MDFATE cap thickness contours (x.0) in cm, brown dots indicate SPI stations, SPI thicknesses are in cm (whole numbers). SPI cap thickness measurements in centimeters are also indicated by brown color ramp and black contours, and labeled as integers. Water depth contours are in meters (e.g., -45)

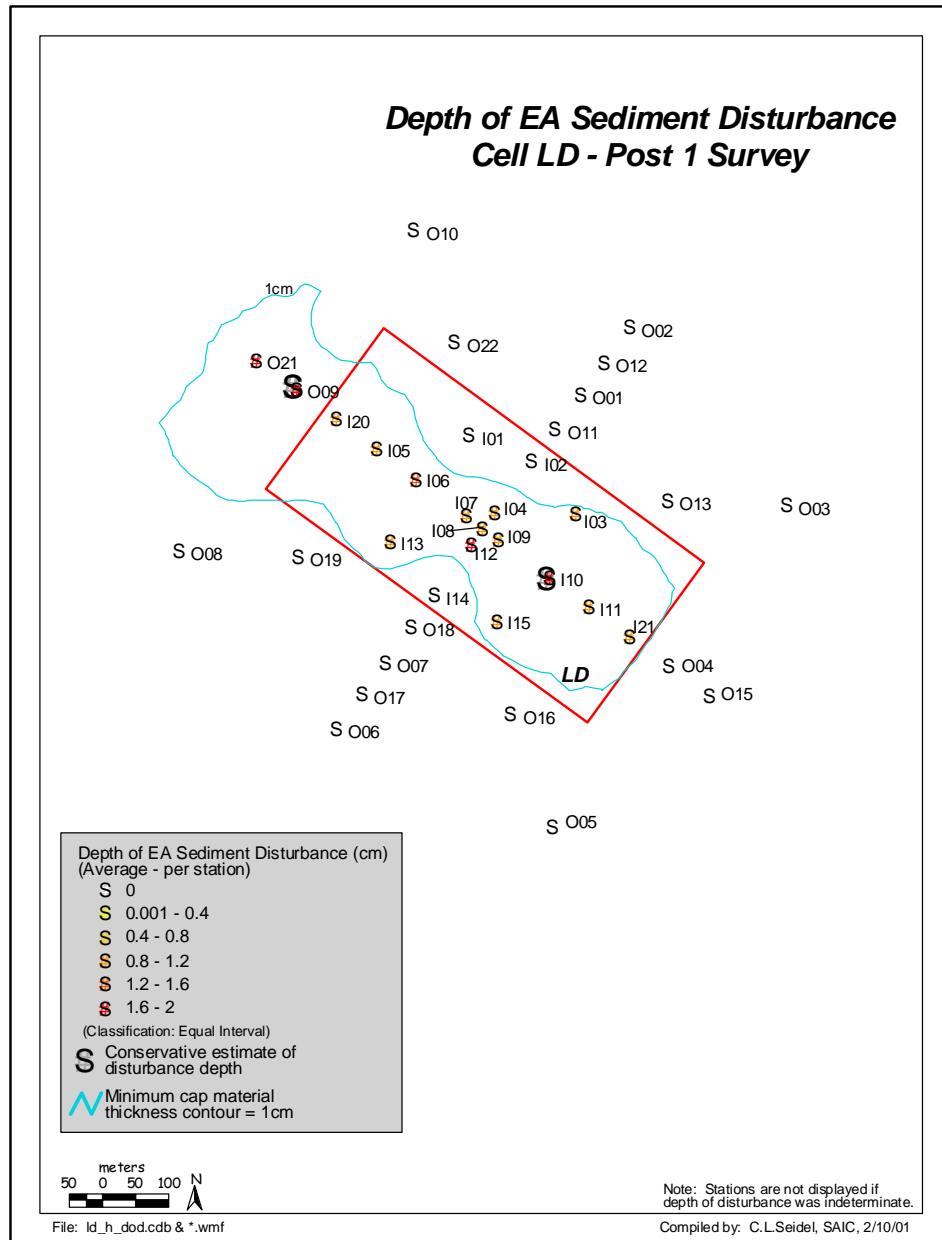


Figure K-33. EA depth of disturbance from placement LD1 (SAIC 2002, Figure 5.7-7)

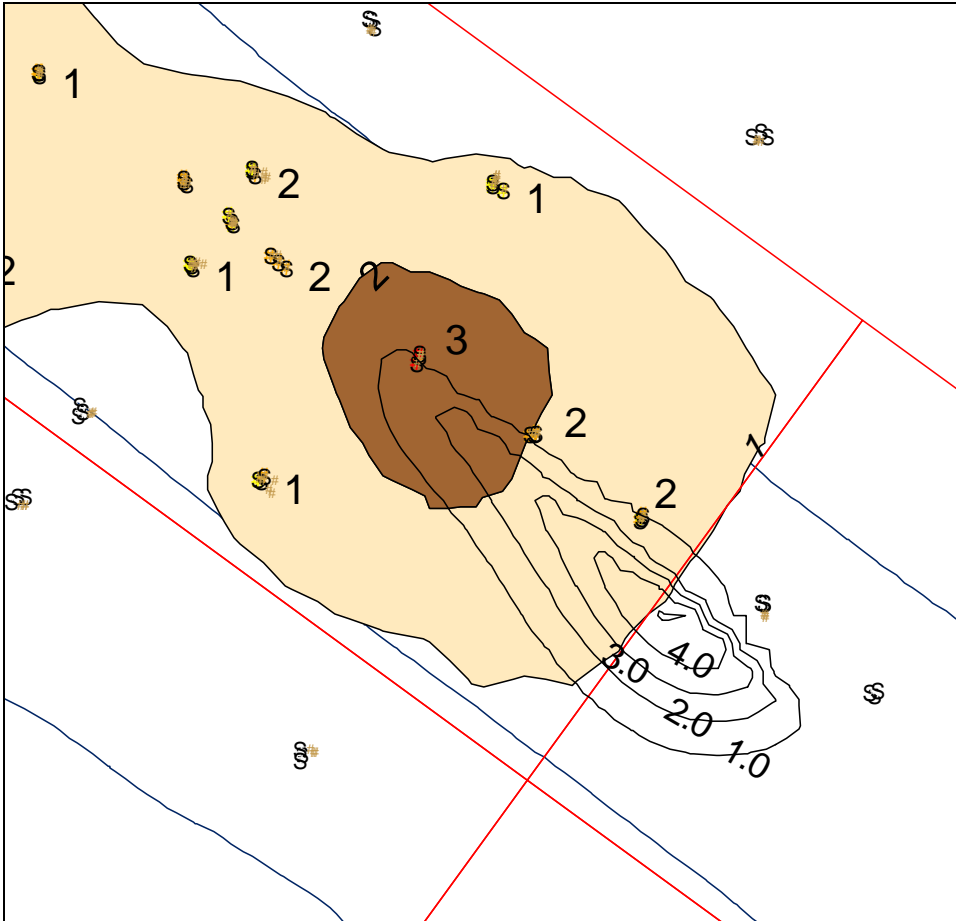


Figure K-34. MDFATE simulation of placement LD1 using conventional placement algorithms. (Contours are in cm, cream colored area is 1-1.5 cm thickness as measured by SPI, dark brown area is 2-2.5 cm in thickness as measured by SPI)

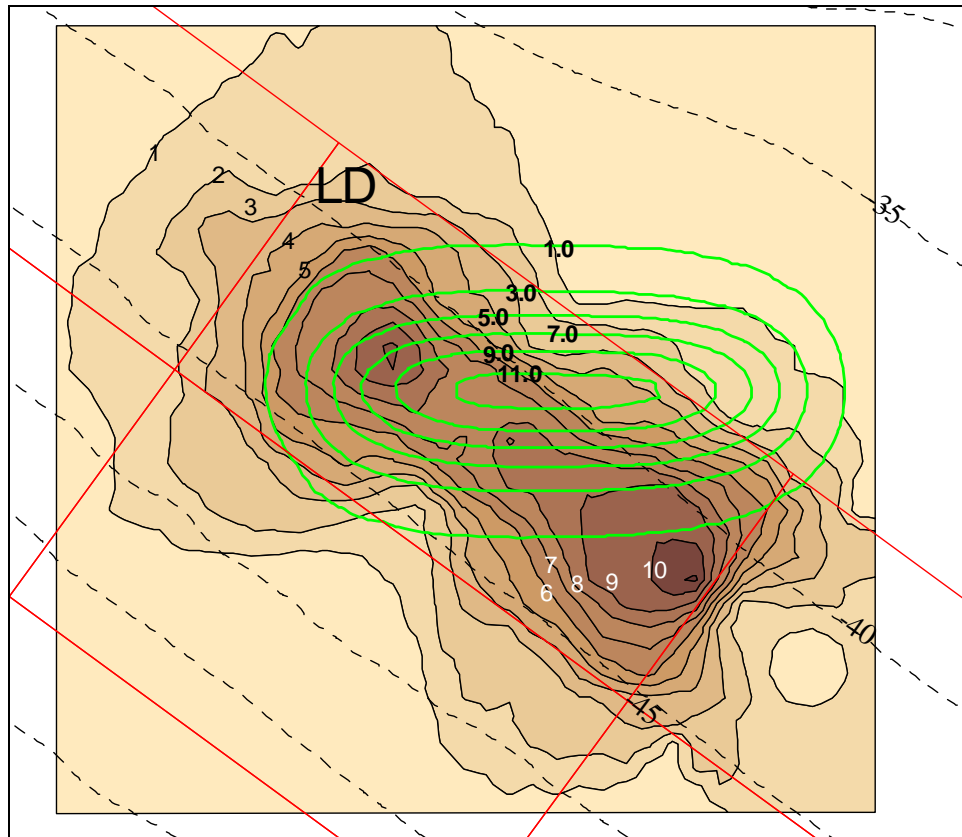


Figure K-35. Cap thickness comparison LD9 placements. MDFATE simulations contours are in centimeters, bright green and labeled with decimals, SPI cap thickness measurements in centimeters are indicated by color ramp and black contours, and labeled as integers. Water depth contours are in meters and displayed as dashed lines

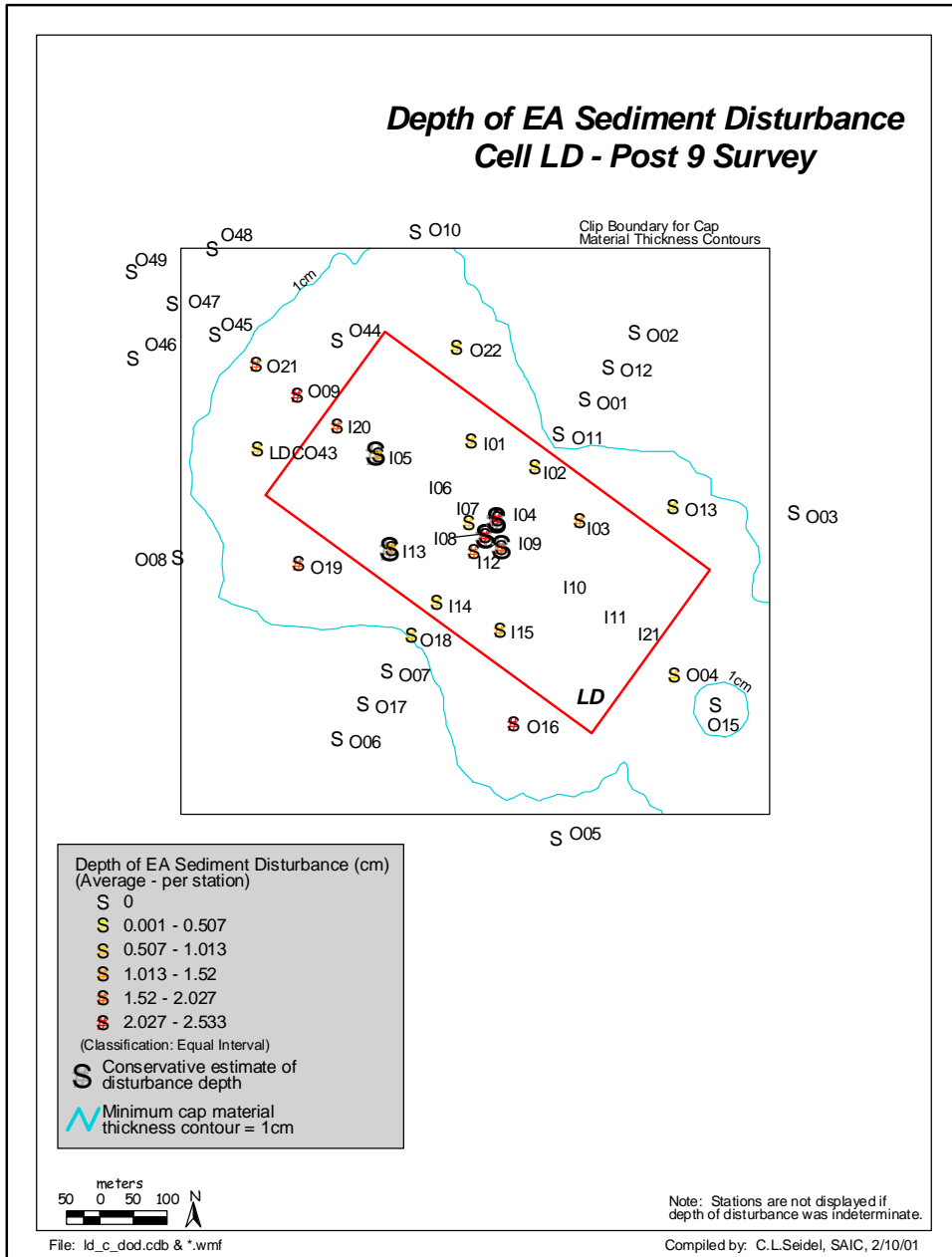


Figure K-36. EA depth of disturbance from placement LD9 (SAIC 2002, Figure 5.7-11)

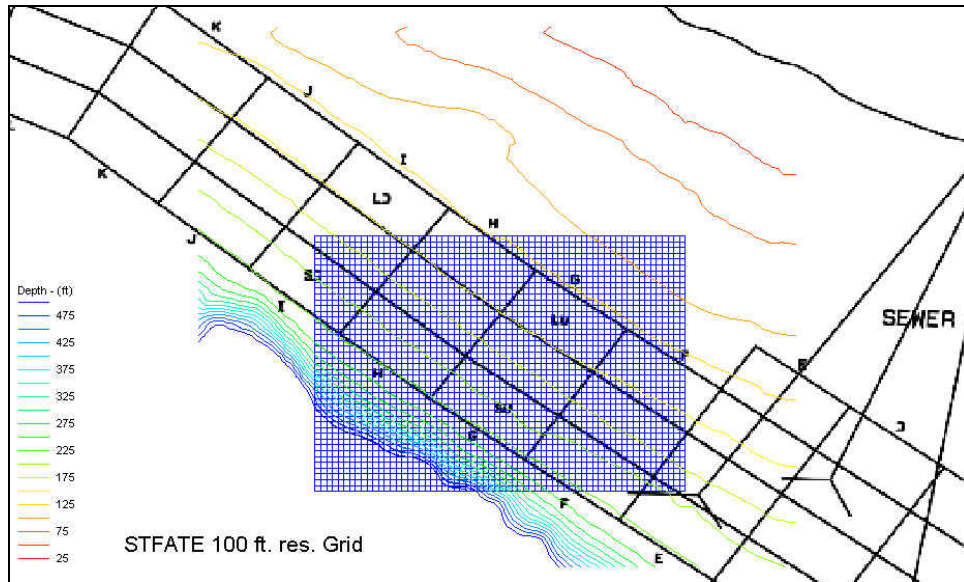


Figure K-37. STFATE numerical grid

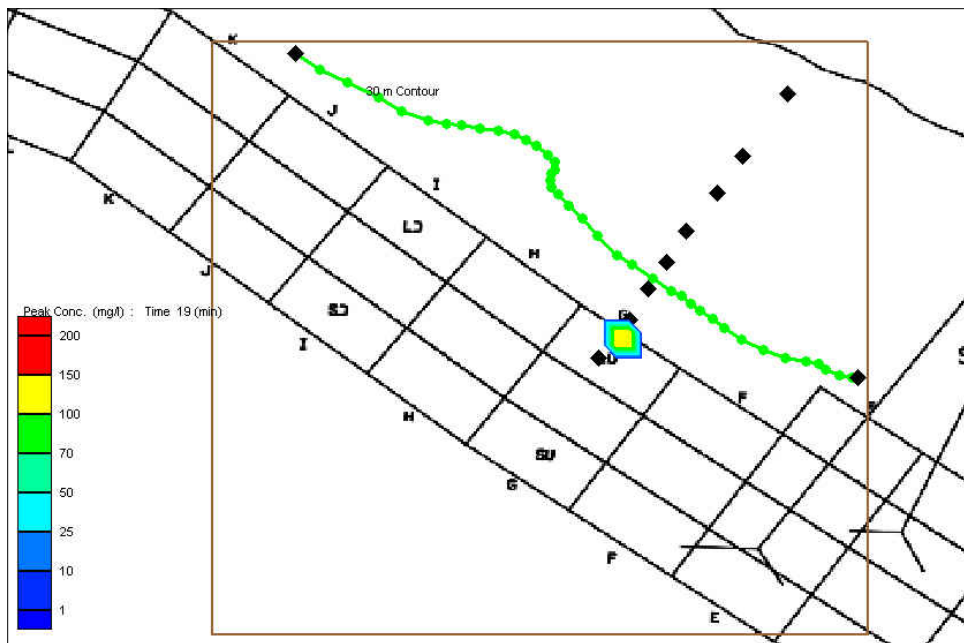


Figure K-38. STFATE simulation of placement in LU, simulated water column concentrations after 19 min

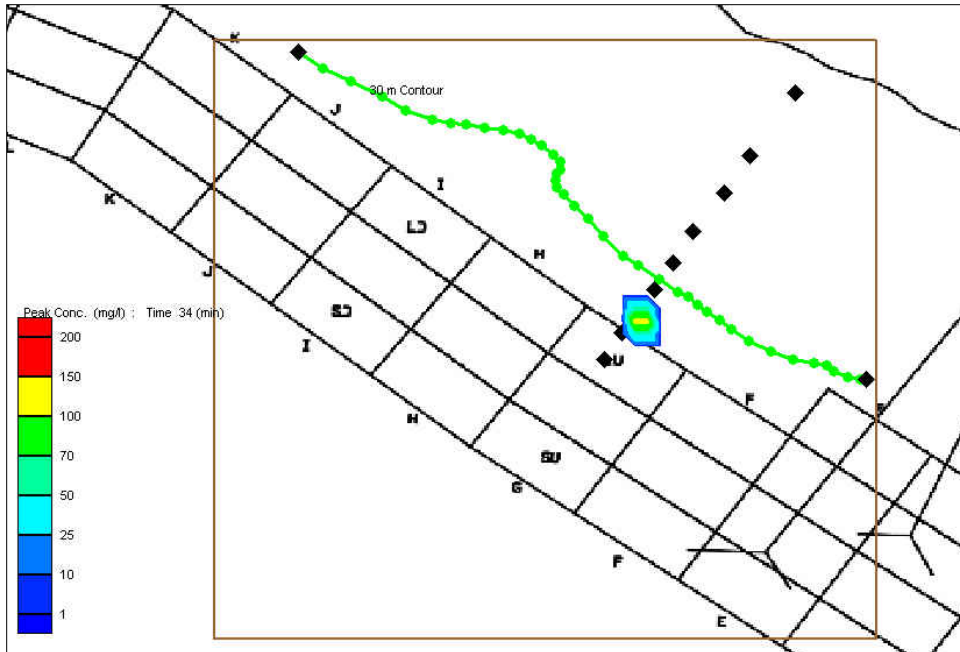


Figure K-39. STFATE simulation of placement in LU, simulated water column concentrations after 34 min

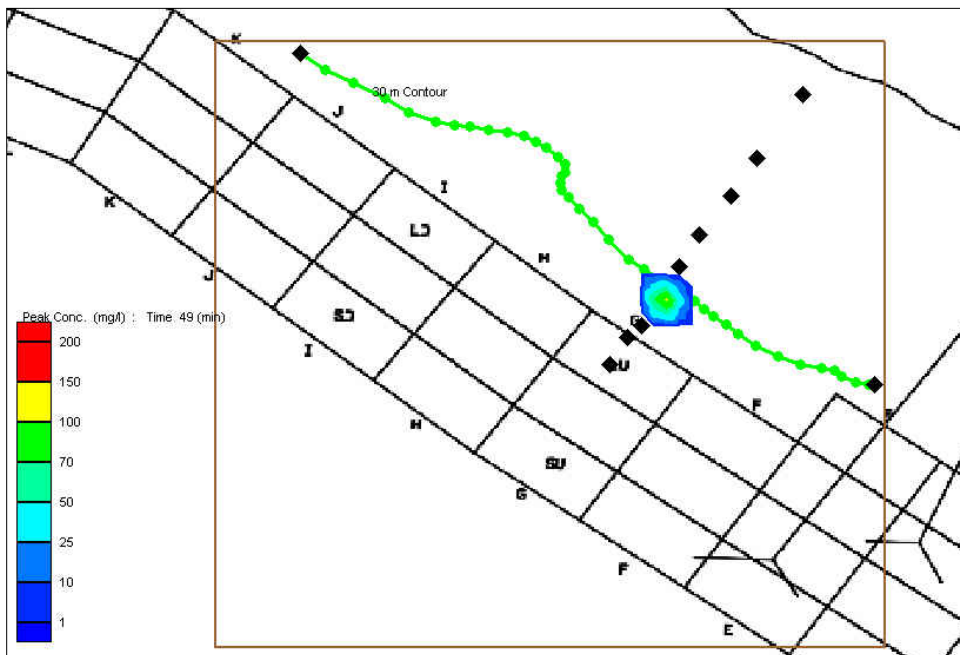


Figure K-40. STFATE simulation of placement in LU, simulated water column concentrations after 49 min

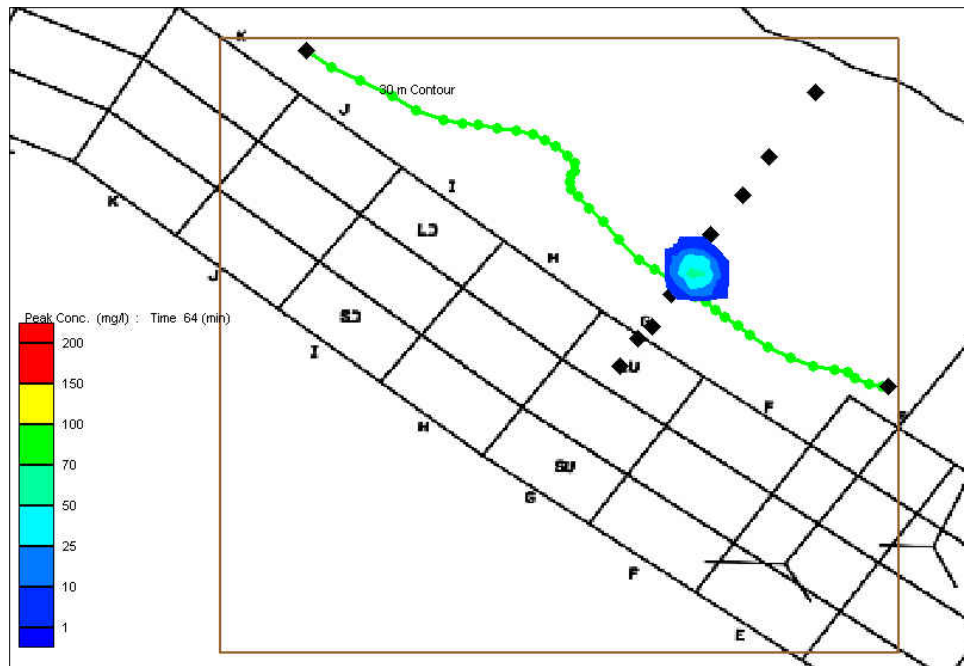


Figure K-41. STFATE simulation of placement in LU, simulated water column concentrations after 64 min

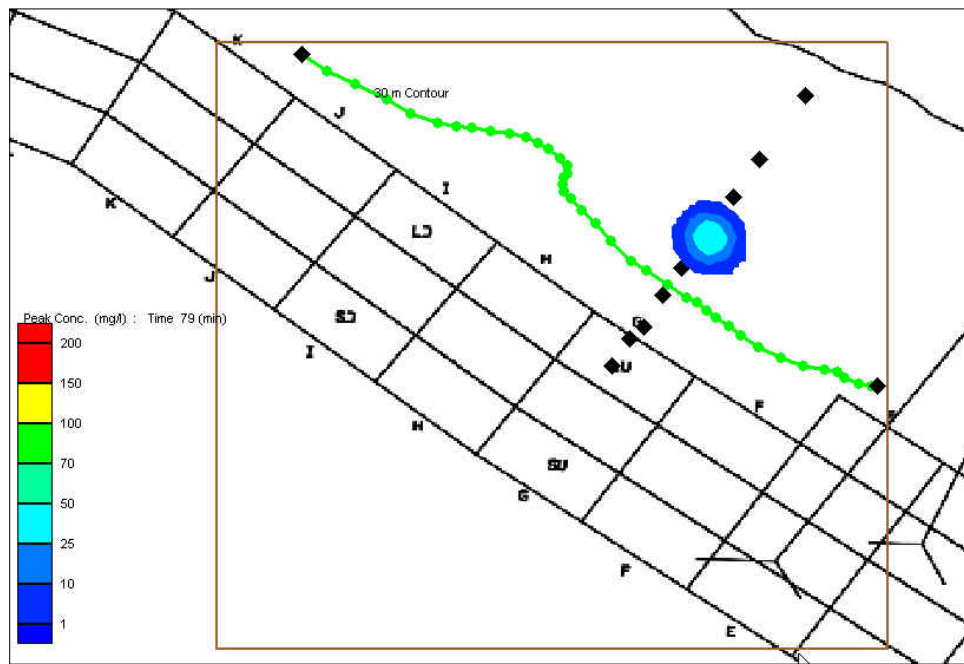


Figure K-42. STFATE simulation of placement in LU, simulated water column concentrations after 79 min

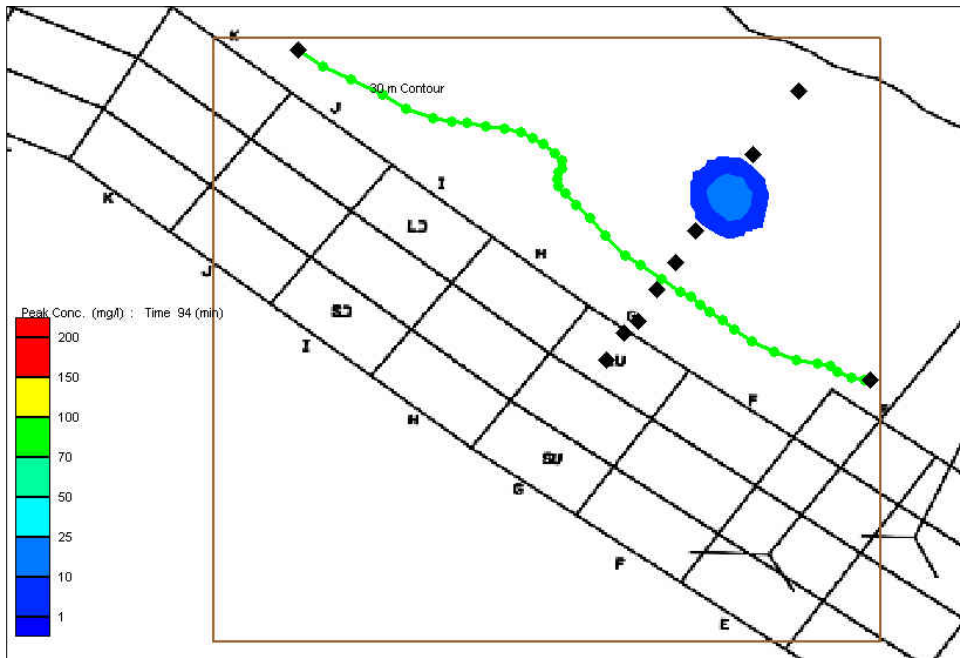


Figure K-43. STFATE simulation of placement in LU, simulated water column concentrations after 94 min

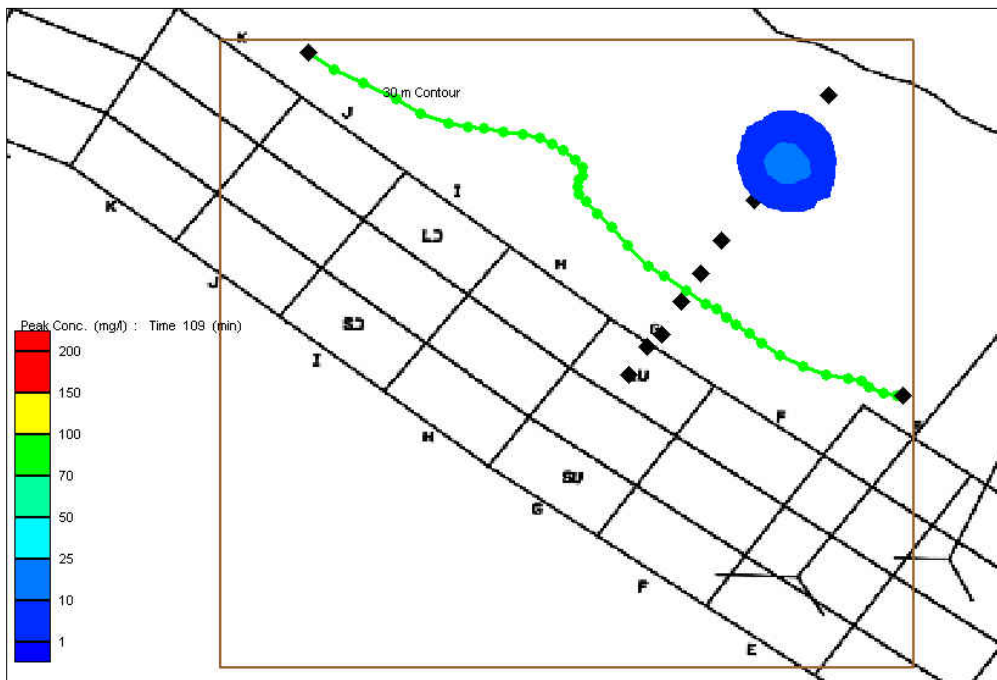


Figure K-44. STFATE simulation of placement in LU, simulated water column concentrations after 109 min

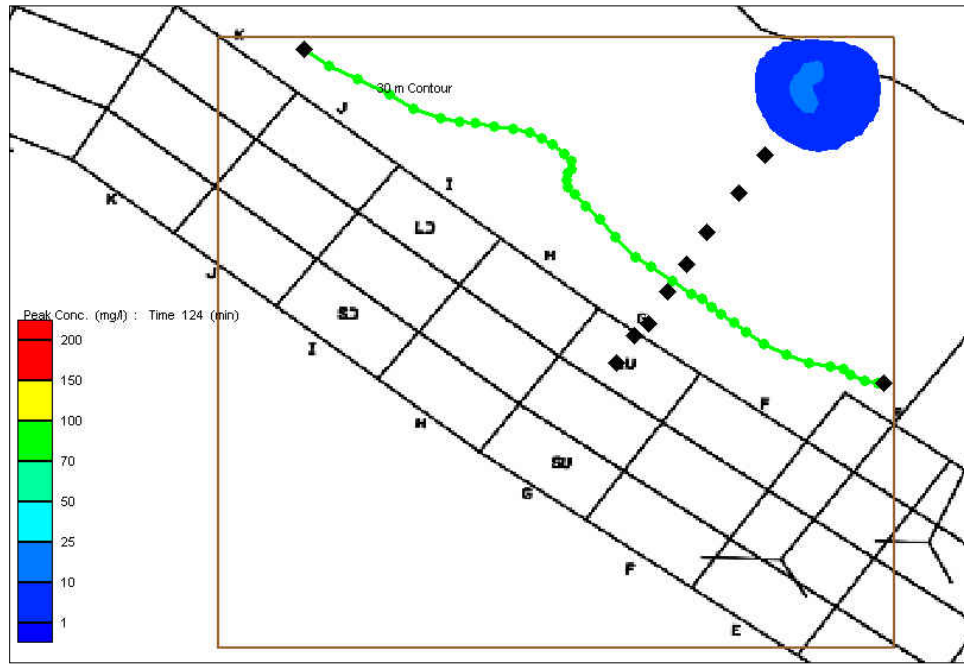


Figure K-45. STFATE simulation of placement in LU, simulated water column concentrations after 124 min

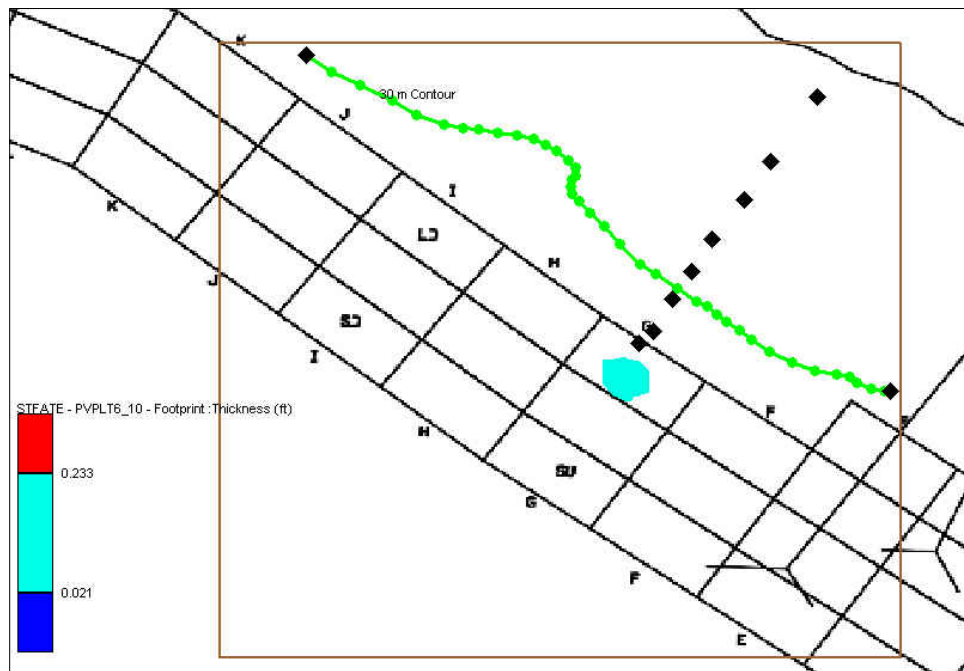


Figure K-46. STFATE simulation of placement in LU, simulated cap thickness

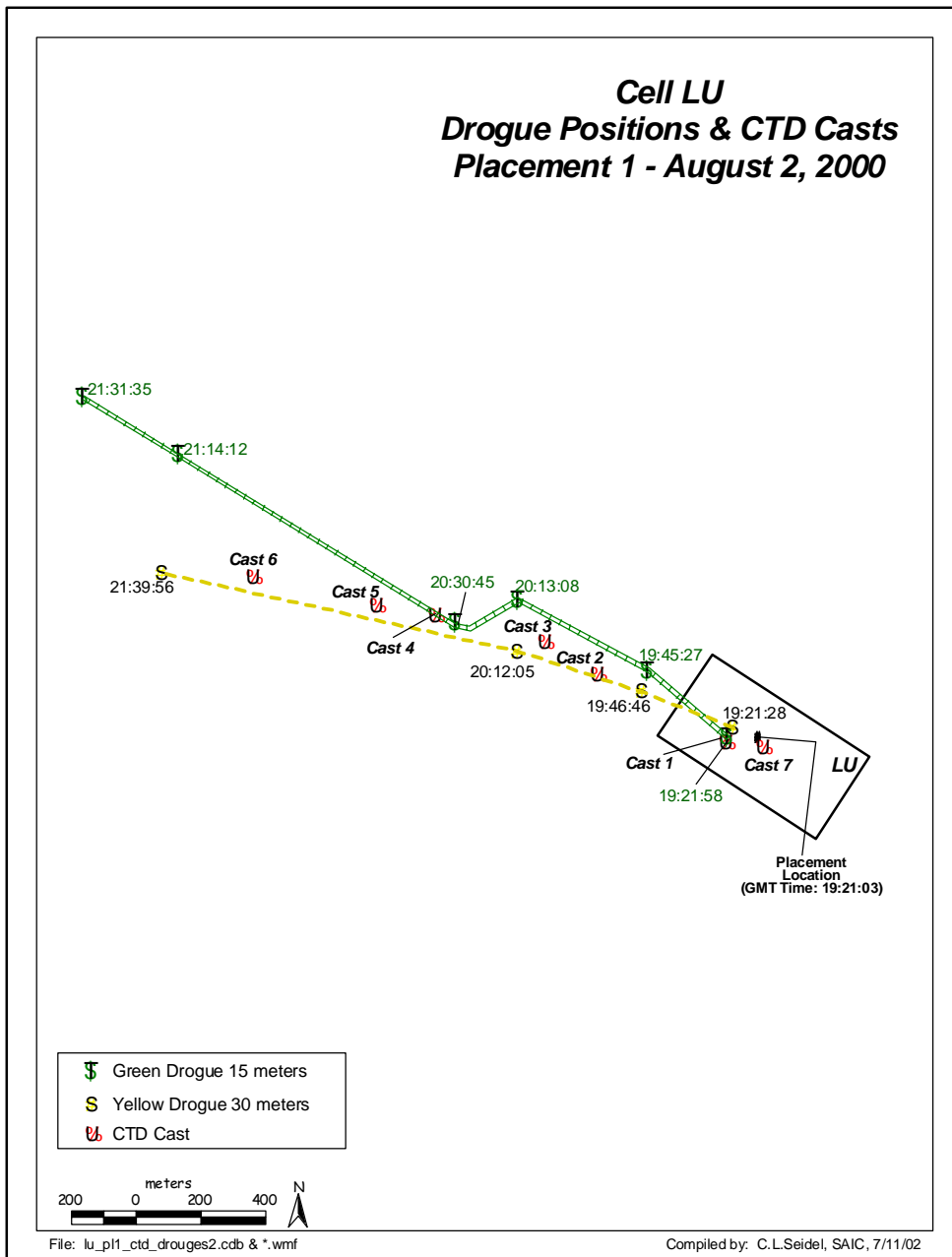


Figure K-47. LU1 drogue paths and CDT stations (SAIC 2002), Figure 3.5-2)

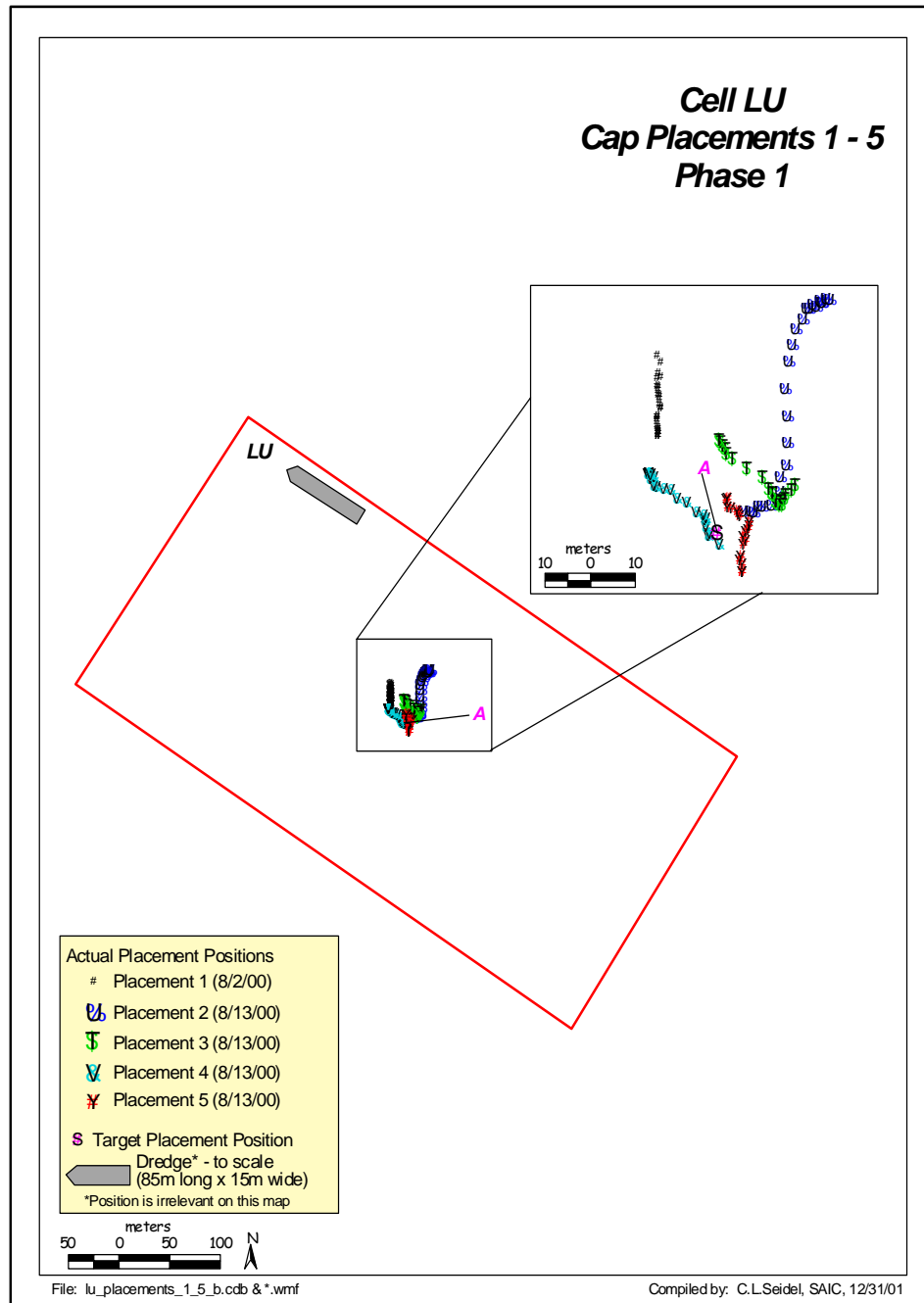


Figure K-48. Drift paths of LU disposals (SAIC 2002, Figure 3.2-5)

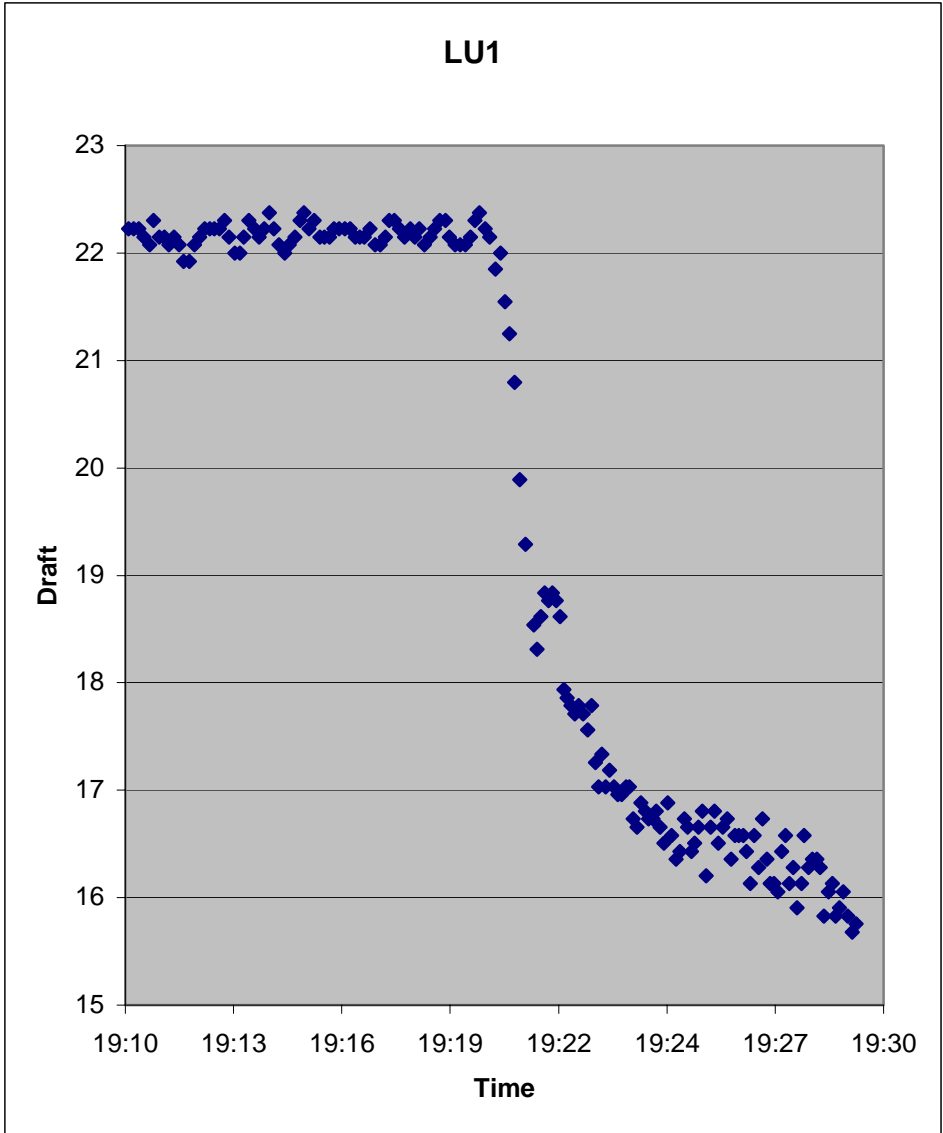


Figure K-49. Vessel draft of LU1 disposal

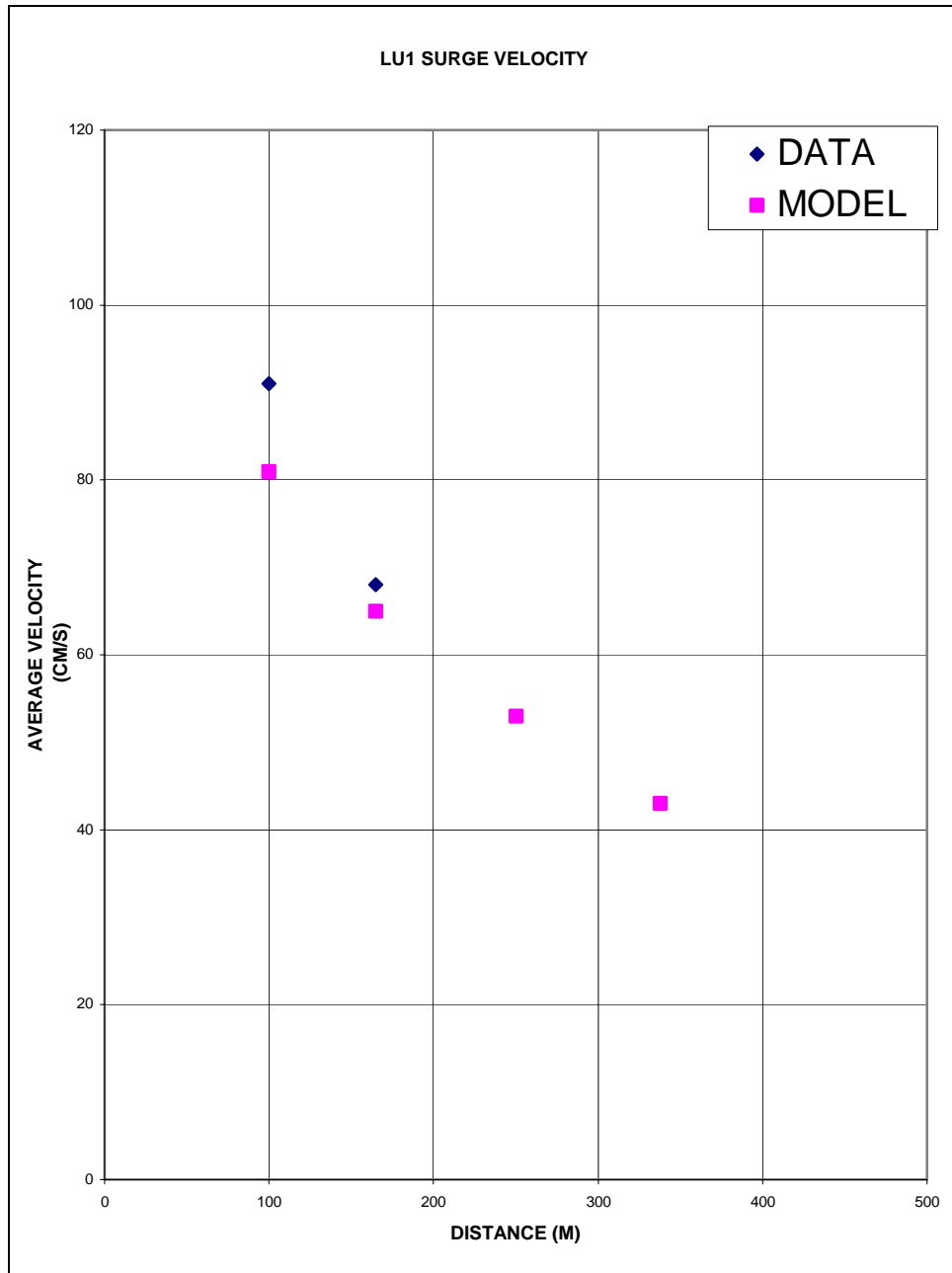


Figure K-50. Comparison of STFATE LU1 average surge speed with field data

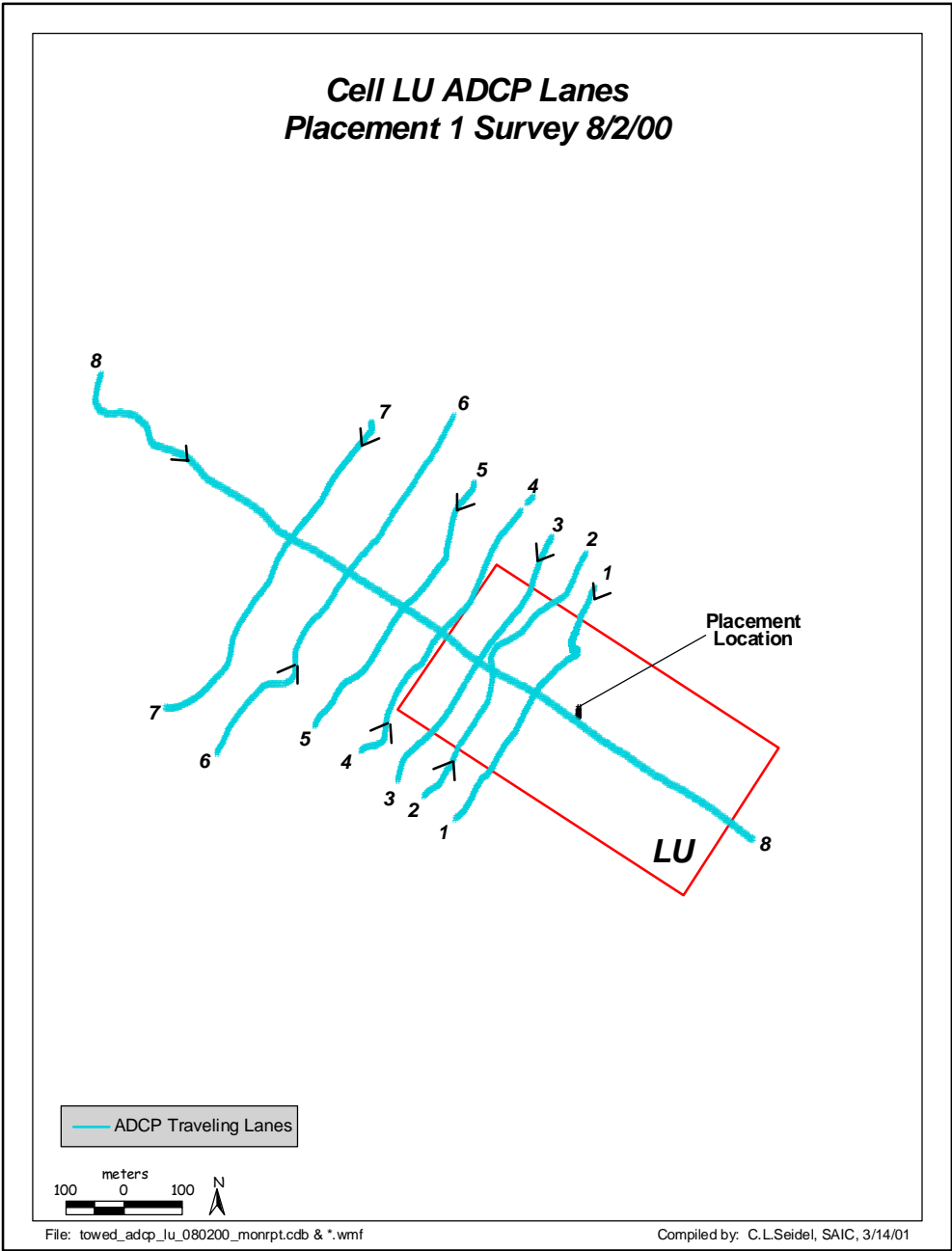


Figure K-51. LU1 transects (SAIC 2002, Figure 3.6-5)

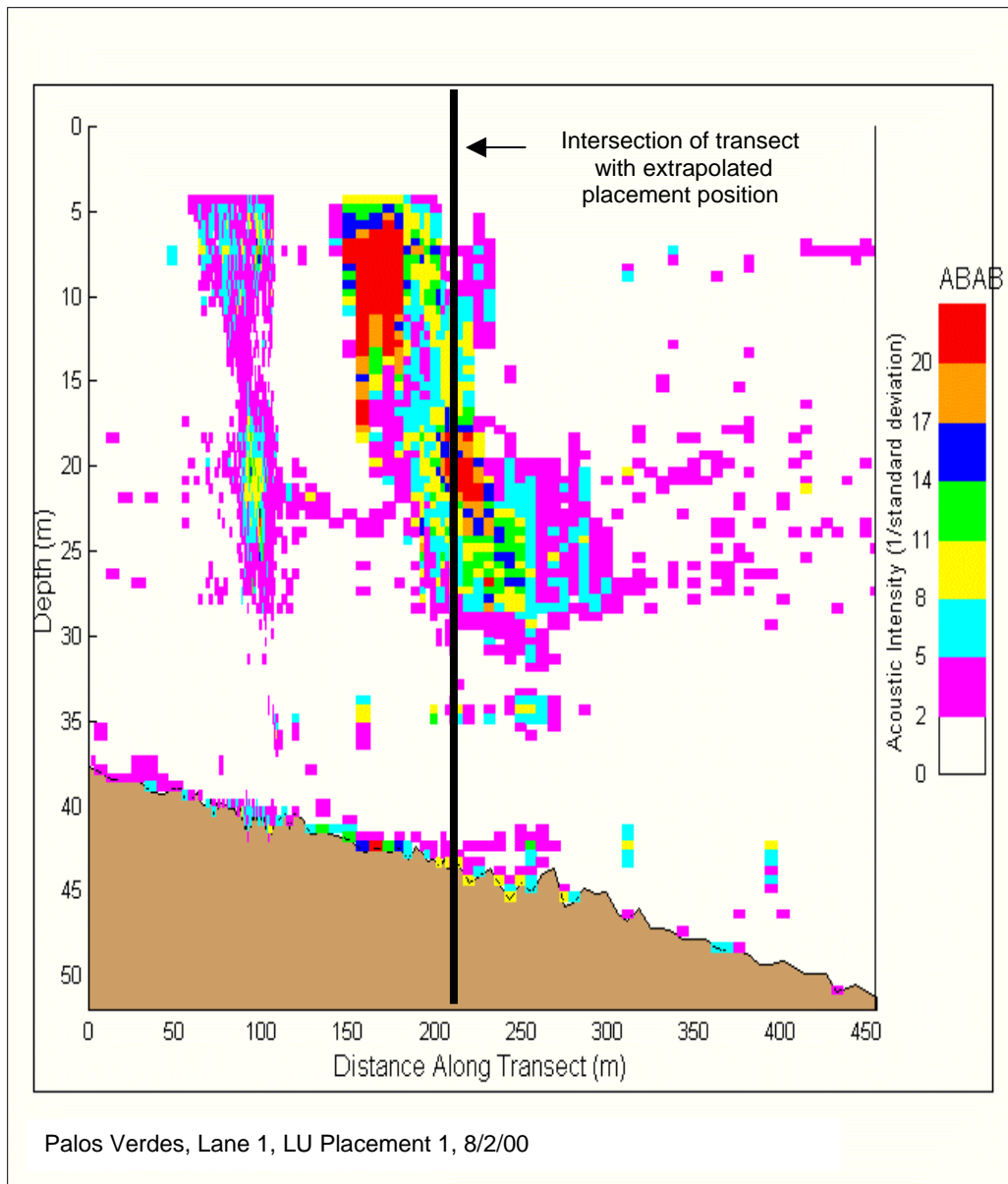


Figure K-52. ABAB along Transect 1 while placement was occurring (SAIC 2002, Figure 3.6-6)

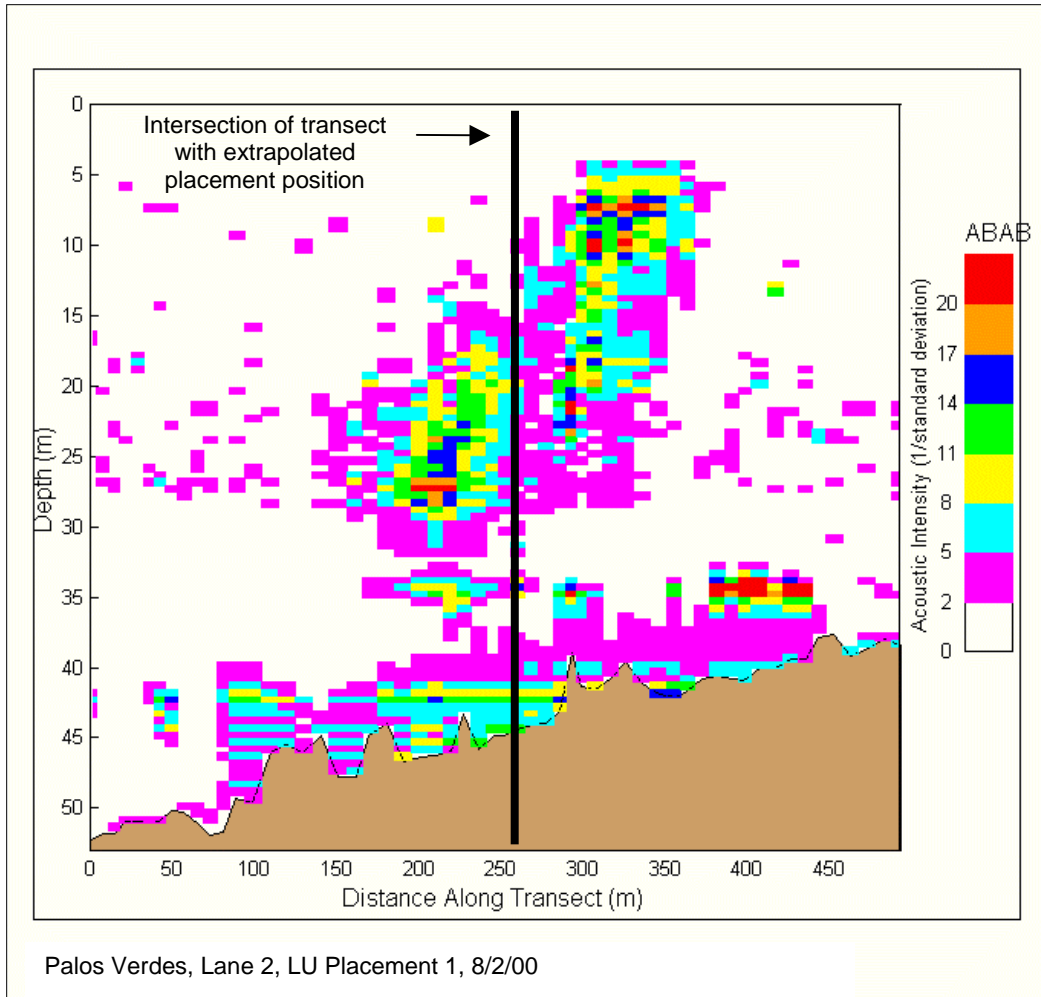


Figure K-53. ABAB along Transect 2 at 2 min after the placement operation ended (SAIC 2002, Figure 3.6-7)

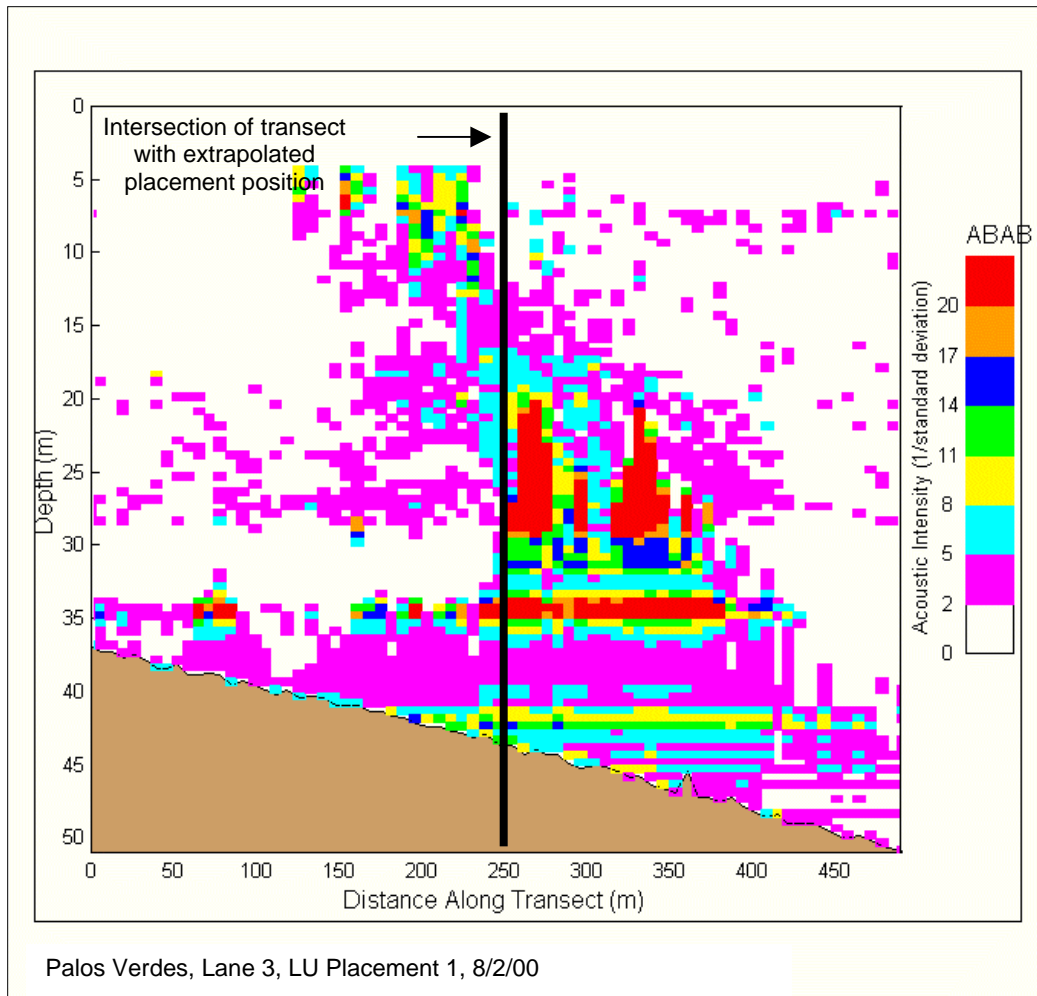


Figure K-54. ABAB along Transect 3 at 9 min after the placement operation ended (SAIC 2002, Figure 3.6-8)

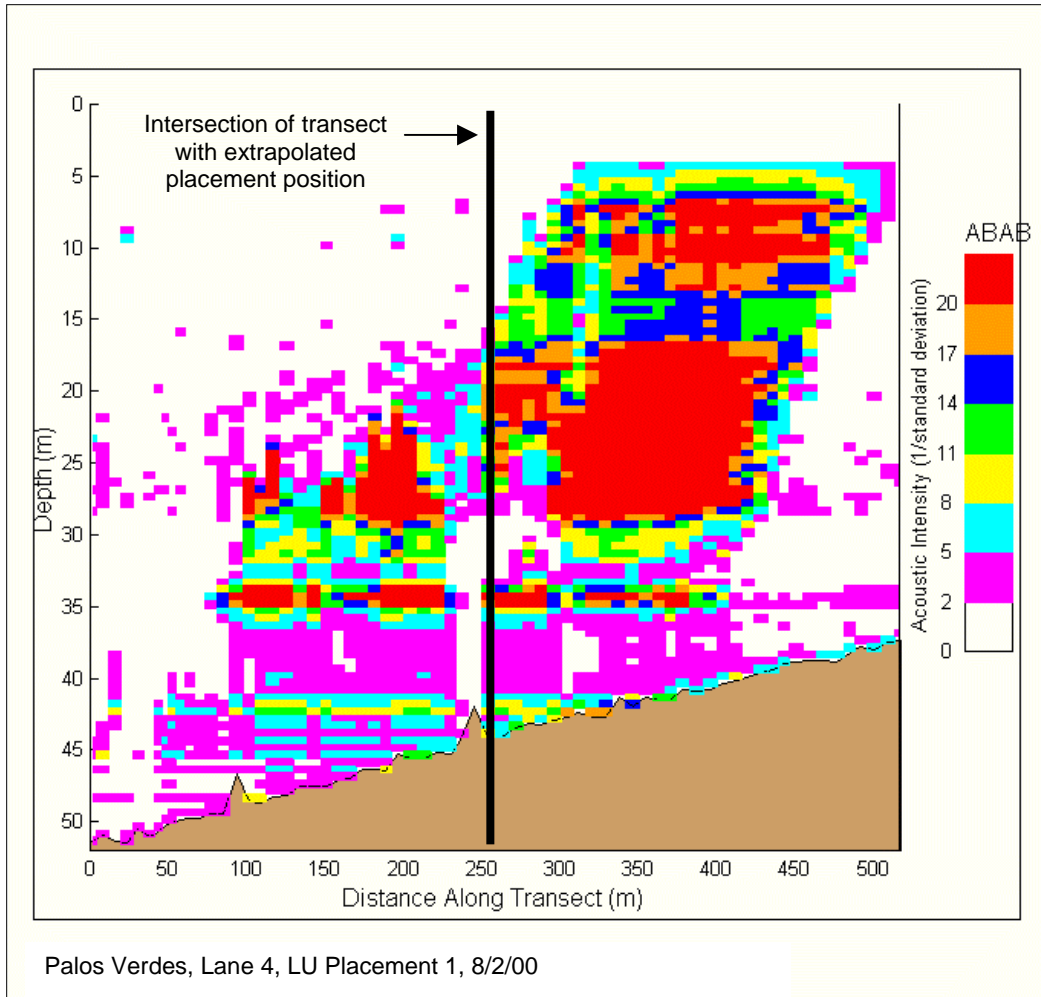


Figure K-55. ABAB along Transect 4 at 16 min after the placement operation ended (SAIC 2002, Figure 3.6-9)

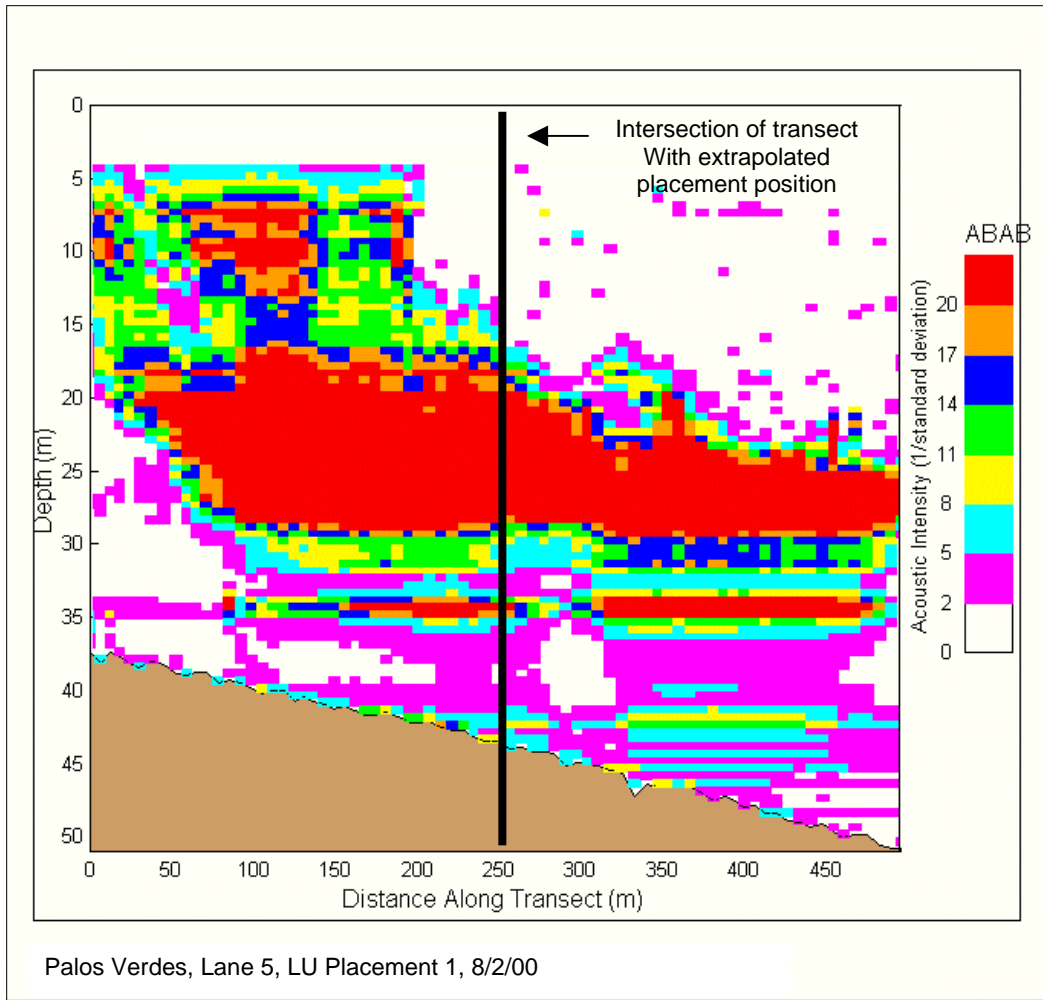


Figure K-56. ABAB along Transect 5 at 22 min after the placement operation ended (SAIC 2002, Figure 3.6-10)

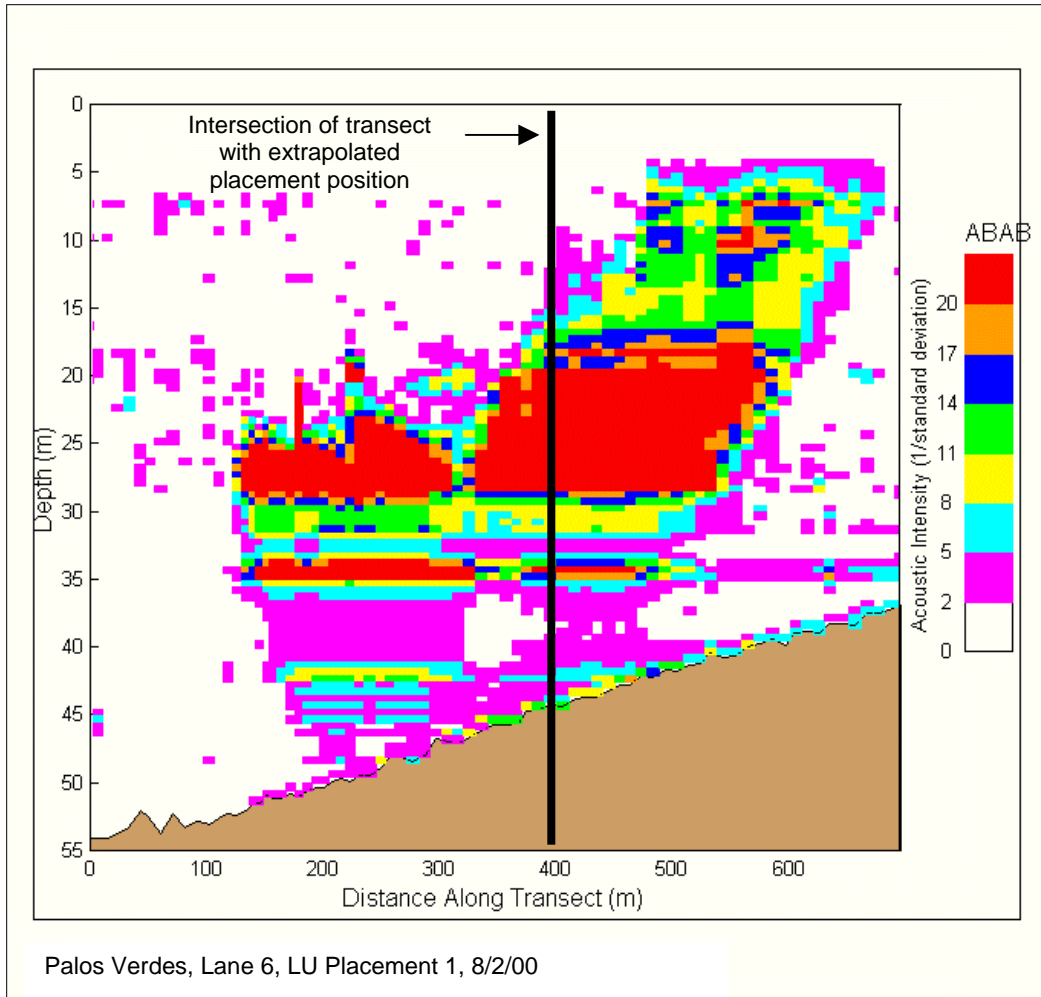


Figure K-57. ABAB along Transect 6 at 30 min after the placement after the placement operation ended (SAIC 2002, Figure 3.6-11)

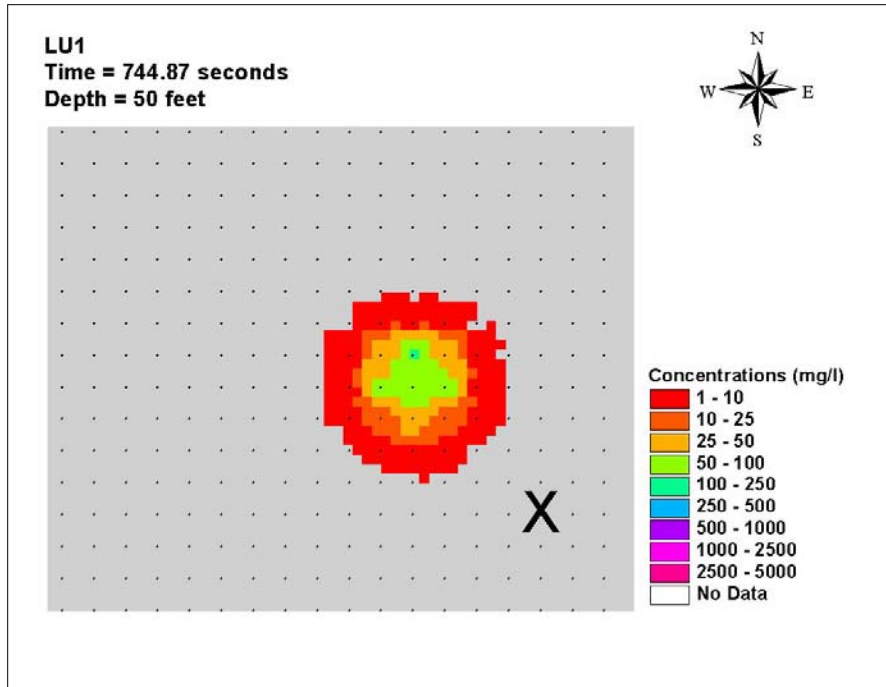


Figure K-58. LU1 plume at end of collapse at 15 m

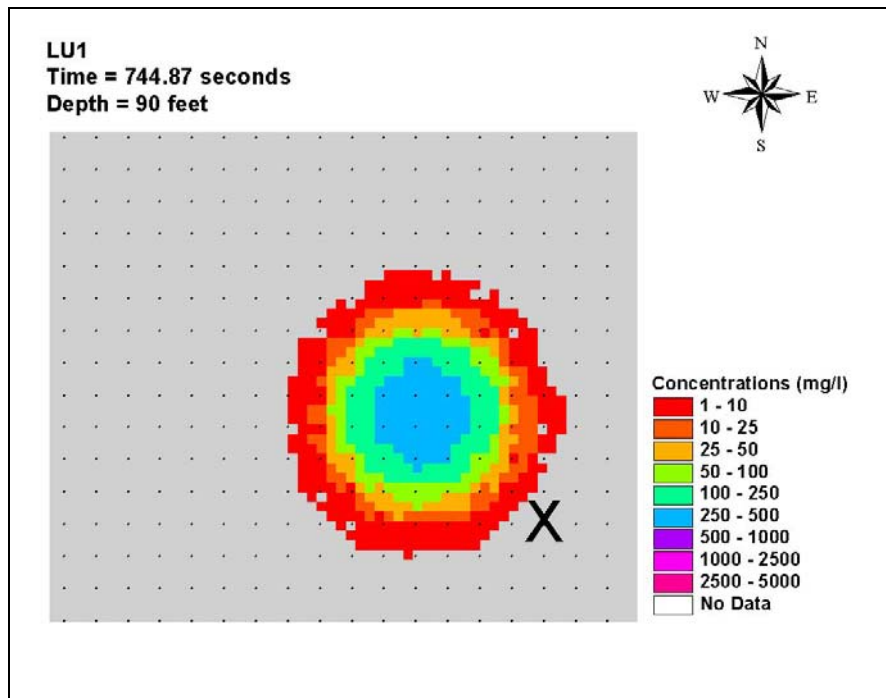


Figure K-59. LU1 plume at end of collapse at 27 m

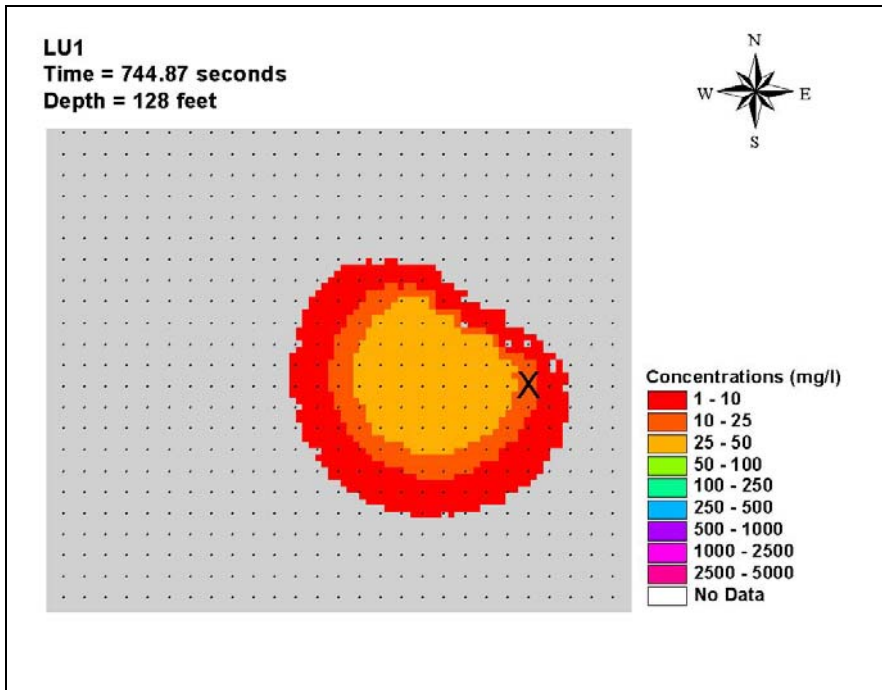


Figure K-60. LU1 plume at end of collapse at 12 m

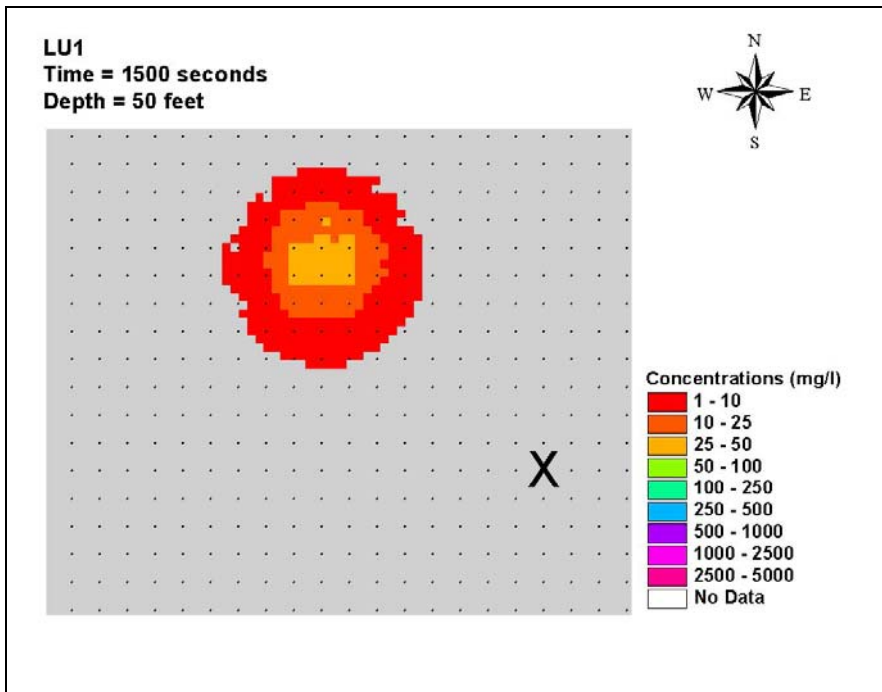


Figure K-61. LU1 plume at 1,500 sec at 15 m

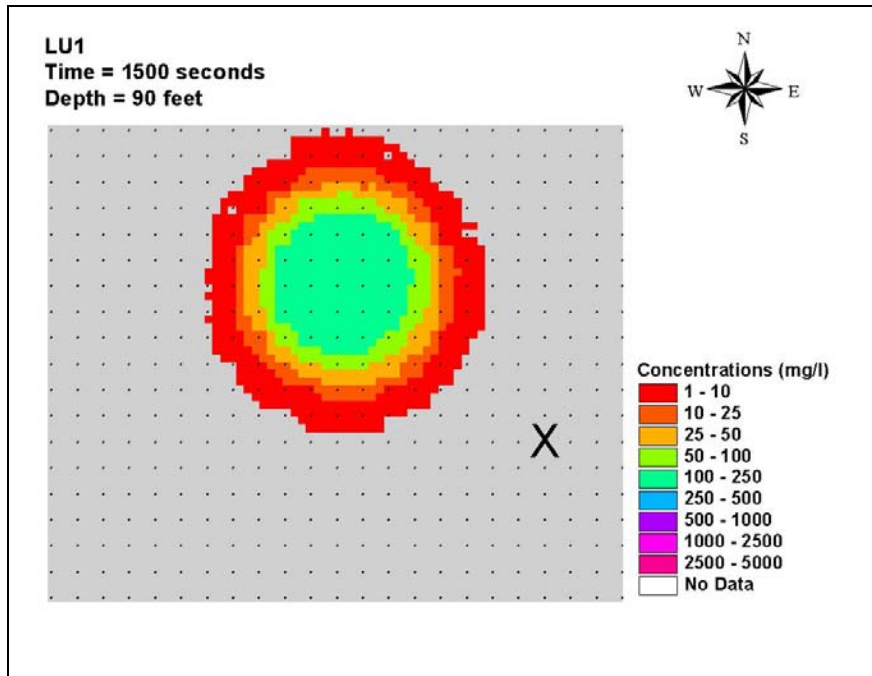


Figure K-62. LU1 plume at 1,500 sec at 28 m

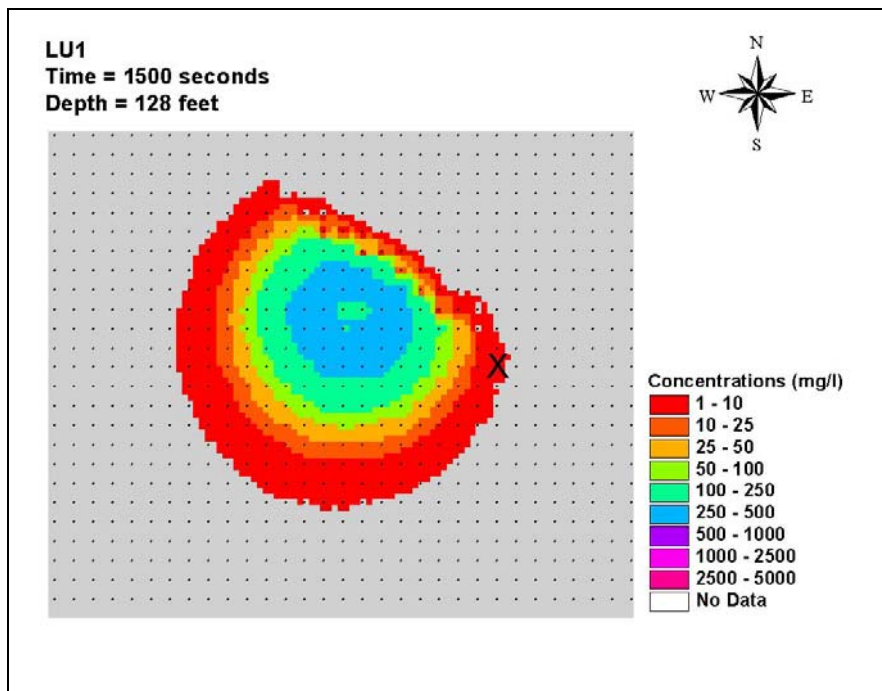


Figure K-63. LU1 plume at 1,500 sec at 39 m

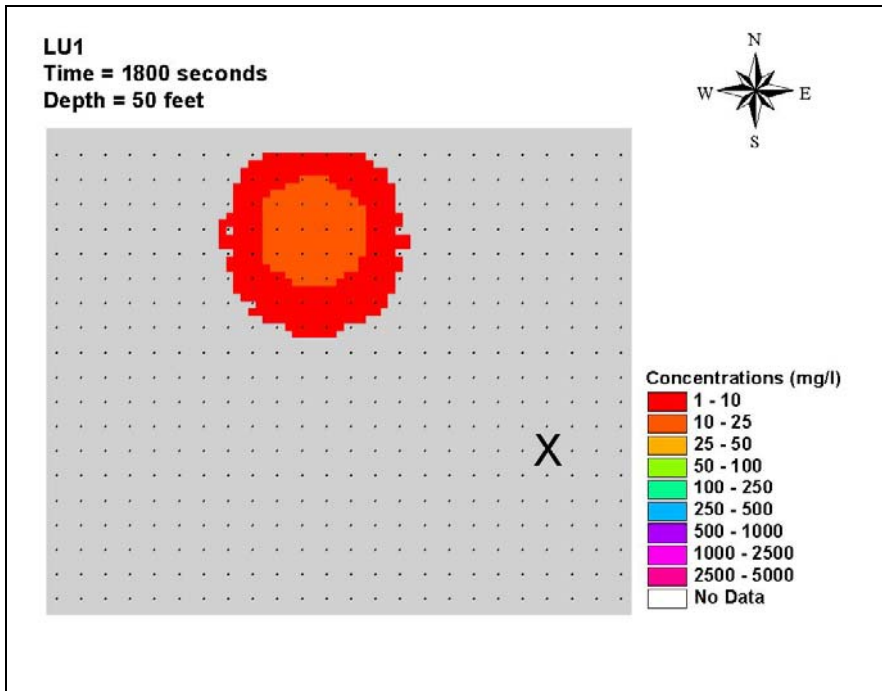


Figure K-64. LU1 plume at 1,800 sec at 15 m

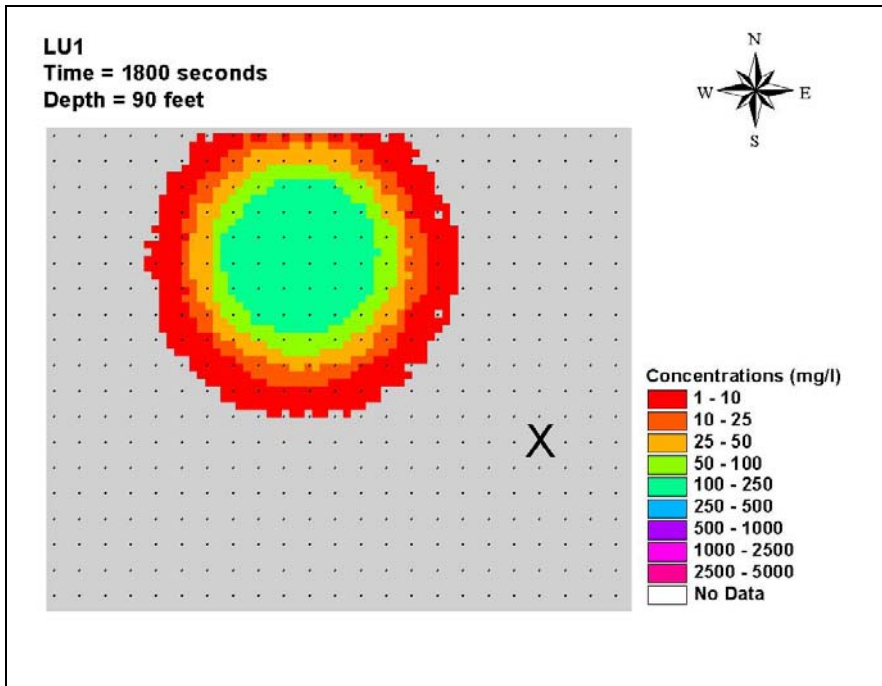


Figure K-65. LU1 plume at 1,800 sec at 27 m

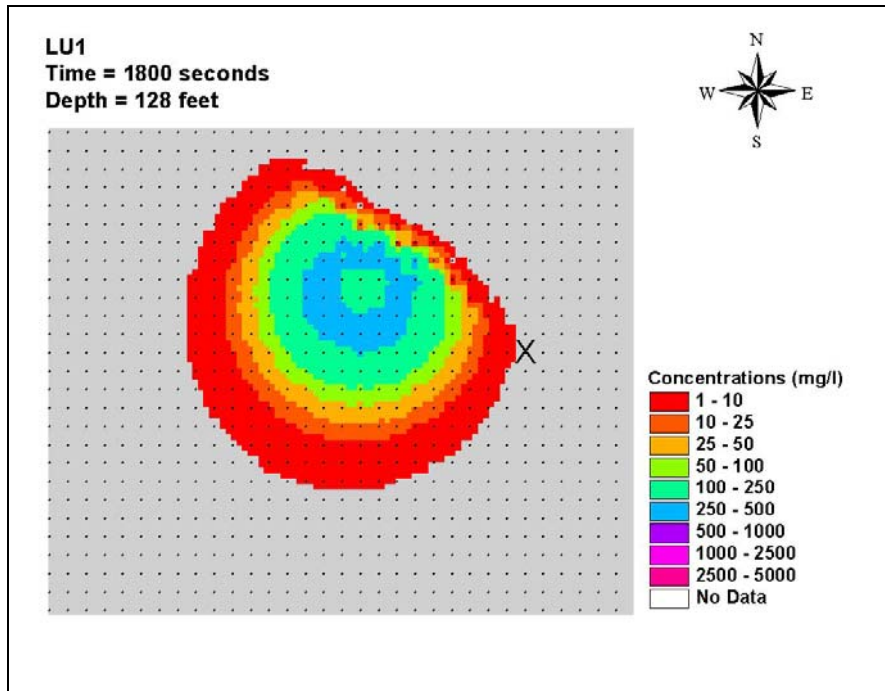


Figure K-66. LU1 plume at 1,800 sec at 39 m

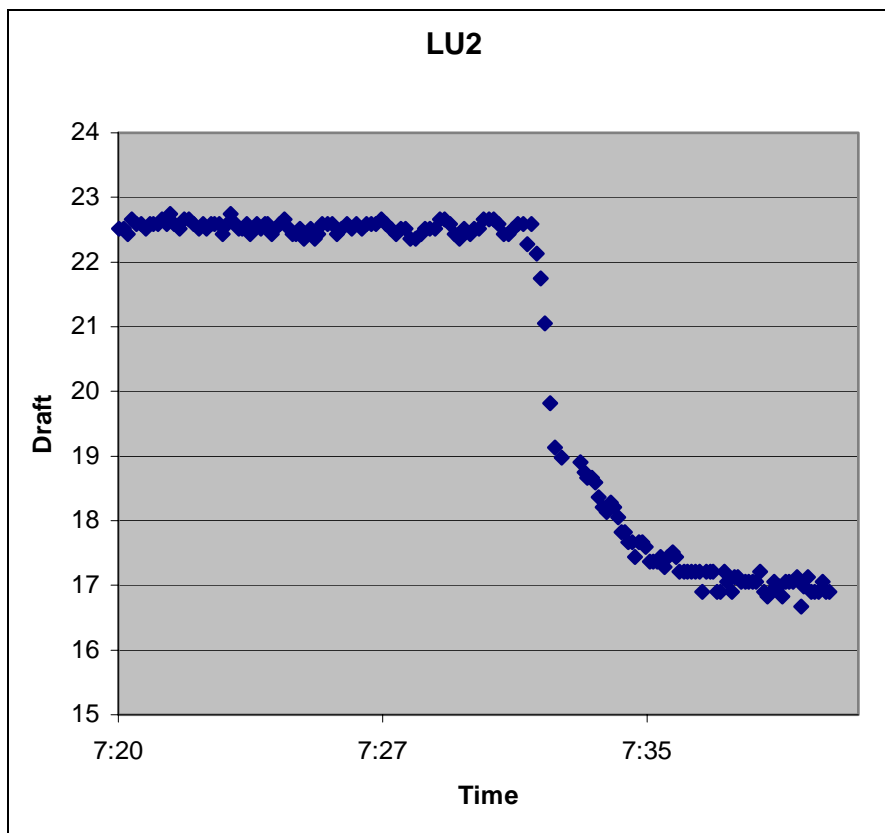


Figure K-67. Vessel draft of LU2 disposal

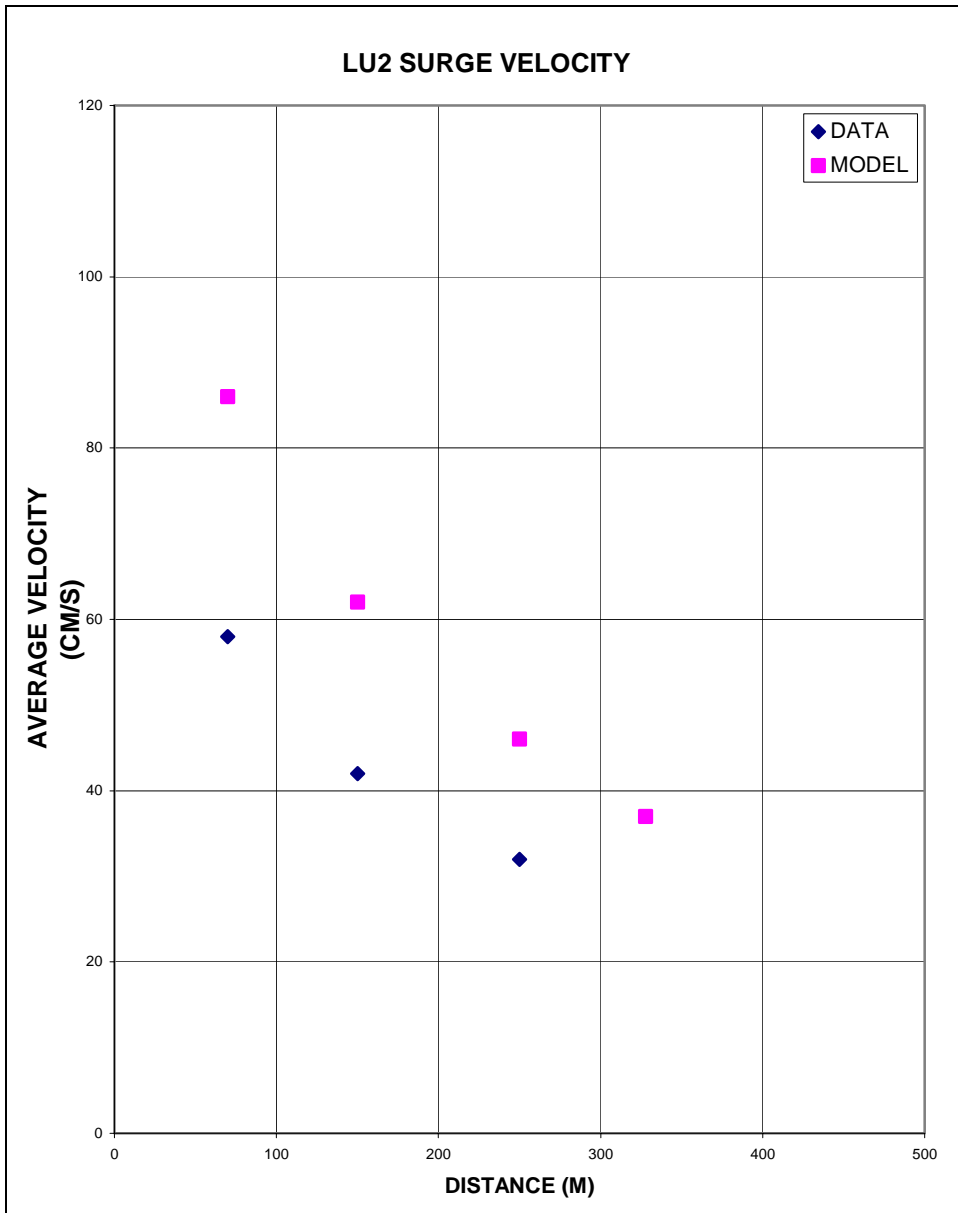


Figure K-68. Comparison of STFATE average surge speed with LU2 field data

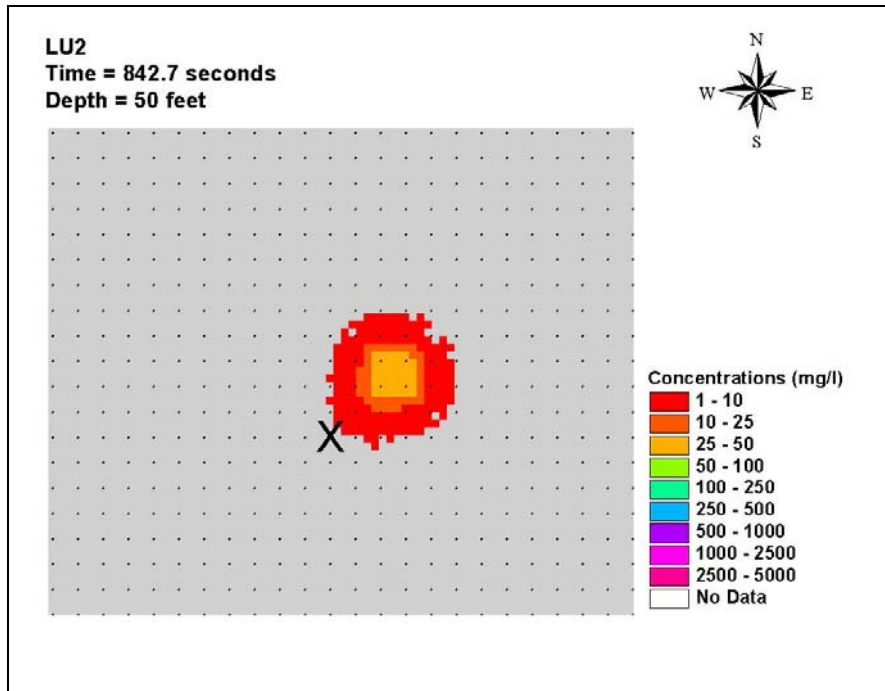


Figure K-69. LU2 plume at end of collapse at 15 m

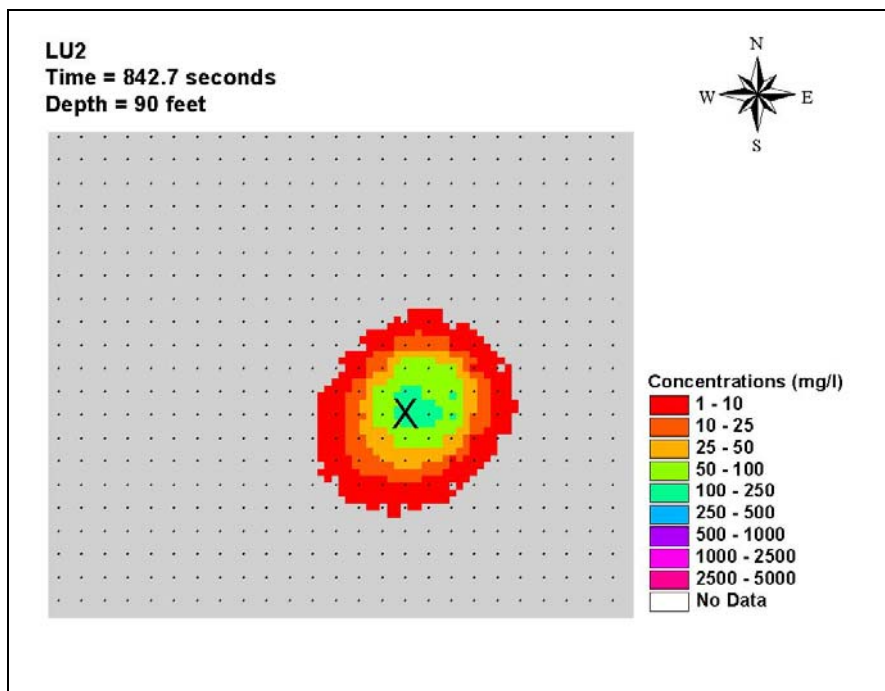


Figure K-70. LU2 plume at end of collapse at 27 m

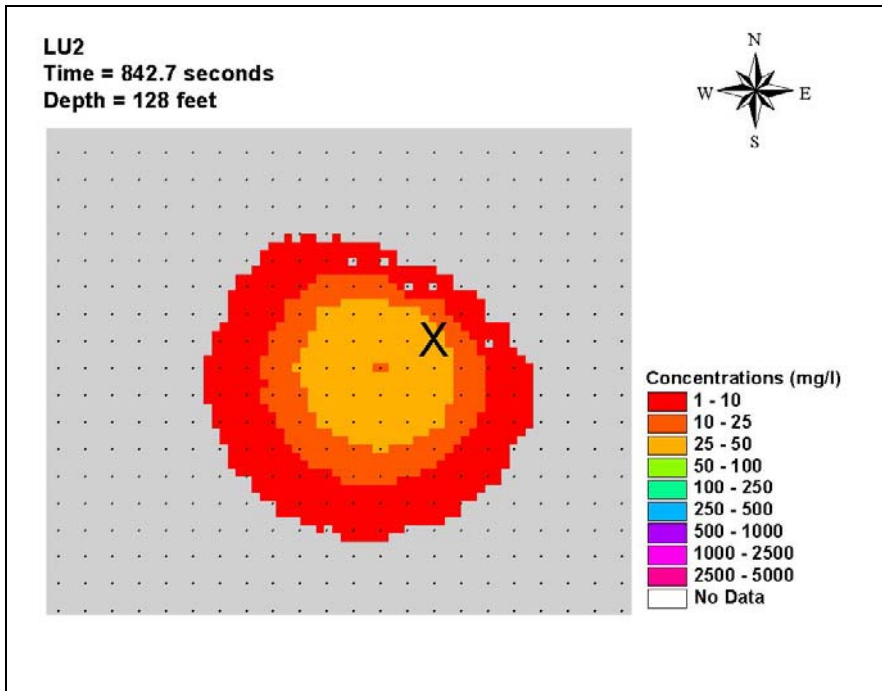


Figure K-71. LU2 plume at end of collapse at 39 m

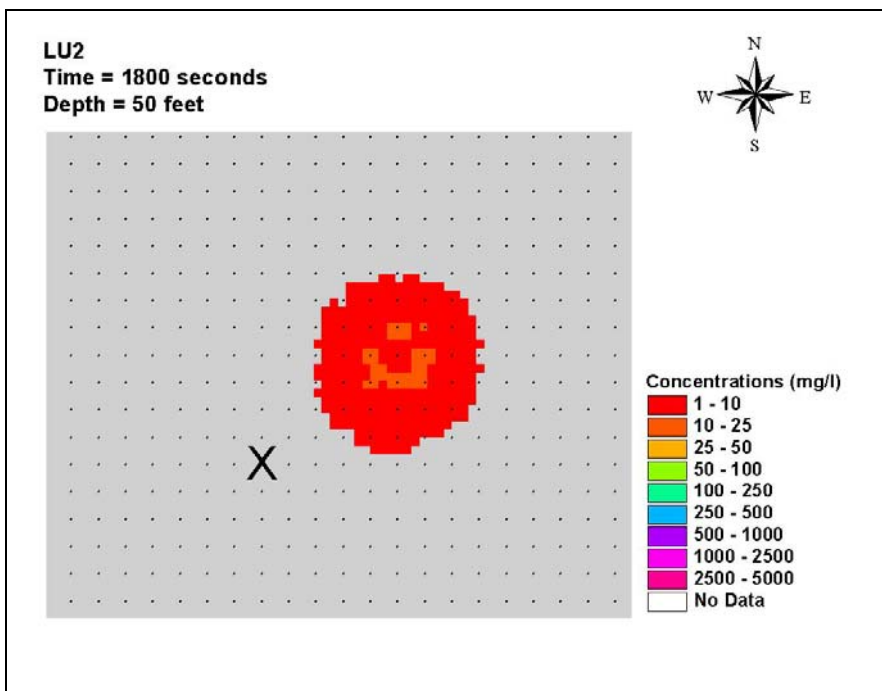


Figure K-72. LU2 plume at 1800 sec at 15 m

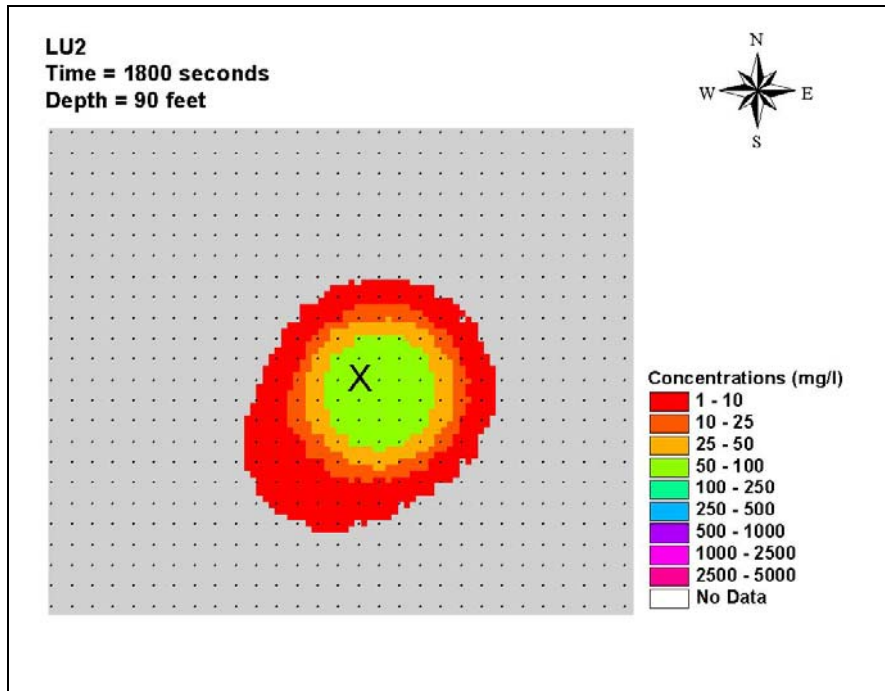


Figure K-73. LU2 plume at 1,800 sec at 29 m

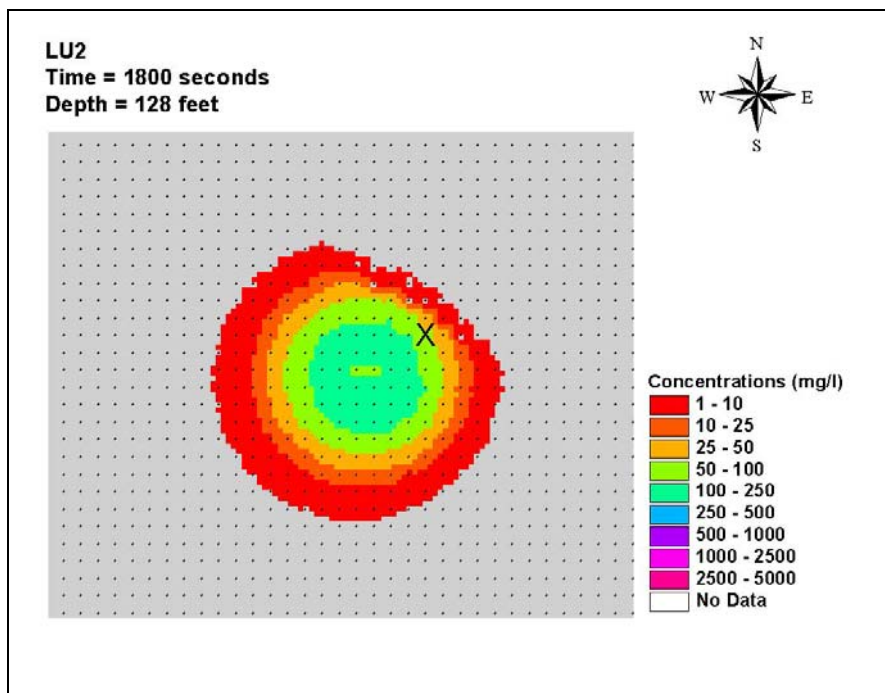


Figure K-74. LU2 plume at 1,800 sec at 39 m

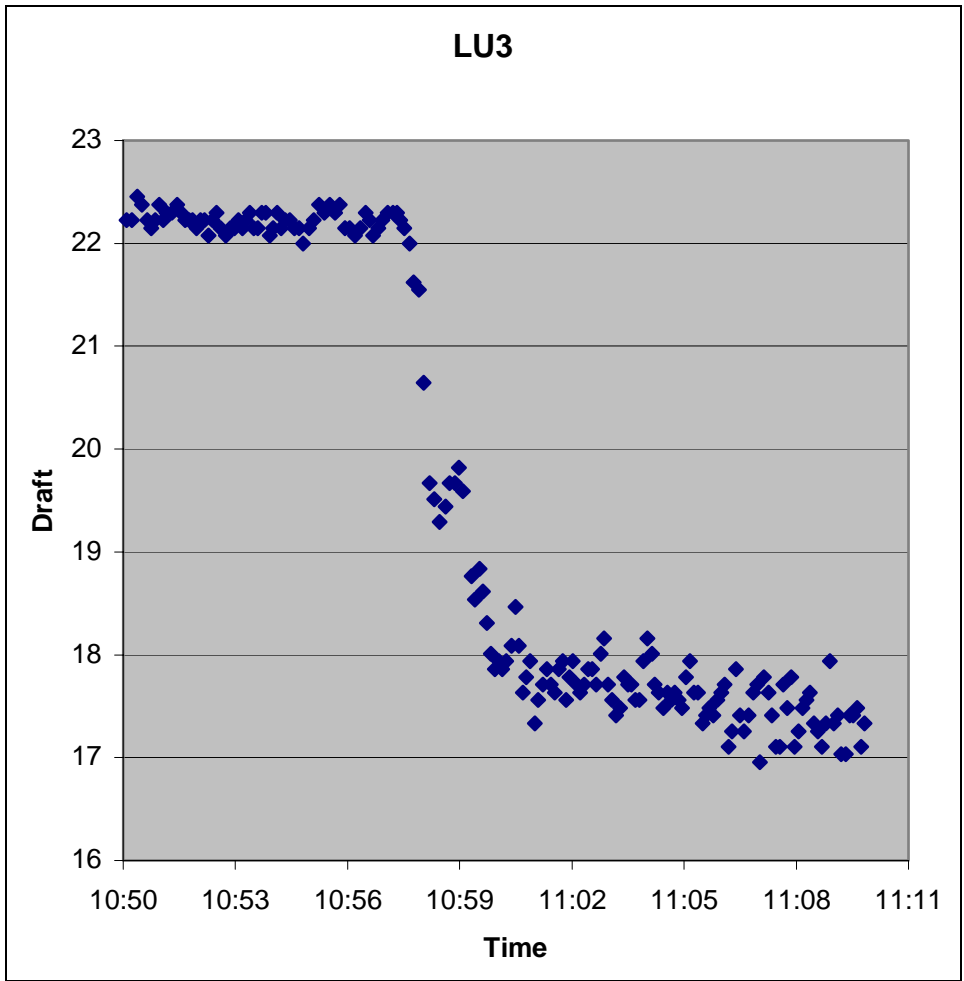


Figure K-75. Vessel draft of LU3 disposal

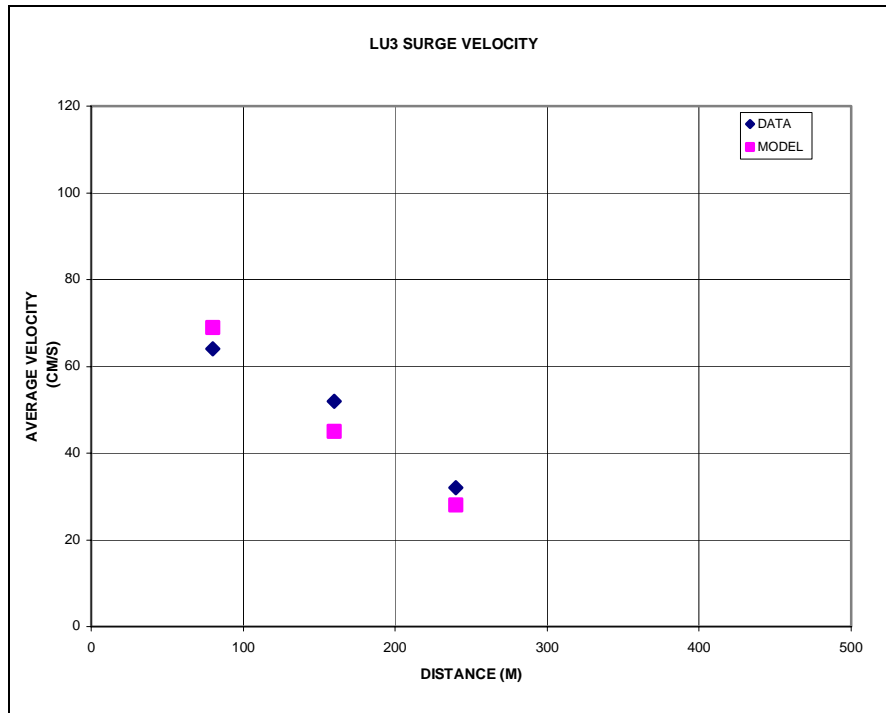


Figure K-76. Comparison of STFACTE average surge speed with LU3 field data

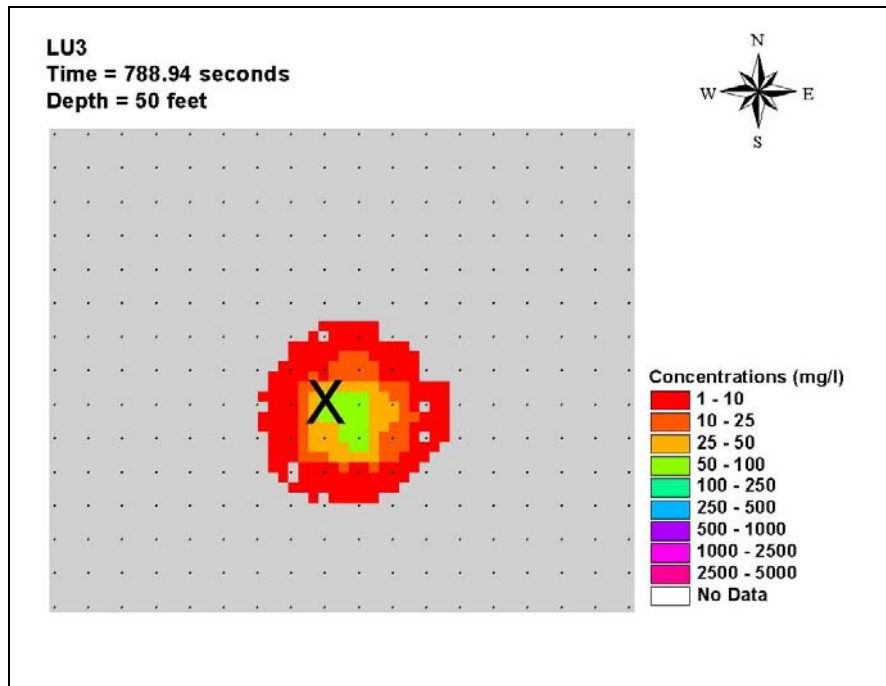


Figure K-77. LU3 plume at end of collapse at 15 m

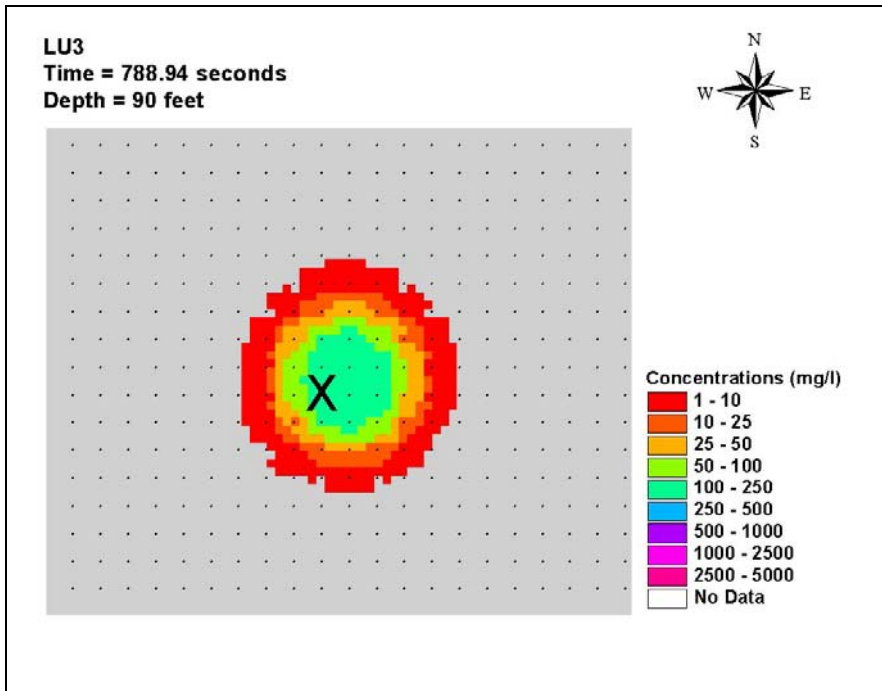


Figure K-78. LU3 plume at end of collapse at 27 m

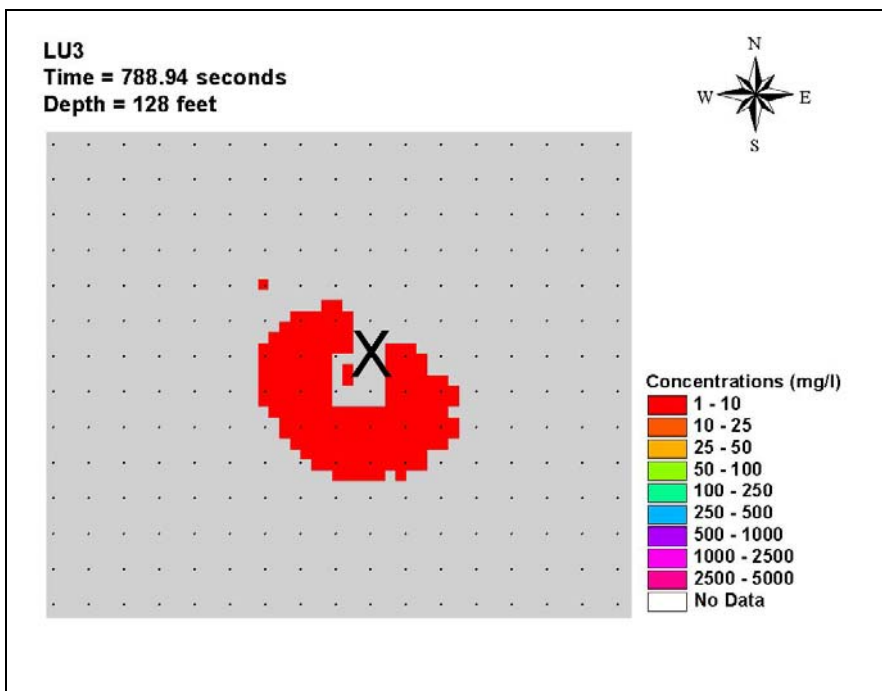


Figure K-79. LU3 plume at end of collapse at 39 m

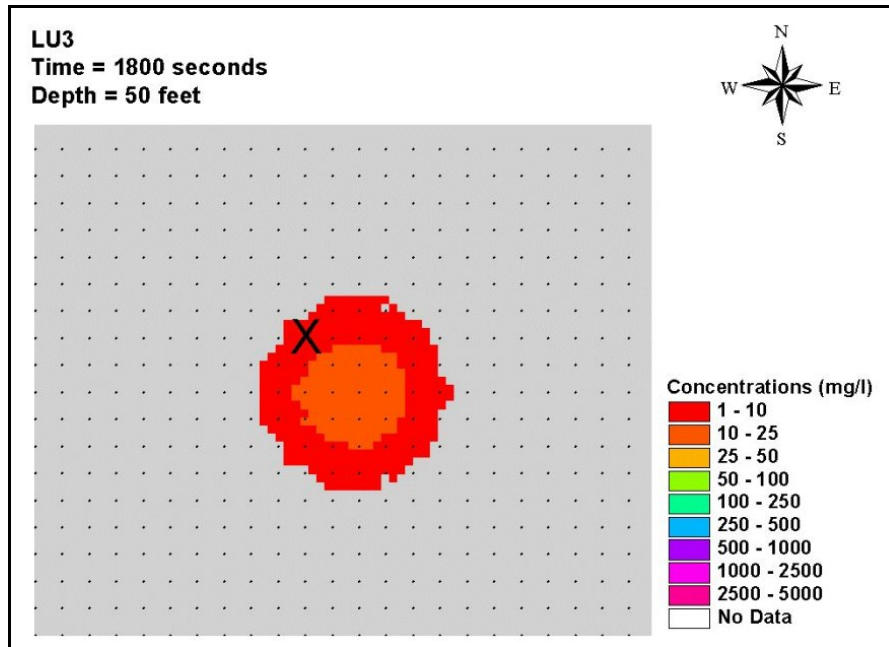


Figure K-80. LU3 plume at 1,800 sec at 15 m

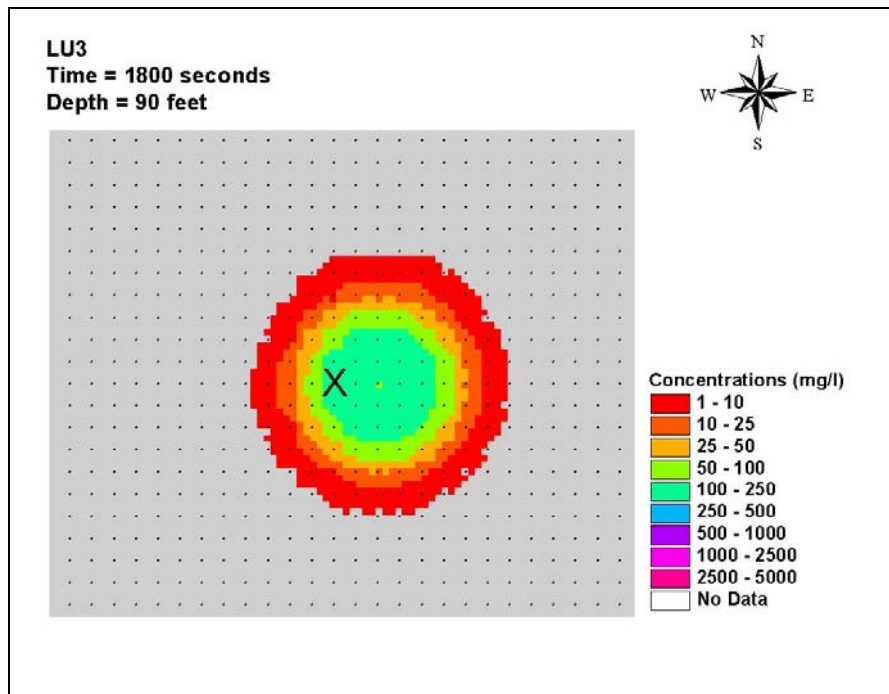


Figure K-81. LU3 plume at 1,800 sec at 27 m

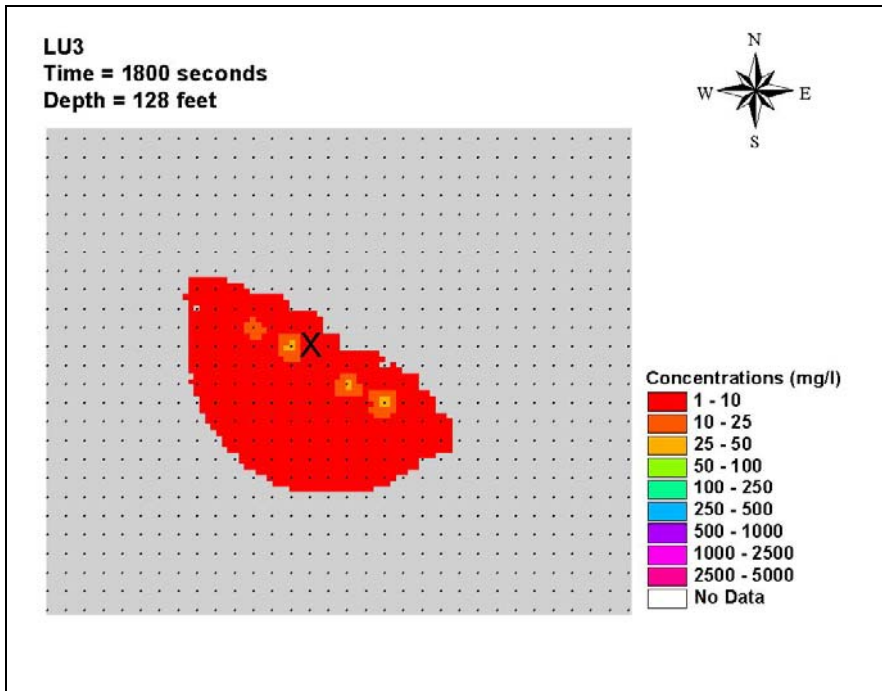


Figure K-82. LU3 plume at 1,800 sec at 39 m

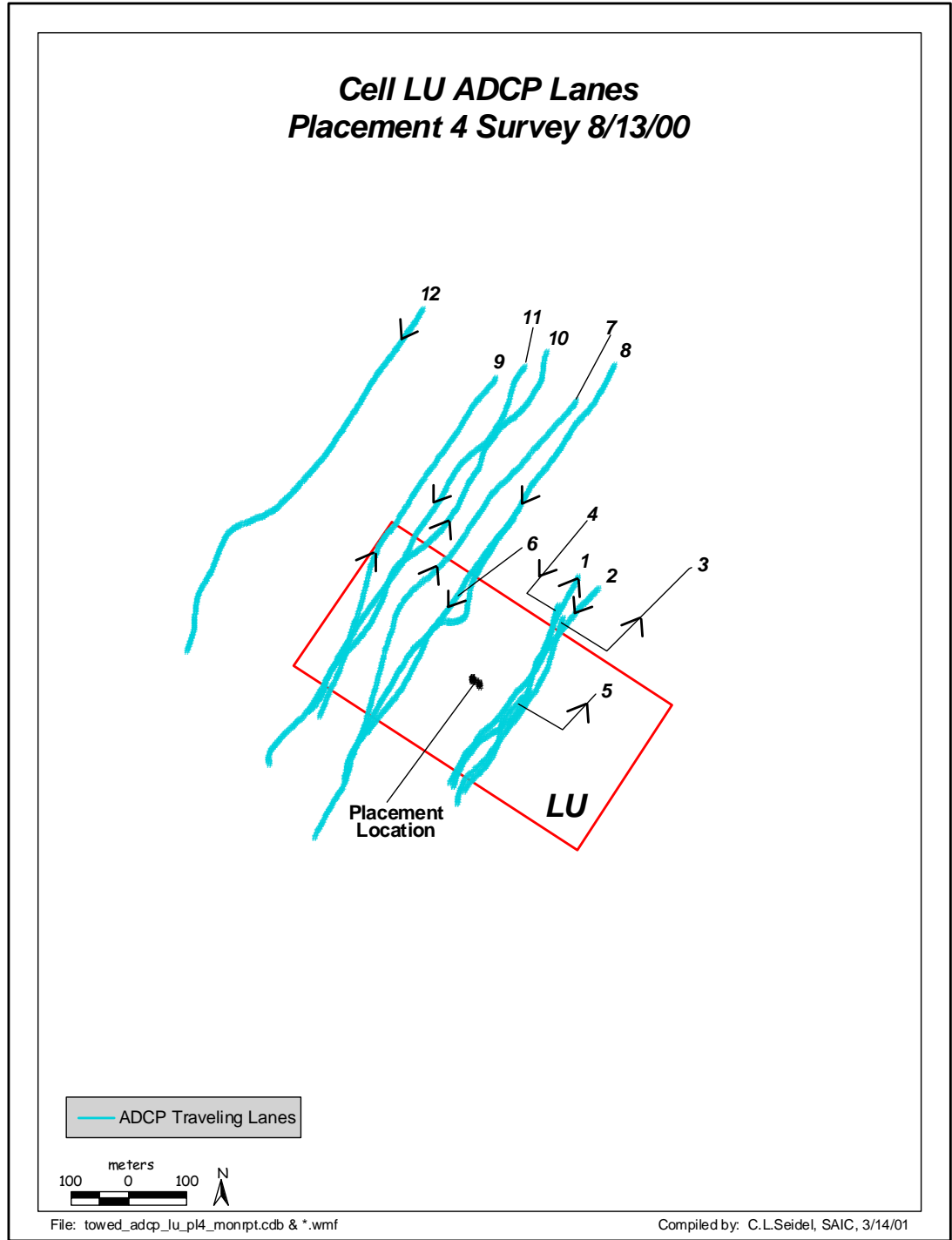


Figure K-83. LU4 transects (SAIC 2002, Figure 3.6-14)

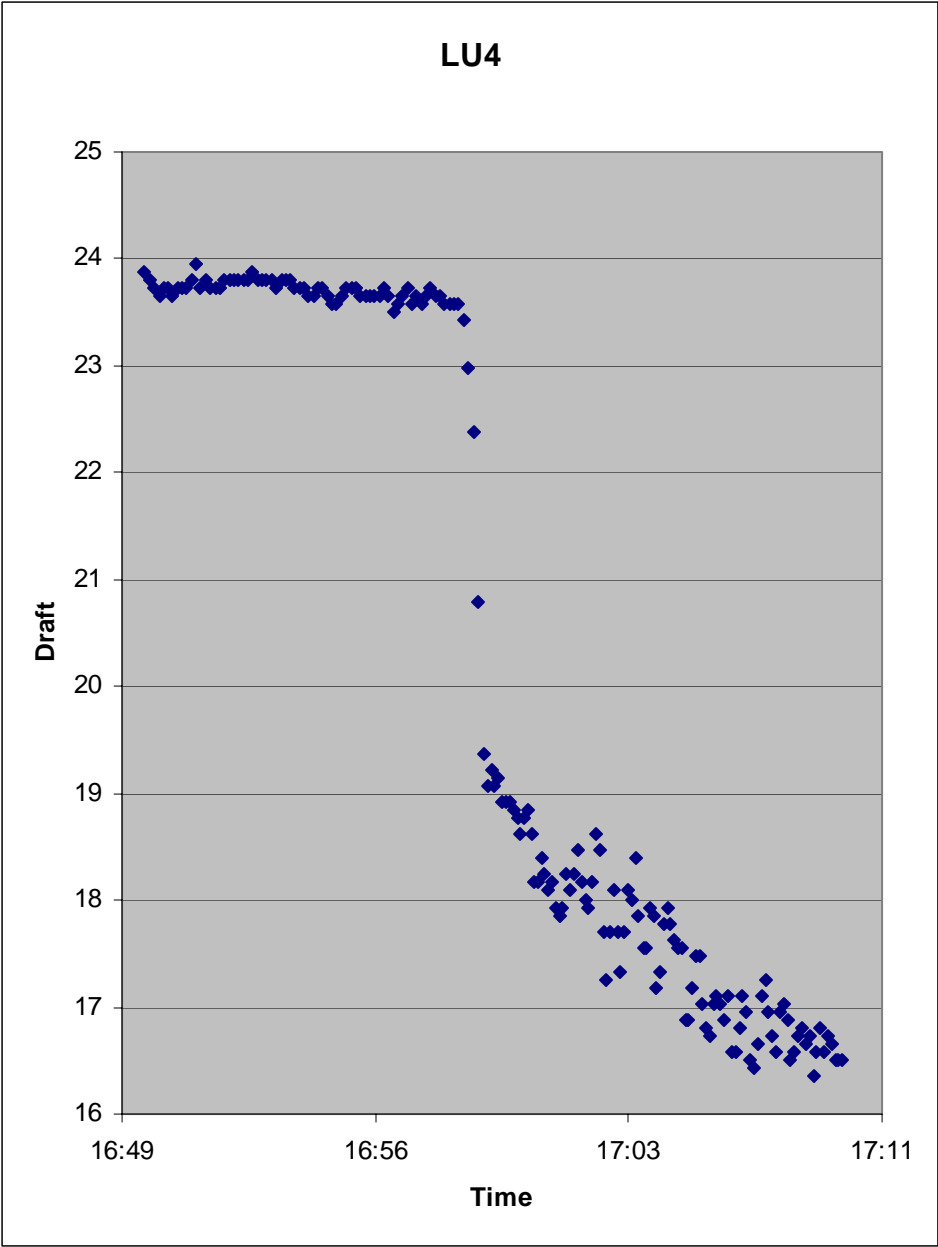


Figure K-84. Vessel draft of LU4 disposal

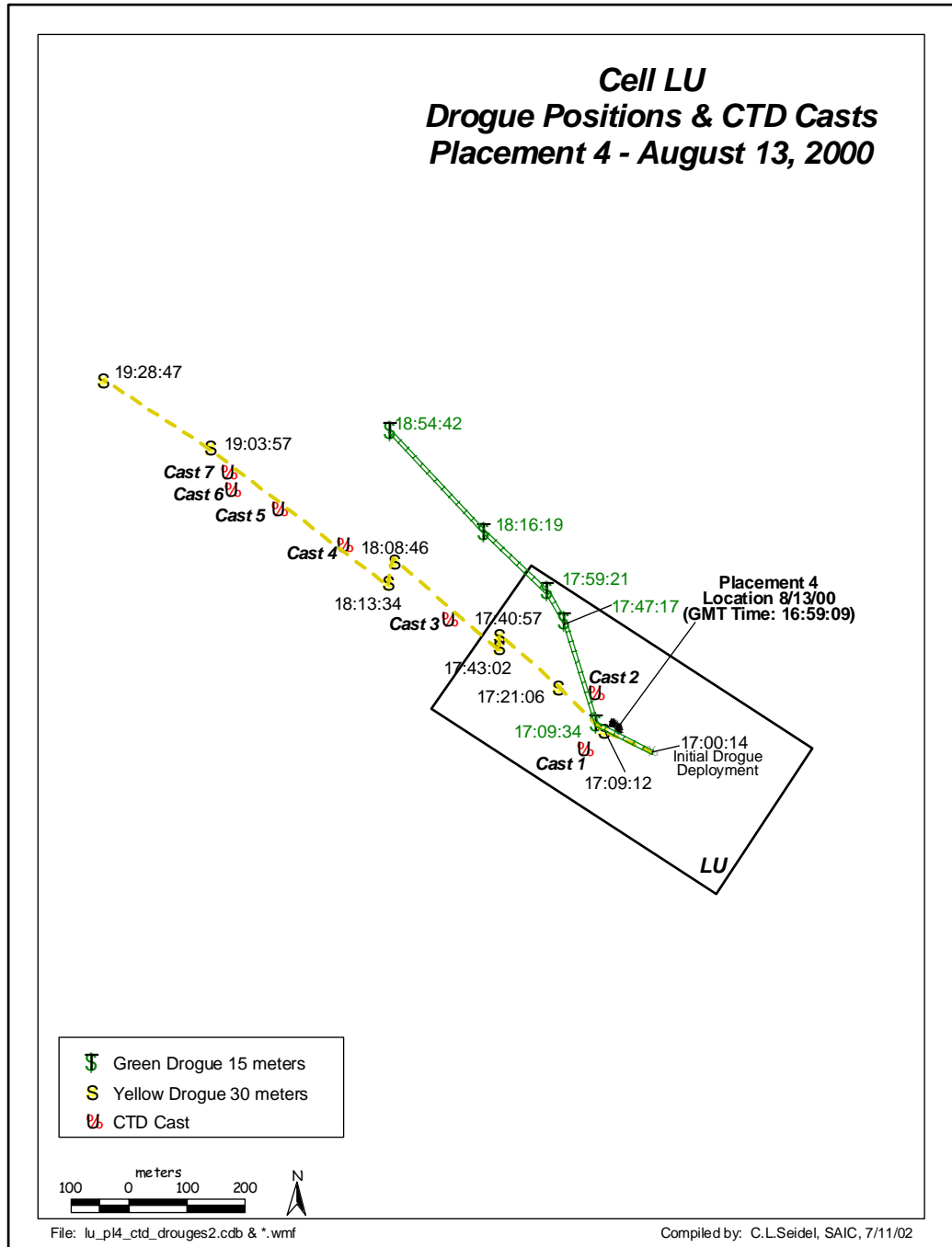


Figure K-85. LU4 drogue paths (SAIC 2002, Figure 3.5-9)

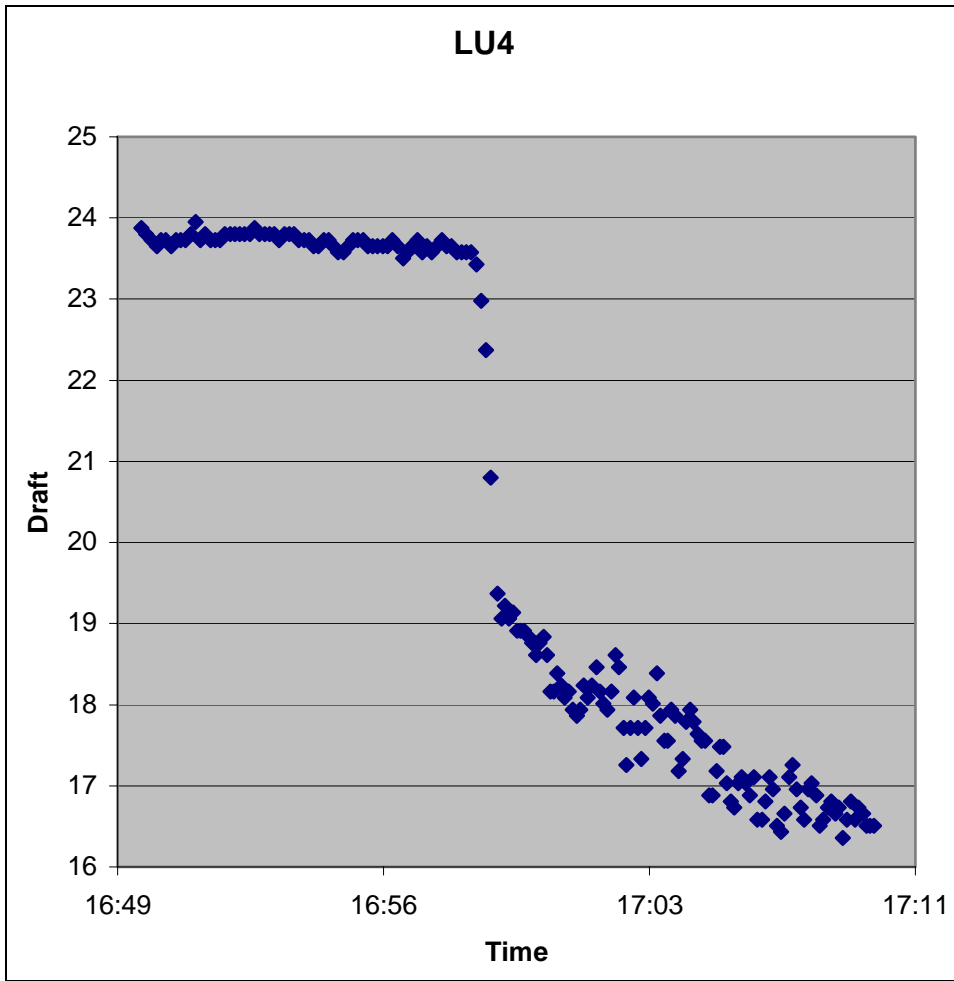


Figure K-86. Comparison of STFATE average surge speed with LU4 field data

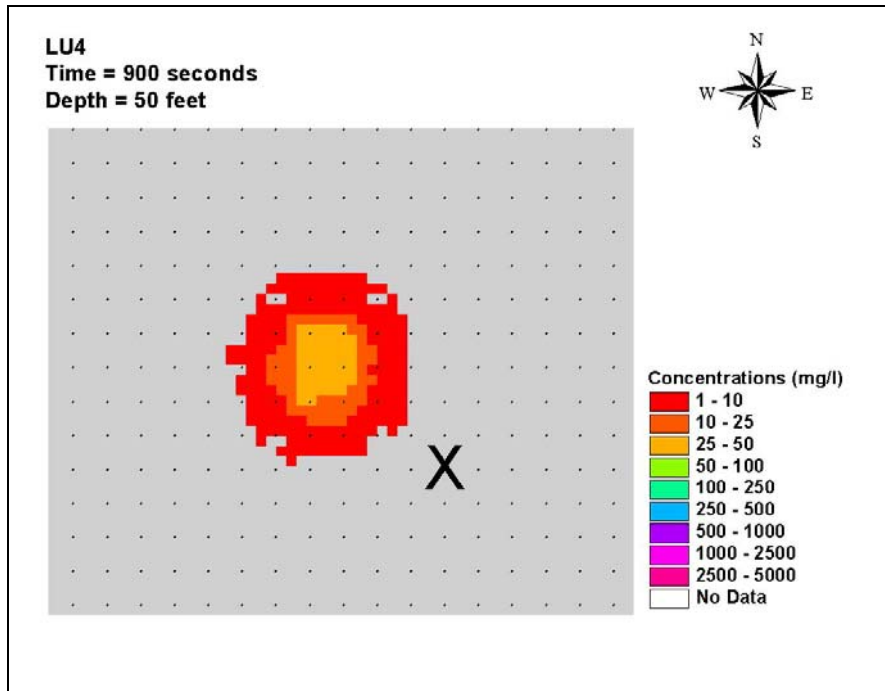


Figure K-87. LU4 plume at 900 sec at 15 m

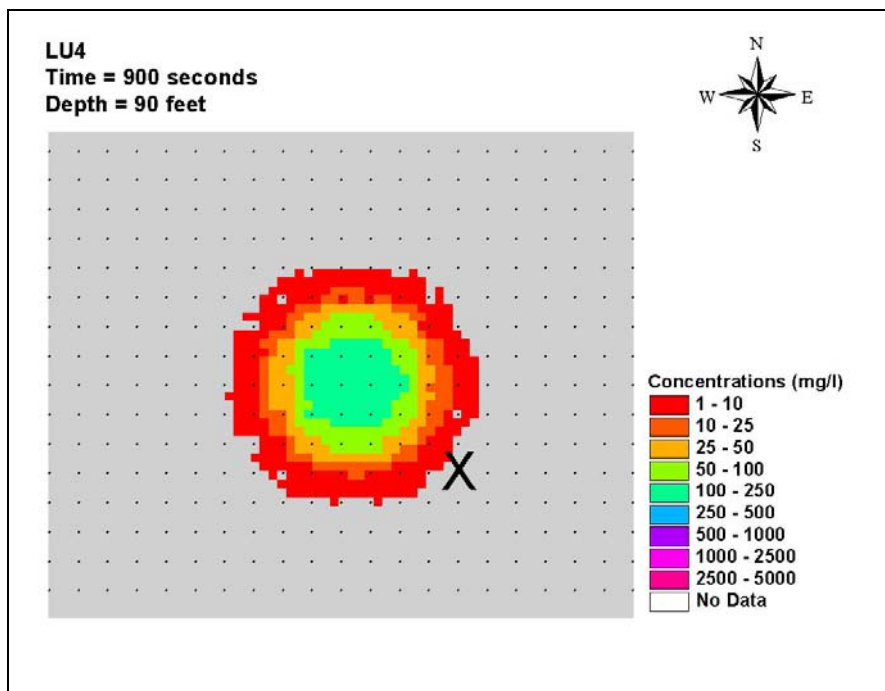


Figure K-88. LU4 plume at 900 sec at 27 m

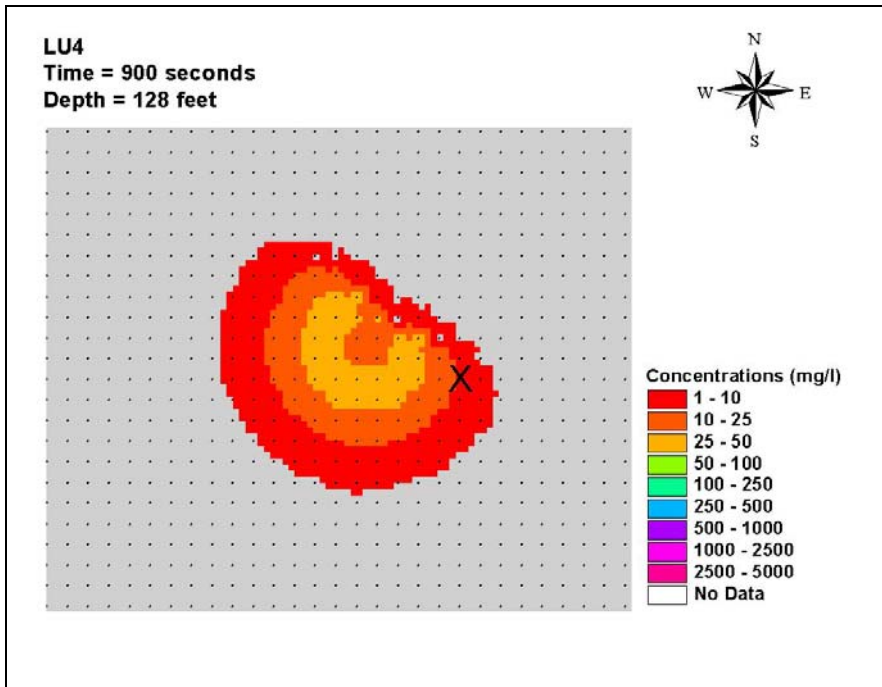


Figure K-89. LU4 plume at 900 sec at 39 m

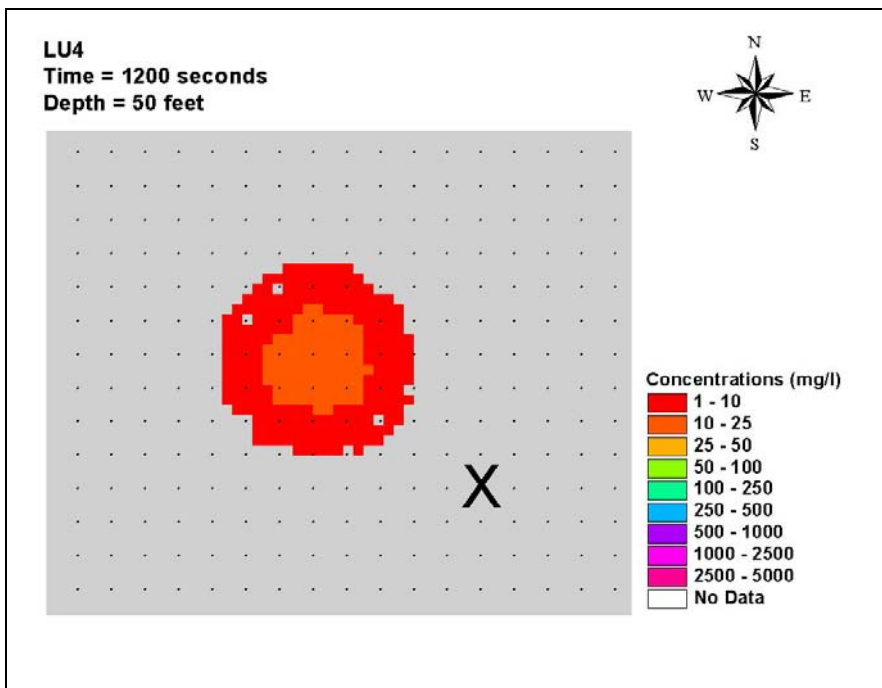


Figure K-90. LU4 plume at 1,200 sec at 15 m

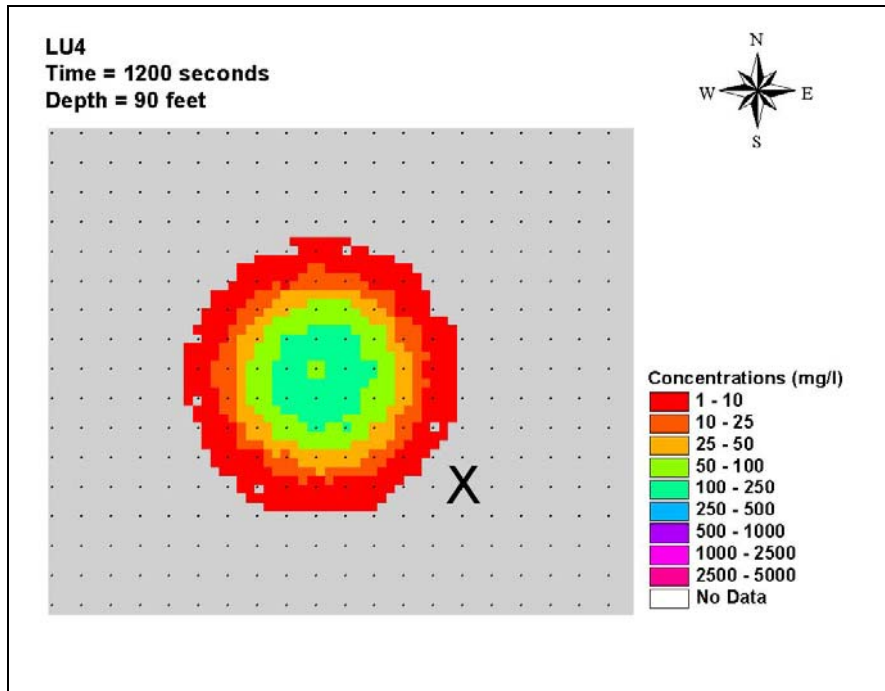


Figure K-91. LU4 plume at 1,200 sec at 27 m

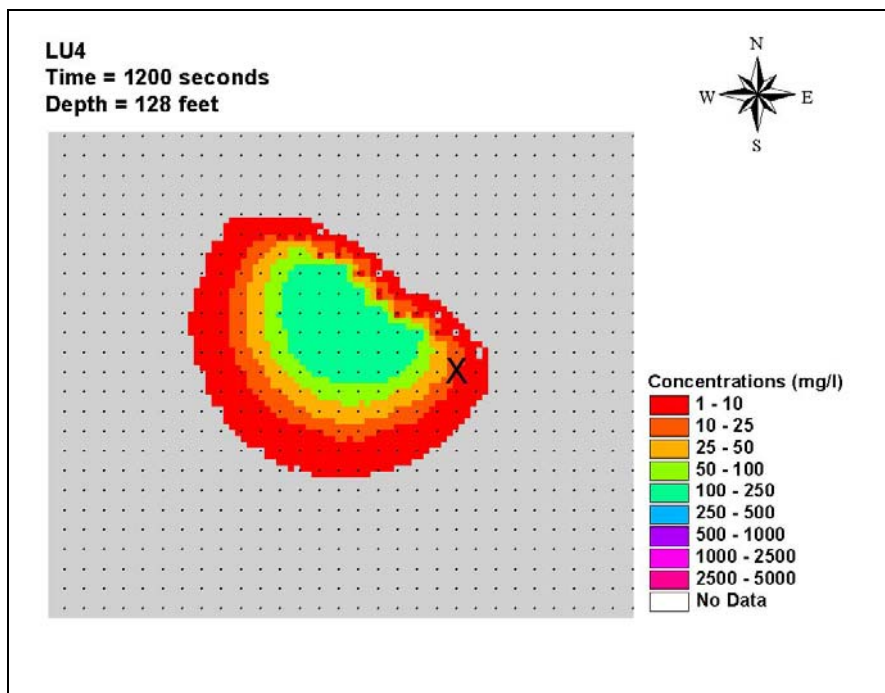


Figure K-92. LU4 plume at 1,200 sec at 39 m

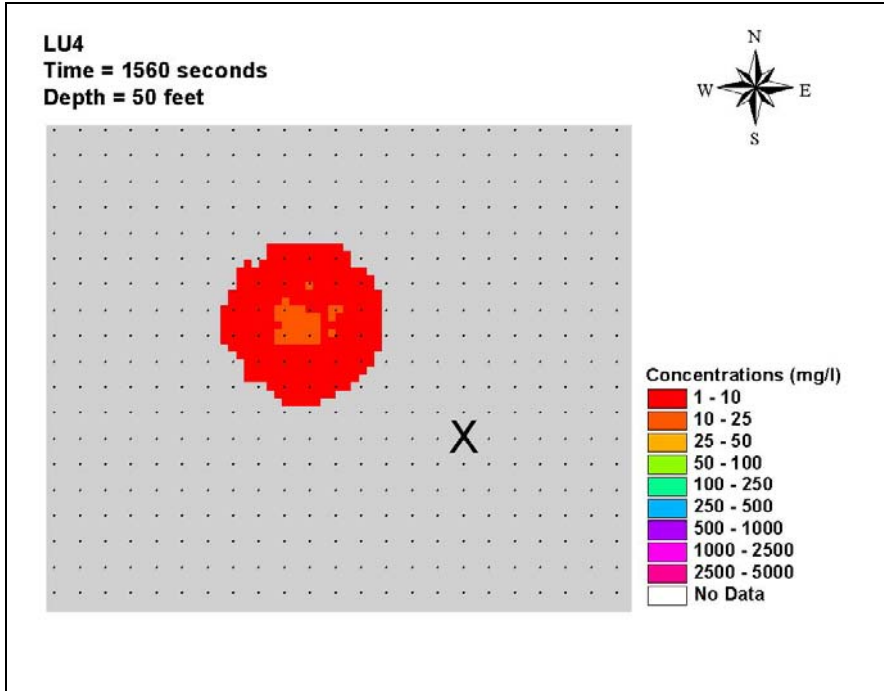


Figure K-93. LU4 plume at 1,560 sec at 15 m

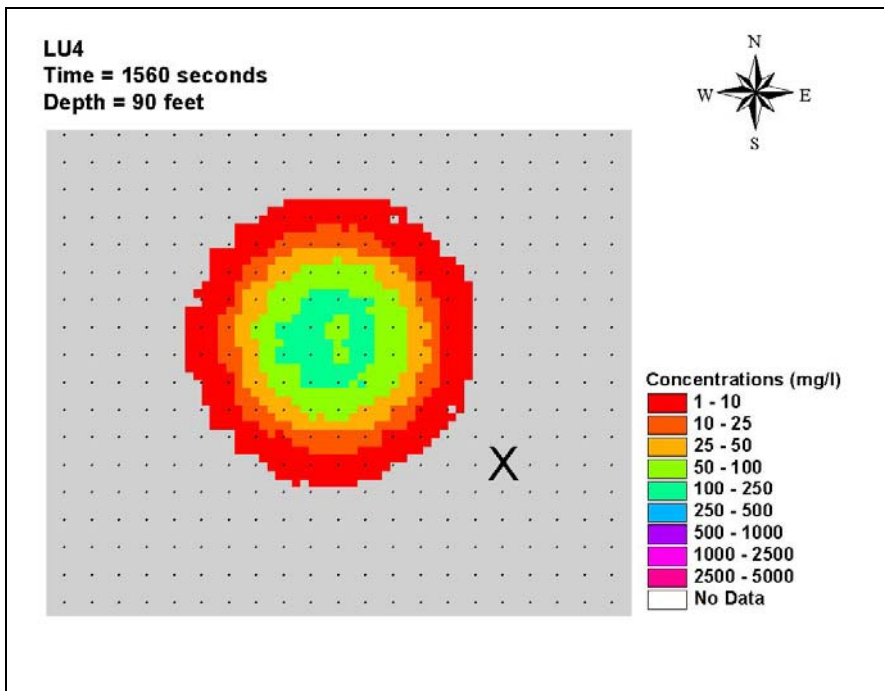


Figure K-94. LU4 plume at 1,560 sec at 27 m

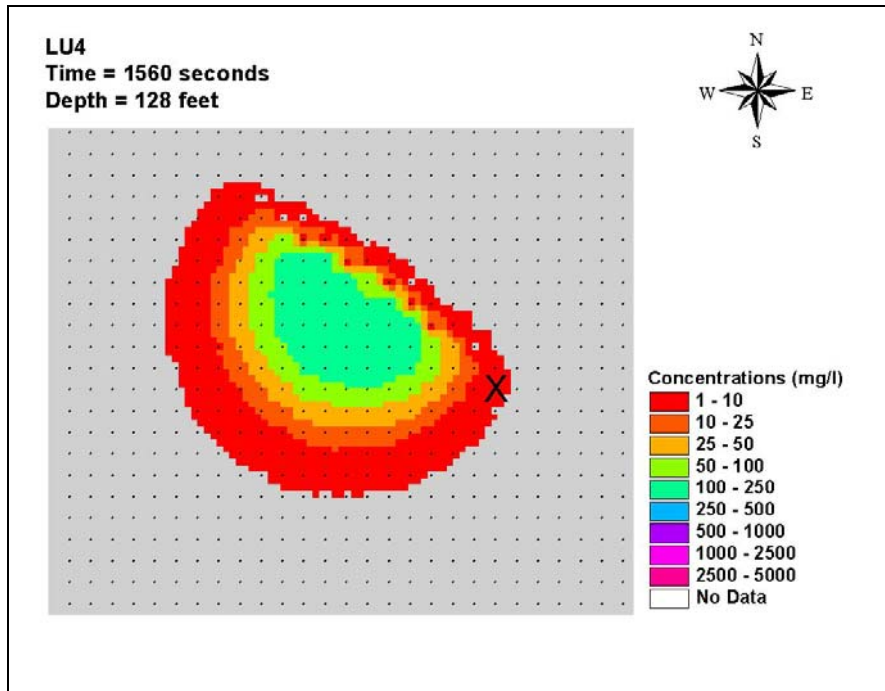


Figure K-95. LU4 plume at 1,560 sec at 39 m

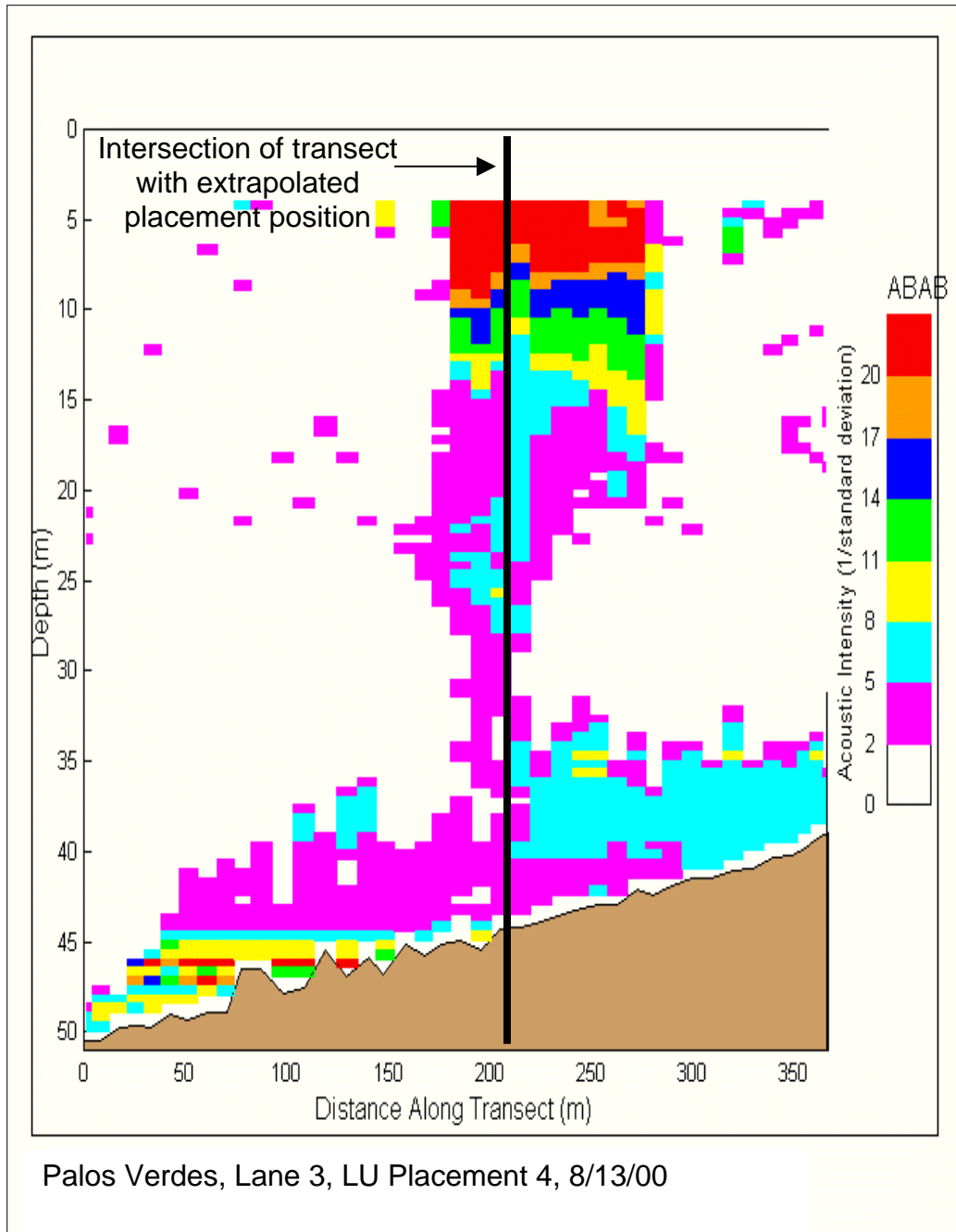


Figure K-96. ABAB along Transect 3 at 5 min after the placement operation ended (SAIC 2002, Figure 3.6-17)

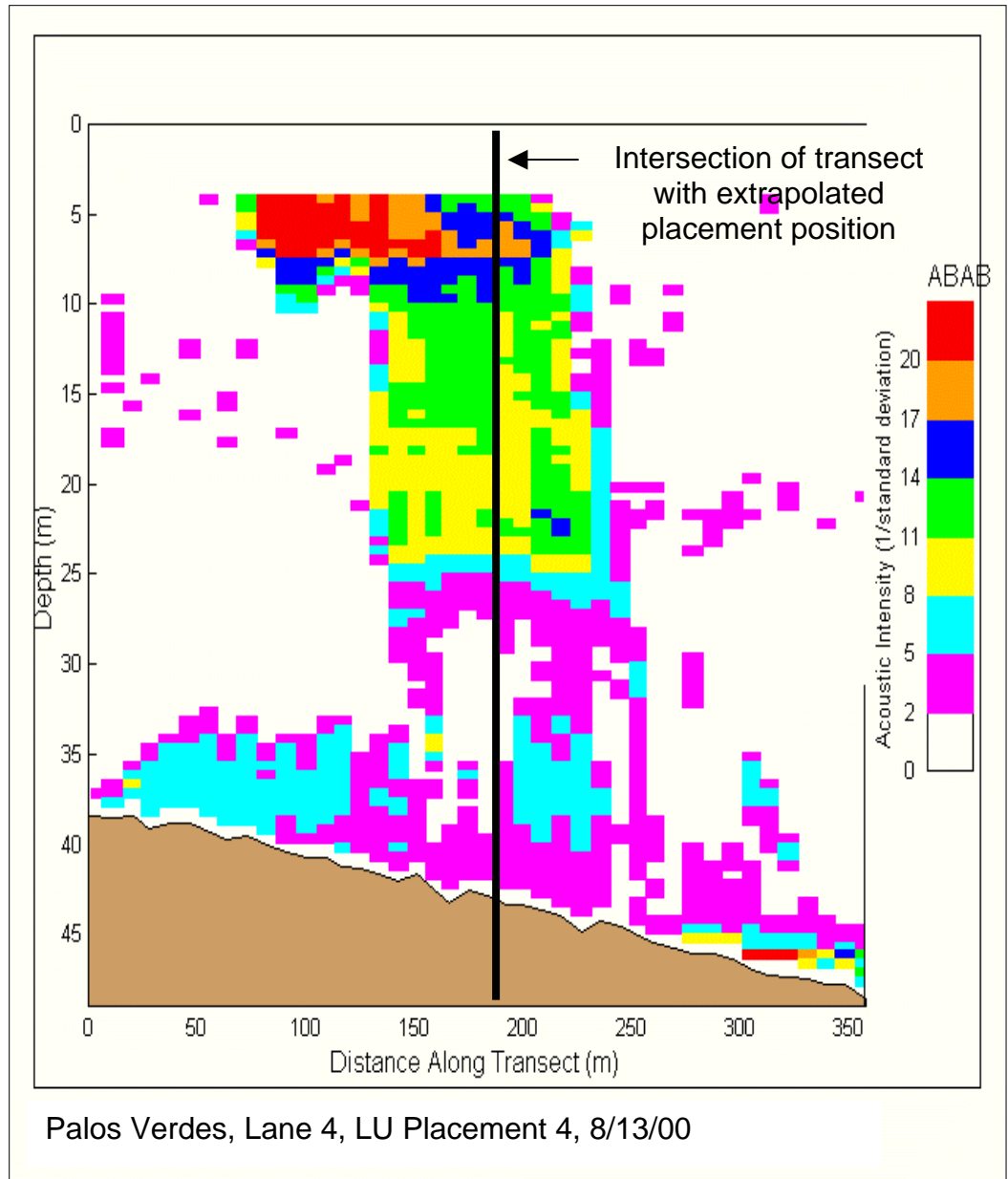


Figure K-97. ABAB along Transect 4 at 8 min after the placement operation ended (SAIC 2002, Figure 3.6-18)

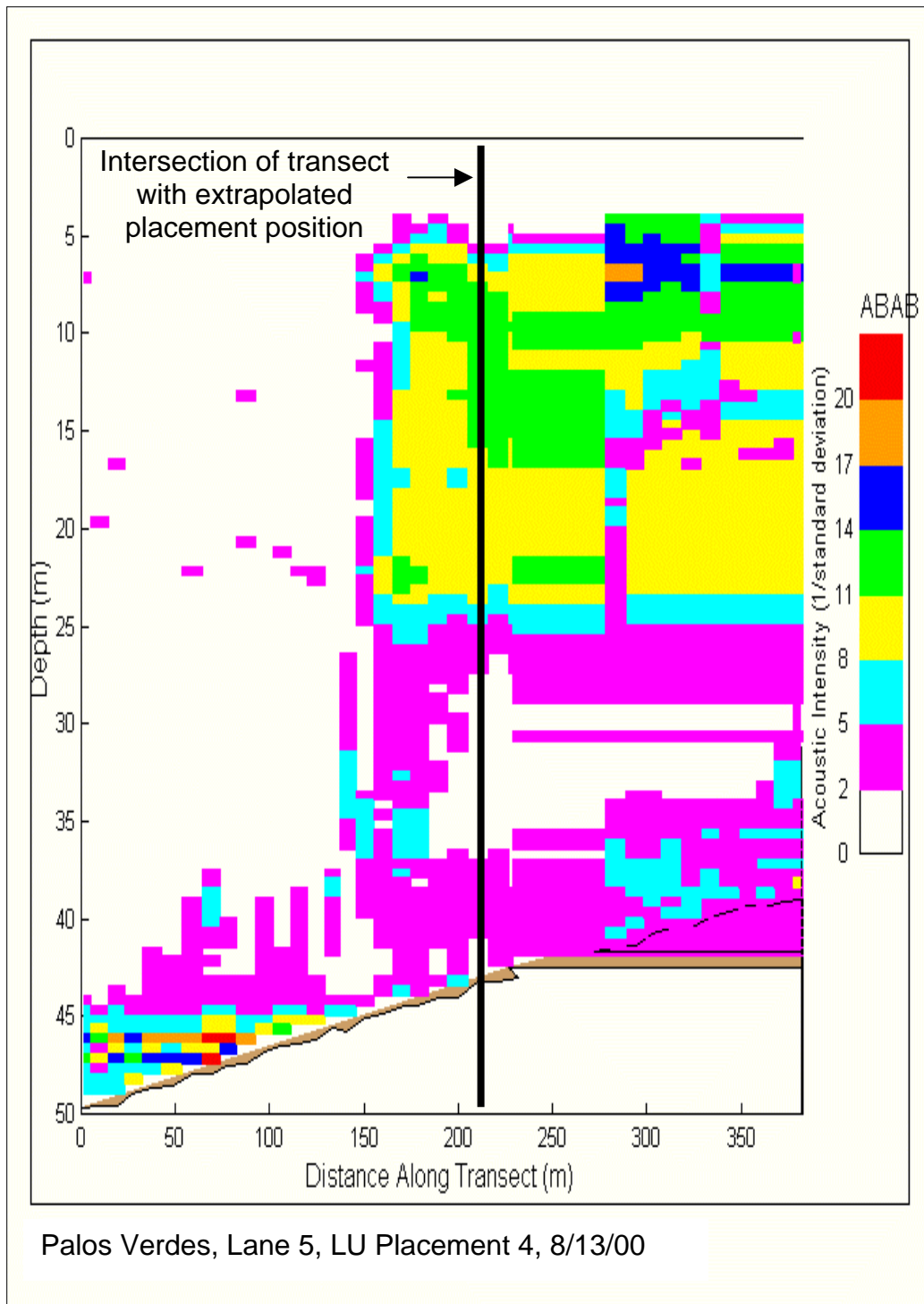


Figure K-98. ABAB along Transect 5 at 12 min after the placement operation ended (SAIC 2002, Figure 3.6-19)

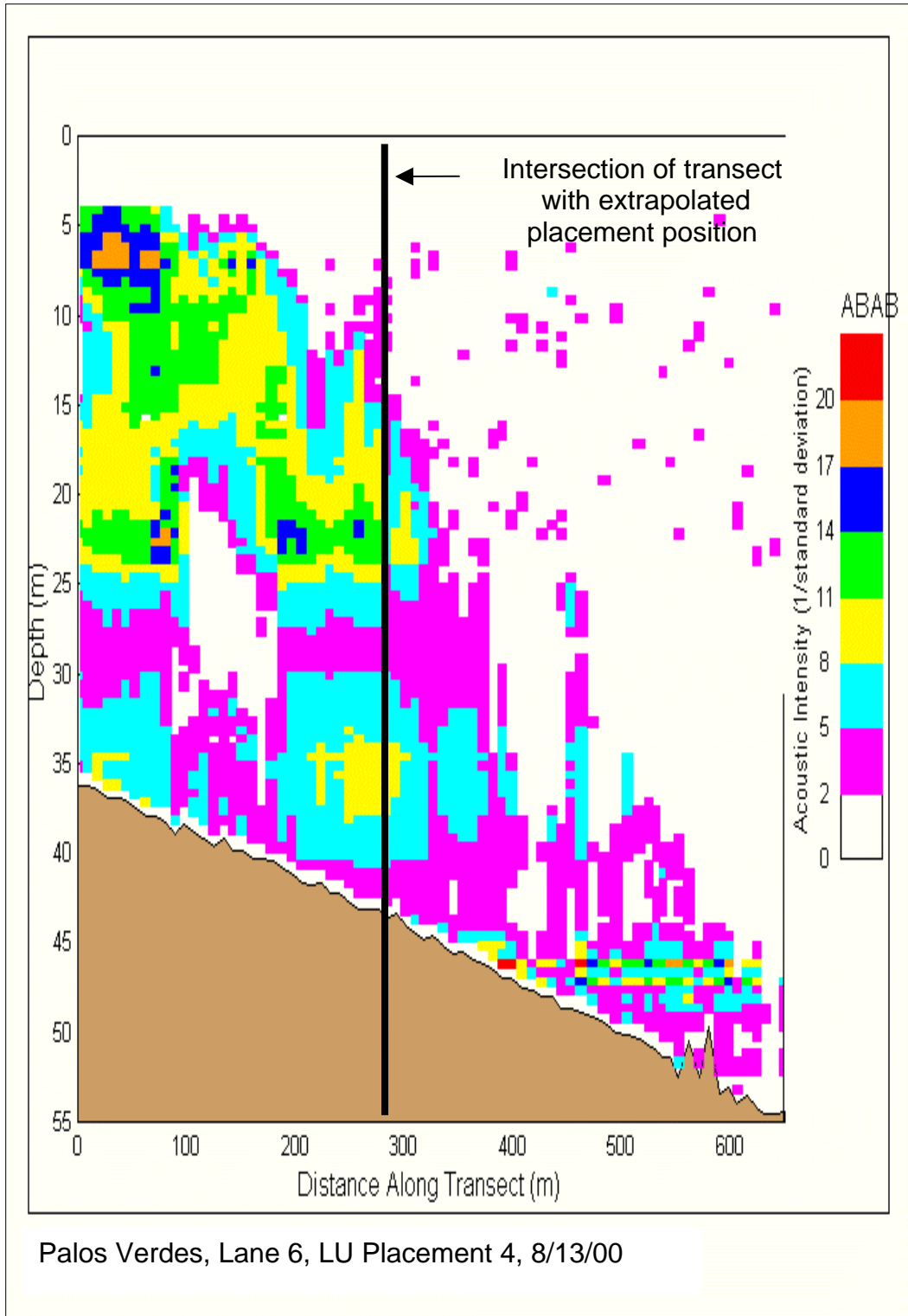


Figure K-99. ABAB along Transect 6 at 17 min after the placement operation ended (SAIC 2002, Figure 3.6-20)

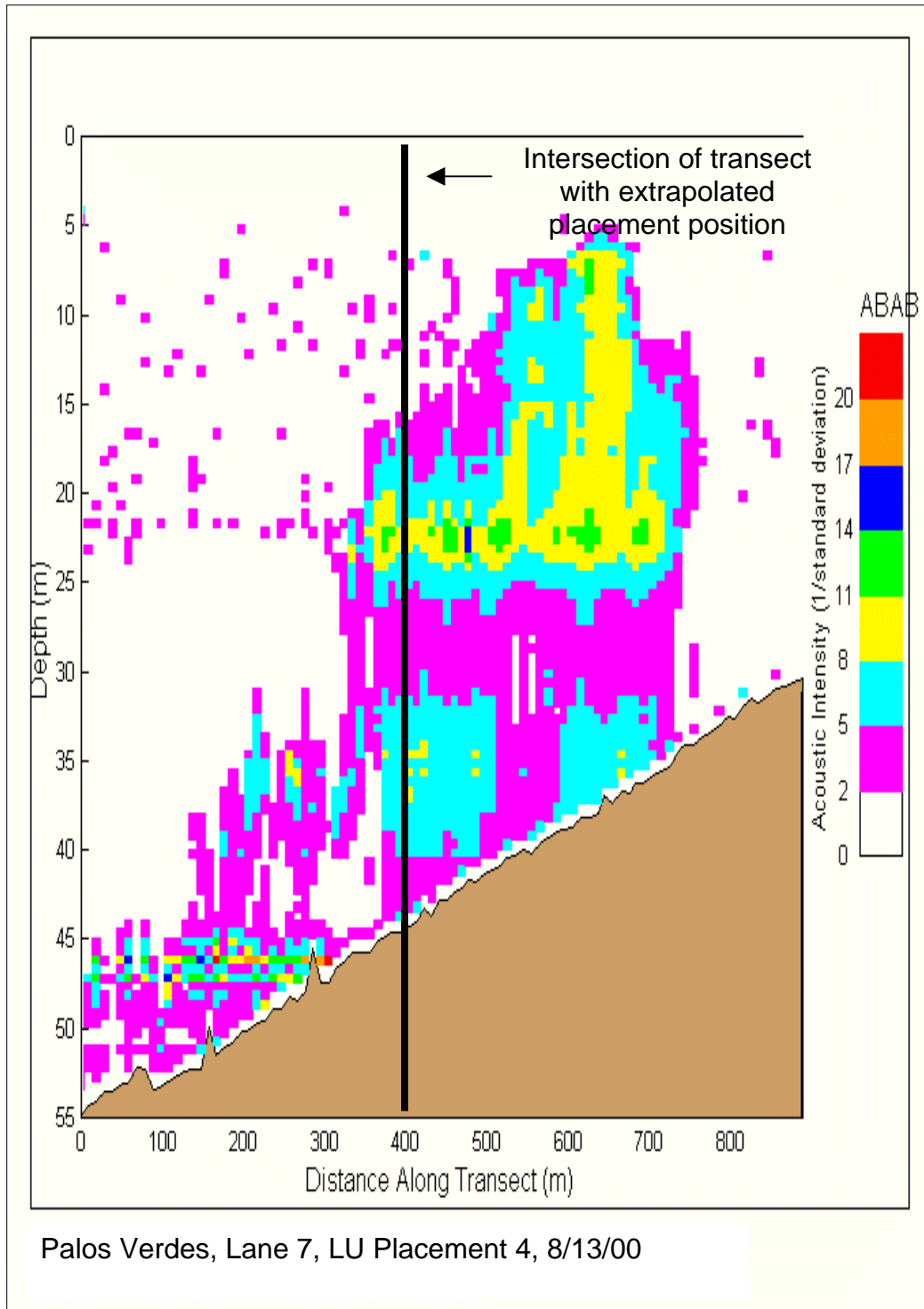


Figure K-100. ABAB along Transect 7 at 23 min after the placement operation ended (SAIC 2002, Figure 3.6-21)

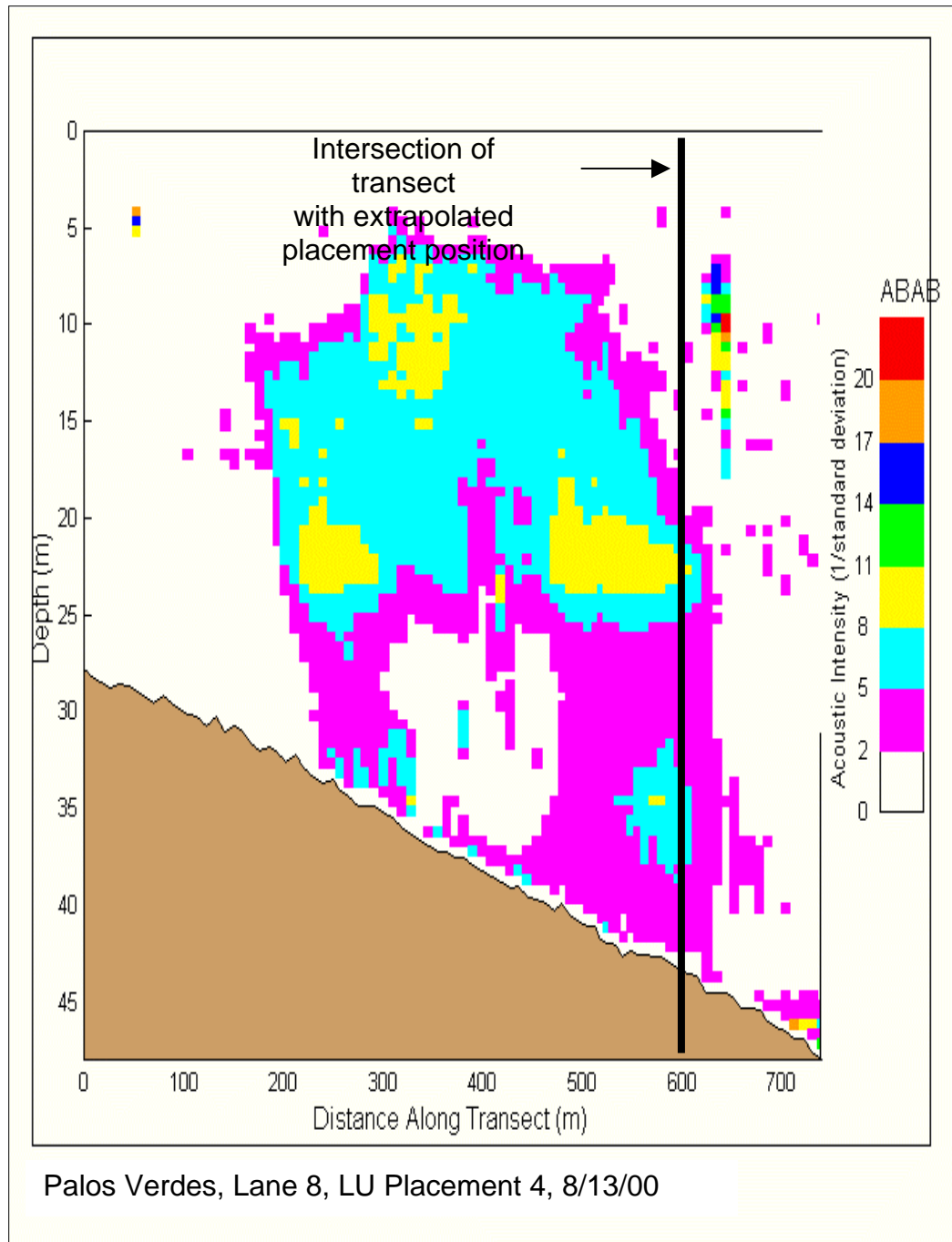


Figure K-101. ABAB along Transect 8 at 31 min after the placement operation ended (SAIC 2000, Figure 3.6-22)

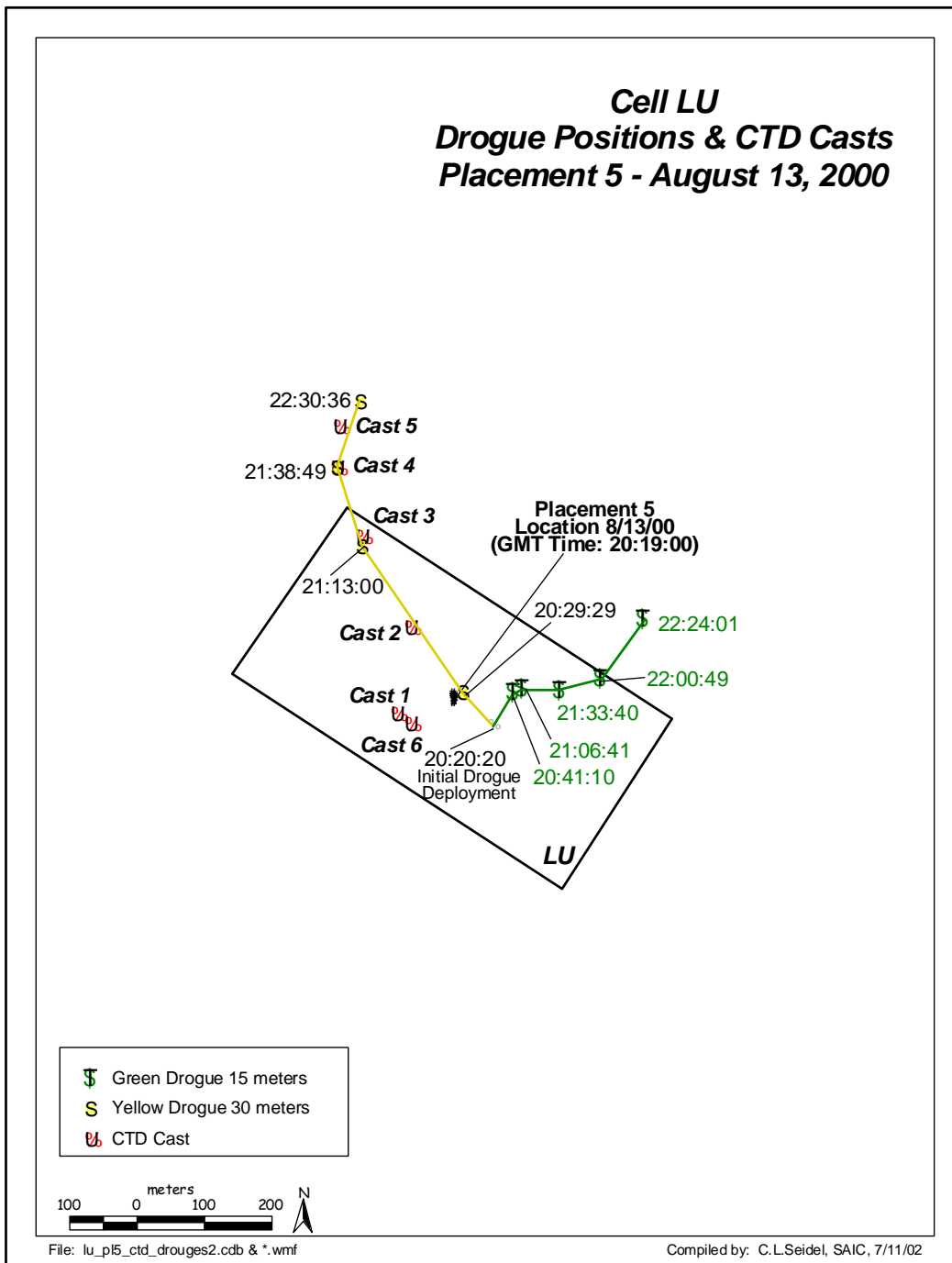


Figure K-102. LU5 drogue paths (SAIC 2002, Figure 3.5-14)

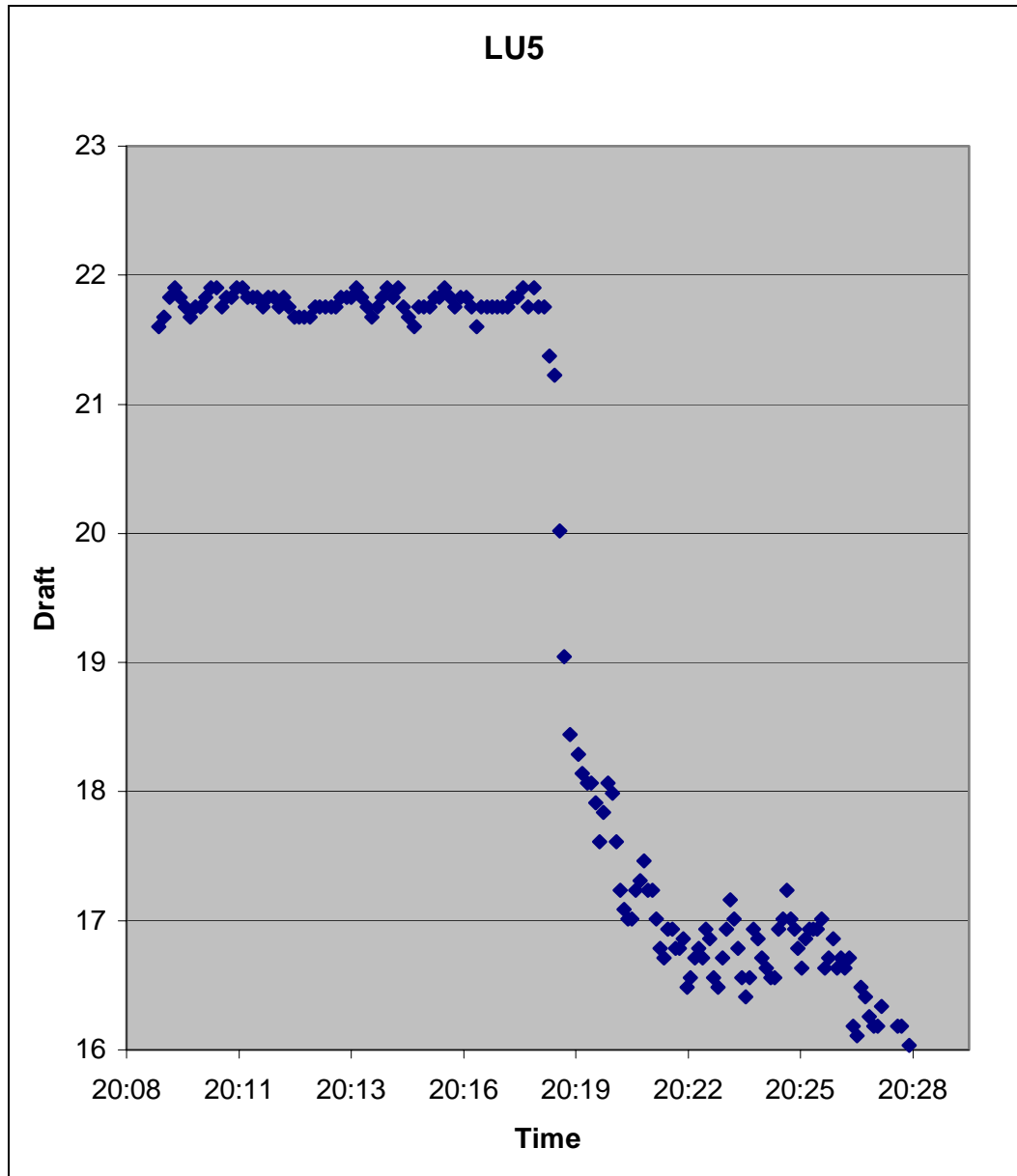


Figure K-103. Vessel draft of LU5 disposal

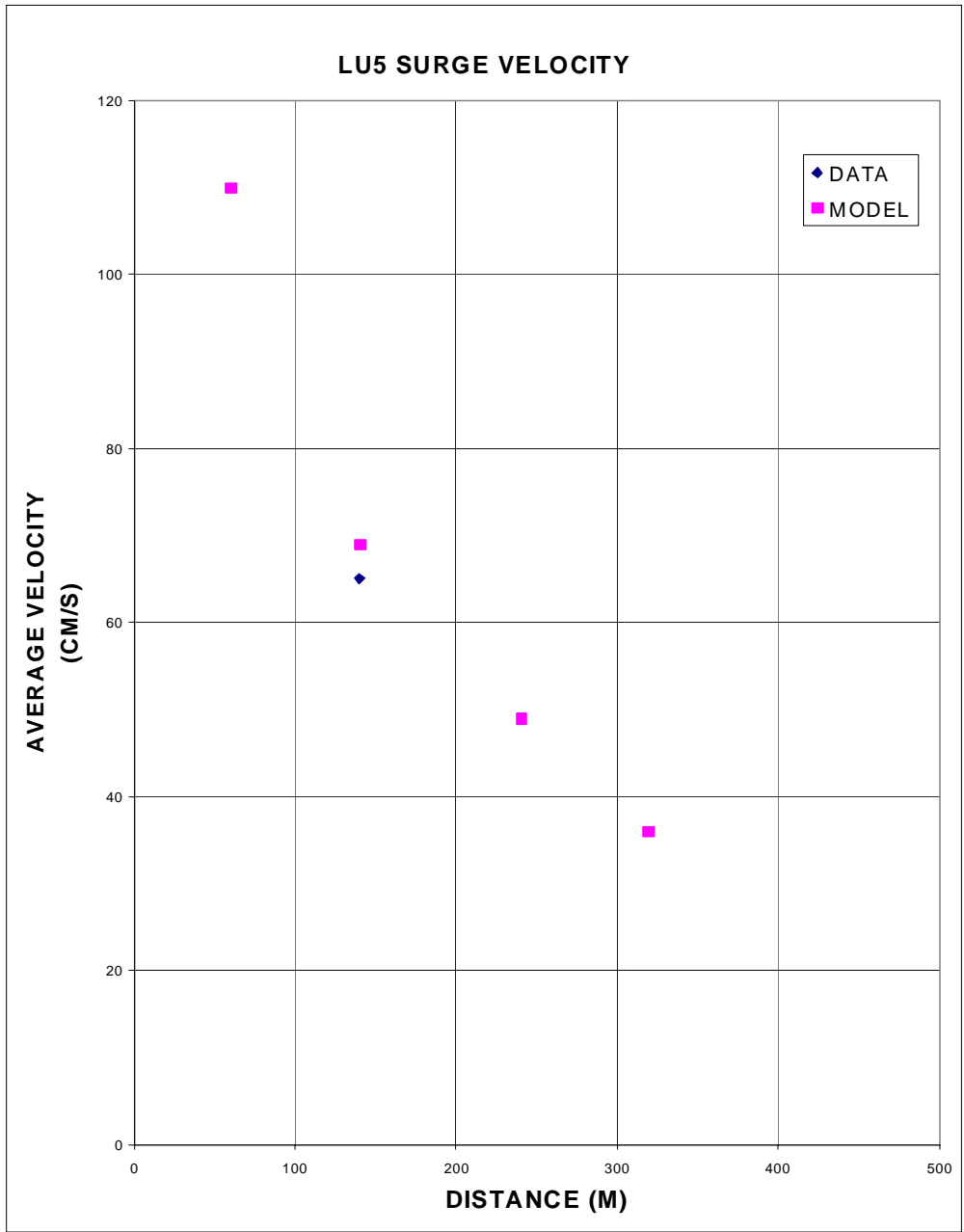


Figure K-104. Comparison of STFATE average surge speed with LU5 field data

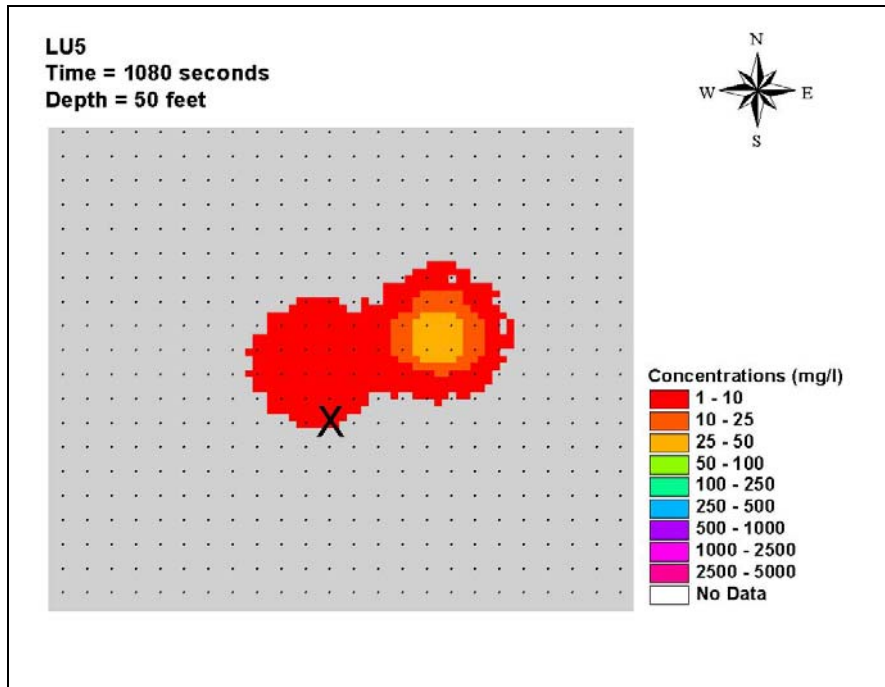


Figure K-105. LU5 plume at 1,080 sec at 15 m

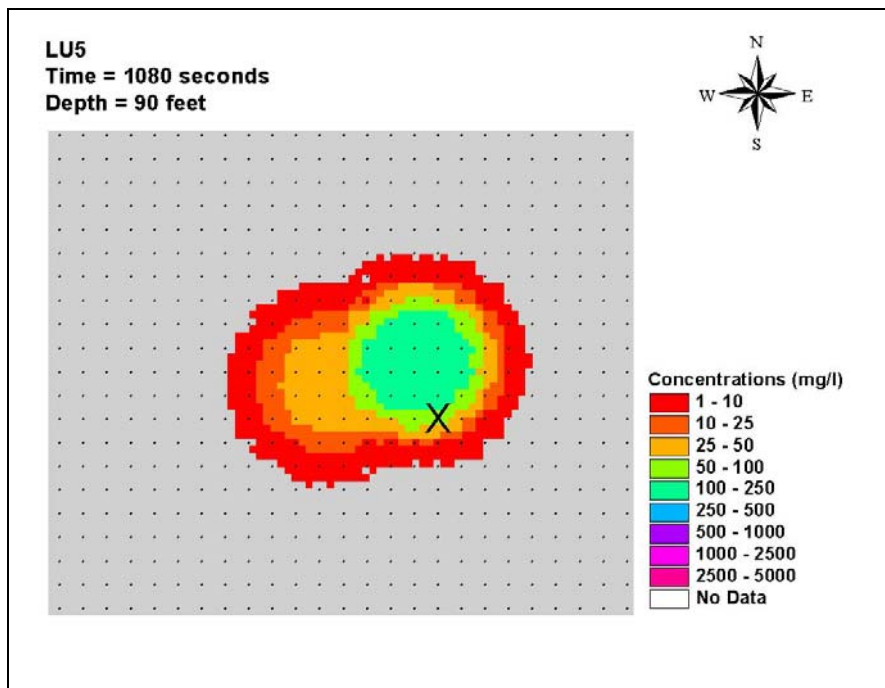


Figure K-106. LU5 plume at 1,080 sec at 27 m

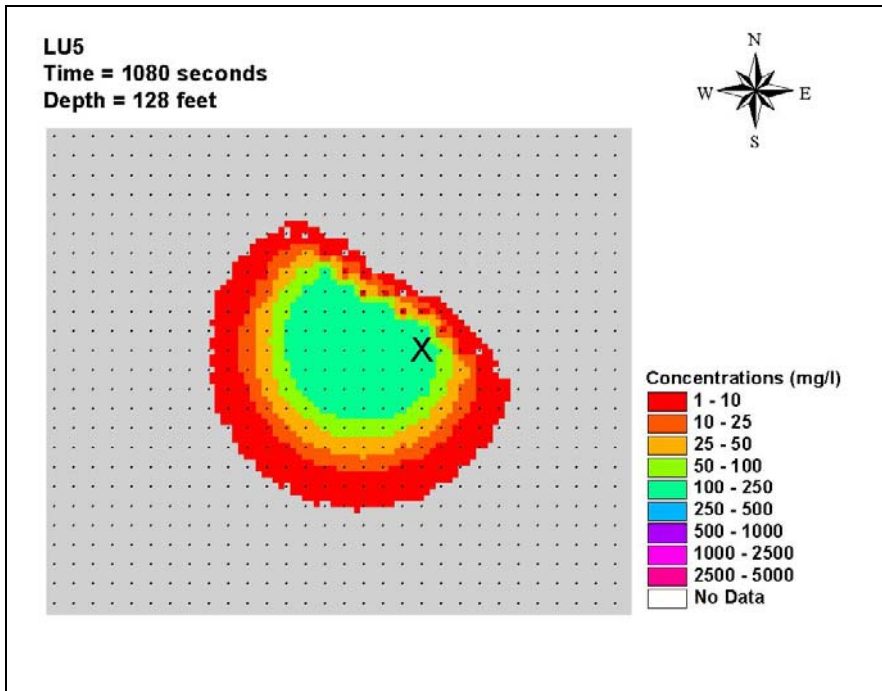


Figure K-107. LU5 plume at 1,080 sec at 39 m

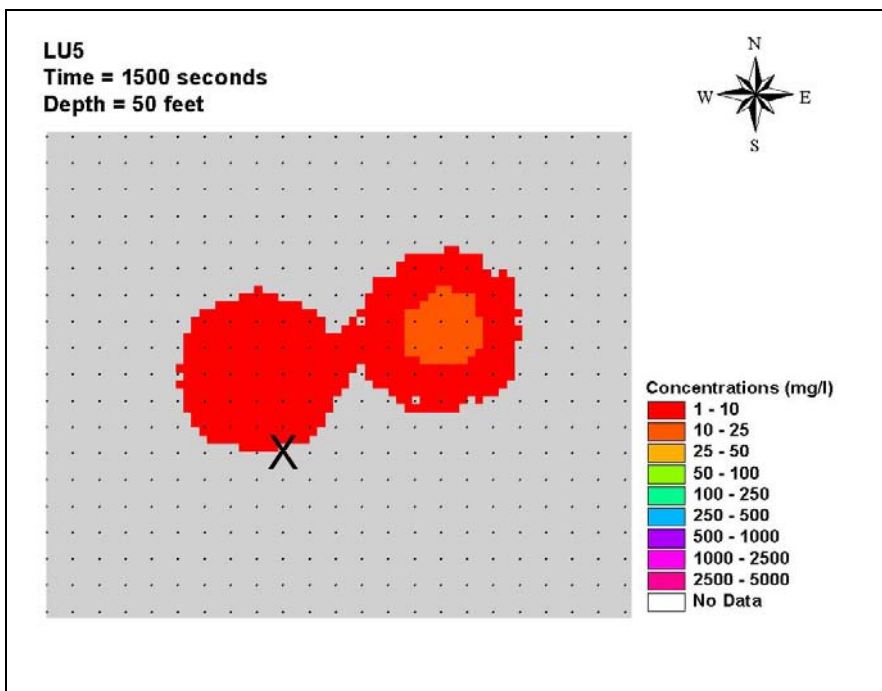


Figure K-108. LU5 plume at 1,500 sec at 15 m

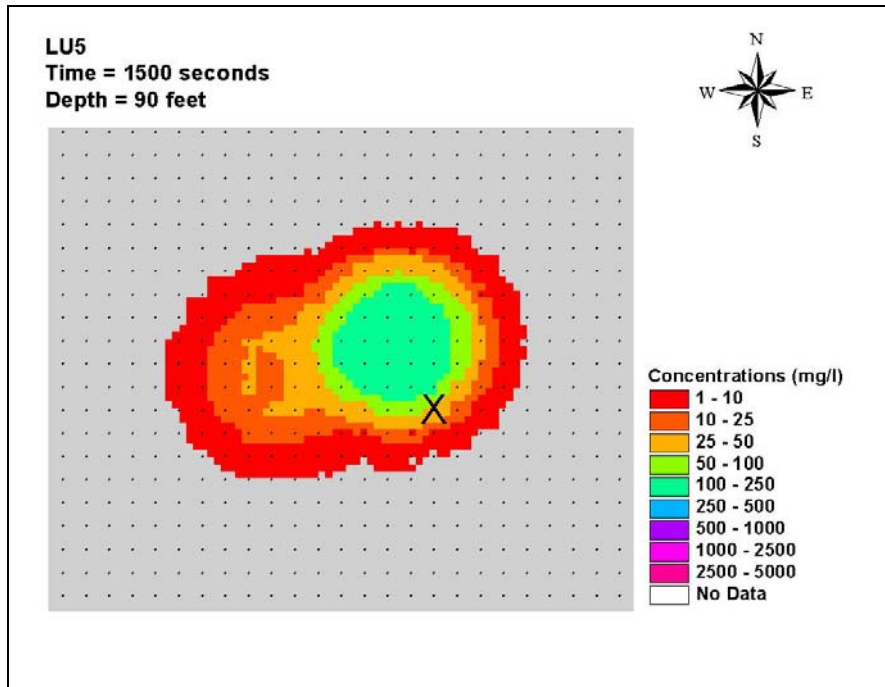


Figure K-109. LU5 plume at 1,500 sec at 27 m

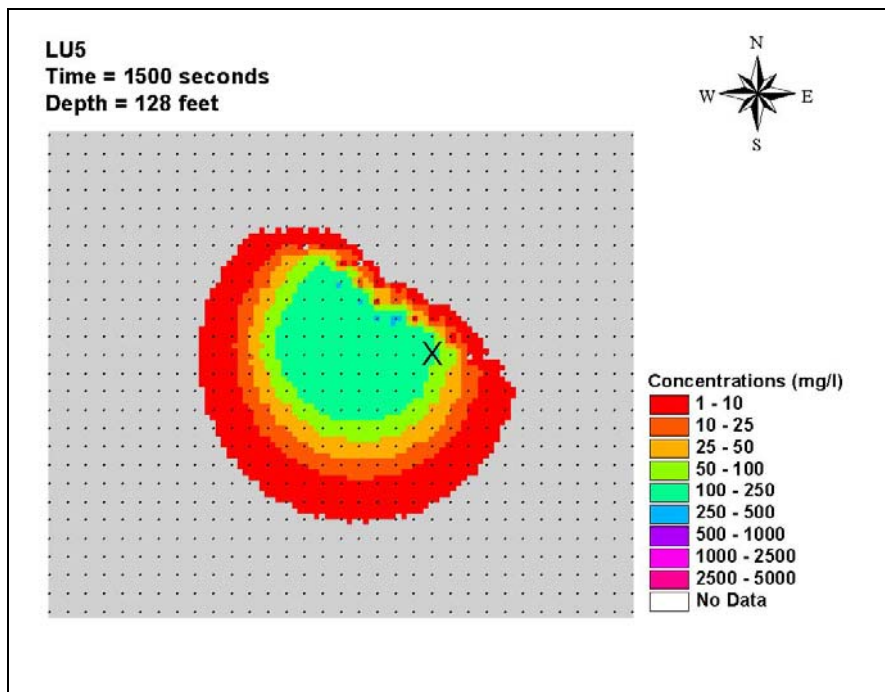


Figure K-110. LU5 plume at 1,500 sec at 39 m

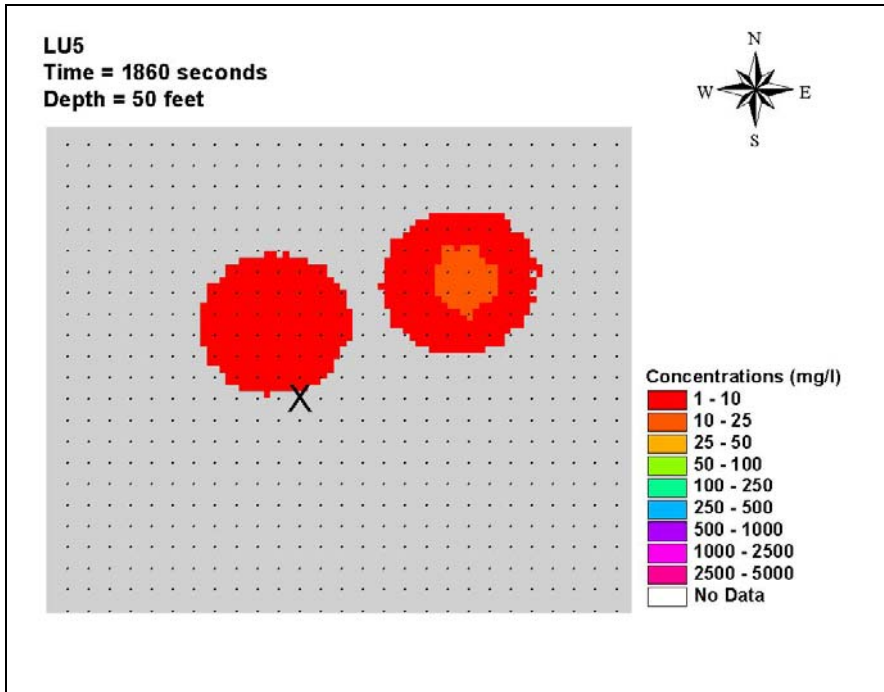


Figure K-111. LU5 plume at 1,860 sec at 15 m

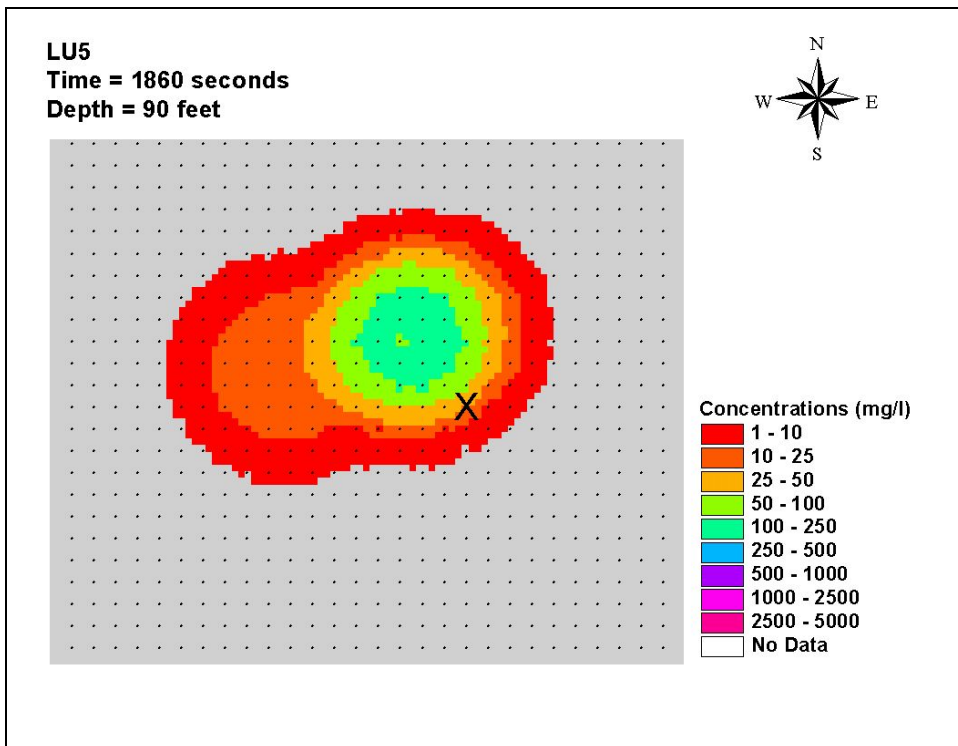


Figure K-112. LU5 plume at 1,860 sec at 27 m

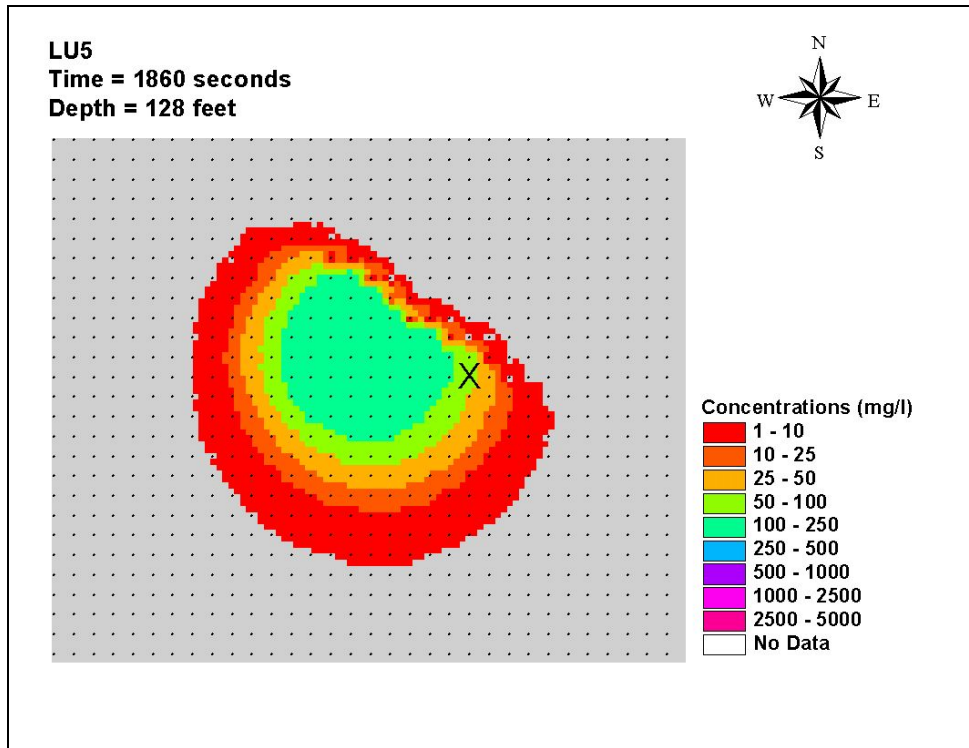


Figure K-113. LU5 plume at 1,860 sec at 39 m

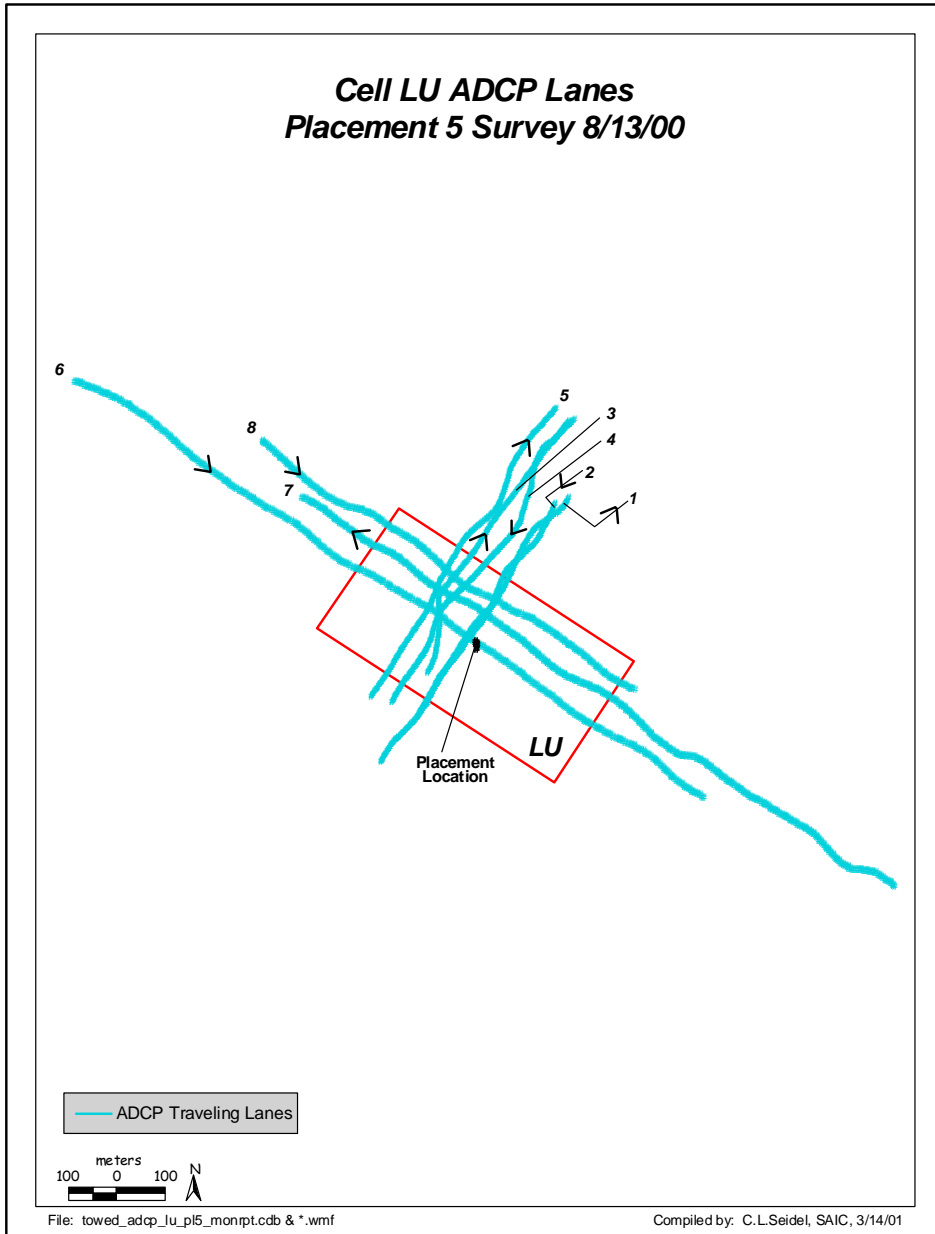


Figure K-114. LU5 transects (SAIC 2002, Figure 3.6-27)

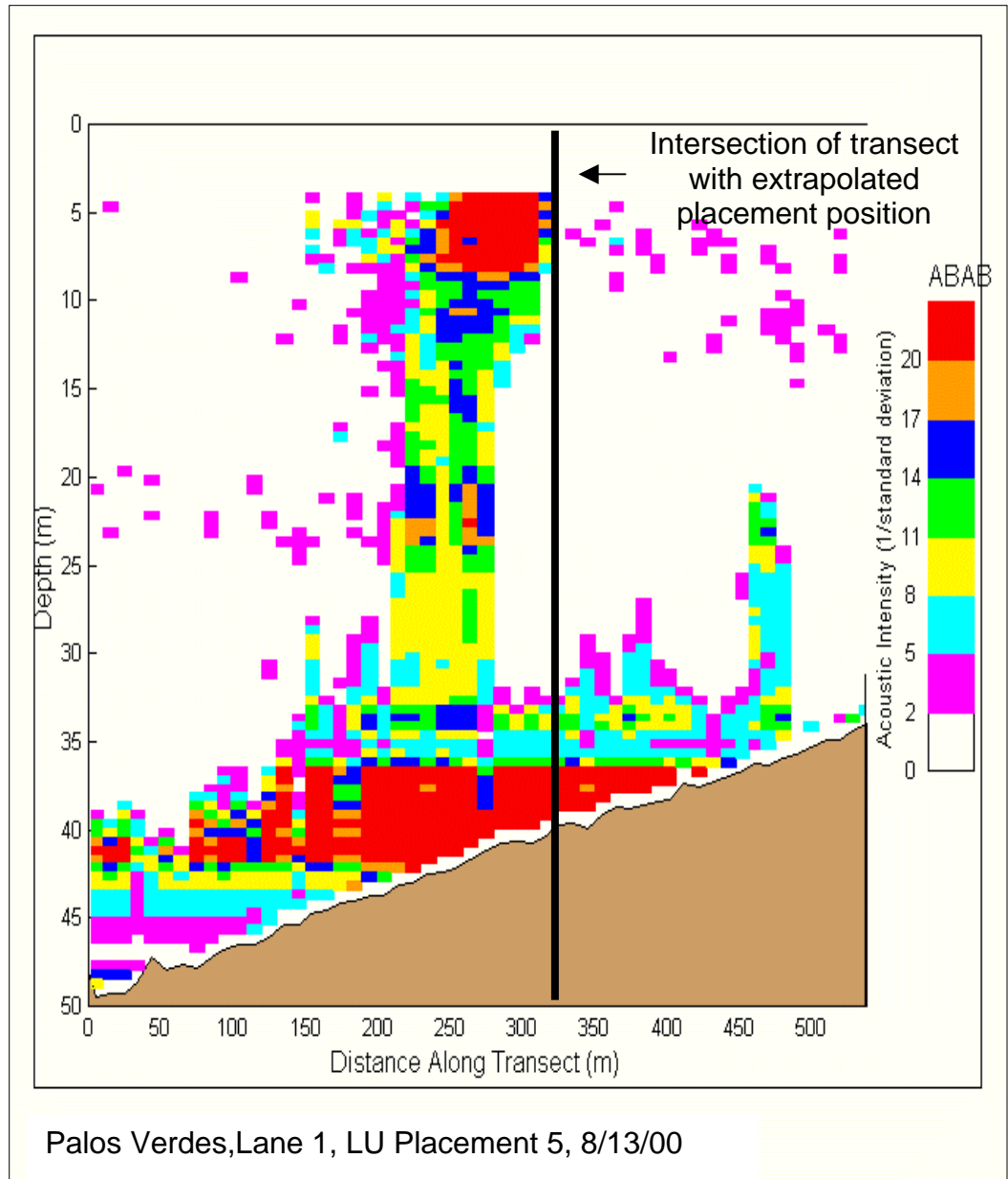


Figure K-115. ABAB along Transect 1 at 8 min after the placement operation ended (SAIC 2002, Figure 3.6-28)

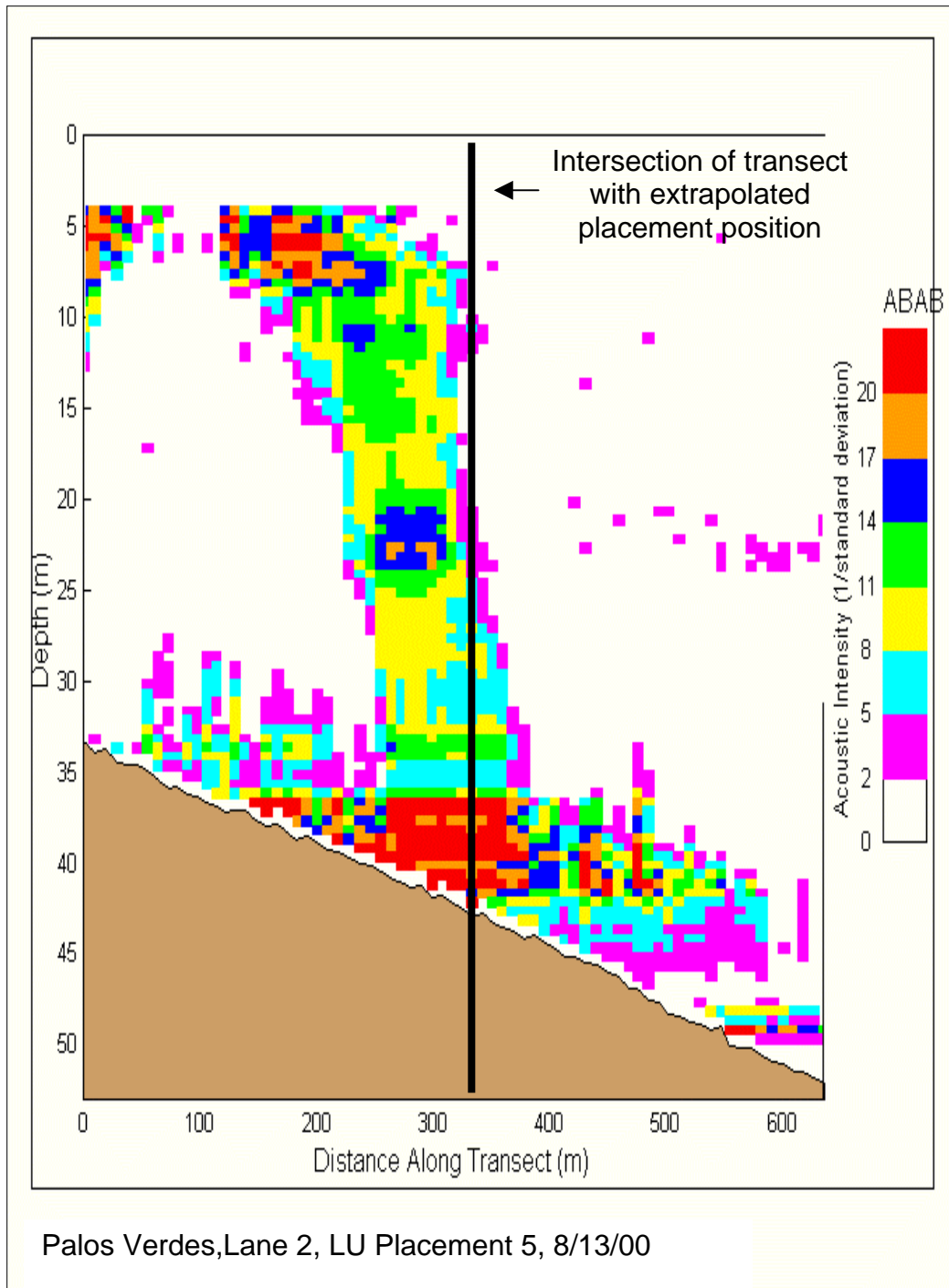


Figure K-116. ABAB along Transect 2 at 15 min after the placement operation ended (SAIC 2002, Figure 3.6-29)

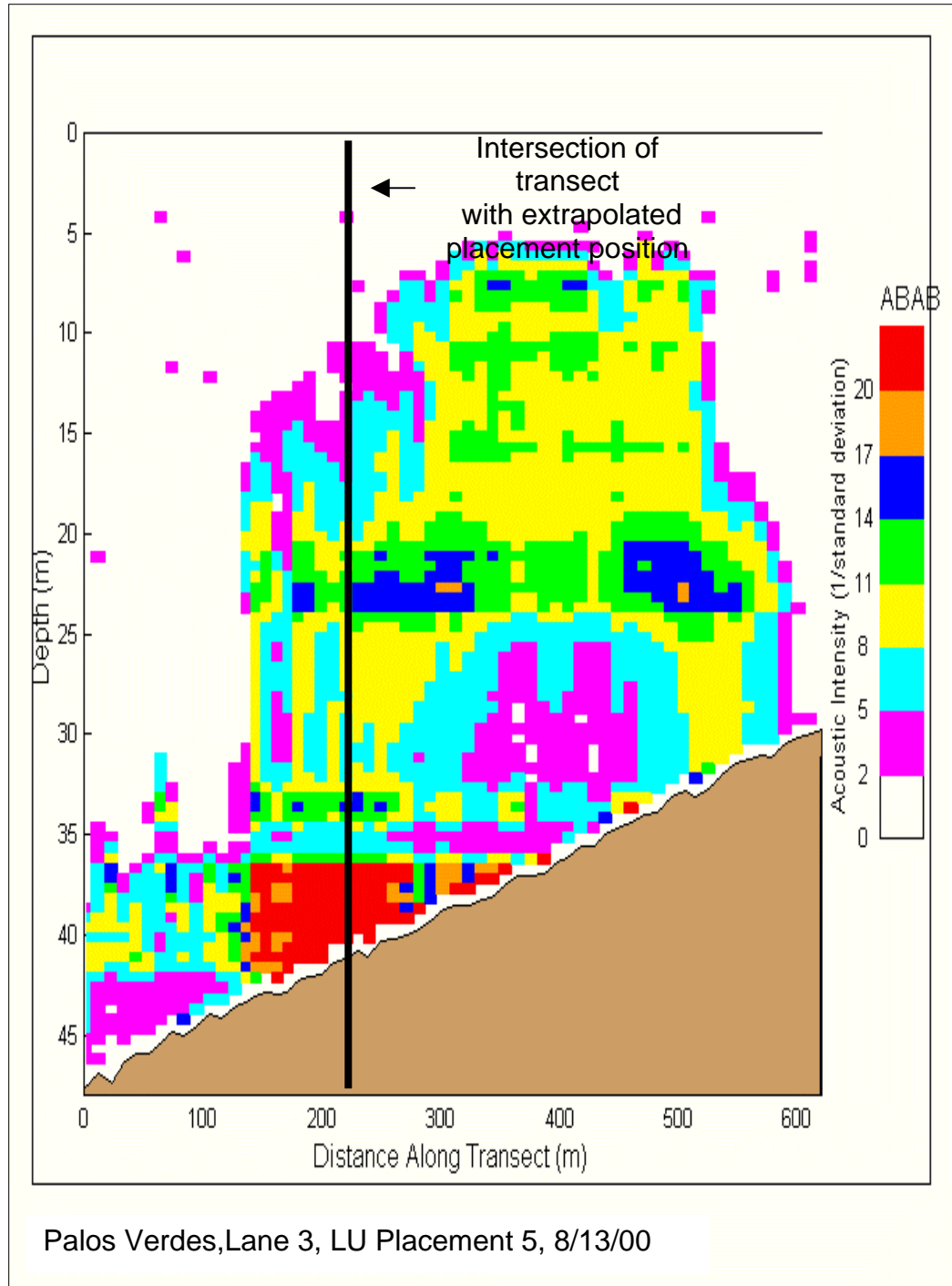


Figure K-117. ABAB along Transect 3 at 22 min after the placement operation ended (SAIC 2002, Figure 3.6-30)

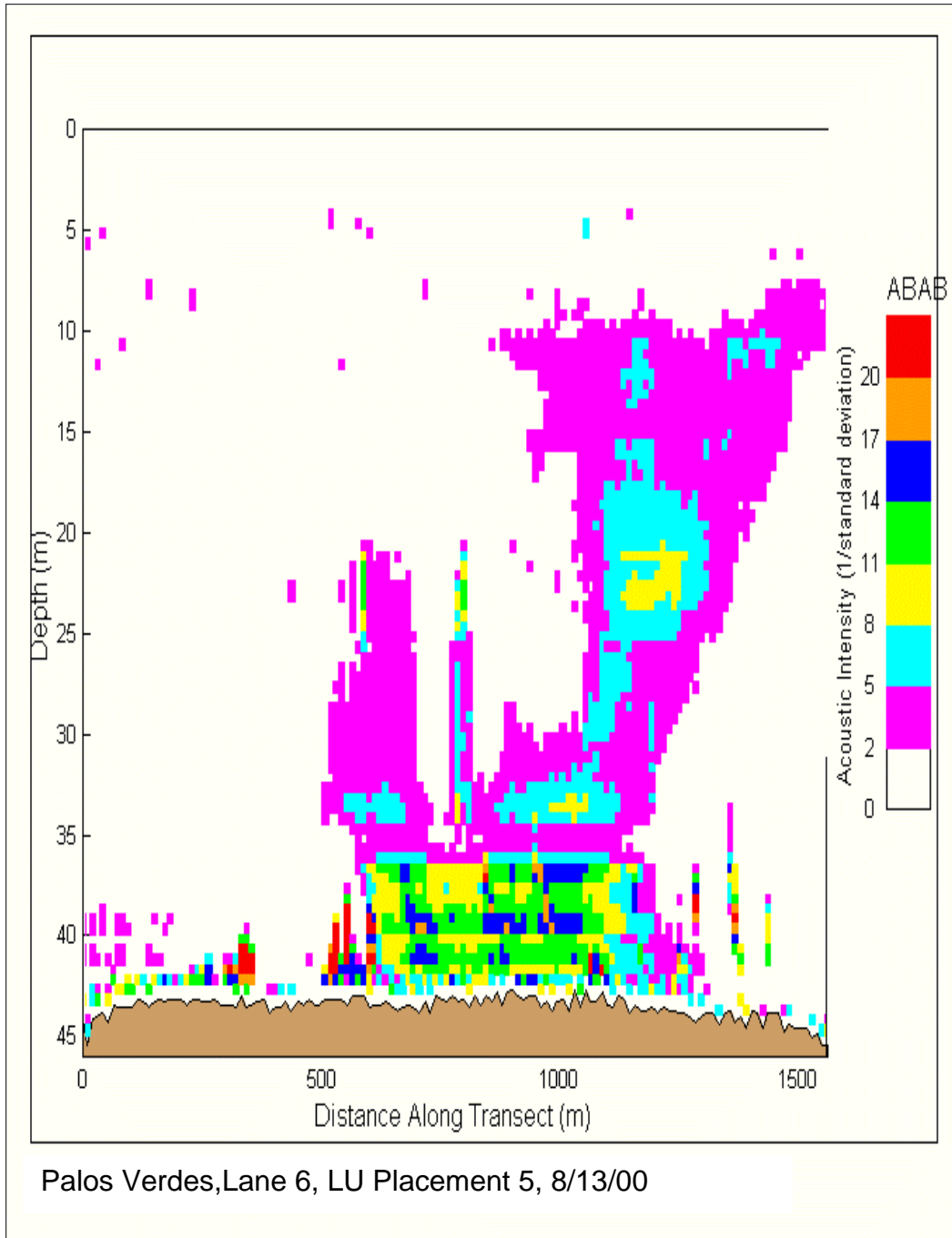


Figure K-118. ABAB along Transect 6 at 49 min after the placement operation ended (SAIC 2002, Figure 3.6-33)

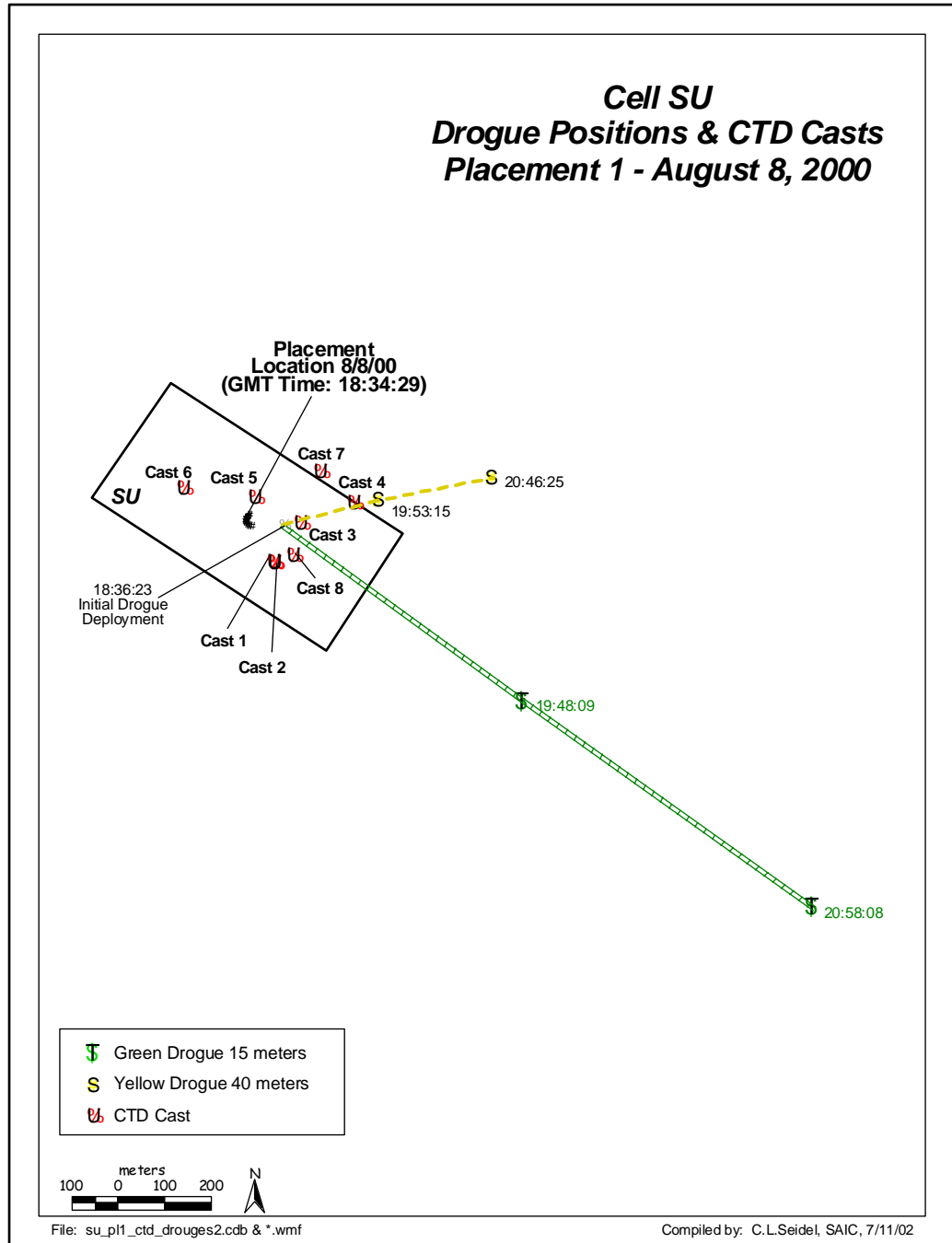
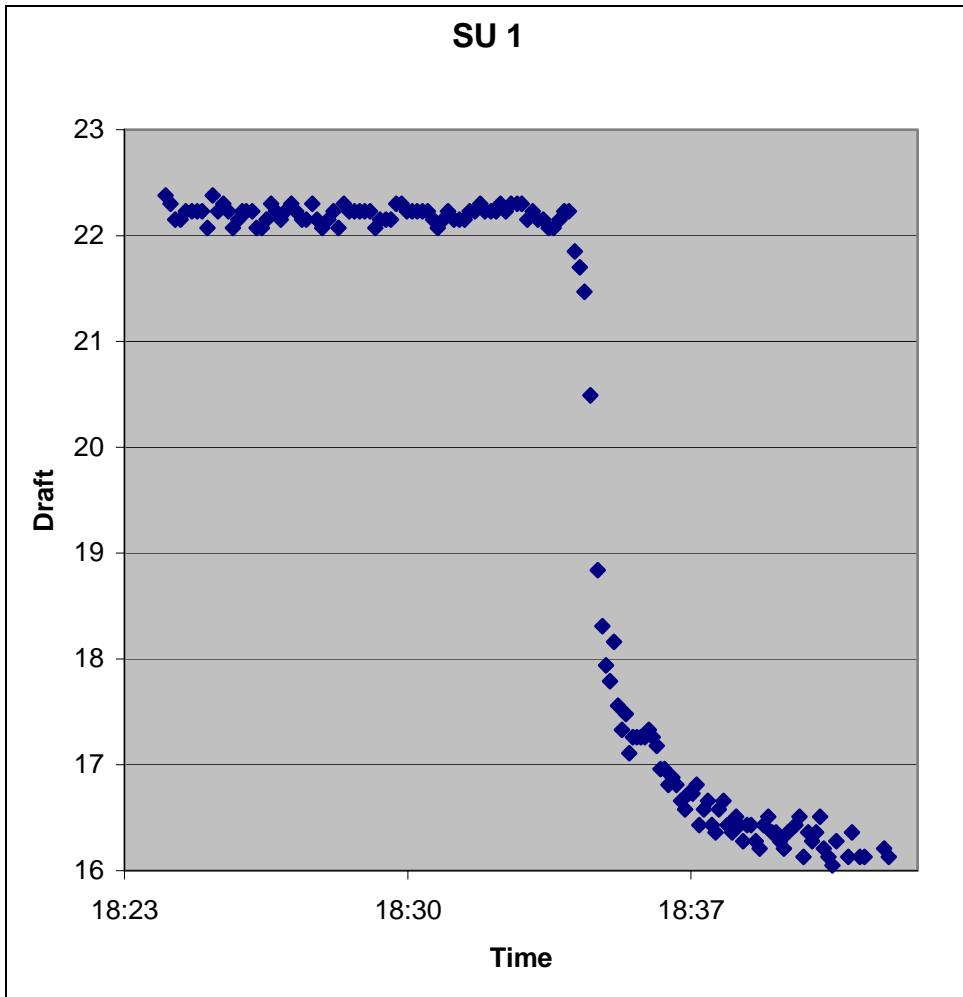


Figure K-119. SU1 drogue paths and CTD stations (SAIC 2002, Figure 4.5-1)



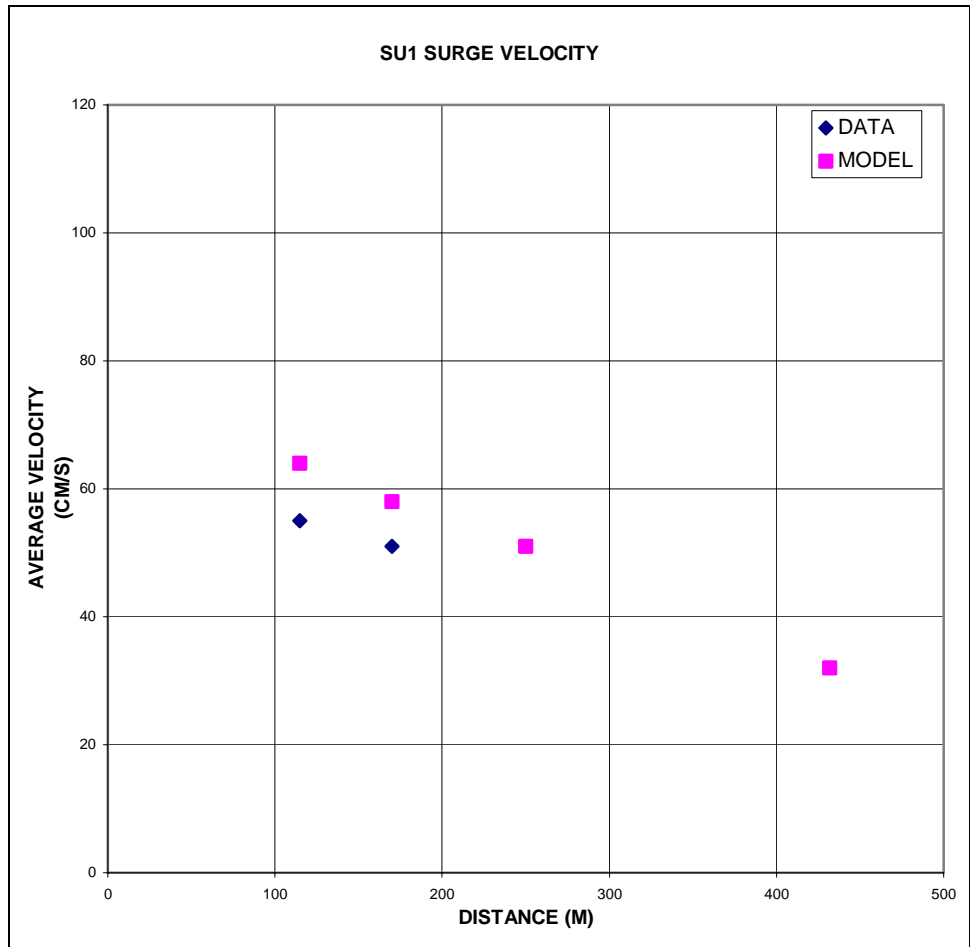


Figure K-121. Comparison of STFATE average surge speed with SU1 field data

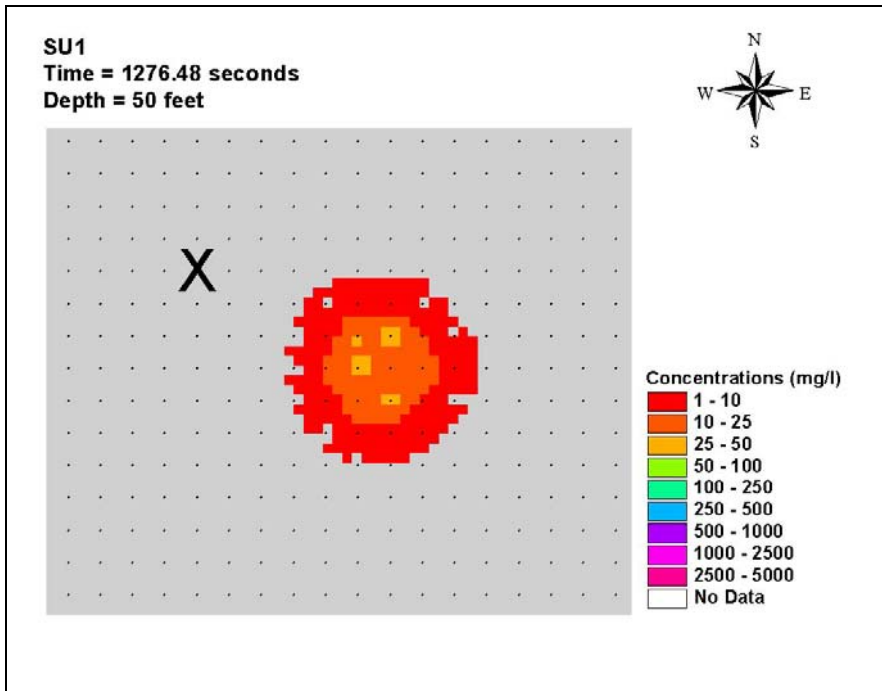


Figure K-122. SU1 plume at end of collapse at 15 m

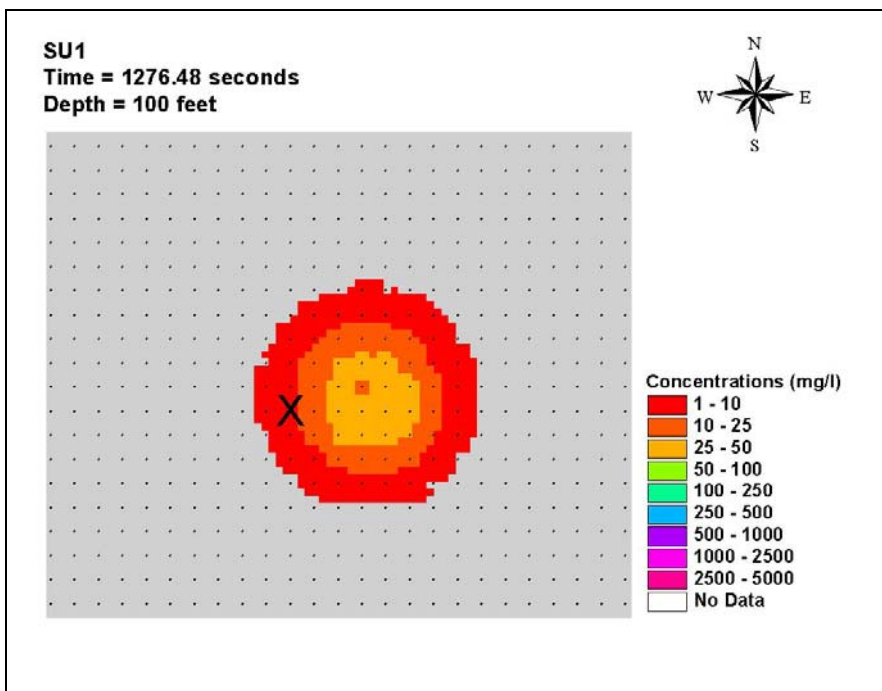


Figure K-123. SU1 plume at end of collapse at 30 m

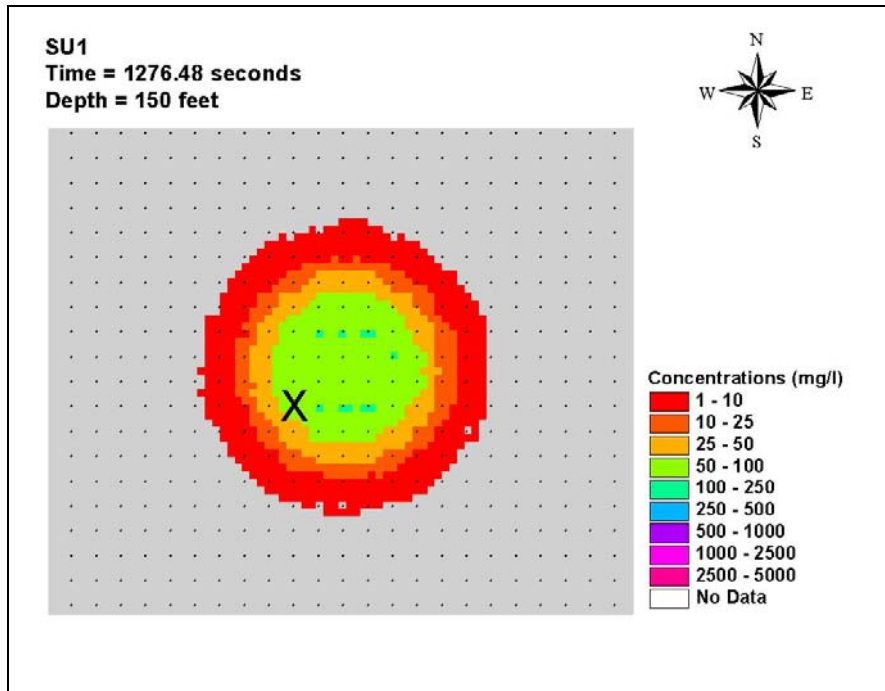


Figure K-124. SU1 plume at end of collapse at 46 m

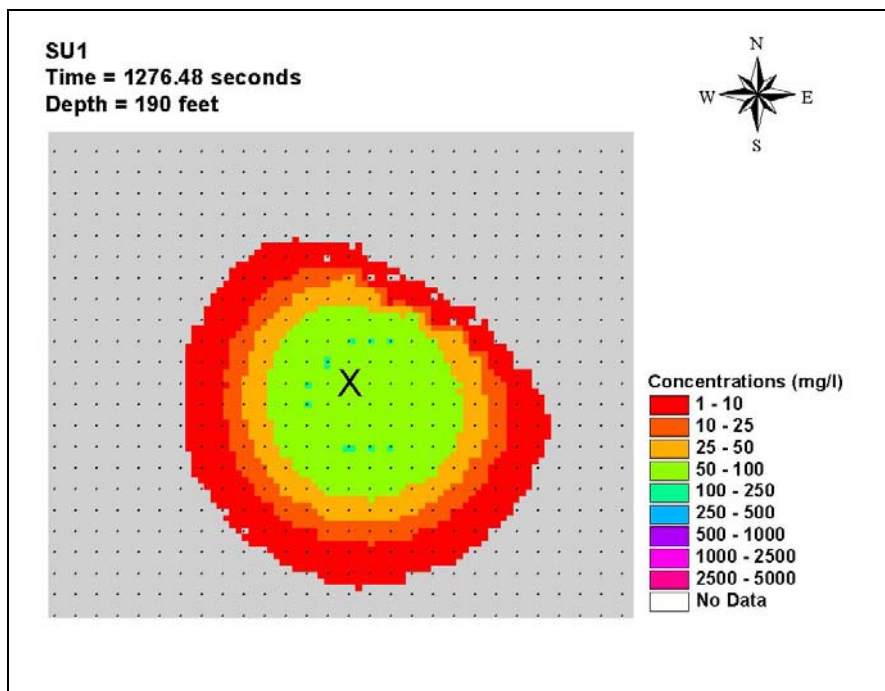


Figure K-125. SU1 plume at end of collapse at 58 m

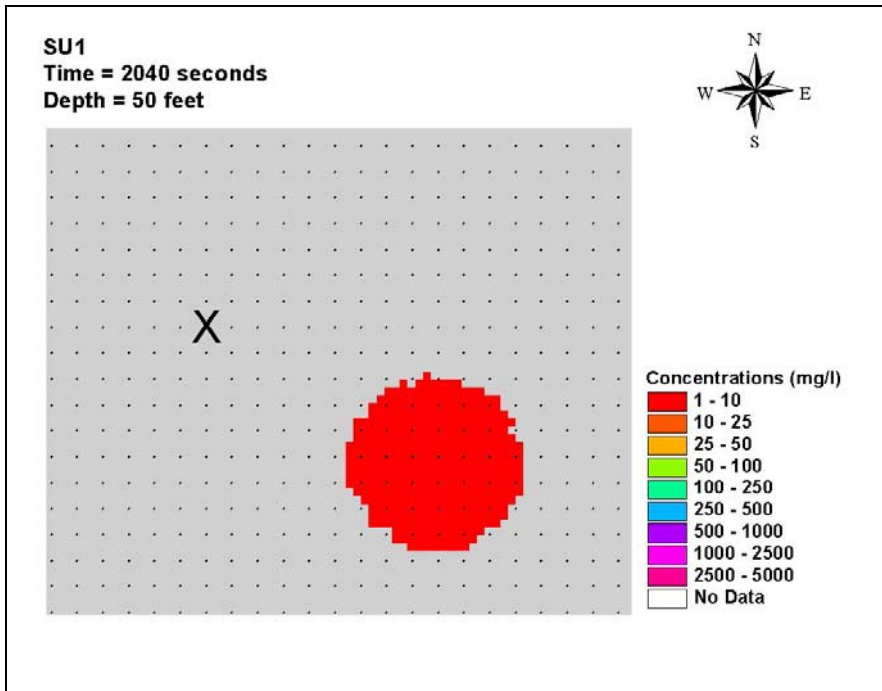


Figure K-126. SU1 plume at 2040 sec at 15 m

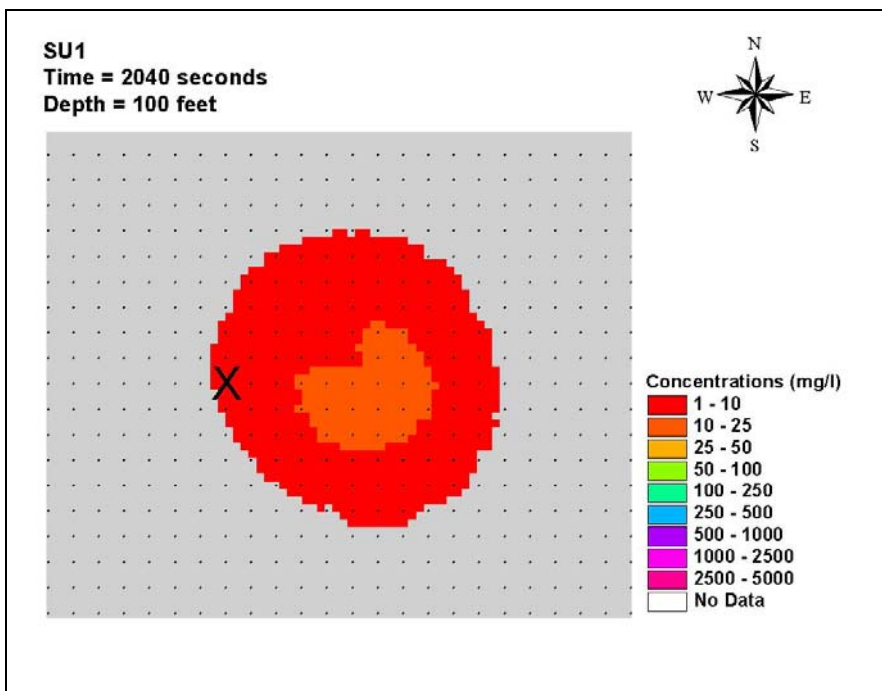


Figure K-127. SU1 plume at 2040 sec at 30 m

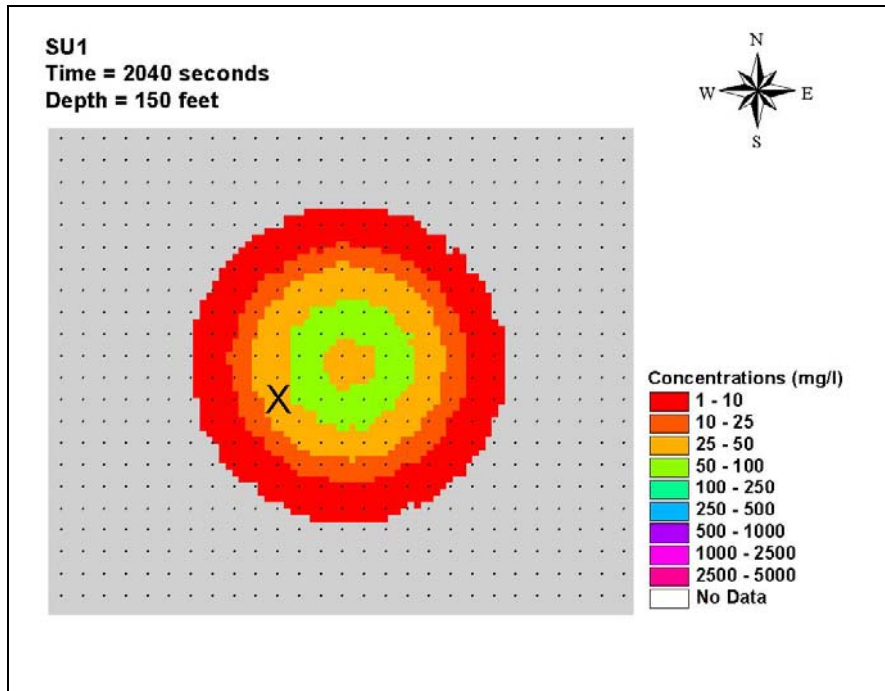


Figure K-128. SU1 plume at 2,040 sec at 46 m

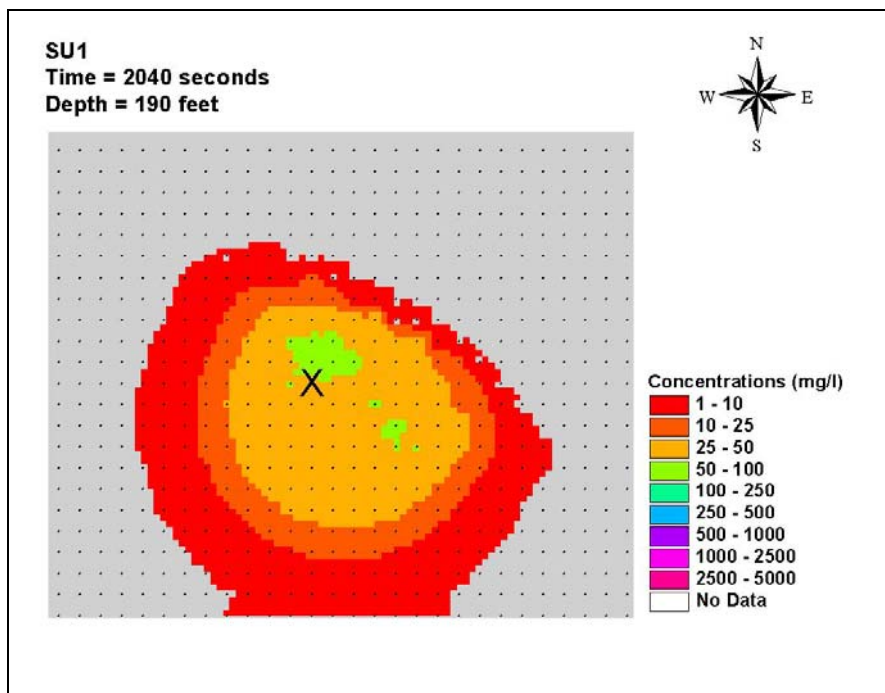


Figure K-129. SU1 plume at 2,040 sec at 58 m

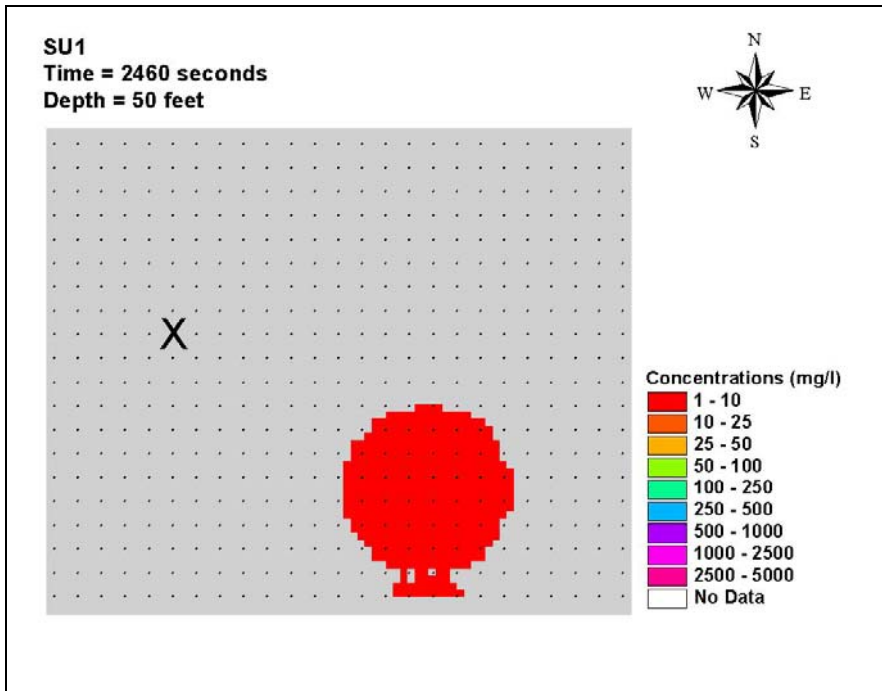


Figure K-130. SU1 plume at 2,460 sec at 15 m

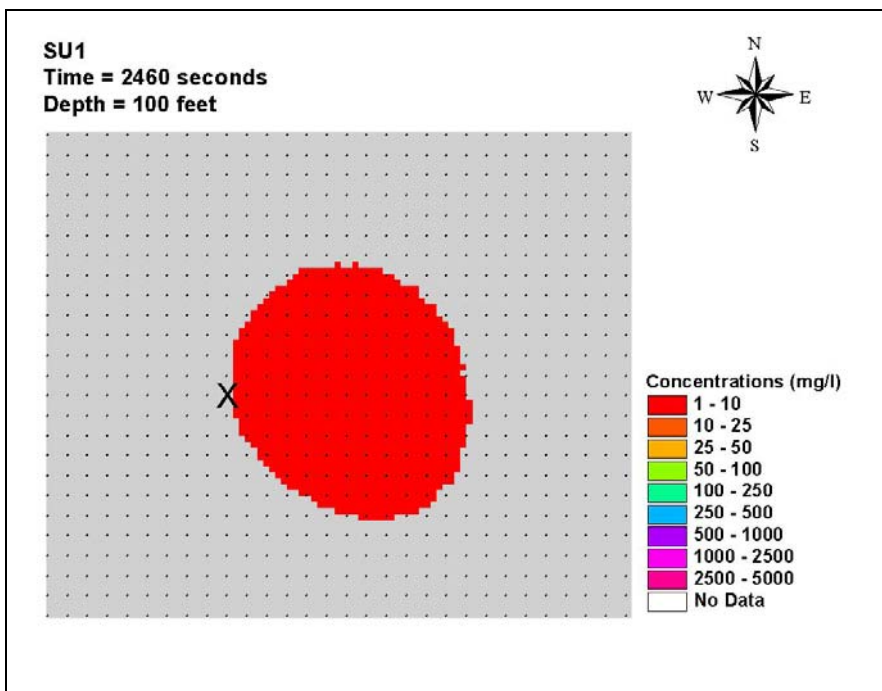


Figure K-131. SU1 plume at 2,460 sec at 30 m

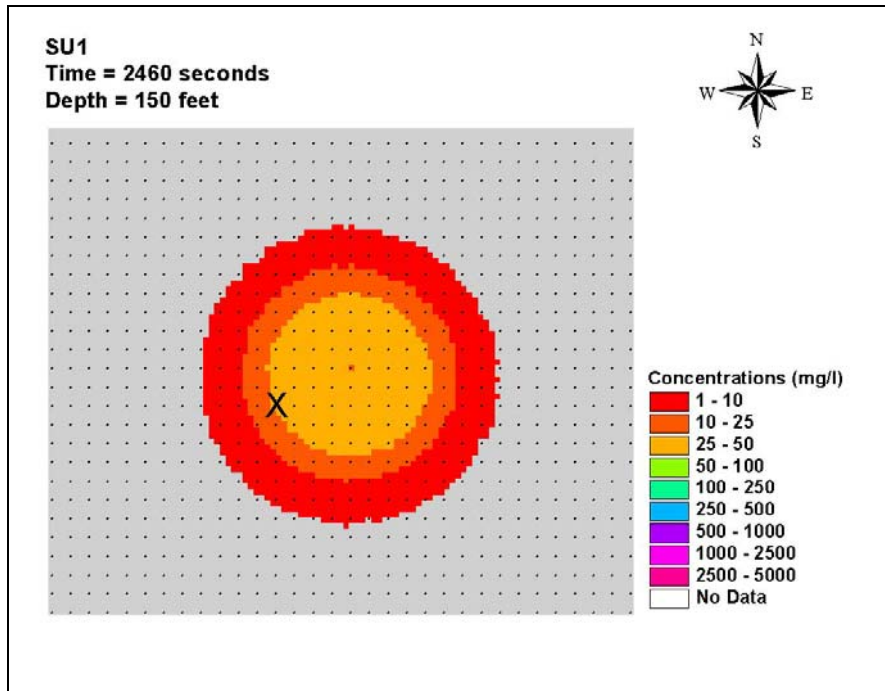


Figure K-132. SU1 plume at 2,460 sec at 46 m

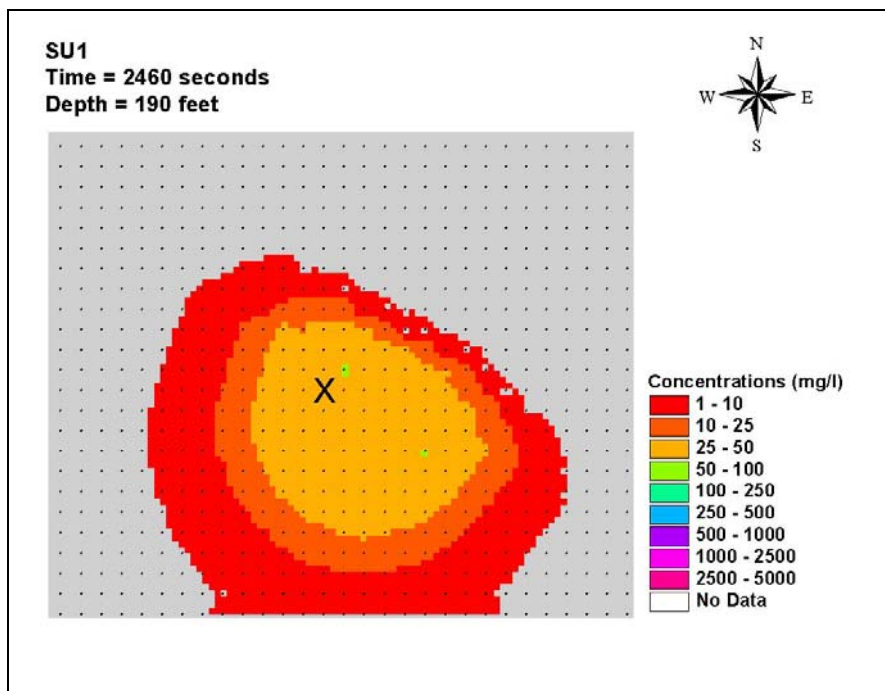


Figure K-133. SU1 plume at 2,460 sec at 58 m

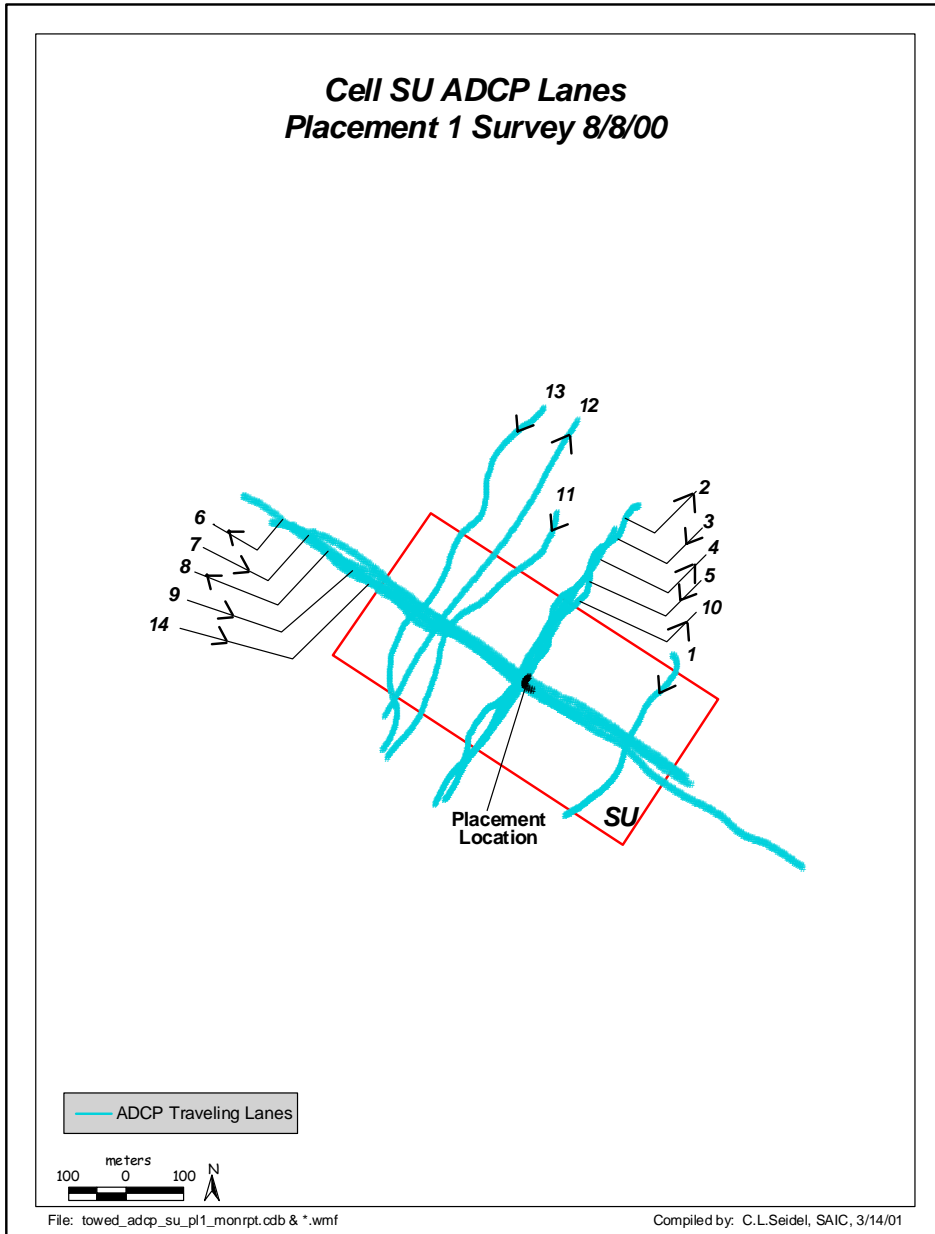


Figure 134. SU1 transects (SAIC 2002, Figure 4.6-2)

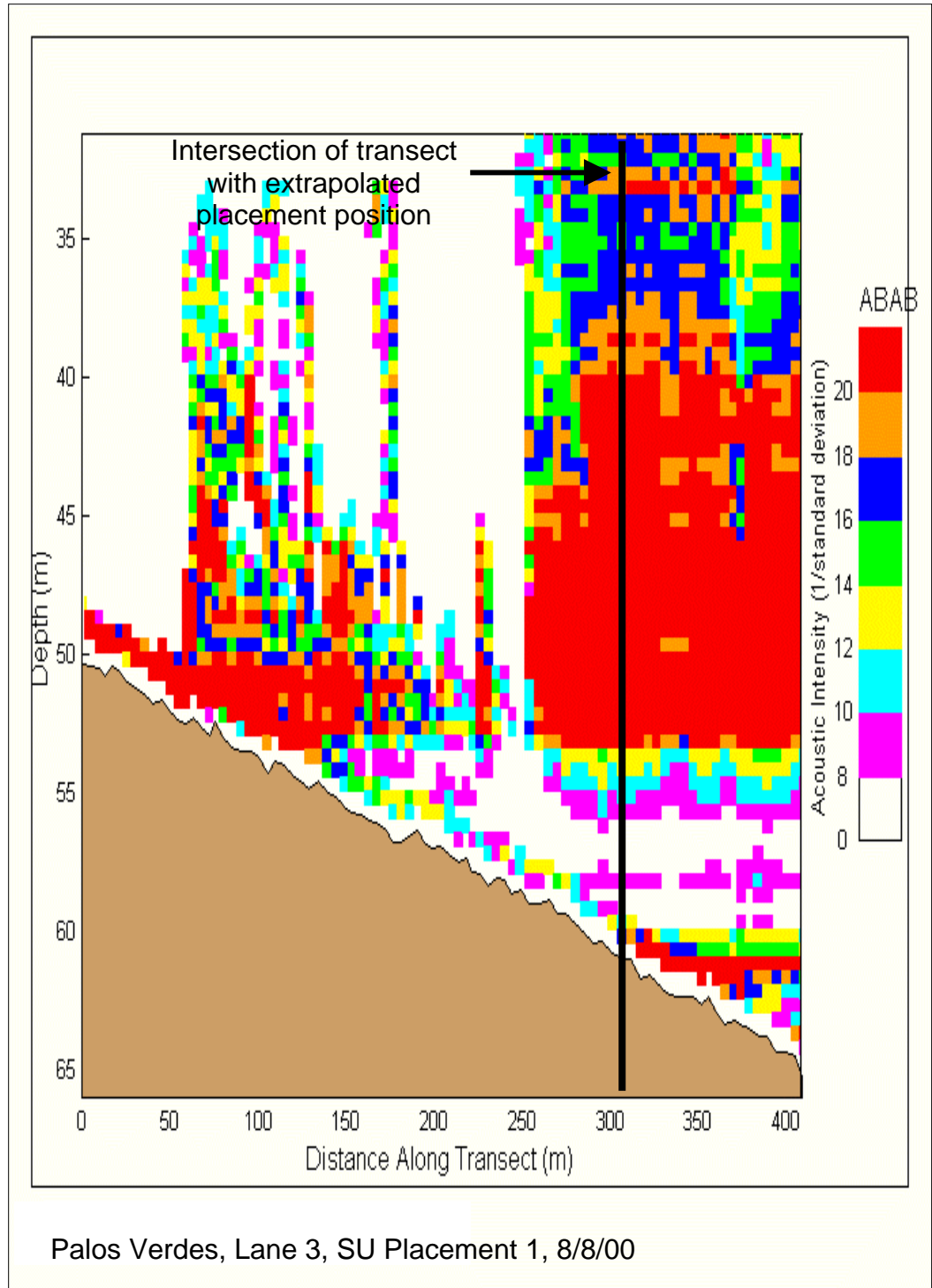


Figure 135. ABAB along Transect 3 at 19 min after the placement operation ended (SAIC 2002, Figure 4.6-4)

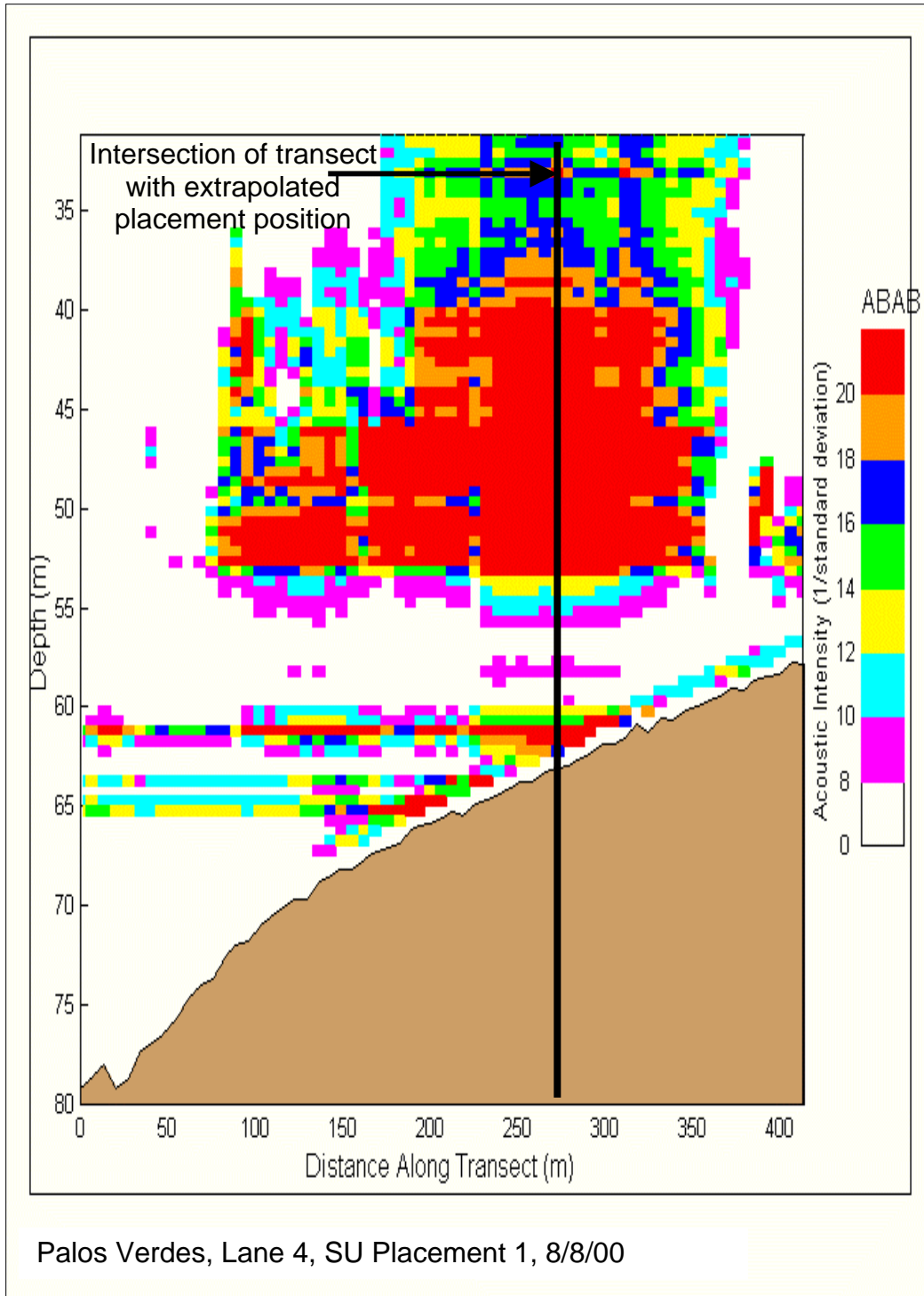


Figure 136. ABAB along Transect 4 at 31 min after the placement operation ended (SAIC 2002, Figure 4.6-5)

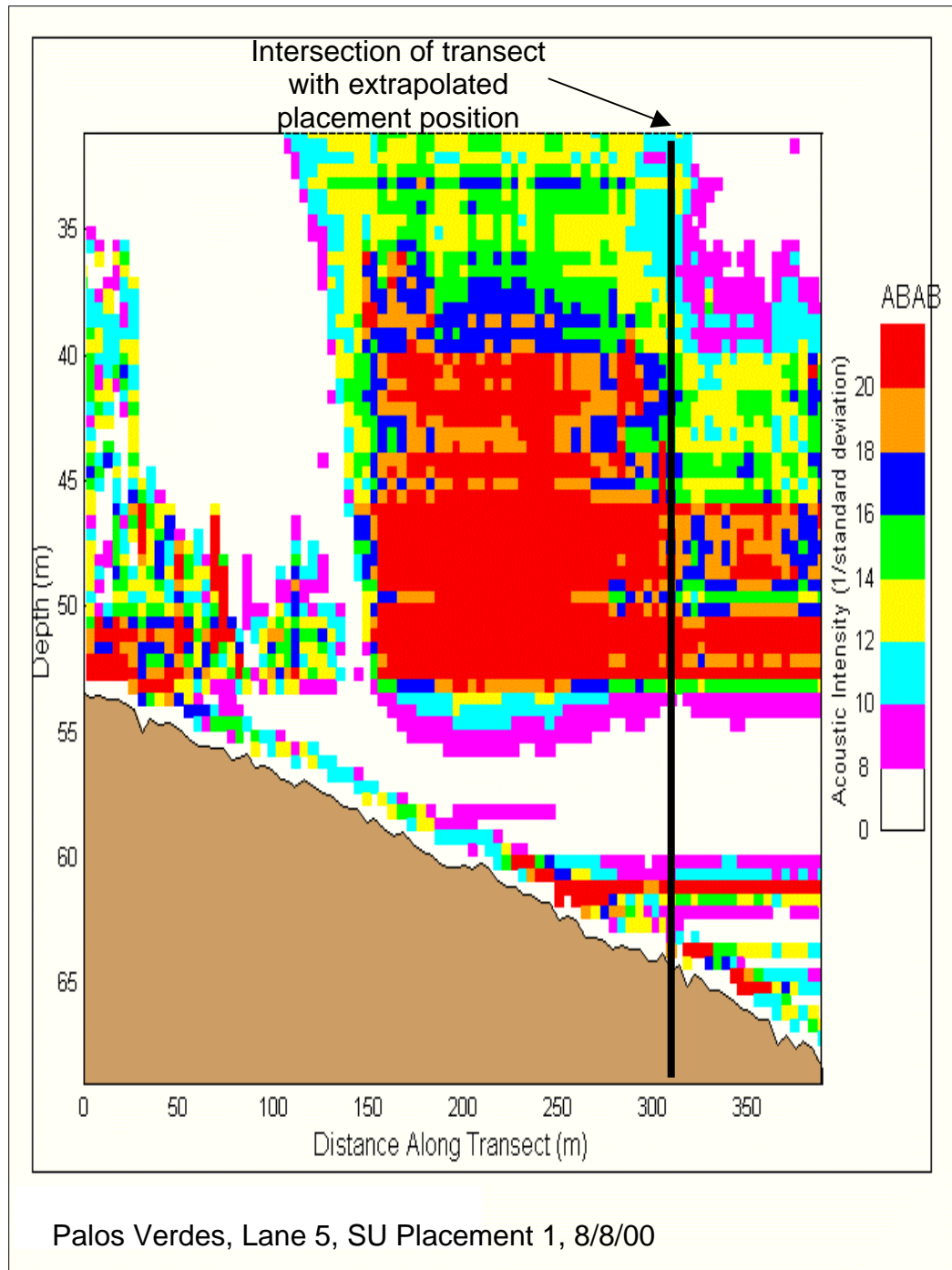


Figure 137. ABAB along Transect 5 at 39 min after the placement operation ended (SAIC 2002, Figure 4.6-6)

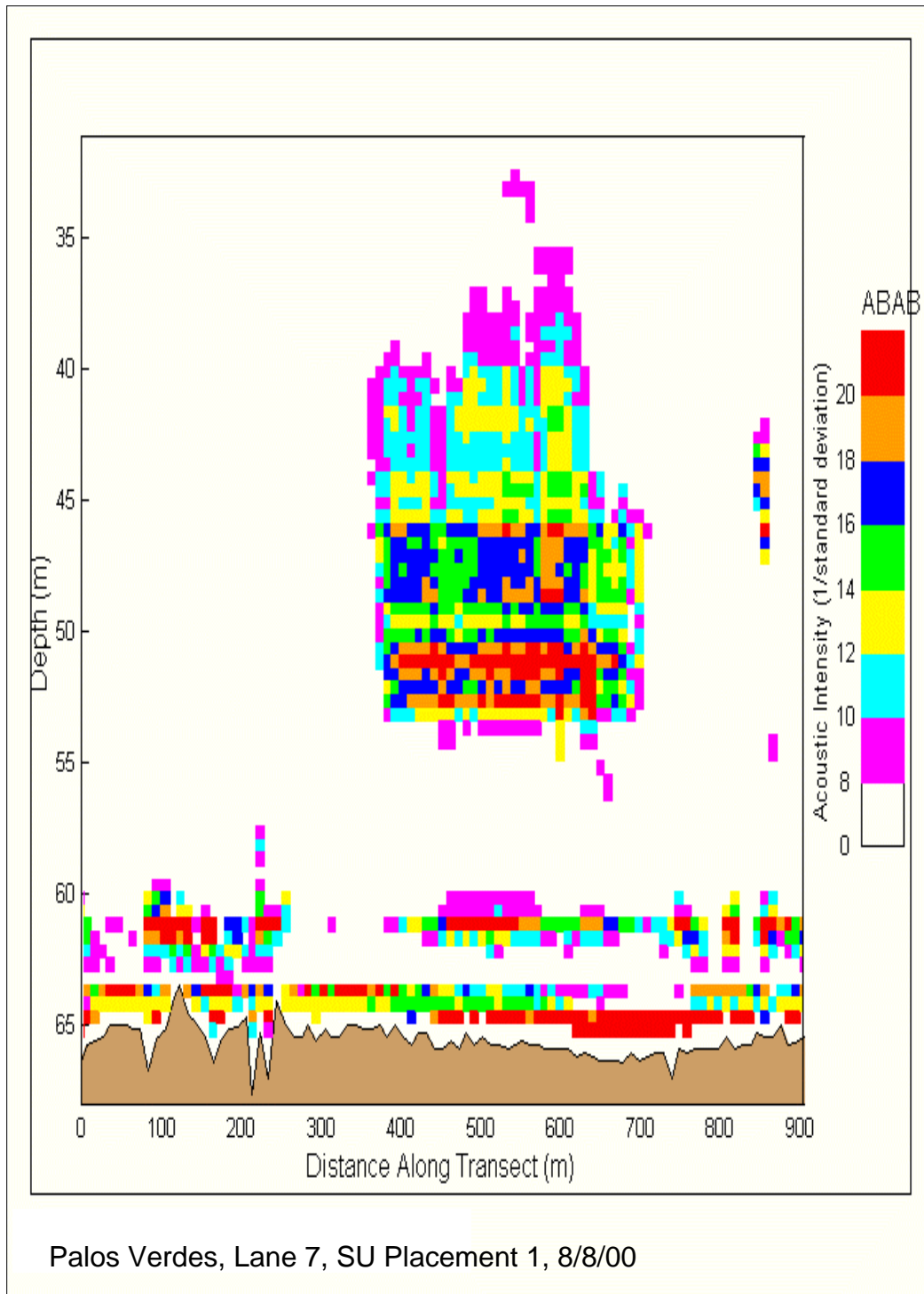


Figure 138. ABAB along Transect 7 at 1 hr after the placement operation ended (SAIC 2002, Figure 4.6-8)

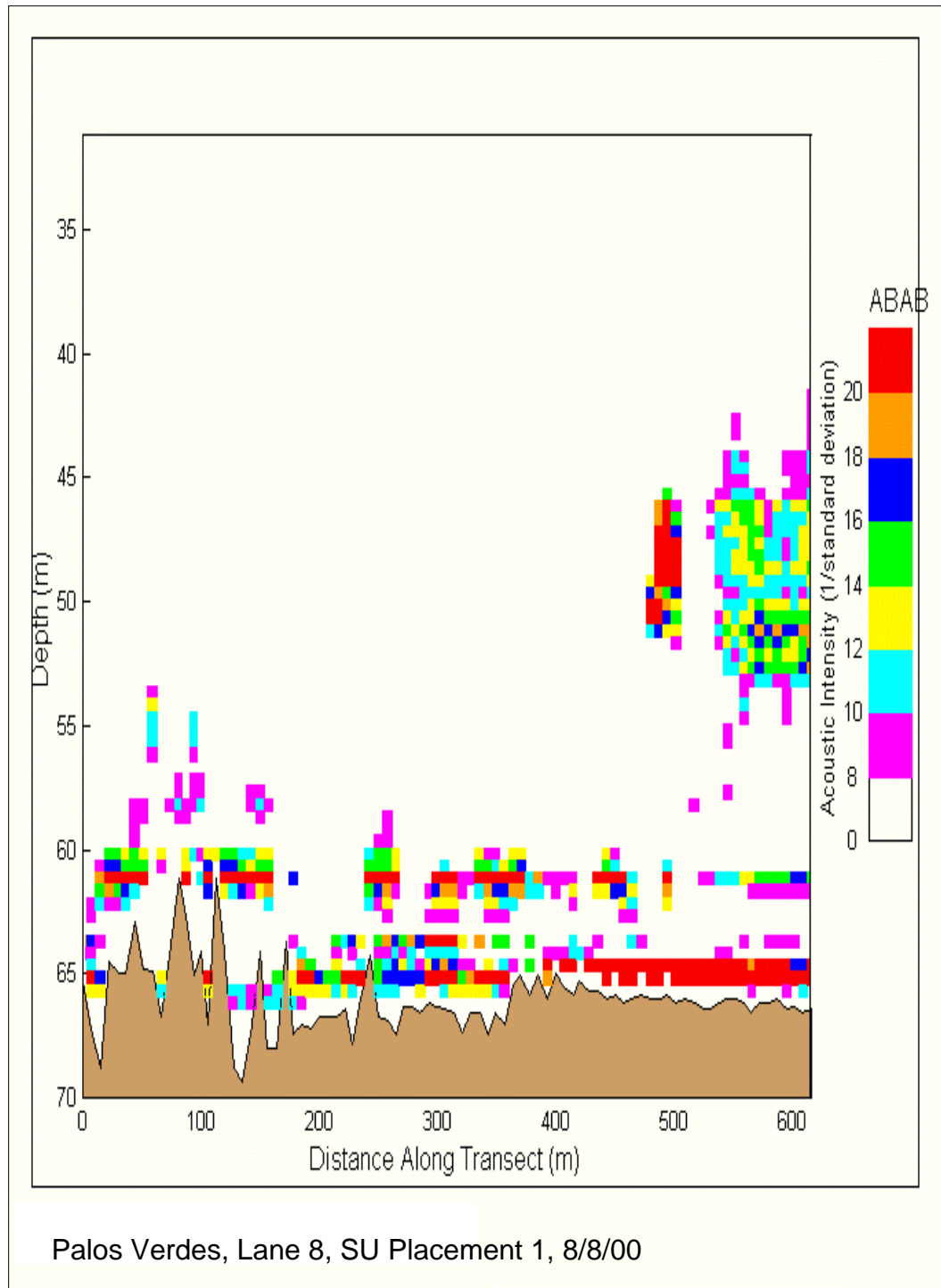


Figure 139. ABAB along Transect 8 at 1 hr 10 min after the placement operation ended (SAIC 2002, Figure 4.6-9)

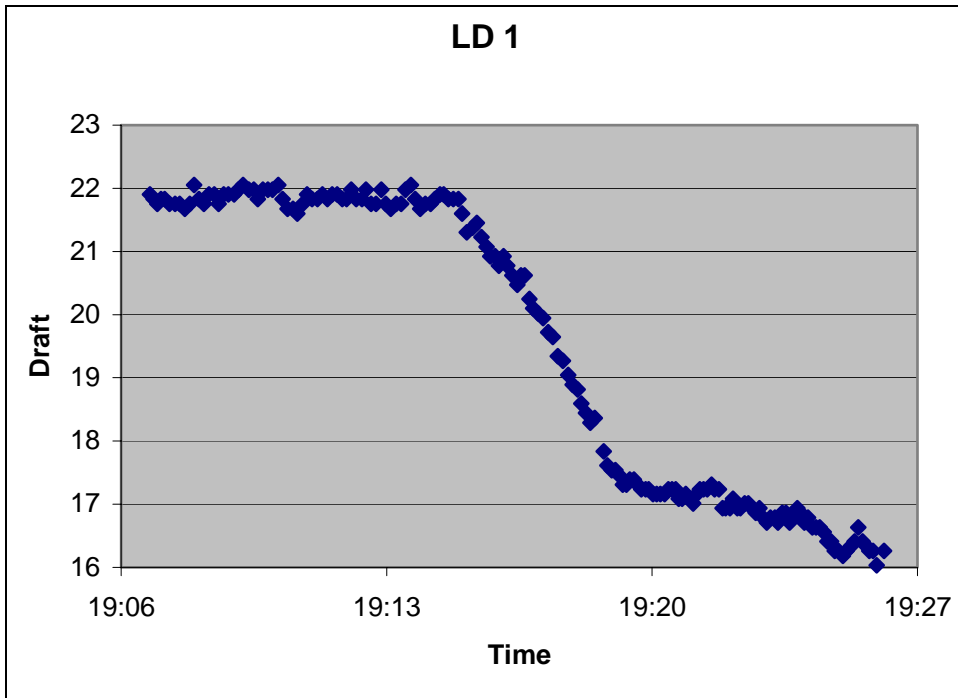


Figure 140. Vessel draft of LD1 disposal

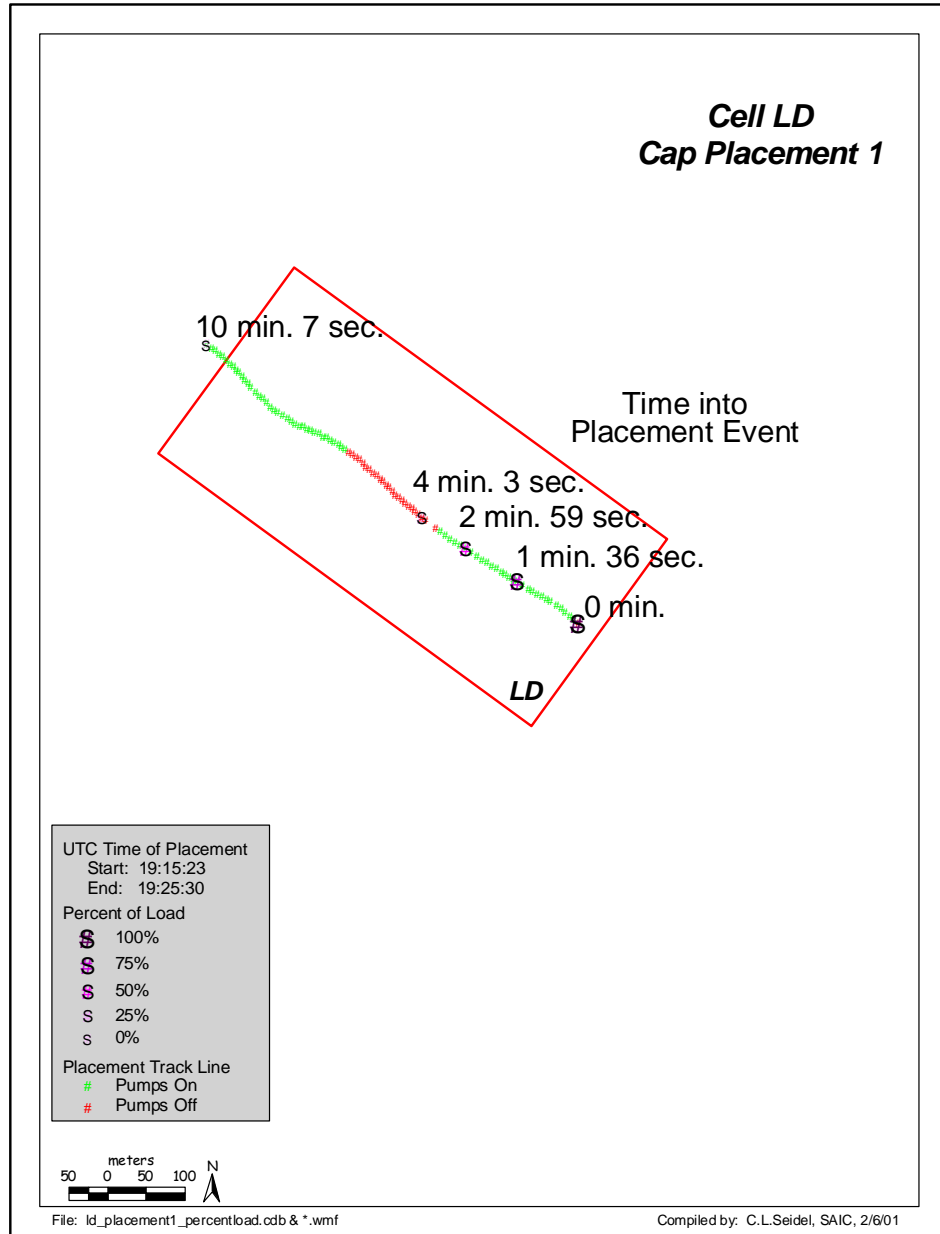


Figure 141. LD1 disposal path (SAIC 2002, Figure 5.2-4)

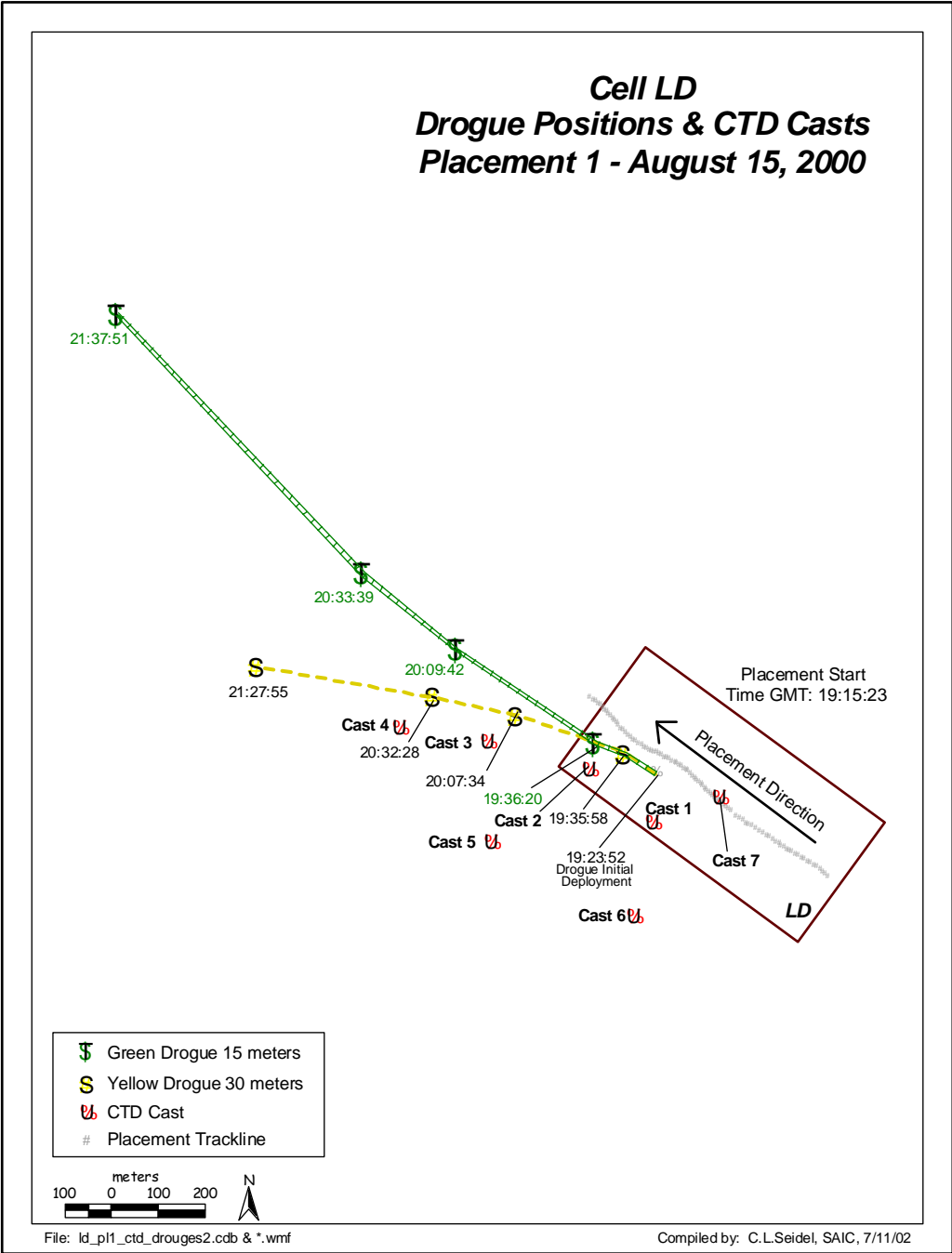


Figure 142. LD1 drogue paths (SAIC 2002, Figure 5.5-1)

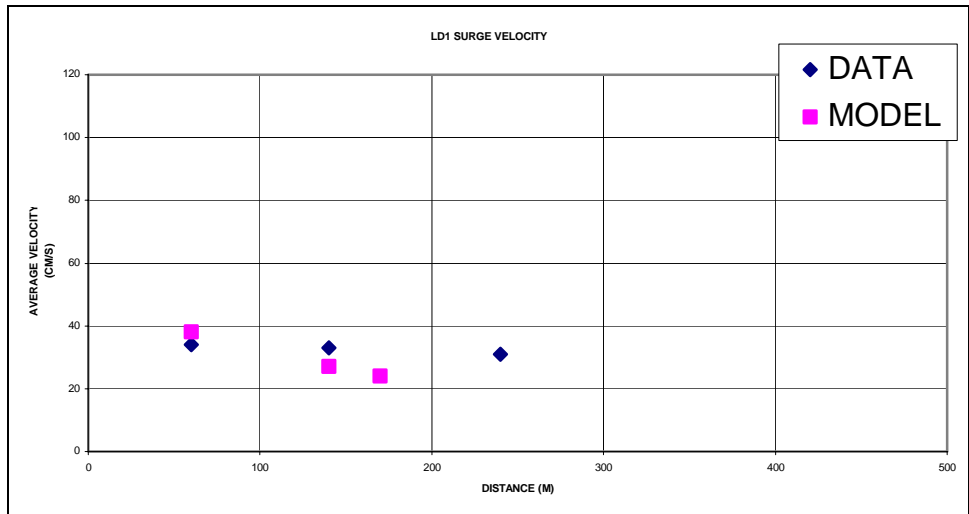


Figure 143. Comparison of STFATE average surge speed with LD1 field data

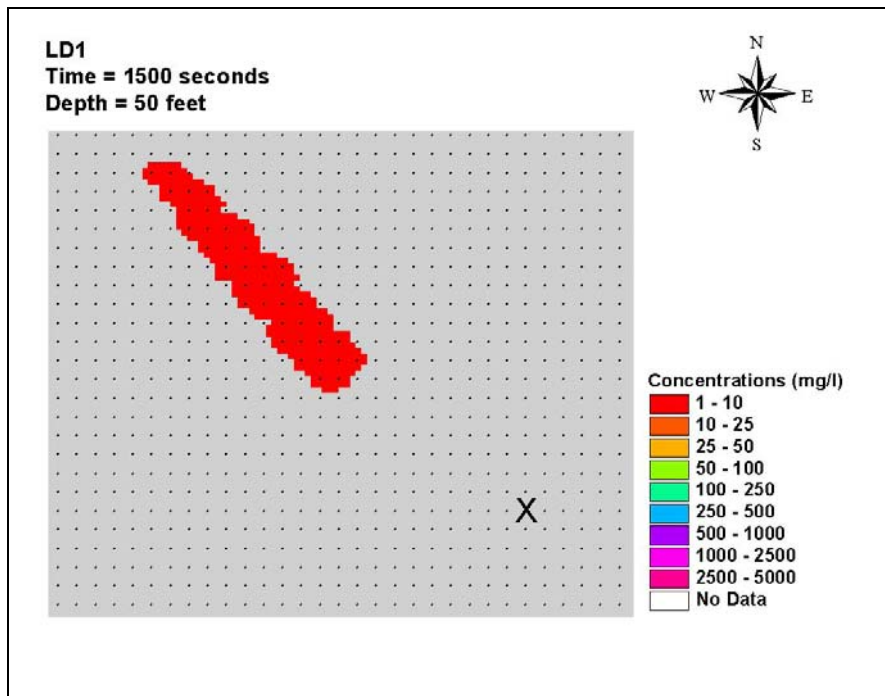


Figure 144. LD1 plume at 1,500 sec at 15 m

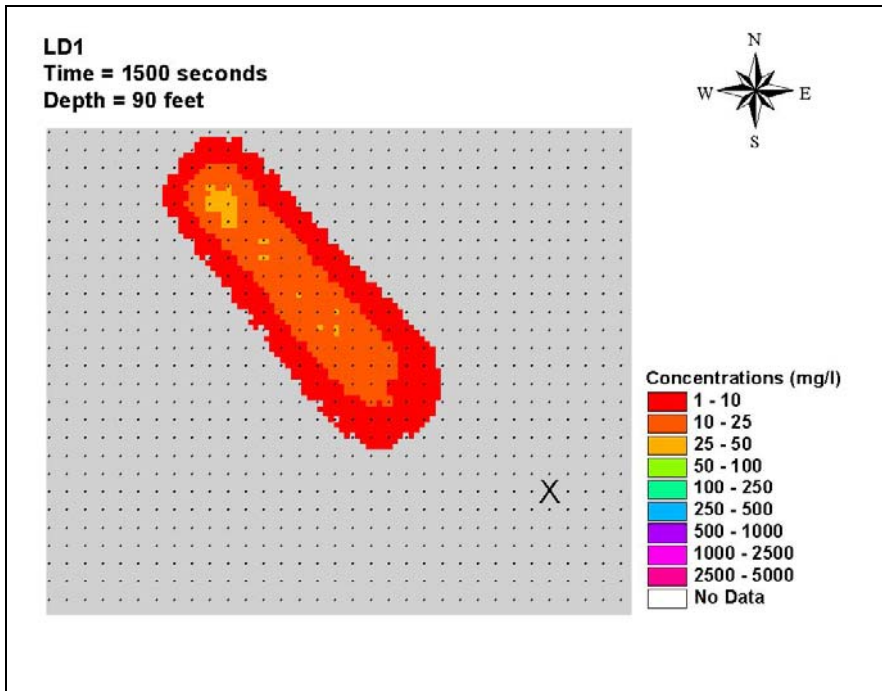


Figure 145. LD1 plume at 1,500 sec at 27 m

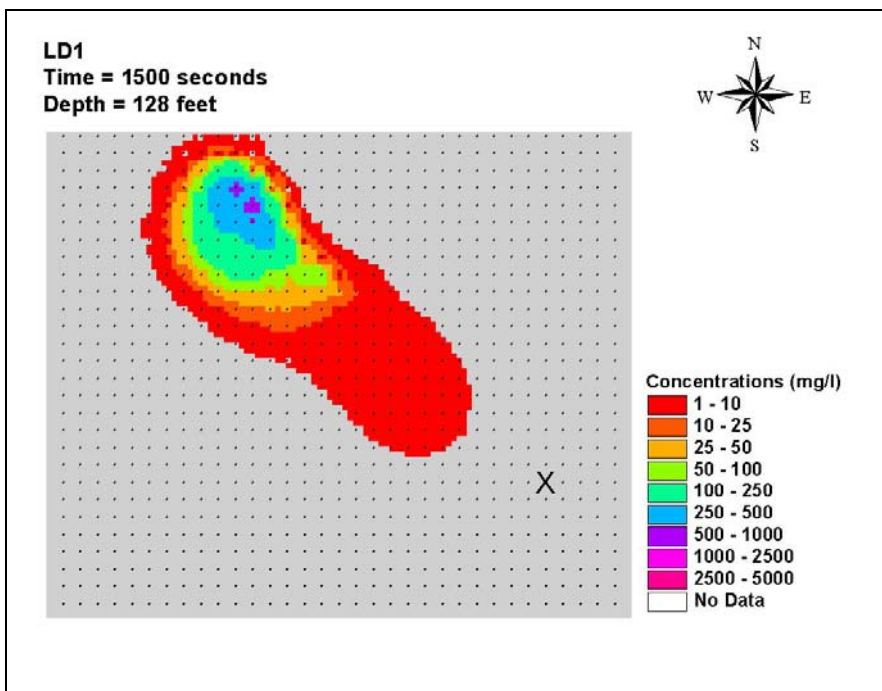


Figure 146. LD1 plume at 1,500 sec at 39 m

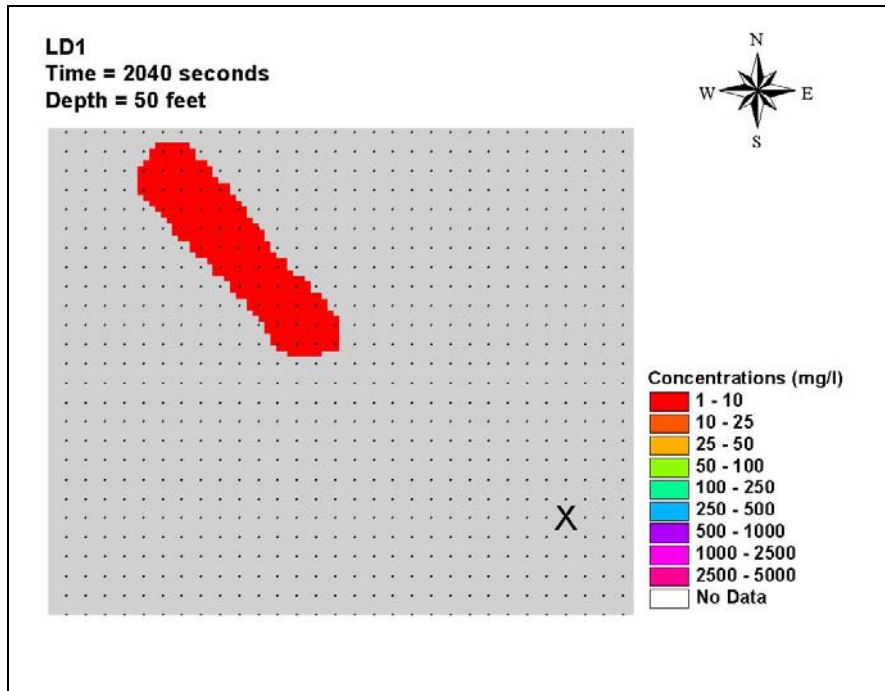


Figure 147. LD1 plume at 2,040 sec at 15 m

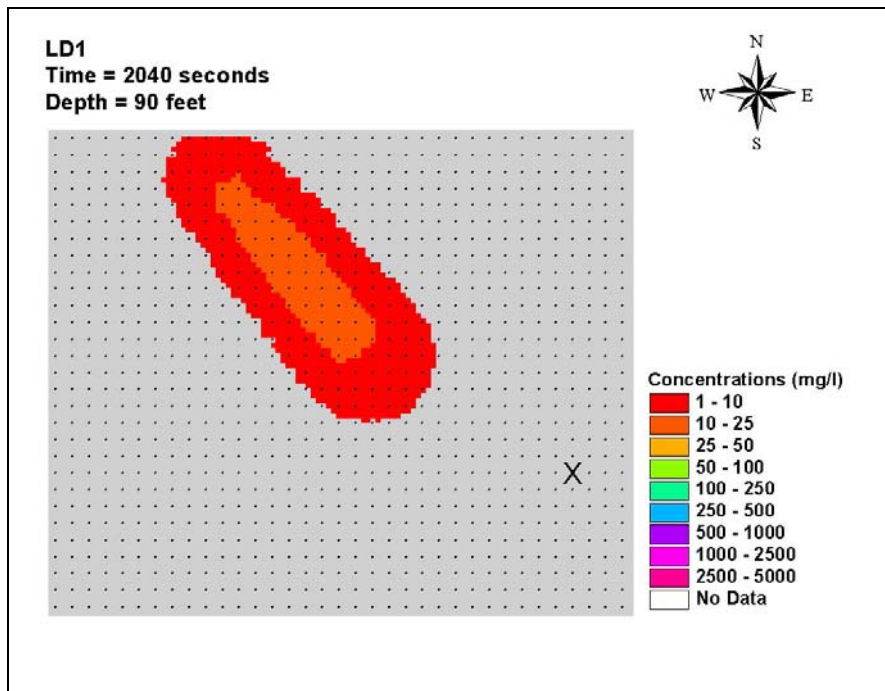


Figure 148. LD1 plume at 2,040 sec at 27 m

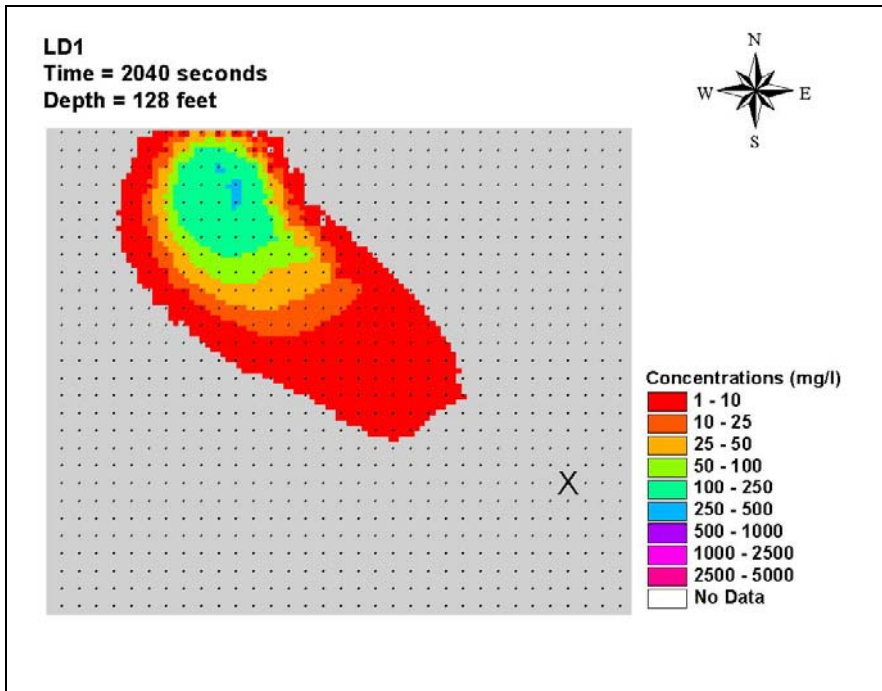


Figure 149. LD1 plume at 2,040 sec at 39 m

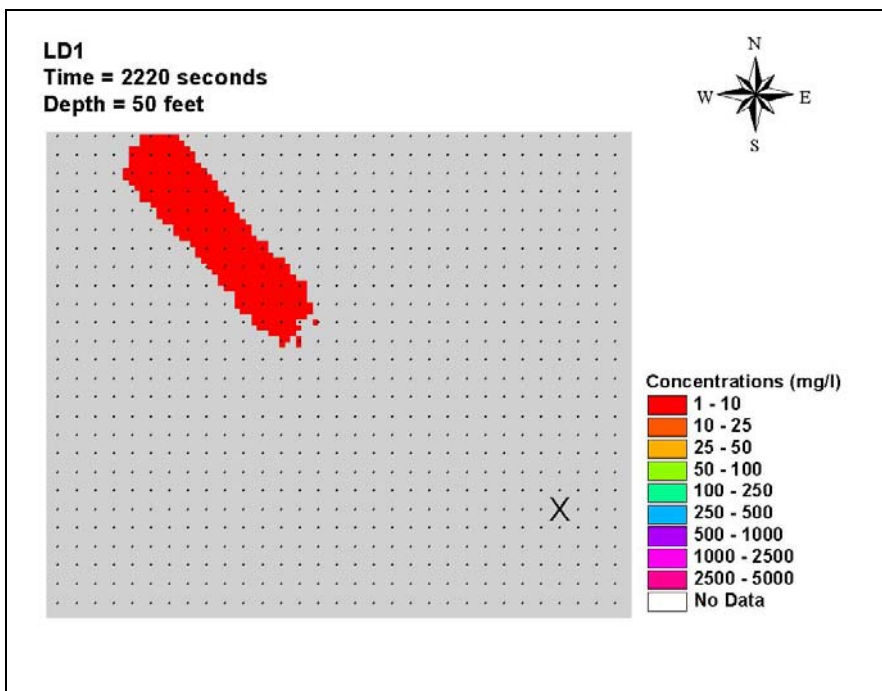


Figure 150. LD1 plume at 2,220 sec at 15 m

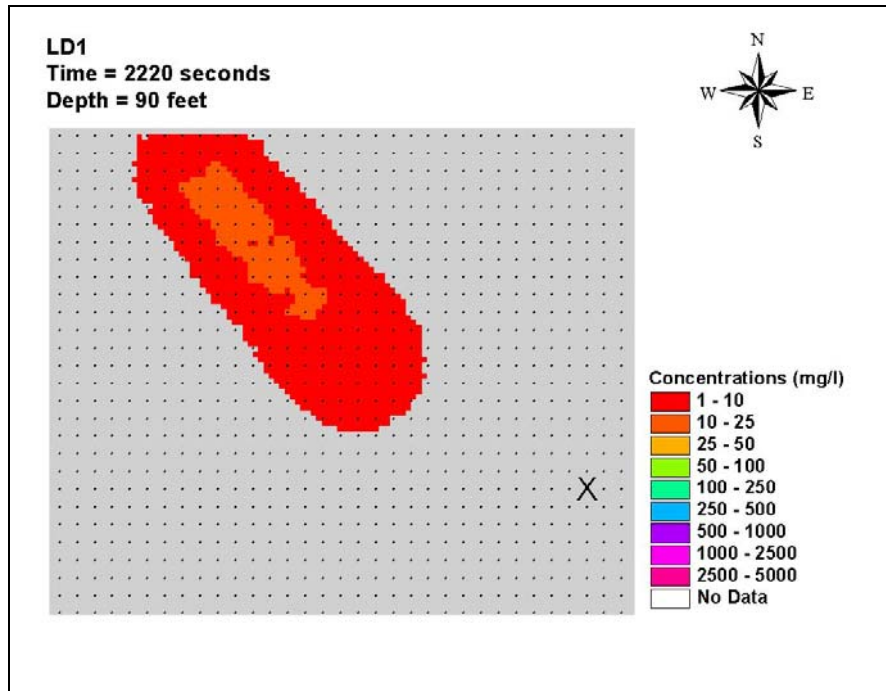


Figure 151. LD1 plume at 2,220 sec at 27 m

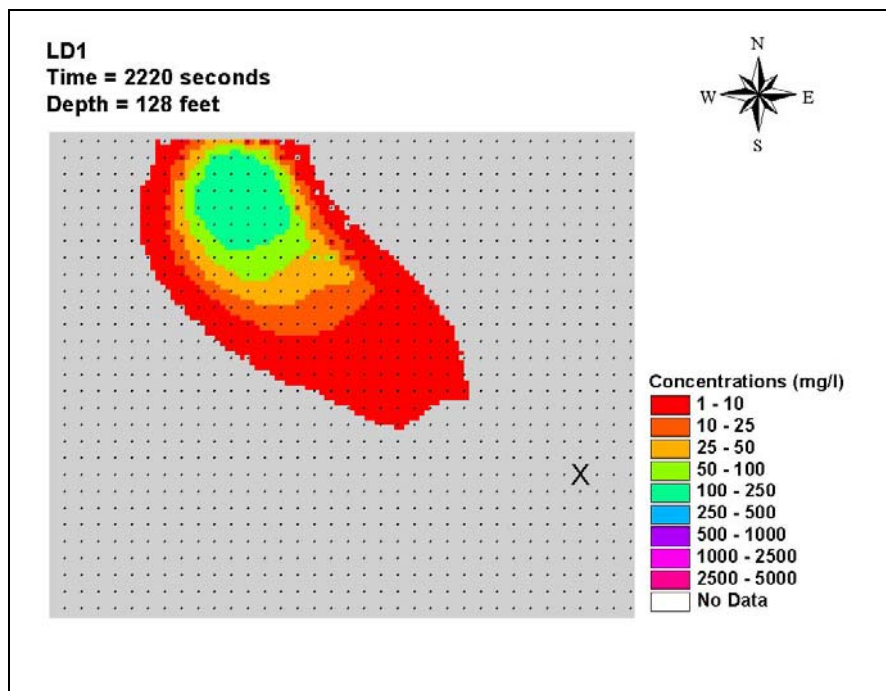


Figure 152. LD1 plume at 2,220 sec at 39 m

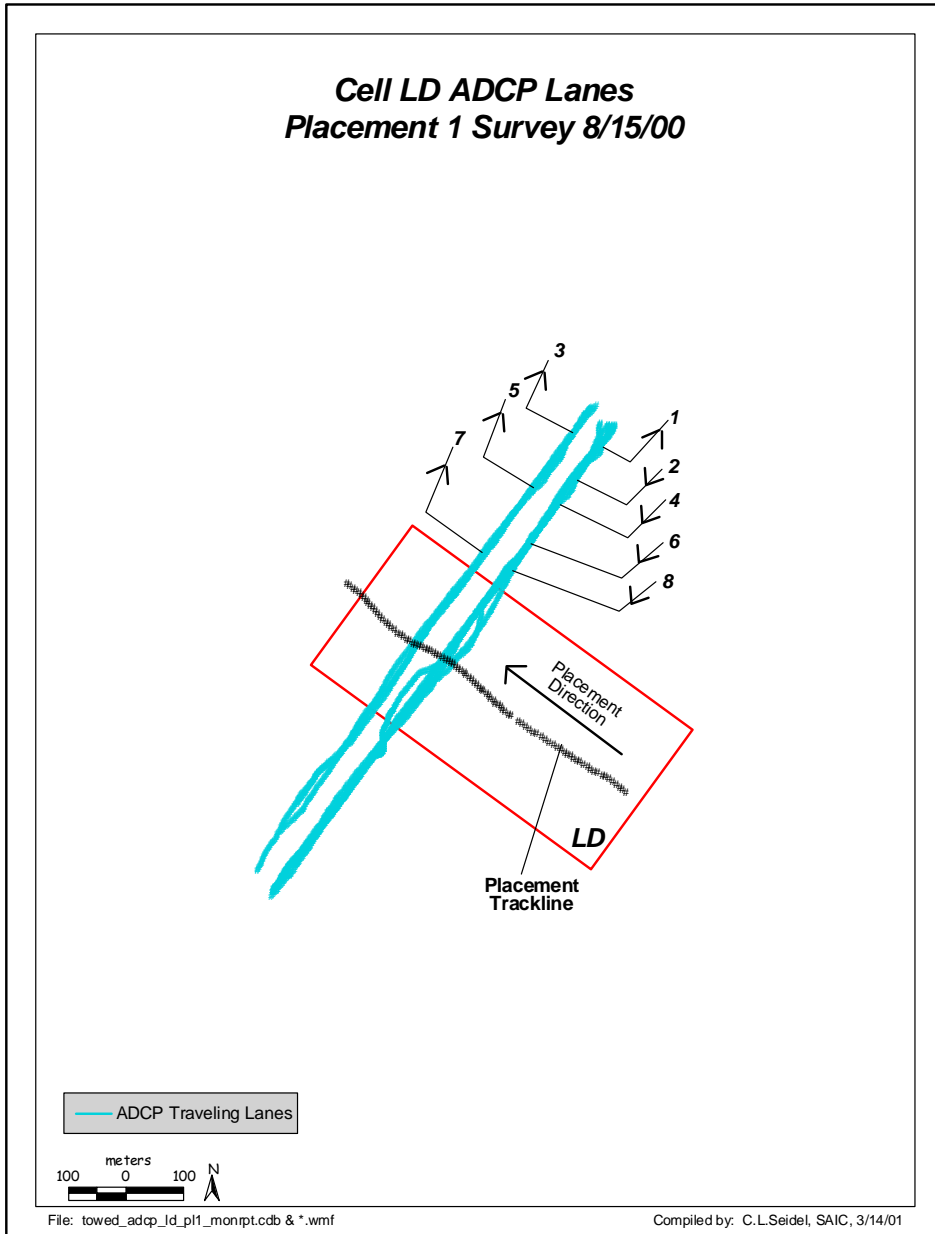


Figure 153. LD1 transects (SAIC 2002, Figure 5.6-3)

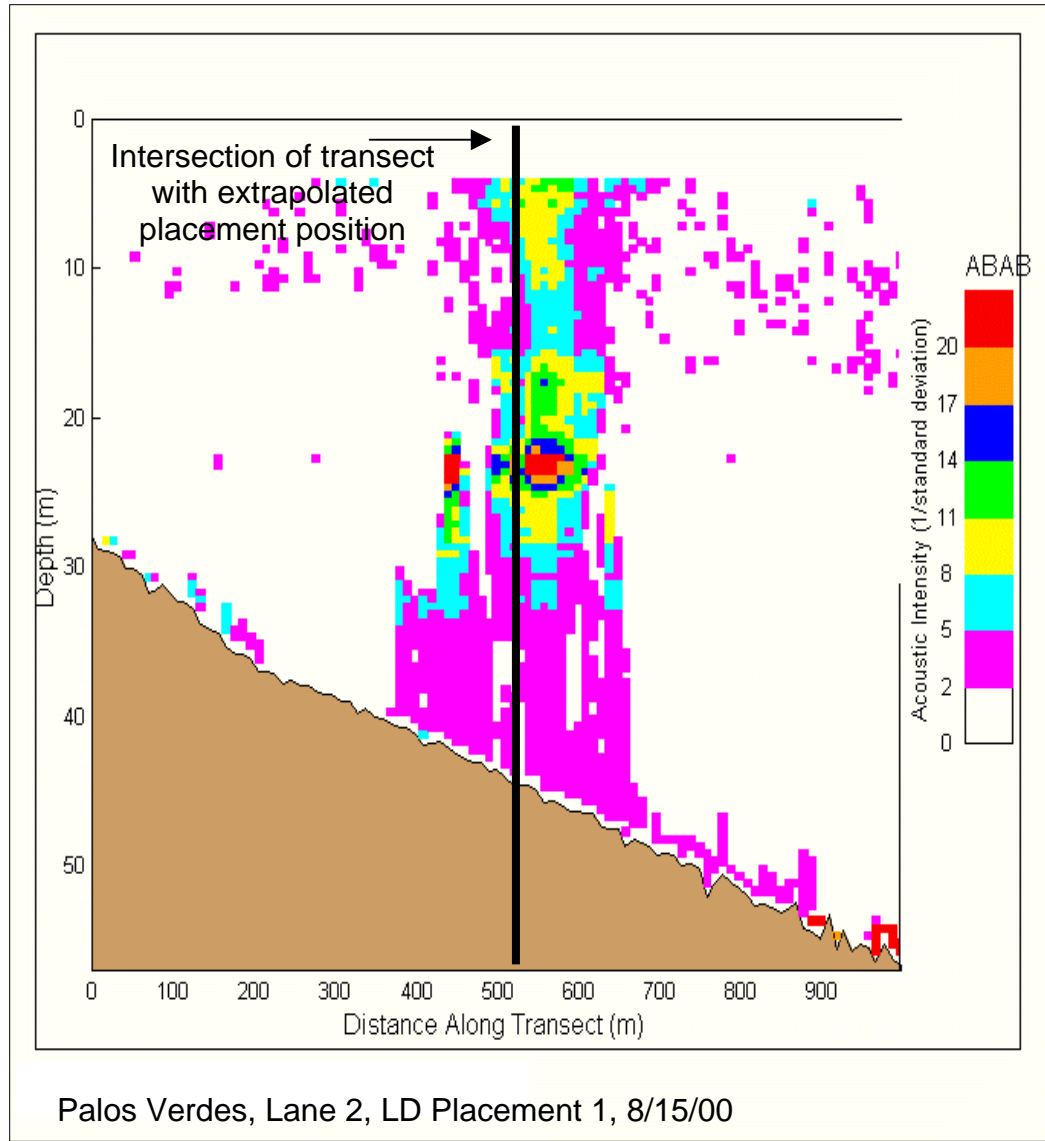


Figure 154. ABAB along Transect 2 at 6 min after the placement ended (SAIC 2002, Figure 5.6-5)

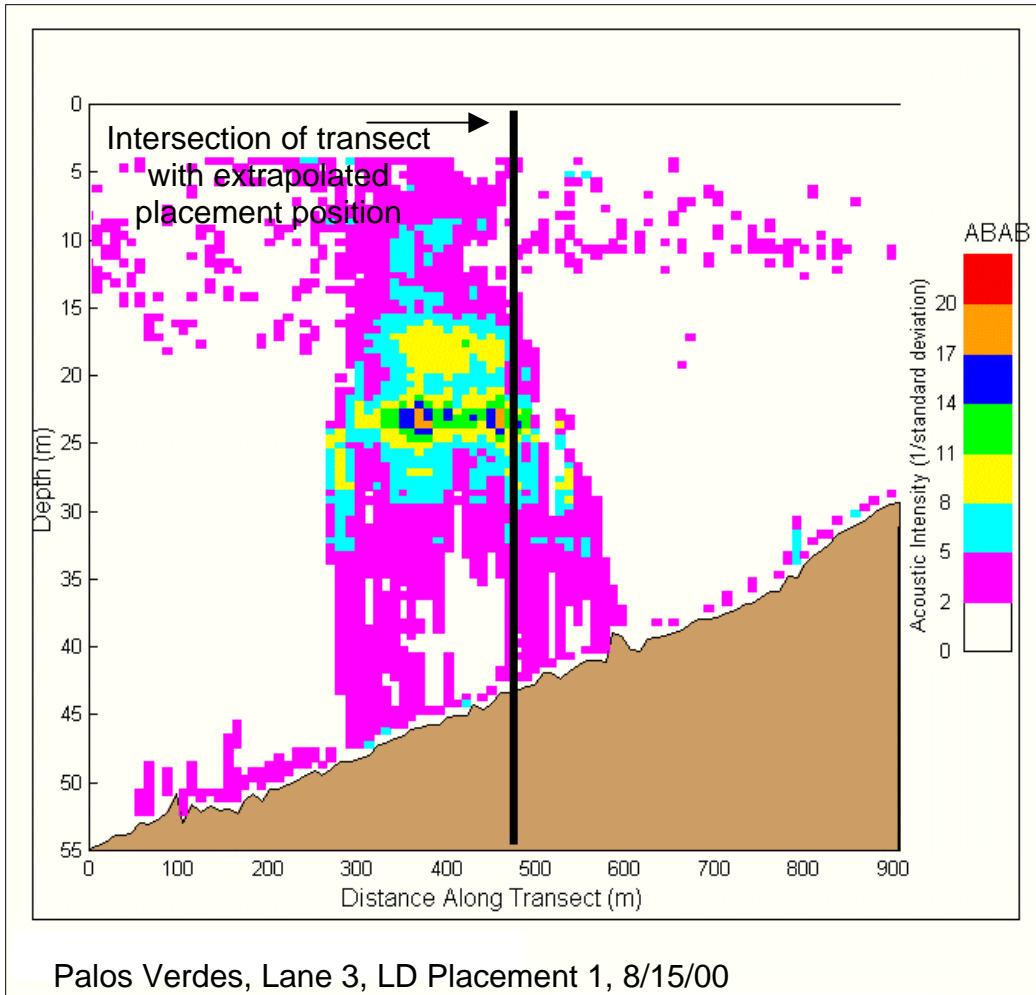


Figure 155. ABAB along Transect 3 at 15 min after the placement ended (SAIC 2002, Figure 5.6-6)

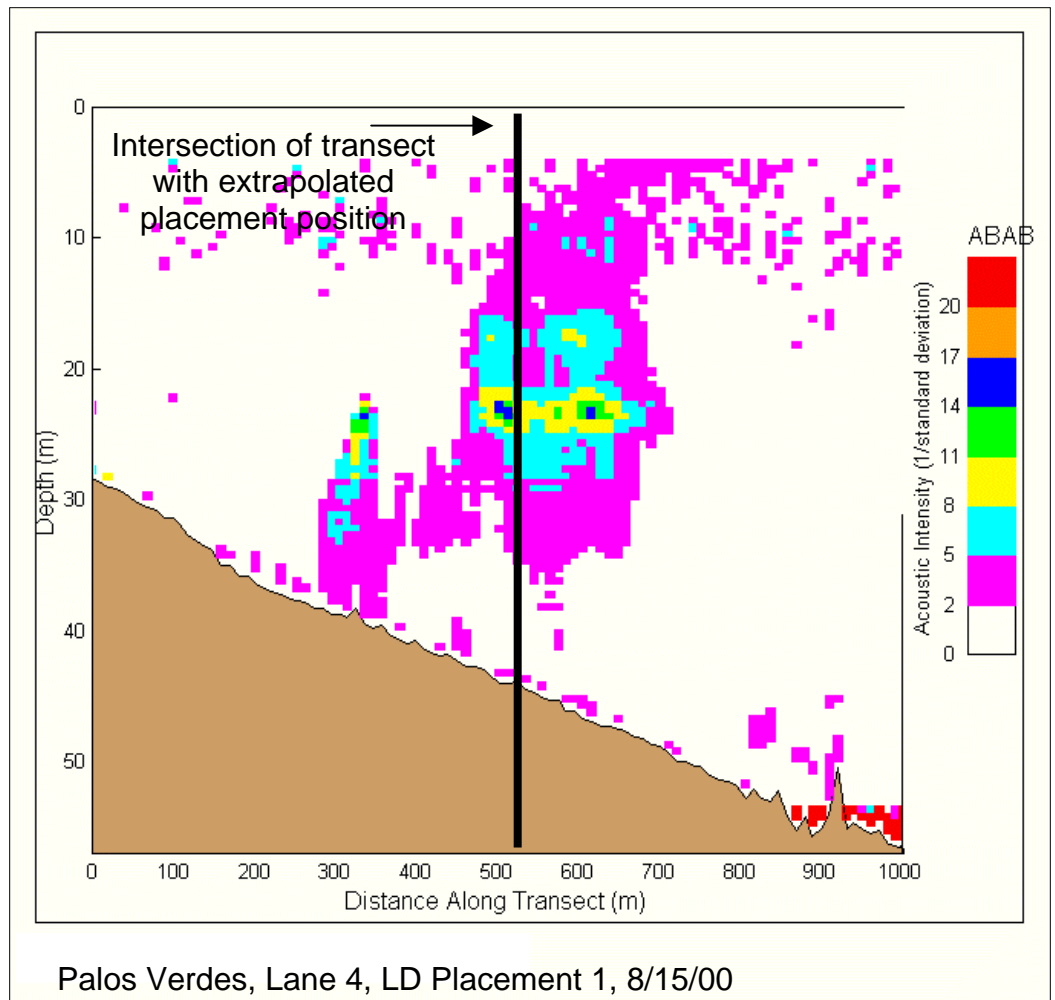


Figure 156. ABAB along Transect 4 at 24 min after the placement ended (SAIC 2002, Figure 5.6-7)

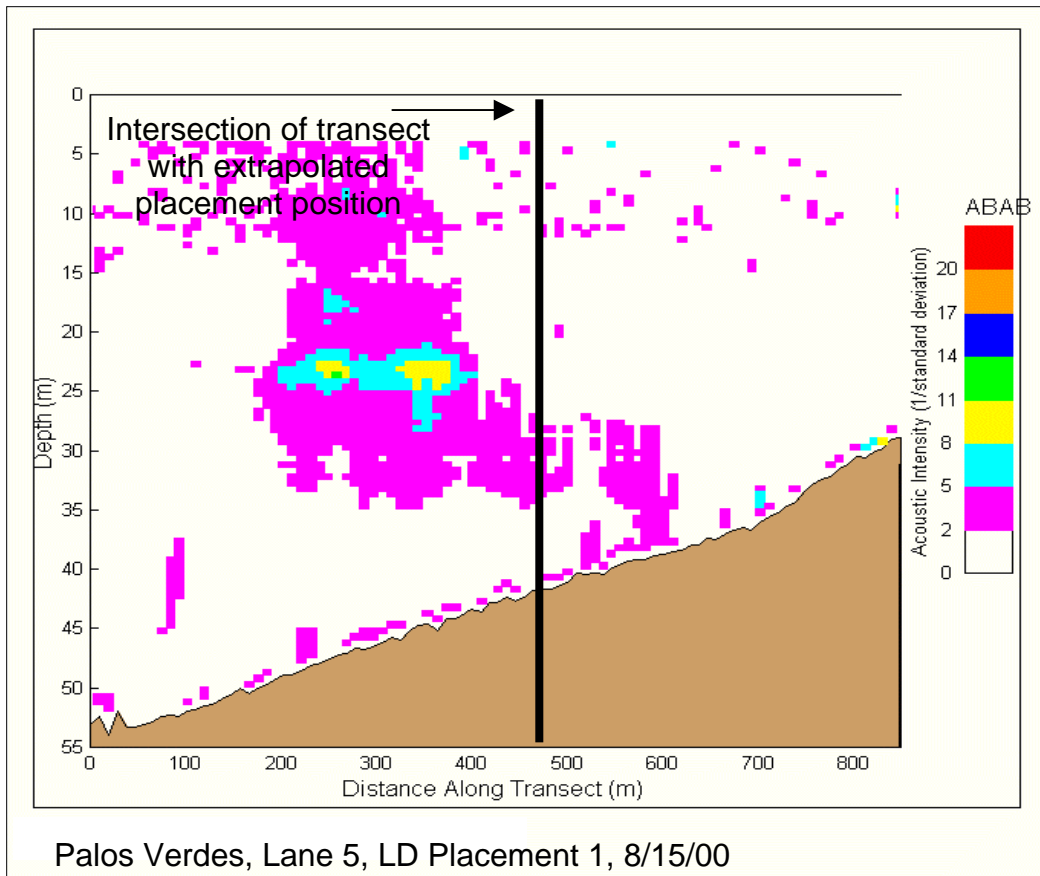


Figure 157. ABAB along Transect 5 at 34 min after the placement ended (SAIC 2002, Figure 5.6-8)

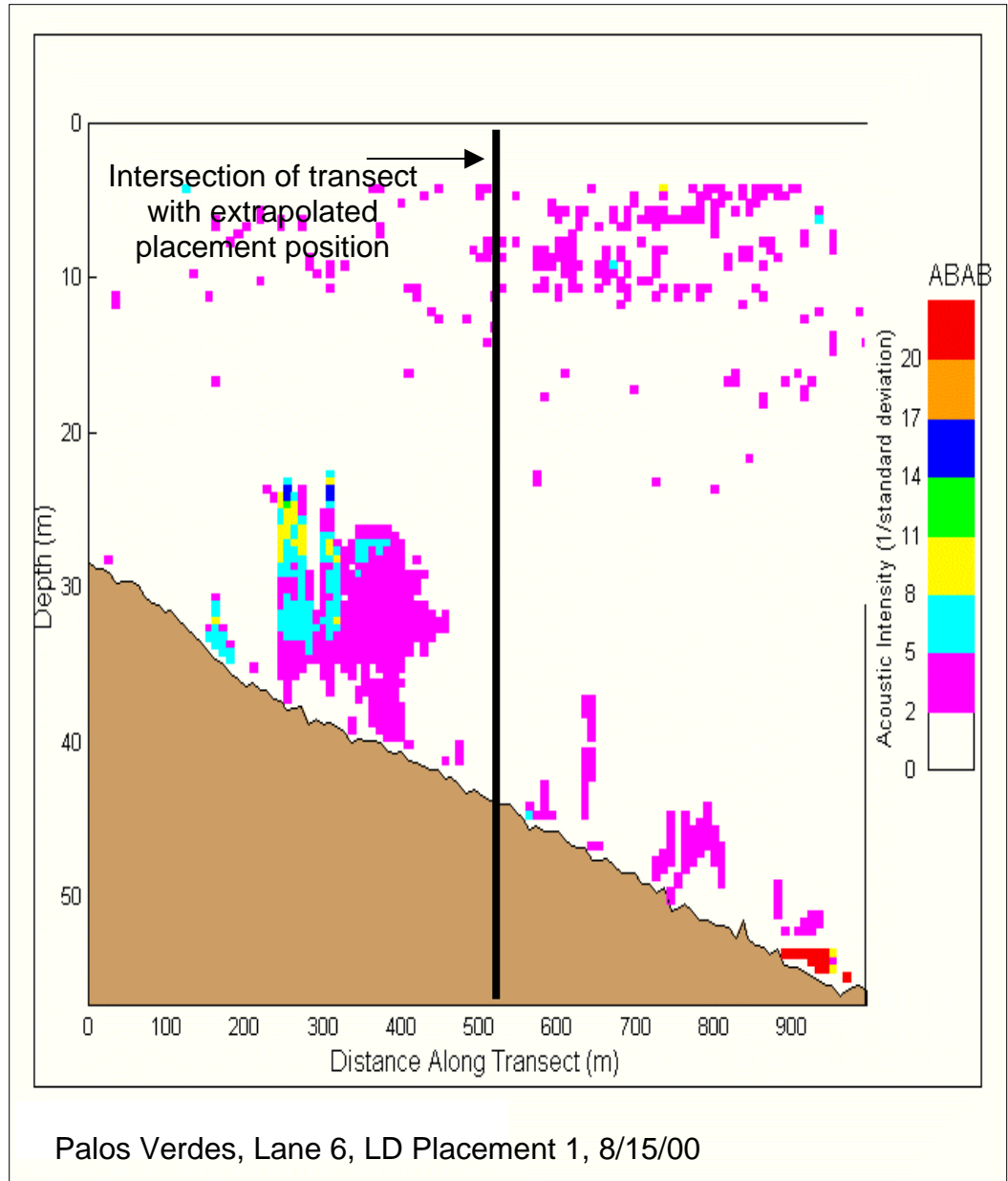


Figure 158. ABAB along Transect 6 at 47 after the placement ended (SAIC 2002, Figure 5.6-9)

Appendix K- Addendum A

Cap Volume Computations

Cap volume estimates

In addition to the MDFATE simulations to predict detailed operational parameters, a good estimate of the in-channel and in-hopper volumes required to construct a pilot cap of a given thickness and area was needed to allow SPL and EPA personnel to make decisions on the volume of material to place during the Palos Verdes Pilot Cap (PVPC) project. An estimate of the volume to be placed was needed to compute a cost for the dredging and placement portion of the Pilot study. The volume to be dredged was then used to determine the best overall combination of cap volume placed and the amount of monitoring to achieve the project objectives. Many of the procedures used for these prior-to-placement volume estimates were developed during the prior *in situ* capping study and are described in Palermo et al. 1999. However, the techniques described in this report are more detailed, based on actual values, and are therefore thought to provide a better estimate of in-channel or in-hopper volumes required for a cap of a specific dimension. These procedures can also be used to make future estimates of required cap volumes. While MDFATE simulations are a part of this procedure, it involves a number of steps beyond those needed for the other MDFATE simulations.

The volume estimates are, in fact, a rough sediment mass balance for the dredging, transportation, and placement process for this project. Because the volume during each phase changes due to differing densities of material, the best method to track the amount of material is by mass. The appropriate mass to volume conversion can then be made as needed. A number of assumptions are required for the mass/volume estimate. In some cases, which are noted, solid information on which to base the assumptions was not readily available. A major part of this effort was to compute the volumes required for a range of capping scenarios (cap thickness and extent). For brevity, only the option selected for implementation during the pilot cap project is presented. The remainder of this section lists the steps required to compute the volume, and describes these steps in detail.

Steps required to compute the PV shelf cap volume. The following steps were followed to compute the in-hopper and in-channel volumes required to produce caps of a specified size. The section following these steps describes how each of these calculations was conducted and the source of the information:

- a. The *in situ* density of the sediment in the channel prior to dredging was determined to estimate the mass of material retained in the dredge during each load and the volume of sediment removed from the channel to create this load.
- b. The mass of the sediments retained by the dredge for each load was computed by estimating the volume and density of the material in the hopper.
- c. NATCO provided an estimate of the sediment volume lost during dredging followed by a subsequent calculation by ERDC.
- d. NATCO estimated any sediment losses that occurred during transportation to the PV shelf.

The following section provides details of information sources and calculation methods to the steps described above.

(1) Queen's Gate *In situ* Channel Density Calculation. The calculation of the Queen's Gate sediments *in situ* density (also called the in-channel density) prior to dredging are the basis for the remainder of the calculations. The *in situ* density prior to dredging was computed indirectly by measuring the weight (mass) of a number of hopper loads, and computing the volume of sediments removed from the channel by bathymetric surveys taken before and after the dredged loads. This information was based on discussions with NATCO personnel. Hopper loads were computed from changes in draft that are converted to the load (weight) of the slurry the dredge is holding. Assuming that gravity is constant over the area, this weight is equivalent to the mass of dredged material. The hopper load is measured in short tons (ST) (2,000 lb). Because SI units were used for this project, the hopper load was converted to a mass in metric tons (MT) (1,000 kg) by the factor of $1 \text{ ST} \cdot .9072 = 1 \text{ MT}$.

Other information from the dredge was required to calculate the *in situ* channel density. Those data included the following:

- a. Lead line soundings were taken inside the hopper to determine the top of the sediment layer that can support the lead weight.
- b. Ullage tables convert the distance from the top of the hopper bin to the sediment surface to a volume of material in the bin. Thus, the volume of reasonably dense solid material in the hopper was computed.
- c. Note that the volume of the more fluid (less dense) slurry above the denser material elevation is not routinely computed, nor is the density of the water in this more fluid slurry routinely measured.
- d. During the contract, accurate before and after hydrographic surveys are taken after a considerable number of loads of dredged material have been removed (say 20 or more). By differencing these surveys, the in-channel volume of removed material is computed. The individual hopper loads taken between the hydrographic surveys are then summed to compute a total mass (weight) of dredged material removed.
- e. The total mass of the sediments in the dredge from all the loads (including both the denser material determined from lead line surveys and the fluid slurry above) is divided by the volume determined from the before and after dredge surveys. This value is the average in channel

in situ density. Note that this value does not include material that overflows during the dredging process and settles outside the channel boundaries. However, if material settles back in the channel, it may be dredged on subsequent loads and would be included in the *in situ* density calculations.

The average in channel density for dredged material removed using the NATCO dredge *Padre Island* (November 1999 to February 2000) was 1.936. This value was provided by NATCO, and was based on correlation of 20 hopper loads with before and after surveys. On 8 June 2000, NATCO provided calculations of *in situ* channel densities from recent dredging with the *Sugar Island*. The more recent *Sugar Island* average channel *in situ* density was 1.84. The earlier *Padre Island* and the more recent *Sugar Island in situ* density values were averaged and rounded to 1.90. This averaged value was used in the calculations of required cap volumes.

- a) **Dredge Load/Volume/Bin Density Calculation.** The density of the material in the hopper bin and the volume of sediments in the hopper was needed by the MDFATE program to determine the actual mass of dredged material placed in the pilot study cells. The average density of the hopper load (solid dredged material and water) is the mass (weight) of material divided by the total volume of material in the hopper. The total volume of the hopper on the Sugar Island was 2,735 cu m (3,578 cu yd).
- b) The mass of the dredged material in the hopper is determined by subtracting the weight of the dredge after loading from the weight of the dredge full. This is done by measuring the change in draft, converting this value to volume and weight of water displaced. For typical loads, the weight of dredged material was about 3,900 tons for the 833 cu m average loads being removed by the Sugar Island. During a typical hopper load on this project, the entire hopper was filled with dredged material (consisting of the solid dredged material that has settled out and the more fluid slurry on top).
- c) Based on these calculations, typical in hopper bulk densities of about 1.3 g/cm³ had routinely been achieved with the Sugar Island during April and May 2000.
- d) When NATCO reports the “load” for the Queen’s Gate dredging, it reports cu m. However, this value is not the number of cu m in the hopper bin. As noted above, the full hopper volume of 2,735 cu m includes a volume of settled sediments and the more fluid slurry above it. Because the contractor is being paid on material removed from the channel, it makes sense to report the load of dredged material removed as the equivalent number of cubic yards that have been removed from the channel. This makes it easier for the Corps to determine progress and make estimated payments.
- e) The load in the dredge was converted to an equivalent volume removed from the channel by the calibration performed by determining the sum of multiple loads in the dredge (as determined by soundings of the hopper) with the measured volume in the channel removed as determined by before and after surveys as described above.

- f) For the Queen's Gate dredging through early June 2000, the sounding volume measured by lead lines were equal to the volume removed as determined by channel bathymetric surveys, i.e., a cubic meter in the hopper as determined by lead line soundings of the solid settled material and the ullage tables was equal to a cubic yard removed from the channel. Note that the bulk density of these two "cubic yards" or "cubic meters" is quite different.
- g) For the pilot study, NATCO assumed three to four passes would be made over the channel during each load in the sandier (more dense) portions of lanes in the channel. NATCO estimated that the typical load taken to the PV shelf and placed using conventional bottom dumping would have a bin density of 1.4 g/cm^3 with a load that was equivalent to 925 cu m of material in the channel. For the majority of MDFATE and STFATE simulations conducted between early June and August 2000, the total mass of solids and water and associated volumes were computed by assuming each load contained 2,735 cu m (3,578 yd³) at an overall bin density of 1.4 gm/cm^3 .

2) Dredge Material Losses During Dredging

- a) Based on NATCO's observations, no measurable net losses of dredged material during dredging were projected. While the dredging was done with overflow, apparently the overflow (the vast majority of which goes through the skimmer and thus is released at a depth equal to the dredge's draft of 3 to 6 m moving vertically downward), stays in the channel. Also, the currents in the channel were relatively low, and tended not to transport material out of the channel. Thus, over the many individual loads required to complete the channel deepening, these overflowed sediments which settle back into the channel were expected to be removed on subsequent loads. NATCO also noted that material deposited on the channel slopes and outside the channel had not been detected, nor had any measurable fluff layers been detected in the channel.
- b) NATCO performed some measurements on the slurry above the solid settled material, the average SG of the slurry was estimated at 1.04. Based on the following assumptions a very rough estimate of volume overflowed per hopper was made:
 - i) Overflow slurry has the same SG as that measured by NATCO.
 - ii) The overflow is assumed to last for 30 min in each load.
 - iii) The inflow rate is 6.1 m/sec through a 0.69 m pipe.

iv) The load in the hopper is the equivalent of 925 cu m at an *in situ* density of 1.90.

c) Based on these assumption, the equivalent *in situ* of volume overflowed is 63.5 cu m or 7 percent of the hopper load.

3) Dredged Material Losses During Transport

a) NATCO did not expect any measurable losses of dredged material during transport to the PV shelf, i.e., no lowering of the skimmers or loss of material through leaking seals.

4) Losses of Dredged Material During Placement

a) Major portions of the MDFATE modeling efforts were to predict the amount of dredged material “lost” during placement. The lost material is material that does not settle out within the MDFATE grid, and thus is not contributing to the cap over the area simulated.

b) A series of single load placements were simulated using MDFATE on 8 June 00. The following were the important input variables.

i) Currents were assumed to be constant at 15 cm at 290 deg. This was thought to be a reasonable amount of current, higher than the bottom currents typically noted in Noble’s (1994) USGS study (5-10 cm/sec), but not as high as the reasonable maximums of 20 to 28 cm/sec.

ii) Dredge velocity was assumed to be 0.1 knots. NATCO indicated the dredge could be held nearly stationary during placements. The 0.1 kts speed is considered nearly stationary.

iii) The volume of material in the hopper was specified as 3,578 cy. The overall volume fraction of solids in the hopper was adjusted based on the 1.4 g/cu cm value provided by NATCO, with the sand, silt and clay fractions adjusted accordingly. See the section on MDFATE results more details on these simulations. The clay was specified as non-cohesive.

iv) Placements at the shallow (LU) cell and deep (SU) cell were simulated.

- v) Placements using the fine, average, and coarse Queen's Gate sediments were simulated.
- vi) From each simulation the maximum elevation and the percentage of material deposited in the grid (compared to the maximum available) was determined.
- vii) For the fine material, a worst case, the percentages retained in the model grid were 76.5 percent at the shallow cell (G3) and 62 percent at the deep cell (G1).

5) Required mound Volumes and Capping Scenarios:

- a) The required mound volumes and capping scenarios are described in Table 4-x. ?
- b) The cap scenarios selected were:
 - i) 15 cm thick by 600 m long by 300 m wide (full cell) at both the shallow and deep cells.
 - ii) 10 spreading loads from borrow area AIII.

6) Conversion of Cap volumes to Hopper and in Channel Volumes. Based on an assumed area over which to place the cap and an assumed cap thickness, the volume of sediments in the cap along with the volume of sediments outside the cap were computed. The as placed cap does not have vertical sides due to cap dispersal during placement, therefore the additional sediment that must be placed to achieve a given thickness, typically 15 cm over the desired cap area, had to be included in the total cap volume estimate.

- a) Using the logic described earlier in this document, the vertical side cap volumes were converted into the required in hopper load and in channel volumes as shown in Table 4-x. ?
 - i) The total volume vertical sides (cubic meters) (Column E) is Column B x Column C x Column D.
 - ii) Column F is the percent volume retained inside the cell to be capped. To achieve the design (15 or 45 cm) thick cap over the entire cell, a

considerable amount of material will end up outside the cell because the material spreads during placement. For the smaller cell in the minimum cap, 300 m long by 100 m wide, the percentages found in the cell provided are simply educated guesses based on results from simulations conducted for the Palermo et al. 1999 report. During the simulations conducted for the Palermo et al. 1999 report, the percent of the material found within a cell 600 m by 300 m was about 50 percent. Several sets of MDFATE simulations were made as part of this volume estimation effort. More detailed results from those simulations can be found in the MDFATE simulations section. From a volume computation perspective, the following information are critical. For the 300 by 600 m by 15 cm thick in Cell G3 (LU), the ratio of the volume required for a cap with vertical sides to the total volume on the bottom was 0.43 (as determined by simulation G3PF2). For 300 by 600 m by 15 cm thick in Cell G1 (SU), the ratio of the volume required for a cap with vertical sides to the total volume on the bottom was 0.23 (as determined by simulation G1FP2).

- iii) The percent retained in the modeled grid (Column G) is based on the MDFATE simulation for the fine sediments. The fine sediments were selected as providing a conservative result. The difference between this volume and 100 percent is assumed to be “lost.” In this case lost is defined as material that will settle outside of the modeled grid or material that was still in suspension when the simulation ended. The MDFATE simulations indicated the percent retained volumes were 87 percent for the material placed in cell G3, and 74 percent for the material placed in cell G1.
- iv) Column H is the percentage of material lost during transportation, estimated by NATCO to be zero.
- v) Column I is the overall multiplier to convert the total cap volume with vertical sides (Column E) to the volume that would have to be in the dredge when it finishes loading. The formula is $= (1 / (\text{col F value} / 100)) * (1 / (\text{col G value} / 100)) * (1 / ((100 - \text{Col H value}) / 100))$. Note that this assumes that the mass of solids/volume ratio is the same in the hopper as on the bottom.
- vi) Column J is the product of the overall multiplier (Column I) and cap volume required with vertical sides (Column E), i.e., how much cap material at the as placed on the shelf void ratio is required to get the desired cap thickness over the cell. Note that this volume is at the in place void ratio specified in MDFATE (1.5 for the fine sediments) and described in the MDFATE simulations. For the fine sediments, this overall as placed void ratio is 1.625. Note there may be some error here because this is the overall void ratio for the sediments

assuming they are present in the cap at the same concentrations as found in the hopper. This will be checked with the program developer, Mr. Rod Moritz.

7) Convert the placed volume back to hopper loads and *in situ* channel volumes:

- a) Column K converts the required cap volume to the equivalent hopper load – in channel volume required. The value of 0.609 is the ratio of the hopper load (mass) as defined by NATCO (925 cu m of in channel material removed) to that mass as found on the seafloor (expressed as 1,520 cu m (1,988 cy)) as predicted by MDFATE for fine sediments with the as placed void ratio assuming all the material reached the seafloor.

- i) Column M is the equivalent number of hopper loads required, or Column L divided by 925 cu m.

Results

Table K14 provides a summary of cap volume calculations. Based on the calculations described above, the following information was used by SPL and EPA to make a decision on the project, i.e., the likely number loads to place at 925 cu m per load for the Queen’s Gate sediments. The modest cap scenario was (600 m long by 300 m wide by 15 cm thick), as modified based on 16 June 2000 MDFATE simulations.

- i) LU – Shallow Cell, G3 – 43,000 cubic meters – 46 hopper loads
- ii) SU – Deep Cell, G1 - 67,300 cubic meters – 73 hopper loads

The resulting total volume was 110,300 cubic meters, equivalent to 119 hopper loads, plus an additional 10 spreading loads from the borrow area.